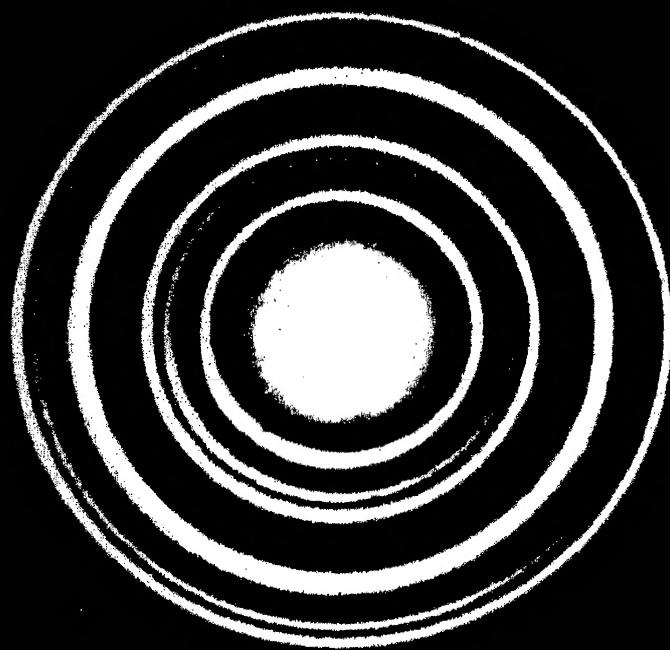




THEORY AND PRACTICE OF  
ELECTRON DIFFRACTION

PLATE I



Polycrystalline  $\text{SnO}_2$ ; transmission pattern

# THEORY AND PRACTICE OF ELECTRON DIFFRACTION

BY

G. P. THOMSON

M.A., F.R.S., Hon. D.Sc. (Lisbon)

PROFESSOR OF PHYSICS IN THE UNIVERSITY OF LONDON AT  
THE IMPERIAL COLLEGE OF SCIENCE AND TECHNOLOGY;  
FORMERLY FELLOW OF CORPUS CHRISTI COLLEGE, CAMBRIDGE

AND

W. COCHRANE

M.A., B.Sc., Ph.D.

ASSISTANT LECTURER IN PHYSICS AT THE IMPERIAL  
COLLEGE OF SCIENCE AND TECHNOLOGY

MACMILLAN AND CO., LIMITED  
ST. MARTIN'S STREET, LONDON

1939

COPYRIGHT

PRINTED IN GREAT BRITAIN  
BY R. & R. CLARK, LIMITED, EDINBURGH

## PREFACE

It is now eleven years since the first discovery by Davisson and Germer that electrons could be diffracted by a crystal, like waves of light by a diffraction grating. Developments in two widely different fields have followed. In the first place the phenomenon has provided the most accurate and the most straightforward test of the assumptions of wave mechanics. It has fully confirmed these assumptions, which now in turn form the basis for the theory of atomic nuclei, perhaps the last great field of research open to the physicist. On the other hand, the method of electron diffraction, especially when the electrons have considerable energies, has been developed as a means of investigating the atomic structure of matter in surface layers, in thin films and in gases, just as X-rays have been used to study the structure of massive crystals.

Although several reports on electron diffraction have appeared, mostly in pamphlet form, there is no general account in English dealing adequately with both aspects of the subject. An early book by one of the authors, *Wave Mechanics of the Free Electron*, was concerned chiefly with the theoretical implications, as the applications to surfaces were only beginning at the time it was written. We are, however, much indebted to the authorities of Cornell University for permission to incorporate certain portions of that book, mainly mathematical, in the present work. Other early accounts are those by Rupp (1930), Mark and Wierl (1931), and Kirchner (1932). These are all necessarily rather out of date. Of the later accounts, that by Hengstenberg and Wolf deals mainly with the theoretical side, a small monograph by Beeching gives a short outline of the subject, and one by Trillat discusses fully some of the applications. While the present work was being prepared, however, there appeared a report by Finch and Wilman in the *Ergebnisse der exakten Naturwissenschaften* on the applications of the method to the study of surface layers, and we take the opportunity of expressing our indebtedness to that excellent account.

We have tried in this book to give a fairly complete treatment of the subject both on the theoretical and practical sides, but the theory has been written from the point of view of the experimental physicist, and we have not attempted to deal fully with the difficult questions of a philosophical character which are involved in a logical formulation of the quantum theory. At the same time we hope that, in our efforts to present a view easy for the practical physicist to grasp, we have said nothing which will be anathema to the orthodox school of quantum physicists.

Although the applications of the electron diffraction method to problems in physics and chemistry have been numerous and successful, we feel that a considerable number of potential users may have been deterred by fear of difficulties in technique and in the interpretation of the results. The former difficulties have been almost completely overcome, and it should not take a competent physicist many weeks to get satisfactory results. The methods are fully described in the chapter on technique (Chapter XVI). The interpretation is perhaps more difficult, but has now been fairly fully worked out. We have described in considerable detail the kinds of patterns usually obtained and how their features are to be explained. Chapters VI, VIII and IX, in which this is done, form the core of the book. Half-tone plates have also been included showing practically all the types of patterns which are found. For the reader who is only interested in the practical applications of the method, Chapters I, II, V, XVIII, XIX and XX may be omitted; it is fortunate that the complicated dynamical theory described in Chapter XIX is comparatively seldom required to explain diffraction patterns, most of the features of which follow from the simpler kinematical theory of Chapters III and VI.

In describing the results achieved by the method we have only given a full description of a limited number of problems, choosing those where a large proportion of the information has been obtained by electron diffraction. This has been done so that it might be possible to give an adequate account, without overloading the book and including matter not strictly relevant to its title. Other applications have been dealt with very briefly in Chapter XV; the object of this chapter is to indicate

the kind of problems which have been successfully attacked by the method, so as to give an indication of its scope to anyone interested in extending its use to problems of his own.

The experimental side of electron diffraction has a great fascination and many of the photographs are striking and beautiful. As a new branch of physics we hope it may interest many who are attracted by scientific curiosity, for electron diffraction combines in an unusual fashion theoretical interest, practical applications and pleasing experiments.

There is one point of nomenclature to which we should like to refer. It is surely time that some distinction was drawn between phenomena such as the formation of spectra by a diffraction grating, or the subject of the present book, and the diffraction of light by a straight edge. In the first case we are dealing with the interference of a discrete number of beams scattered by certain lines or centres ; in the second the interference is between the infinitesimal wavelets from the portion of the wave-front not obstructed by the obstacle. There seems to be a case for restricting the use of the word ' diffraction ' to the latter. Would ' interfraction ' be too bizarre for the former ?

In view of the statement which appeared in the *Zeitschrift für Physik*, vol. 95, p. 801, it is difficult to know how to deal with the numerous papers published by E. Rupp. We have, however, made brief mention of some of his results in cases where they seemed to be of interest.

In addition to the acknowledgements already made, we wish to record our thanks to Professor G. I. Finch, Professor F. Kirchner, Dr. H. Boersch, Dr. C. A. Murison and Dr. R. O. Jenkins for the loan of prints of electron diffraction patterns and for permission to make reproductions from them ; also to Dr. L. O. Brockway for permission to reproduce Table XX ; and to Dr. G. Aminoff for the loan of the drawings of Figs. 57 and 58. We are also grateful to Dr. M. Blackman for discussion on some theoretical points, and to Dr. Gertrud Scharff for keeping us informed of the literature on the subject. Messrs. T. W. J. Riches, G. R. Green and E. S. Parke rendered valuable assistance in the preparation of the diagrams and plates.

For permission to reproduce certain figures we should like to express our indebtedness to the Royal Society, the Physical

viii THEORY AND PRACTICE OF ELECTRON DIFFRACTION

Society, the Faraday Society, the American Physical Society, the American Chemical Society, the National Academy of Sciences, la Société française de Physique, the Institute of Physical and Chemical Research (Tokyo) ; to Messrs. Methuen & Co., Ltd., and Messrs. G. Bell & Sons, Ltd. ; and to the proprietors of the following journals : *The Philosophical Magazine*, *Physica*, *Annalen der Physik*, *Ergebnisse der exakten Naturwissenschaften*, *Zeitschrift für Physik*, *Physikalische Zeitschrift*, *Wissenschaftliche Veröffentlichungen aus dem Siemens-Konzern*, *Japanese Journal of Physics* and *The Bell System Technical Journal*.

G. P. THOMSON  
W. COCHRANE

SOUTH KENSINGTON  
March 1939

# CONTENTS

## CHAPTER I

	PAGE
GENERAL THEORY OF WAVES . . . . .	I

## CHAPTER II

DE BROGLIE'S WAVE MECHANICS . . . . .	12
---------------------------------------	----

## CHAPTER III

ELEMENTARY THEORY OF WAVE DIFFRACTION BY CRYSTALS .	20
---	----

## CHAPTER IV

EXPERIMENTAL EVIDENCE FOR ELECTRON WAVES . . . . .	29
--	----

## CHAPTER V

THEORETICAL INTERPRETATION . . . . .	57
--------------------------------------	----

## CHAPTER VI

EXTENDED THEORY OF DIFFRACTION . . . . .	70
--	----

## CHAPTER VII

CONSIDERATION OF INTENSITIES OF DIFFRACTION . . . . .	86
---	----

## CHAPTER VIII

SOME SECONDARY EFFECTS . . . . .	106
----------------------------------	-----

## CHAPTER IX

THE PRINCIPAL TYPES OF DIFFRACTION PATTERN AND THEIR INTERPRETATION . . . . .	126
--	-----

## CHAPTER X

THE MEASUREMENT OF INNER POTENTIAL . . . . .	155
--	-----

# x THEORY AND PRACTICE OF ELECTRON DIFFRACTION

## CHAPTER XI

	PAGE
STUDY OF THE GROWTH OF CRYSTALS . . . . .	162

## CHAPTER XII

OXIDES . . . . .	177
------------------	-----

## CHAPTER XIII

POLISH . . . . .	185
------------------	-----

## CHAPTER XIV

OILS, GREASES, ETC. ; LUBRICATION . . . . .	197
---	-----

## CHAPTER XV

MISCELLANEOUS APPLICATIONS . . . . .	211
--------------------------------------	-----

## CHAPTER XVI

TECHNIQUE . . . . .	216
---------------------	-----

## CHAPTER XVII

DIFFRACTION BY GAS MOLECULES . . . . .	246
--	-----

## CHAPTER XVIII

SLOW ELECTRONS . . . . .	263
--------------------------	-----

## CHAPTER XIX

DYNAMICAL THEORY . . . . .	283
----------------------------	-----

## CHAPTER XX

POLARISATION . . . . .	311
------------------------	-----

NAME INDEX . . . . .	352
----------------------	-----

SUBJECT INDEX . . . . .	329
-------------------------	-----

## LIST OF PLATES

I. Polycrystalline $\text{SnO}_2$ ; transmission pattern .	. <i>Frontispiece</i>
II. (a) Celluloid; (b) Gold; (c) Platinum, magnetically deflected patterns; (d) Aluminium . . . . .	Facing page 40
III. (a) Mica, thin sheet ( <i>Kikuchi</i> ); (b) Mica, medium thickness ( <i>Kikuchi</i> ) . . . . .	80
IV. (a) Mica, thick sheet ( <i>Finch</i> ); (b) Fluorite cube face, beam approximately parallel to cube edge ( <i>Finch</i> ); (c) Iron single crystal; cylindrical film, showing scattering up to $162^\circ$ from incident beam ( <i>Boersch</i> ) . . . . .	112
V. (a) Beaten gold foil ( <i>Trillat</i> and <i>Oketani</i> ); (b) Cadmium iodide, inclined film, (001) orientation ( <i>Kirchner</i> ); (c) Molybdenite, inclined film, rotated during exposure ( <i>Finch</i> ); (d) Sputtered platinum; normal pattern; (e) Platinum sputtered in oxygen at low voltage; probably mainly di-oxide; (f) Sputtered platinum, (111) orientation . . . . .	128
VI. (a) Etched silver crystal, cube face, beam parallel to cube edge; (b) Diamond, natural (111) face; (c) Rock-salt, cleavage face; (d) Etched zinc blende, (110) face, beam parallel to cube-face diagonal ( <i>Finch</i> ) . . . . .	144
VII. (a) Oriented $\text{PbO}$ on molten lead ( <i>Jenkins</i> ); (b) Cobalt deposit on copper single crystal, (110) face, beam parallel to cube edge; (c) Thin silver deposit on copper single crystal, (110) face, beam parallel to cube-face diagonal . . . . .	172
VIII. (a) Polished gold, reflection; (b) Polished gold, transmission; (c) Nickel deposit on copper crystal, (110) face, beam parallel to cube-face diagonal; (d) Lard ( <i>Murison</i> ); (e) Vaseline ( <i>Murison</i> ); (f) Stearic acid ( <i>Murison</i> ) . . . . .	190
IX. (a) Anthracene ( <i>Finch</i> ); (b) Polished graphite ( <i>Jenkins</i> ); (c) Comparison photograph, graphite and gold ( <i>Finch</i> ); (d) Spinel fracture ( <i>Finch</i> ) . . . . .	210
X. (a) Mica powder ( <i>Finch</i> ); (b) Paraffin, $\text{C}_{32}\text{H}_{66}$ ( <i>Finch</i> ); (c) Rotation photograph from zinc blende cleavage face ( <i>Miyake</i> ); (d) $\text{CCl}_4$ vapour ( <i>Wierl</i> ) . . . . .	252



## CHAPTER I

### GENERAL THEORY OF WAVES

IN this chapter will be given some of the fundamental properties of wave motion which will be needed later on. The treatment of wave motion in elementary textbooks of physics, and even in some that are fairly advanced, is usually so simplified that points of considerable importance for our purposes fail to appear at all.

It is not an easy matter to define wave motion with generality and precision. Even the mathematical definition of it as the solution of a differential equation is open to objection, for there are several modifications of the usual form which are equally well entitled to be considered wave equations. It seems best to start from familiar instances and show how the conception of what constitutes a wave can be gradually broadened. Fundamentally a wave is an effect which has a definite value at a definite place and time, but in general varies continuously from place to place and from time to time. In one specially important and simple type of wave the variation with time is the same everywhere, and is simple harmonic. Such a wave is called a monochromatic wave. At a single point the effect

$$\psi = a \sin (nt + \delta),$$

where  $a$  is the amplitude,  $n/2\pi$  is the frequency ( $2\pi/n$  is the period) and  $nt + \delta$  will be called the phase. (In some books this name is applied to  $\delta$  alone.) The simplest wave of this type is the plane wave of constant amplitude

$$\psi = a \sin \left( nt \pm \frac{2\pi x}{\lambda} \right), \quad . \quad . \quad . \quad (1)$$

where  $\lambda$  is called the wave-length. Another form is the spherical wave

$$\psi = \frac{c}{r} \sin \left( nt \pm \frac{2\pi r}{\lambda} \right). \quad . \quad . \quad . \quad (2)$$

## 2 THEORY AND PRACTICE OF ELECTRON DIFFRACTION

It should be noted that a monochromatic wave implies the existence of the motion for all values of  $t$  from  $-\infty$  to  $+\infty$ ; thus a wave which has a beginning or an end cannot be strictly monochromatic.

The two cases of waves we have quoted come under the general form

$$\psi = a_{xyz} \sin (nt - \phi_{xyz}), \quad . \quad . \quad . \quad (3)$$

where  $a$  and  $\phi$  are functions of the space coordinates but not of the time. Though this expression includes forms of motion which are not generally classed as waves, it is of interest to examine some general properties of it. We define a wave front as a surface over which  $\phi$  is constant. It is thus a surface of constant phase at a given time. Consider a surface which moves so as always to be a surface of the same constant phase (Fig. 1), *i.e.* such that  $nt - \phi_{xyz} = c$ . As  $t$  changes,  $\phi$  must do

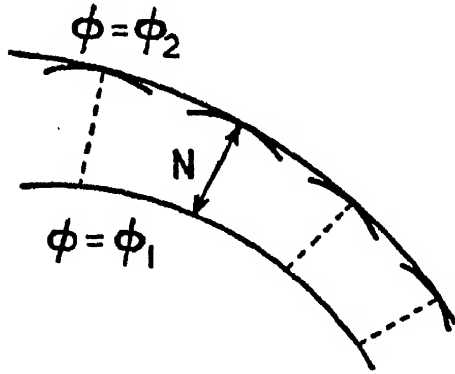


FIG. 1

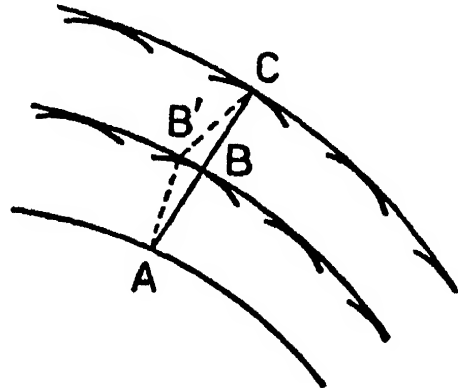


FIG. 2

so too, thus the surface moves. If  $\phi = \phi_1$ ,  $\phi = \phi_2$ , represent two adjacent positions at times  $t_1$  and  $t_2$ , then  $nt_1 - \phi_1 = nt_2 - \phi_2$ , and if  $N$  is the length of the common normal the speed with which the surface  $\phi$  moves normal to itself is

$$\lim_{t_1 \rightarrow t_2} \frac{N}{t_1 - t_2} = \lim_{\phi_1 \rightarrow \phi_2} \frac{Nn}{\phi_1 - \phi_2} = \frac{n}{|\text{grad } \phi|}.$$

We will call this speed ' $v$ ' the phase speed,

$$v = \frac{n}{\left[ \left( \frac{\partial \phi}{\partial x} \right)^2 + \left( \frac{\partial \phi}{\partial y} \right)^2 + \left( \frac{\partial \phi}{\partial z} \right)^2 \right]^{\frac{1}{2}}}. \quad . \quad . \quad (4)$$

Since  $\phi$  is a function of the coordinates,  $v$  will also in general be so. If  $v$  were known, this method would make it possible to determine the way in which a wave front progresses. The well-known Huygens construction involves this idea with the additional assumption that  $v$  is determined only by the properties of the medium, and in particular is a constant if the medium is homogeneous. This assumption is quite unjustified even if the medium is everywhere the same, for  $v$  has been arrived at by a kinematic, not a dynamic argument. However, for the two simple types of waves quoted above it is easy to see that  $v = n\lambda/2\pi$  and is therefore constant. Though generally regarded as a wave theorem, Huygens' construction (for isotropic media) implies nothing not already given by geometrical optics. It is well known that these can be summed up in Fermat's principle that the path of a ray is such that the time taken for the light to go along it is a maximum or minimum as compared with any adjacent possible path between the two points. Since the Huygens wavelets represent the distances travelled by the light in equal times, a line drawn everywhere normal to their envelope will have the Fermat property, and be a geometrical ray, ABC and AB'C (Fig. 2) differing only to the second order of small quantities. Thus Huygens wave fronts are no more than a set of surfaces orthogonal to the geometrical rays.

It is best at this point to start a different line of argument. The typical expressions (1) and (2) for  $\psi$  which we have given satisfy a differential equation of the form

$$\frac{\partial^2 \psi}{\partial x^2} + \frac{\partial^2 \psi}{\partial y^2} + \frac{\partial^2 \psi}{\partial z^2} = \frac{1}{V^2} \frac{\partial^2 \psi}{\partial t^2}, \quad (5)$$

where the wave velocity  $V$  is written for  $n\lambda/2\pi$ . This equation is often spoken of as the wave equation *par excellence*, though, as we shall see, other forms are also used. If  $V$  is a constant, the simplest case, all plane waves of constant amplitude are propagated with equal speed, and it is easy to see that for such waves  $v = V$ . The same is true for the type of spherical waves considered above.

If we agree to consider any solution of the above equation as a wave, it is at once seen that such waves can be superposed. For if  $\psi_1$ ,  $\psi_2$  are two solutions,  $\psi_1 + \psi_2$  is also a solution. This

#### 4 THEORY AND PRACTICE OF ELECTRON DIFFRACTION

principle of superposition is not exactly true for real waves of finite amplitude in material media; in water waves it ceases to be true for waves of quite moderate amplitude compared with their length, and even for sound ceases to hold for violent sounds, such as those due to explosions. There is, however, no evidence at present to suggest that it fails for any of the types of light wave, or for the electron waves with which this book chiefly deals, and the agreement with experiment of theoretical calculations based on this assumption is extremely exact in the case of visible light. We must, however, be prepared to consider  $V$  as a function of the coordinates and even sometimes of the time.  $V$  is known as the wave velocity. When  $V$  is a constant, a mathematical theorem due to Kirchhoff<sup>1</sup> shows that if  $\psi$  satisfies differential Equation (5) the value of  $\psi$  at any place and time,  $\psi(x_0y_0z_0, t_0)$ , is determined by the values of  $\psi$  taken over a closed surface surrounding  $x_0y_0z_0$ ,<sup>2</sup> and calculated at a time  $t_0 - r/V$ , where  $r$  is the distance from the element of the surface to the point  $x_0y_0z_0$ , together with the values of

$$\frac{\partial \psi(x_0y_0z_0, t_0 - r/V)}{\partial x}, \quad \frac{\partial \psi(x_0y_0z_0, t_0 - r/V)}{\partial y}, \quad \frac{\partial \psi(x_0y_0z_0, t_0 - r/V)}{\partial z},$$

over the same surface. The surface must be drawn so as not to contain any singularities such as sources or sinks of energy. Physically this theorem means that the equation represents a motion which is propagated everywhere with speed  $V$ , so that the condition at a point is determined by the conditions at distant points at an earlier time, the time interval being that required for the effect to travel between the two points with speed  $V$ . This theorem is the mathematical justification for the Fresnel treatment of diffraction problems, but it is not a complete justification. The argument runs thus. The effect at a point  $P$  (Fig. 3) can be calculated from the known effects over the surface  $ABC$ , which is supposed continued to infinity so as to surround  $P$  with a hemisphere at infinity. The effect of the hemisphere is neglected because the phases of the dis-

<sup>1</sup> For a proof of this theorem see Drude's *Optics*, p. 179 (Longmans, Green & Co., New York, 1913).

<sup>2</sup> Here, and elsewhere, when no confusion is likely to arise, coordinates are written without commas or parentheses.

turbance at points on it will be distributed at random and will cancel. Thus the effect at P appears as an integral taken over the surface ABC. The integral actually is

$$\int \frac{dS}{4\pi} \left[ \cos(N, r) \frac{\partial}{\partial r} \left( \frac{\psi(t - r/V)}{r} \right) - \frac{1}{r} \frac{\partial}{\partial N} \psi(t - r/V) \right],$$

where N is the normal to the surface ABC.

If ABC is a plane (it is to be remembered that it is an arbitrary surface, not even necessarily a wave front), and if the wave system is one of plane waves parallel to it, given by  $\psi = a \sin(nt - 2\pi x/\lambda)$ , the integrand for large values of  $r$  becomes

$$\frac{a}{2\lambda r} (1 + \cos \theta) \cos \left( nt - \frac{2\pi r}{\lambda} \right),$$

where  $\theta$  is the angle between  $r$  and the normal to the wave front. Fresnel's diffraction theory is equivalent to assuming that, if part of the wave is blocked by an obstacle in the plane ABC, the remainder will continue to produce an effect at P corresponding to the above expression, so that the total effect is obtained by integrating the expression over the part of ABC which has not been

blocked out. This assumption is in fact inexact; it would imply a displacement which changes discontinuously near the screen and so is not a solution of the original differential equation. It is thus inconsistent with the original starting point of the argument. It appears, however, from the few cases in which an exact solution of the wave equation with suitable boundary conditions is possible, that the Fresnel approximation is extremely close except within a few wavelengths of the screen. As is well known, it is in excellent agreement with the experiments.

A similar differential equation can be used as the definition of waves when V is a function of  $xyz$ . In such a case Kirchhoff's theorem will break down, but unless V varies

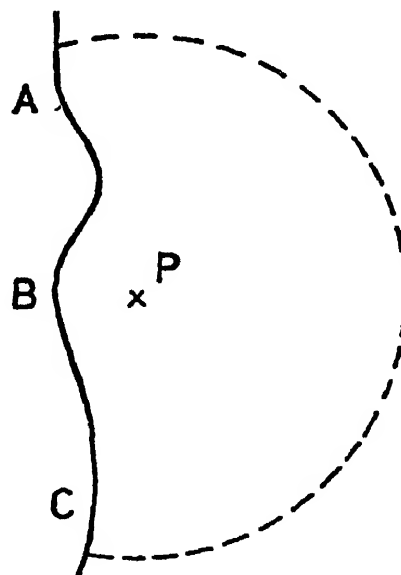


FIG. 3

## 6 THEORY AND PRACTICE OF ELECTRON DIFFRACTION

appreciably in a wave-length the same general idea of propagation from point to point will continue to hold.

The form  $\psi = a \sin (nt - \phi)$  is equivalent to  $\psi = ae^{i(nt - \phi)}$ , where the imaginary part is to be taken at the end. Substituting in

$$\nabla^2 \psi = \frac{1}{V^2} \frac{\partial^2 \psi}{\partial t^2}$$

and equating real and imaginary parts, we find

$$a \nabla^2 \phi + 2 \sum_{xyz} \frac{\partial a}{\partial x} \frac{\partial \phi}{\partial x} = 0$$

and

$$\nabla^2 a - a \sum_{xyz} \left( \frac{\partial \phi}{\partial x} \right)^2 = - \frac{n^2}{V^2} a.$$

If  $a$  is constant these reduce to

$$\nabla^2 \phi = 0 \quad \text{and} \quad V^2 = \frac{n^2}{\sum_{xyz} \left( \frac{\partial \phi}{\partial x} \right)^2},$$

*i.e.*  $V = v$ . In such a case we can write

$$\psi = c \sin n \left( t - \int \frac{dr}{V} \right),$$

since

$$v = \frac{n}{\partial \phi / \partial r},$$

where  $r$  is the normal to the wave front. Thus  $\psi$  is fully determined by conditions along a line. This line, which is always normal to the wave front, may be called a ray and the circumstances of the motion may be expressed in terms of geometrical optics, successive wave fronts being determined by Huygens' construction. This will occur even when  $a$  is variable if  $\nabla^2 a = 0$ , an instance being the spherical wave for which  $a = 1/r$ . We see, then, that in order that the waves should contain information which could not be obtained by geometrical optics, it is necessary that their amplitude should be variable and should not satisfy Laplace's equation. If  $a$  is known, the equation

$$a \nabla^2 \phi + 2 \sum_{xyz} \frac{\partial a}{\partial x} \cdot \frac{\partial \phi}{\partial x} = 0$$

is a restriction on  $\phi$  showing that the original assumption  $\psi = a \sin (nt - \phi)$  is too general to be a solution of the differential equation. Notice that this condition does not contain  $V$ .

In considering the difference between  $V$  and  $v$ , it should be remembered that the former is regarded as a physical property of the medium at the given time and place, while the latter is defined from the kinematics of an assumed wave and may be different for different waves at a given place, even if the frequency is kept constant.

Still assuming that the waves are solutions of

$$\nabla^2 \psi = \frac{1}{V^2} \frac{\partial^2 \psi}{\partial t^2},$$

two important cases arise according as  $V$  does or does not depend upon the frequency. As is well known, in many cases waves travel at speeds which vary with the frequency of the waves. This is so for water waves, and for light waves in a dispersive medium. We shall see that it is true also for electron waves.

Now the most general effect at any given place can be represented over a limited period of time by a series of sines and cosines — a Fourier series. Thus

$$\begin{aligned} \psi(t) = & a_1 \sin \frac{t\pi}{T} + a_2 \sin \frac{2t\pi}{T} + \dots + a_m \sin \frac{mt\pi}{T} + \dots \\ & + b_0 + b_1 \cos \frac{t\pi}{T} + b_2 \cos \frac{2t\pi}{T} + \dots + b_m \cos \frac{mt\pi}{T}, \quad (6) \end{aligned}$$

where the expression is valid between  $t = -T$  and  $t = T$ . If the time interval is made very large, from  $-\infty$  to  $+\infty$ , the series passes into a Fourier integral which may be regarded as meaning that the effect can be regarded as the sum of a number of vibrations of all possible periods. The amplitude corresponding to any period, or rather to any infinitesimal range of periods, depends on the form of the function of the time which the integral is to represent. The Fourier integral is usually written

$$\psi(t) = \frac{1}{2\pi} \int_{-\infty}^{\infty} \psi(\kappa) d\kappa \int_{-\infty}^{\infty} \cos \alpha(\kappa - t) d\alpha$$

and, on expanding,

$$\psi(t) = \int_{-\infty}^{\infty} f_1(\alpha) \sin \alpha t d\alpha + \int_{-\infty}^{\infty} f_2(\alpha) \cos \alpha t d\alpha, \quad (7)$$

where  $f_1(\alpha)$ ,  $f_2(\alpha)$  are functions of  $\alpha$ . The analogy between (7) and the Fourier series (6) is readily apparent. We can now write down an expression for a plane wave of any form. Consider

$$\begin{aligned} \psi(x, t) = \int_{-\infty}^{\infty} F_1(\lambda) \sin \frac{2\pi}{\lambda}(x - Vt) d\lambda \\ + \int_{-\infty}^{\infty} F_2(\lambda) \cos \frac{2\pi}{\lambda}(x - Vt) d\lambda. \quad (8) \end{aligned}$$

Clearly it satisfies the wave equation (5). When  $t=0$  it represents the most general expression in  $x$ , the  $\alpha$  of Fourier's integral (7) being replaced by  $2\pi/\lambda$  and  $x$  substituted for  $t$ . If  $x$  and  $t$  increase so that  $x - Vt$  is constant, the expression is unchanged; hence, if the origin of  $x$  is shifted to the right with velocity  $V$ , the expression is a function of  $x$  only. It is thus a disturbance moving with velocity  $V$  without change of form. Clearly this argument only holds if  $V$  is independent of  $\lambda$ , or, in other words, of the frequency. Thus, if  $V$  is constant, a plane wave of any form can be propagated unchanged.

It should be noticed that this constancy of form has only been proved for infinite plane waves. If, for example, there is diffraction, the waves of different wave-length will be treated differently and there will be more or less sorting out of the waves. This is of course what happens when white light is analysed by a diffraction grating. When  $V$  is a function of  $\lambda$ , even a plane wave will not travel unchanged unless it happens to be of simple sine curve form or in one or two other quite exceptional cases. The medium in this case is said to be dispersive, and it is important to consider the kind of changes which occur in waves transmitted in such a medium.

Take first a disturbance represented by the sum of two simple waves A and B of equal amplitude and nearly the same frequency (Fig. 4). We have

$$\begin{aligned} \psi &= a \sin (nt - 2\pi x/\lambda) + a \sin (n't - 2\pi x/\lambda') \\ &= 2a \sin (nt - 2\pi x/\lambda) \cos \left\{ t \frac{n - n'}{2} - \pi x (1/\lambda - 1/\lambda') \right\} \end{aligned}$$

approximately. This is the well-known expression for 'beats' in sound and can be regarded as representing a wave C (Fig. 4)

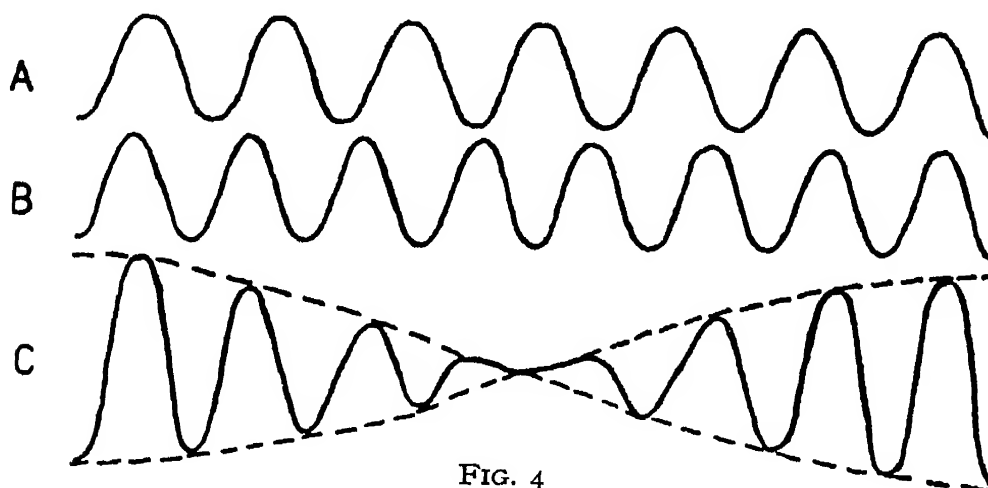


FIG. 4

whose intensity slowly varies. The intensity factor is in form a wave, and the velocity of this 'wave of amplitude' is

$$\frac{n - n'}{2\pi/\lambda - 2\pi/\lambda'} = -\lambda^2/2\pi \cdot \frac{dn}{d\lambda}$$

in the limit. Since

$$\frac{n}{2\pi} = \frac{V}{\lambda'}$$

this can also be written

$$V - \lambda \frac{dV}{d\lambda}.$$

If the phase is written  $nt - mx$  it assumes the simple form  $dn/dm$ . This is known as the group velocity and plays a very important part in the study of waves in a dispersive medium. We shall denote it by  $U$ .

The two waves of nearly the same wave-length form what is called a group and the group velocity is the velocity with which a peculiarity associated with the group, such as a maximum of amplitude, will advance. The group velocity may be quite different from the wave velocity. For example, in the case of gravity waves on the surface of deep water it is just half the wave velocity. A rather more general kind of group is one formed of waves whose wave-length varies continuously over a small range of wave-length  $\delta\lambda$ . Such a group

has only one maximum of amplitude when all the component waves are in phase, but if  $\delta\lambda$  is very small the amplitude will vary very slowly on both sides of this point. For many approximate calculations it is more convenient to regard an irregular disturbance as composed of a large number of such elementary groups than as analysed into its primary Fourier components. Thus, consider the spreading of a splash over the surface of water. If surface tension is neglected,

$$V = \left(\frac{g\lambda}{2\pi}\right)^{\frac{1}{2}}, \quad U = \frac{1}{2}V.$$

Take the Fourier analysis first. The irregular splash can be analysed into Fourier components, to each of which corresponds a wave of different wave-length. Initially these waves are all in phase at the origin of the splash, but get out of step and cancel farther out. As time goes on the waves are propagated with different velocities. At any given place and time most of them have phases distributed at random and so cancel, but there will be a certain range of wave-lengths which are nearly in phase, because the initial 'out-of-stepness' due to their varying wave-length is just balanced by that due to their varying speed. But these are precisely the waves whose group velocity has carried them from the origin, where all were initially in phase, to the point in question at the given time. Thus the predominant effect is due to a certain group. The condition for stationary phase at a distance  $x$  and time  $t$  is clearly

$$tn - \frac{2\pi x}{\lambda} = tn' - \frac{2\pi x}{\lambda'} \quad \text{or} \quad x/t = \text{Lt} \frac{n - n'}{2\pi/\lambda - 2\pi/\lambda'} = U.$$

Thus  $x = Ut$ , and we can find what group will be the prominent one at a given place and time by finding the velocity  $x/t$  with which it must have moved and using the expression

$$U = \frac{1}{2} \left(\frac{g\lambda}{2\pi}\right)^{\frac{1}{2}}$$

to find  $\lambda$ . Such a treatment is of course approximate only; a truly elementary group, for which  $\delta\lambda$  is infinitesimal, is

infinite in length, but the treatment becomes more and more exact the larger  $x$  and  $t$ .

The actual wave-crests move with the speed  $V$ , twice as fast as the group, and their motion is an accelerated one for they are continually getting to places where the predominant wave-length of the group is longer, and both wave and group speed is greater.

The idea has been expressed mathematically by Lord Kelvin. In an integral of the type

$$\psi = \frac{1}{2\pi} \int_0^\infty f(m) e^{i(nt - mx)} dm,$$

where  $f(m)$  varies slowly with  $m$ , the only important parts are those for which the phases of the exponentials agree, otherwise they vary nearly evenly from 0 to  $2\pi$  and the terms corresponding to them cancel out. This means that  $nt - mx$  is stationary for varying  $m$ , therefore  $t \frac{dn}{dm} - x = 0$ . But  $U = \frac{dn}{dm}$ , hence  $U = x/t$  as before, and the groups move out with their group velocity.

## CHAPTER II

### DE BROGLIE'S WAVE MECHANICS

DURING the first quarter of this century several difficulties had arisen in atomic physics. The chief of these were : the difficulty of reconciling the photo-electric effect with the facts of interference ; the arbitrary nature of the hypotheses required to give Planck's equation ; and a growing conviction that, in spite of its great successes, the Bohr-Sommerfeld theory was inadequate to account for some of the spectroscopic results even with the additional hypothesis of electronic spin.

The publication of L. de Broglie's doctor's thesis <sup>1</sup> in 1924, and a paper by him in the *Philosophical Magazine* of the same year, were the first signs of a satisfactory way out of these difficulties.<sup>2</sup> De Broglie started from the idea that Einstein's equation  $E = h\nu$  represents a fundamental relation between energy and frequency. By the theory of relativity a particle of resting mass  $m_0$  has associated with it energy  $m_0c^2$ , where  $c$  is the velocity of light, and should therefore have an inherent frequency  $\nu_0 = \frac{m_0c^2}{h}$ . De Broglie regarded this as the frequency of a pulsation in the space surrounding the particle. We may write this as  $\psi = a \sin 2\pi\nu_0 t_0$ , leaving it for the moment an open question whether  $a$  is a function of the coordinates or not ;  $t_0$  is the time measured for an observer at rest with the particle. Now suppose the particle to move with velocity  $u$  along the  $x$  axis. We find on applying the Lorentz transformation

$$\psi = a \sin \frac{2\pi\nu_0}{(1 - u^2/c^2)^{\frac{1}{2}}} \left( t - \frac{ux}{c^2} \right),$$

where  $t$  and  $x$  refer to the new axes. This expression is a wave if  $a$  is a constant and in some cases when it is not (p. 6).

<sup>1</sup> L. de Broglie, *Dissertation* (Masson, Paris, 1924).

<sup>2</sup> De Broglie, *Phil. Mag.* 47, p. 446 (1924) ; *Ann. de phys.* 3, p. 22 (1925) ; De Broglie and Brillouin, *Wave Mechanics* (Blackie, London, 1928).

The frequency is

$$\nu = \frac{\nu_0}{(1 - u^2/c^2)^{\frac{1}{2}}} = \frac{m_0 c^2}{h(1 - u^2/c^2)^{\frac{1}{2}}} = \frac{mc^2}{h},$$

where  $m$  is the apparent mass relative to the new axes, thus the relation  $E = h\nu$  remains true. We may write

$$\psi = a \sin 2\pi\nu(t - x/V),$$

where  $V = c^2/u$  is the wave velocity. It is clearly greater than the velocity of light. This is apparently contradictory to the principle of relativity that no signal can be transmitted faster than light. The contradiction is only apparent, however, for the transmission of a signal by waves is analogous to the case of a sudden disturbance of water considered in the last chapter, and we have seen that it is the group velocity which determines how fast the disturbance of a given wave-length will spread. Let us find the group velocity; it is the relation between  $x$  and  $t$  when the phase is stationary for varying frequency, *i.e.* varying  $u$ .

$$\text{Thus} \quad t \cdot \frac{d\beta}{du} - \frac{x}{c^2} \frac{d(\beta u)}{du} = 0, \quad \text{where} \quad \beta = \frac{1}{(1 - u^2/c^2)^{\frac{1}{2}}}.$$

The group velocity

$$U = \frac{x}{t} = \frac{c^2 \cdot d\beta/du}{\beta + u \cdot d\beta/du}, \quad \text{but} \quad \frac{d\beta}{du} = \frac{\beta u}{c^2 - u^2},$$

$$\text{therefore} \quad U = \frac{c^2 u / (c^2 - u^2)}{1 + u^2 / (c^2 - u^2)} = u.$$

The group velocity is thus the speed of the particle, which of course never exceeds that of light. The wave-length  $\lambda$  of the plane wave is given by

$$\lambda = \frac{V}{\nu} = \frac{c^2}{u\nu} = \frac{mc^2}{mu\nu} = \frac{h}{mu},$$

where  $m$  is the apparent mass. Since  $mu$  is the momentum, even on the relativity mechanics,  $\lambda$  is  $h/(\text{momentum})$ . If we eliminate  $u$  between the expressions for  $\lambda$  and  $V$ , remembering that  $m$  is a function of  $u$ , we find

$$V^2 = c^2 + \frac{\lambda^2 m_0^2 c^4}{h^2}.$$

Thus the waves show dispersion (as they must since the wave and group speeds are different), and in the sense of normal optical dispersion or of that of gravity water waves. The waves go through the group which constitutes the electron, from behind with great speed; but at present the picture is incomplete because, though we have calculated a group velocity, our wave expression is still that of an endless monochromatic wave which, at least when  $\alpha$  is constant, has no variation in amplitude and does not constitute a group. The result must be regarded as tentative and requires to be generalised. This is done by invoking de Broglie's second main idea, which is that the waves act as a guide for the particles and determine their motion. The ordinary Newtonian mechanics, or rather their relativistic generalisation, are thus to be replaced by laws which involve the conception of waves.

We have seen that wave motion degenerates into ray motion when  $v = V$ . In such a case Huygens' construction holds in the simple form and from it can be deduced Fermat's principle that

$$\delta \int_A^B \frac{ds}{V} = 0.$$

It was pointed out by Hamilton that this principle has a close mechanical analogue, for the Newtonian mechanics of a single particle in a conservative field of force can be summed up in the condition

$$\delta \int_A^B m u \, ds = 0.$$

The integral is called the 'action' and is denoted by  $S$ . If we take for  $V$  the expression found above, namely  $c^2/u$ , Fermat's principle becomes

$$\delta \int_A^B \frac{u}{c^2} ds = 0;$$

writing  $E = mc^2$ , this gives

$$\delta \int_A^B \frac{mu}{E} ds = 0;$$

for a particle moving in a conservative field  $E$  is constant and the above is equivalent to the action equation. Thus in the special cases in which waves of the type considered above

are equivalent to rays, these rays are the possible Newtonian trajectories of the particle for different initial conditions. We may, therefore, hope that in the generalised case, in which a translation into geometrical optics is no longer possible, the waves we have considered will continue to tell us something about the motion of the particles.

We wish to obtain a wave equation of the form

$$\frac{\partial^2 \psi}{\partial x^2} + \frac{\partial^2 \psi}{\partial y^2} + \frac{\partial^2 \psi}{\partial z^2} \equiv \nabla^2 \psi = \frac{1}{V^2} \frac{\partial^2 \psi}{\partial t^2}. \quad (1)$$

If  $\psi$  is to vary with the time as  $e^{i2\pi\nu t}$ , we have

$$\nabla^2 \psi = -\frac{4\pi^2\nu^2}{V^2} \psi.$$

Now

$$V = \frac{c^2}{u} = \frac{mc^2}{mu} = \frac{h\nu}{mu}.$$

On the relativity mechanics

$$E = \frac{m_0 c^2}{(1 - u^2/c^2)^{\frac{1}{2}}} + F,$$

where  $F$  is the potential energy, while

$$mu = \frac{m_0 u}{(1 - u^2/c^2)^{\frac{1}{2}}}.$$

Solving for  $u$  in the first equation and substituting, we get

$$mu = \frac{1}{c} [(E - F)^2 - m_0^2 c^4]^{\frac{1}{2}}. \quad (2)$$

In ordinary mechanics we have  $E' = F + \frac{1}{2}mu^2$  giving

$$mu = [2m_0(E' - F)]^{\frac{1}{2}}. \quad (3)$$

The equations thus become

$$\nabla^2 \psi + \frac{4\pi^2}{h^2 c^2} [(E - F)^2 - m_0^2 c^4] \psi = 0 \quad (4)$$

for relativity, and

$$\nabla^2 \psi + \frac{8\pi^2 m_0}{h^2} (E' - F) \psi = 0 \quad (5)$$

for ordinary mechanics. It should be noticed that the value which this last equation gives for the wave velocity if  $F = 0$  is

$$\frac{h\nu}{mu} = \frac{\frac{1}{2}mu^2}{mu} = \frac{1}{2}u.$$

The omission of the 'energy of constitution'  $m_0c^2$  has entirely altered the wave speed, but the wave-length is still  $h/mu$  where we no longer distinguish between  $m$  and  $m_0$ .

One reason for choosing  $h\nu/mu$  as the expression for  $V$  instead of, for example,  $c^2/u$ , is that it corresponds to a relativistic generalisation of the original equation  $E = h\nu$ . It is well known that associated with an energy in relativity is a momentum, the whole forming a 'four-vector', while associated with a frequency are three space components; we can take these as proportional to the component wave numbers along the axes. We have, in fact, as one four-vector  $(E/c, mu)$  and as another  $(\nu/c, 1/l)$  where  $l$  is some length. If this is taken as a wave-length there will be a corresponding wave velocity  $V'$  such that  $\nu/V' = 1/l$ . Now the time component of the first of these four-vectors is  $h$  times that of the second. It is reasonable to suppose that the same relation holds between the space components. This means  $mu = h\nu/V'$ , which, if  $V' = V$ , is the relation we have used.

The wave equation we have obtained is sufficiently generalised to cover any case of the motion of a particle of known energy in a field of force determined by a scalar potential. It does not, as yet, include the effects of magnetic fields. But we have still to consider in what way the motion of the particle is connected with the wave in those cases where the waves are not such as to be equivalent to geometrical optics, and these are of course precisely the cases in which we are interested, for it is here that we may hope for new results not predicted by the older dynamics. It may be noticed at the start that since  $\lambda = h/mu$  the wave mechanics will give results indistinguishable from Newtonian mechanics as  $h/mu$  becomes indefinitely small, *i.e.* for heavy bodies and large speeds, for it is well known that wave optics approaches geometrical optics as a limit as the wave-length becomes indefinitely small. De Broglie suggested that the electron is

a point singularity in the wave.<sup>1</sup> But the interpretation now generally accepted is that made by Schrödinger, to whom Equation (5) is due and who has used it with great success in the investigation of the stationary state of atoms. He takes  $|\psi|^2$  as a measure of the 'electric density'. For a single electron this is nearly equivalent to saying that the same quantity measures the probability per unit volume of the presence of the electron at any point.<sup>2</sup> Schrödinger also has modified the equation so as to eliminate the energy, and obtains a form which should hold for all particles of the given mass in the given potential field. In the equation

$$\nabla^2\psi + \frac{8\pi^2m_0}{h^2}(E' - F)\psi = 0,$$

$\psi$  varies with the time according to the factor  $e^{i\frac{2\pi}{h}E't}$ , thus

$$E'\psi = \frac{h}{2\pi i} \frac{\partial\psi}{\partial t},$$

and making this substitution we have

$$\nabla^2\psi - \frac{8\pi^2m_0}{h^2}F\psi = \frac{i4\pi m_0}{h} \frac{\partial\psi}{\partial t}. \quad (6)$$

As long as  $\psi$  varies as  $e^{i\frac{2\pi}{h}E't}$  this is mathematically identical with the last equation, but it is a more convenient form because it is a single equation which holds whatever the energy of the particle may be, while the former is a family of equations each valid for one particle frequency (or energy). The latter equation has also been assumed to hold in cases when  $F$  includes the time explicitly, for example, when an electron in an atom is disturbed by the field of an electromagnetic wave. It would be unreasonable to make such a generalisation in the former equation, for in a case like this the energy of the electron is not constant.

It has been pointed out by de Broglie<sup>3</sup> and others that one can arrive at the above equations by a formal process which gives an easy generalisation to the case of problems

<sup>1</sup> L. de Broglie, *J. Phys.* 7, p. 321 (1926).

<sup>2</sup> The 'probability' interpretation was first introduced by Born (*Zeits. für Phys.* 38, p. 803, 1926) in his wave-mechanical treatment of the scattering of electrons by single atoms.

<sup>3</sup> De Broglie, *J. Phys.* 7, p. 31 (1926).

involving more than one particle. Write the equation of energy in the form  $E = H(xyzp_xp_y p_z)$ , where  $H$  is expressed as a function of the coordinates (which, however, must be rectangular) and their conjugate momenta  $p_xp_y p_z$ , and  $E$  is the numerical value of the energy. Form an operator by replacing  $p_x$  by  $\frac{h}{2\pi i} \frac{\partial}{\partial x}$ , and so on; then the equation in the form containing  $E$  is given by

$$H\left(xyz \frac{h}{2\pi i} \frac{\partial}{\partial x} \dots\right)\psi = E\psi,$$

and that in the general form by writing

$$H\left(xyz \frac{h}{2\pi i} \frac{\partial}{\partial x} \dots\right)\psi = \pm \frac{h}{2\pi i} \frac{\partial \psi}{\partial t}, \quad (7)$$

where either sign may be taken. Since the function  $H$  is the well-known Hamiltonian expression for the energy, this can be generalised directly to any number of particles. For two electrons, for example, the change consists in replacing  $\nabla^2\psi$  by

$$\left(\frac{\partial^2}{\partial x_1^2} + \frac{\partial^2}{\partial y_1^2} + \frac{\partial^2}{\partial z_1^2} + \frac{\partial^2}{\partial x_2^2} + \frac{\partial^2}{\partial y_2^2} + \frac{\partial^2}{\partial z_2^2}\right)\psi,$$

where  $(x_1y_1z_1)$  and  $(x_2y_2z_2)$  are the coordinates of the two electrons. The solution for  $\psi$  is thus a function of six coordinates and the 'waves' cannot be described in three-dimensional space. The solution cannot even, in general, be expressed as the product of a function of  $(x_1y_1z_1)$  alone into one of  $(x_2y_2z_2)$  alone.

The presence of ' $i$ ' in the general wave equation raises some curious points. We are not concerned here, as in the usual oscillation problem, with the real part of  $\psi$  but rather with its modulus. Corresponding to any  $\psi$  is a conjugate  $\psi^*$  which is a solution of the equation with the other choice of the ambiguous sign;  $\psi\psi^* = |\psi|^2$  is the quantity which, following Schrödinger, we shall use as expressing a physical reality. In Chapter V we shall consider the occurrence of imaginaries.

Now that we have an equation which is not limited to monochromatic waves, we can envisage the electron as a group formed of waves of nearly but not quite the same frequency.

If the frequency range continuously over a small finite range, such a group will have a prolonged, but finite, region of large amplitude and on each side will tail away to zero. Owing to the great difference in wave and group velocities fresh waves are always entering the group from behind, and disappearing at its front edge. As the group advances it grows longer, for the different elementary groups composing it spread out owing to their difference in speed. The group is not strictly monochromatic and the wave-length varies slightly from point to point, but as the group spreads the variation grows less and less. The speed with which that part of the group advances, whose wave-length differs from  $\lambda$  by less than some assigned small quantity, is  $u$  where  $\lambda = h/mu$ . If  $\lambda$  refers to the main central portion of the group,  $u$  is the speed of the particle to which the group most nearly corresponds.

### Refractive Index

The wave velocity is  $V = c^2/u$ . If the particle is accelerated,  $V$  changes and the corresponding waves will change from a nearly monochromatic wave corresponding to one value of  $V$  to one corresponding to another. Now

$$V = \frac{c^2}{u} = c^2 \left( \frac{m}{2T} \right)^{\frac{1}{2}},$$

where  $T$  is the kinetic energy and relativity is neglected. For a conservative field of force

$$T = E' - F \text{ and } V = c^2 \left[ \frac{m}{2(E' - F)} \right]^{\frac{1}{2}}.$$

This gives a second type of dispersion, one which depends on  $F$ . We may express the result by saying that a field of force of potential energy  $F$  has a refractive index for a particle of energy  $E'$  given by

$$\mu = \left( 1 - \frac{F}{E'} \right)^{\frac{1}{2}}.$$

The same result can be obtained from Equation (5) by comparing it with  $\nabla^2 \psi = \frac{1}{V^2} \frac{\partial^2 \psi}{\partial t^2}$ .

# CHAPTER III

## ELEMENTARY THEORY OF WAVE DIFFRACTION BY CRYSTALS

As most of the experiments with which we shall be concerned in the following chapters deal with the diffraction of electron waves by crystals, it seems desirable to include here some account of the theory of crystal diffraction as worked out for X-rays. No attempt is made to deal fully with this subject in the present chapter: we shall consider only those results which are required for our immediate purpose.

A crystal may be defined as a solid whose structure repeats itself periodically in each of three dimensions. The smallest element from which the whole structure can be built by a mere process of repetition is called the 'unit cell'. This 'unit cell' can always be taken as a parallelepiped. If a number of these parallelepipeds are placed together as in the crystal, their corners form a three-dimensional array of points called the 'crystal lattice'. The lattice of points can be supposed moved parallel to itself in any way, it being immaterial what point of the repeating pattern is taken as representative of the unit. The cell corresponding to a given point lattice can be drawn in an infinite number of ways. The dotted lines in Fig. 5 show one way, other ways are indicated by the full lines. The unit cell has, necessarily, always the same volume, being the smallest volume from which the crystal can be built by repetition.

Directions parallel to a set of three intersecting edges of a unit cell are called the directions of the crystal axes, and the lengths of these edges are the lengths of the axes. Any possible natural surface of the crystal passes through a set of lattice points called a 'net plane', though many such net planes seldom or never occur as natural surfaces. If the lengths of the axes are  $a$ ,  $b$ ,  $c$ , then the equation of a net plane through lattice points on the axes, at distances  $pa$ ,  $qb$  and  $rc$  from

some lattice point taken as origin is

$$\frac{x}{pa} + \frac{y}{qb} + \frac{z}{rc} = 1. \quad (1)$$

The numbers  $p$ ,  $q$  and  $r$  are of course integers and the axes are in general oblique. If

$$x' = \frac{x}{a}, \quad y' = \frac{y}{b}, \quad z' = \frac{z}{c},$$

the equation of the plane may be written

$$qrx' + rpy' + pqz' = pqr.$$

This may be reduced to  $hx' + jy' + kz' = \text{an integer}$ , where  $h$ ,  $j$ ,  $k$  have no common factor. The integers  $(hjk)$  are known as the

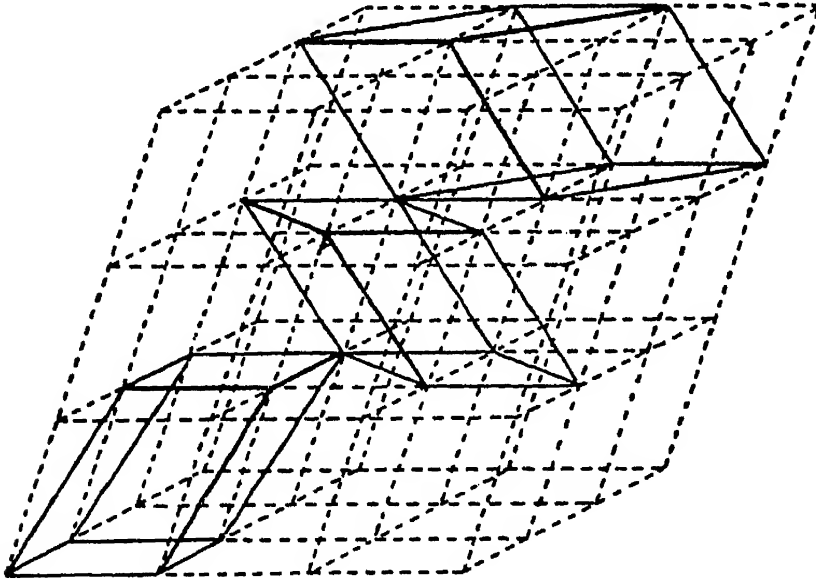


FIG. 5

Miller indices of the set of planes parallel to the above. One of these planes is

$$hx' + jy' + kz' = 1. \quad (2)$$

It is a known algebraical theorem that this equation has an infinite number of solutions in integers for all integral values of  $(hjk)$  prime to each other, negative integers being admitted. The set of planes

$$hx' + jy' + kz' = N \quad (3)$$

clearly has also an infinite number of integral solutions in

$x'y'z'$ , for all integral (and zero)  $N$ , and planes for successive values of  $N$  are equally spaced. Now a point characterised by integral values of  $x'y'z'$  is a lattice point, so that we have a set of equally spaced planes each passing through a (doubly) infinite set of lattice points, the one through the origin being

$$hx' + jy' + kz' = 0, \quad . \quad . \quad . \quad (4)$$

and the next  $hx' + jy' + kz' = 1$  or  $hx/a + jy/b + kz/c = 1$ . Clearly if  $N$  is not an integer, no integral values of  $x'y'z'$  can satisfy the equation. Equation (3) represents the complete set of planes in this direction.

### Diffraction

Each unit cell of the crystal lattice contains the same amount of matter similarly arranged. Suppose that plane

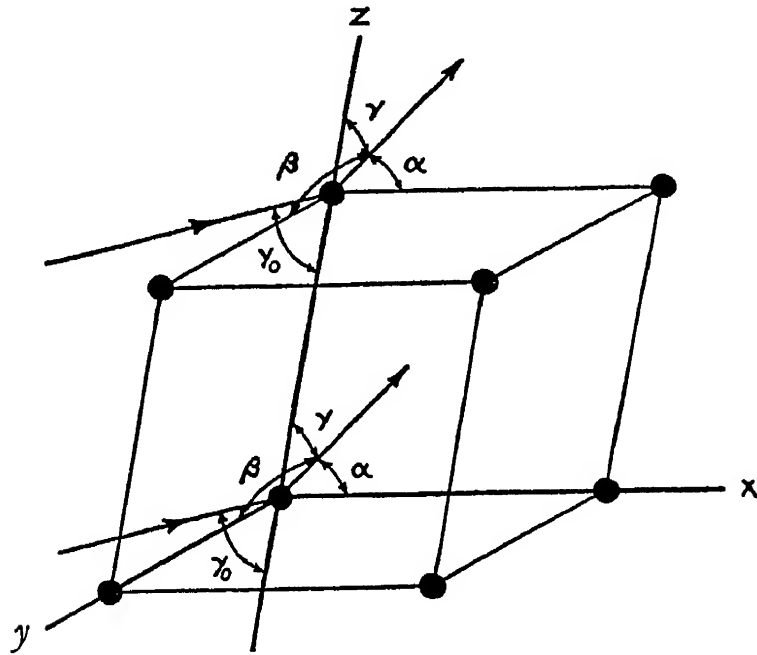


FIG. 6

waves fall on the crystal and that, to take the simplest case first, each unit cell contains one particle capable of scattering the waves. We wish to determine in what directions, if any, the scattered waves will reinforce one another. We may draw the crystal lattice so that the lattice points fall on any part of the pattern of which the crystal is formed. Choose the scattering points as in Fig. 6. Then if the incident wave

normal makes angles,  $\alpha_0, \beta_0, \gamma_0$  with the axes, and we consider parallel scattered rays in a direction with angles  $\alpha, \beta, \gamma$ , the path difference between the rays from the scattering point at the origin and that from the point at  $(a00)$  is  $a(\cos \alpha_0 - \cos \alpha)$ . Similarly the path differences for the rays from  $(0b0)$  and  $(00c)$  are  $b(\cos \beta_0 - \cos \beta)$  and  $c(\cos \gamma_0 - \cos \gamma)$  respectively. The scattered rays are taken as parallel, because we shall be observing effects at a distance from the crystal very large compared with the distance apart of the atoms. If, now, we have simultaneously,

$$\begin{aligned} a(\cos \alpha_0 - \cos \alpha) &= l\lambda, \\ b(\cos \beta_0 - \cos \beta) &= m\lambda, \\ c(\cos \gamma_0 - \cos \gamma) &= n\lambda, \end{aligned}$$

where  $l, m, n$  are integers, and  $\lambda$  is the wave-length of the rays, then the diffracted rays, not merely from the four lattice points which we have considered but from all points of the crystal lattice, will be in phase. For we can proceed from the origin to any point of the lattice by a repetition of steps corresponding to the three axes, and each of these steps is shown by the above equations to involve a path difference of a whole number of wave-lengths. If  $\lambda$  is given and  $\alpha_0, \beta_0, \gamma_0$ , there are three equations for  $\alpha, \beta, \gamma$ ; but these last are not independent, being connected with the angles between the axes by an identical relation, *e.g.* if the axes are rectangular

$$\cos^2 \alpha + \cos^2 \beta + \cos^2 \gamma = 1.$$

Thus, in general there is no solution of the above equations and no diffracted beam with monochromatic waves. If, however, white light is used, a number of solutions become possible, corresponding to different choices of the integers  $lmn$ . These in the case of X-rays form the well-known Laue patterns obtained when 'white' X-rays are passed through a single crystal and received on a photographic plate.

The conditions for a diffracted beam have been expressed in a different and very convenient manner by W. L. Bragg. The path difference between wavelets from the origin and those from  $(x'y'z')$  is

$$\Sigma x'a(\cos \alpha_0 - \cos \alpha) \quad \text{or} \quad \lambda(lx' + my' + nz').$$

This can be zero for integral values of  $x'y'z'$  if  $lmn$  as defined by the above equations are integral, and the locus of  $x'y'z'$  for zero path difference will be the plane

$$lx' + my' + nz' = 0. \quad . \quad . \quad . \quad . \quad (5)$$

Now the condition that the scattered rays, in a certain direction from a number of points in a plane illuminated by parallel light, shall be in phase (path difference *zero*) is that the direction shall be that of the reflected ray as given by

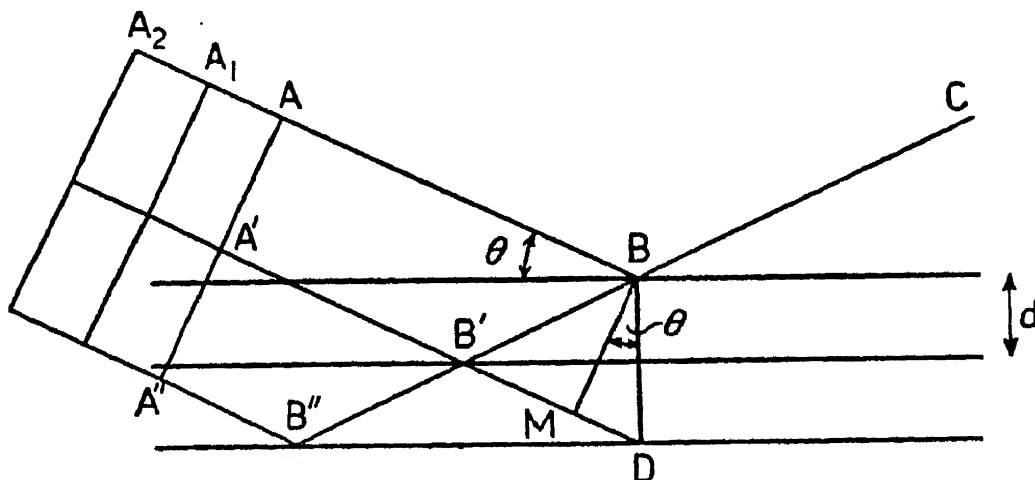


FIG. 7

geometrical optics. This is easily seen from the fact that the Huygens construction gives the law of reflection by a plane.

Conversely, if we take a direction corresponding to reflection from one of the planes of the crystal, all the scattering centres in that plane will be in phase. The same will be true of any parallel plane, and the condition that the whole reinforce reduces to the condition that reflected waves from a series of parallel planes shall strengthen each other. This condition can easily be found. In Fig. 7 let  $BC$  be the reflected ray and  $AB$ ,  $A'B'$ , be incident rays. Let  $AA'A''$  be perpendicular to  $AB$ . The condition is that  $AB + BC + N\lambda = A'B' + B'C$  or  $N\lambda = B'B + A'B' - AB$ . Produce  $A'B'$  to cut the third plane in  $D$  and draw  $BM$  perpendicular to  $A'D$ . Then  $B'D = B'B$  and  $B'B + A'B' - AB = MD = 2d \sin \theta$ , where  $\theta$  is the glancing angle. Thus the condition is

$$2d \sin \theta = N\lambda.$$

This gives the angle at which a crystal plane must be set to give an intense diffracted beam by 'reflection'.

By comparing Equations (4) and (5) we see that the Miller indices ( $hjk$ ) of a Bragg plane are proportional to the Laue numbers  $lmn$  corresponding to the same diffracted beam. If  $lmn$  have a common factor  $N'$  this will be the least number, other than *zero*, to which the expression  $lx' + my' + nz'$  can be equal for integral values of  $x', y', z'$ . It is, therefore, the number of wave-lengths path difference between the atoms in one Bragg plane and those in the one which lies nearest it. Thus  $N'$  is equal to the Bragg  $N$ , the 'order' of the reflection.

To apply the Bragg law we need to know the distance between successive planes. If  $\lambda, \mu, \nu$  are the angles  $yoz, zox, xoy$  between the axes, the length of the perpendicular from the origin on the plane  $hx/a + jy/b + kz/c = 1$  is  $d$ , where

$$d^2 = \frac{1 - \cos^2 \lambda - \cos^2 \mu - \cos^2 \nu + 2 \cos \lambda \cos \mu \cos \nu}{\frac{h^2}{a^2} \sin^2 \lambda + \frac{j^2}{b^2} \sin^2 \mu + \frac{k^2}{c^2} \sin^2 \nu + \frac{2hj}{ab} (\cos \mu \cos \lambda - \cos \nu) + \frac{2jk}{bc} (\cos \mu \cos \nu - \cos \lambda) + \frac{2kh}{ca} (\cos \lambda \cos \nu - \cos \mu)}$$

Bragg's law runs :

$$2 \sin \theta =$$

$$\Lambda \left[ \frac{l^2 \sin^2 \lambda + \frac{m^2}{b^2} \sin^2 \mu + \frac{n^2}{c^2} \sin^2 \nu + \frac{2mn}{bc} (\cos \nu \cos \mu - \cos \lambda) + \frac{2ln}{ca} (\cos \lambda \cos \nu - \cos \mu) + \frac{2lm}{ab} (\cos \mu \cos \lambda - \cos \nu)}{1 - \cos^2 \lambda - \cos^2 \mu - \cos^2 \nu + 2 \cos \lambda \cos \mu \cos \nu} \right]^{\frac{1}{2}},$$

where  $\Lambda$  is written for the wave-length to avoid confusion with the angle, and the 'order'  $N$  is allowed for by writing  $lmn$  for  $N(hjk)$ . For rectangular axes this reduces to

$$2 \sin \theta = \lambda \sqrt{\frac{l^2}{a^2} + \frac{m^2}{b^2} + \frac{n^2}{c^2}},$$

and for cubic axes with cube side  $a$

$$2a \sin \theta = \lambda \sqrt{l^2 + m^2 + n^2},$$

where  $\lambda$  now denotes the wave-length as usual.<sup>1</sup>

<sup>1</sup> In accordance with a convention introduced by W. L. Bragg we shall, after this, replace the symbols ( $hjk$ ),  $lmn$ , by the usual letters for Miller indices ( $hkl$ ) and distinguish between their use as Miller indices and their use as Laue numbers by enclosing them in brackets in the first case, thus: ( $hkl$ ) Miller indices,  $hkl$  Laue numbers. In the preceding analysis it was, of course, necessary to employ distinct sets of symbols.

### Structure Factor

So far we have considered only one scattering point in each unit cell. If there are many, or if there is a continuous distribution of scattering matter, the above analysis gives the condition that the wave scattered by any one point shall reinforce the waves from corresponding points in the other unit cells. The scattered waves from the different points in each unit cell will interfere among themselves, reinforcing in some directions and tending to cancel in others. The resultant intensity will thus be the product of two factors, one of which has maxima, as found above, in directions determined by the crystal axes and the indices  $hkl$ . The other depends on the grouping of the scattering matter in the unit cell. The second factor may cause the entire disappearance of some of the maxima and the weakening of others ; but of course it can never cause a diffraction maximum in a place not given by the above formula.

### Cubic Crystals

While there are comparatively few crystals whose unit cell is a cube, there are a large number which can be represented

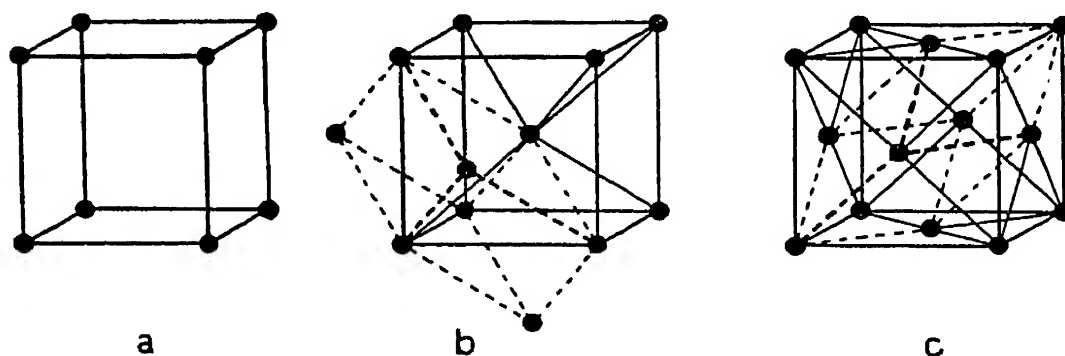


FIG. 8

by equal rectangular axes, by a slight artifice. These are the crystals which belong to the body-centred and the face-centred cubic types. The lattices of these crystals are shown in Fig. 8 (b) and (c), together with the simple cubic lattice at (a). Take Fig. 8 (b) : if we place at the centre of a simple cube a point representing exactly the same atom or group of atoms as that represented by the points at the corners, we obtain a

'body-centred cube'. A lattice made up of these has twice as many points as a simple cubic lattice of the same size.<sup>1</sup> The cube is no longer the unit cell for it contains two units. One way in which a true unit cell can be drawn is shown by the dotted lines (Fig. 8), but it is far more convenient to keep to the rectangular axes, though it means taking into account the interference between the waves scattered by the two units in the cube. For example, take a plane perpendicular to one of the cubic axes. The spacing is no longer equal to the cube edge, but is halved, for other parallel planes can be drawn through the centres of the spheres; these contain the same density of points as the original ones. Hence all the odd orders of reflection from this plane will be destroyed by the interference of the waves from the two kinds of planes. In general if  $hkl$  are Laue numbers corresponding to a certain direction  $\alpha\beta\gamma$ , the path difference between rays from opposite points of a cube diagonal is  $(h+k+l)\lambda$ , and that between the origin and the centre of the cube is  $\frac{1}{2}(h+k+l)\lambda$ . Hence for the centre points to be in phase with the others  $h+k+l$  must be even. The other diffraction maxima will be destroyed by interference.

Fig. 8 shows at (c) a face-centred cube formed by adding a group at the centre of each cube face. The cube now contains 4 groups, whose coordinates may be taken to be  $(000)$ ,  $(\frac{1}{2}\frac{1}{2}0)$ ,  $(0\frac{1}{2}\frac{1}{2})$ ,  $(\frac{1}{2}0\frac{1}{2})$ . The condition for phase agreement between these and the original point is

$$\frac{h+k}{2}, \quad \frac{k+l}{2}, \quad \frac{l+h}{2},$$

all integers. This implies that  $hkl$  are all even or all odd. The first few possible sets are thus 111, 200, 220, 311, 222, 400.

### ' Powder ' Method

A method which has been used a great deal in the examination of metals by X-rays is the Hull-Debye-Scherrer method. If a substance composed of a vast number of very small

<sup>1</sup> Note that a point at the corner of a cube is shared by 8 cubes and counts  $\frac{1}{8}$ , similarly a point on an edge counts  $\frac{1}{4}$  and one on a face counts  $\frac{1}{2}$ .

crystals oriented at random is irradiated by monochromatic X-rays, some among the crystals will be set at such an angle that they are in the right attitude to reflect the X-rays from one particular face. If there are sufficient crystals, reflections will be found from every possible face. The deviation of the rays from the direction of the original beam is  $2\theta$ , where  $2d \sin \theta = N\lambda$  (Fig. 9). The diffracted rays thus form a series

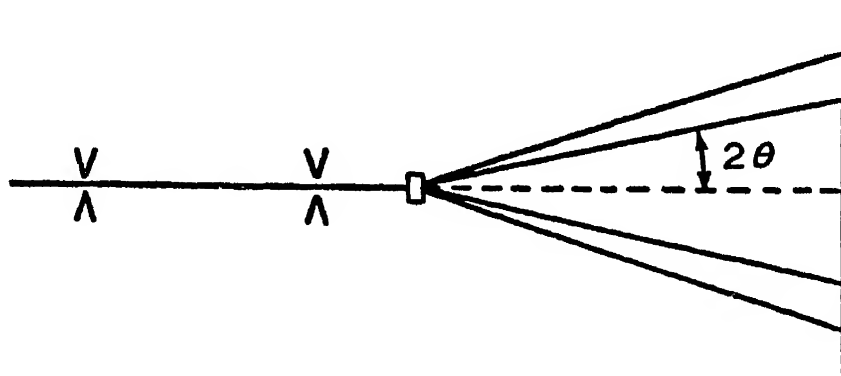


FIG. 9

of cones round the incident beam as axis, one for each value of  $d$ . If a photographic plate is placed perpendicularly to the incident beam, the intersections of these cones will give a pattern of concentric circles on the plate. Each point on one of the circles is caused by a different fragment of crystal, and if the crystals are not sufficiently numerous or are not arranged entirely at random with regard to the direction of the incident rays, the circles may be incomplete and appear as a series of spots, or as arcs varying in intensity. As in the case of the optical diffraction grating, high resolving power requires the cooperation of a large number of diffracting centres and if the crystals are too small the rings will be broadened. Since the crystals are arranged at random, waves from one crystal will have no definite phase relation with those from another, and there will be no interference between them.

## CHAPTER IV

### EXPERIMENTAL EVIDENCE FOR ELECTRON WAVES

It was suggested by Elsasser<sup>1</sup> that evidence for the wave nature of electrons would be found from their interaction with crystals. Clearly, very strong support for the theory would be obtained if it were possible to measure some quantity which could be regarded as a wave-length, and if it were found that the values agreed with the formula  $\lambda = h/mu$ . The measurement of a wave-length suggests a diffraction grating, which is in essence a device for producing a number of regularly spaced wavelets from one primary wave. If we substitute the numerical values of  $h$  and  $m$  in the above formula and write

$$\frac{1}{2}mu^2 = \frac{eP}{300},$$

where  $P$  is the potential drop in volts equivalent to the energy of the electron, we get

$$\lambda = \sqrt{\frac{150}{P}} \times 10^{-8} \text{ cm.} \quad . \quad . \quad . \quad (1)$$

Thus for electrons of manageable hardness the wave-lengths are comparable with those of X-rays. For the measurement of X-ray wave-lengths crystals are used, each atom of which may be regarded as producing a scattered wavelet, the wavelets from corresponding atoms in the different unit cells having phases whose regular relations we have considered in Chapter III. Now electrons also are scattered by atoms, in some cases without loss of energy or change of wave-length, and it was thus reasonable to hope that the interference of these wavelets should give similar effects to those obtained from X-rays.

<sup>1</sup> W. Elsasser, *Naturwiss.* 13, p. 711 (1925).

### Davisson and Germer's Experiments

The first experiments on these lines were made by Davisson and Germer.<sup>1</sup> The general idea was that a beam of homogeneous electrons, of energy varying in different experiments from 65 to 600 volts, was allowed to fall normally on a single crystal of nickel cut with a (111) plane in the surface. Nickel forms a face-centred cubic lattice. The scattered electrons were received in a Faraday cylinder which could be moved so as

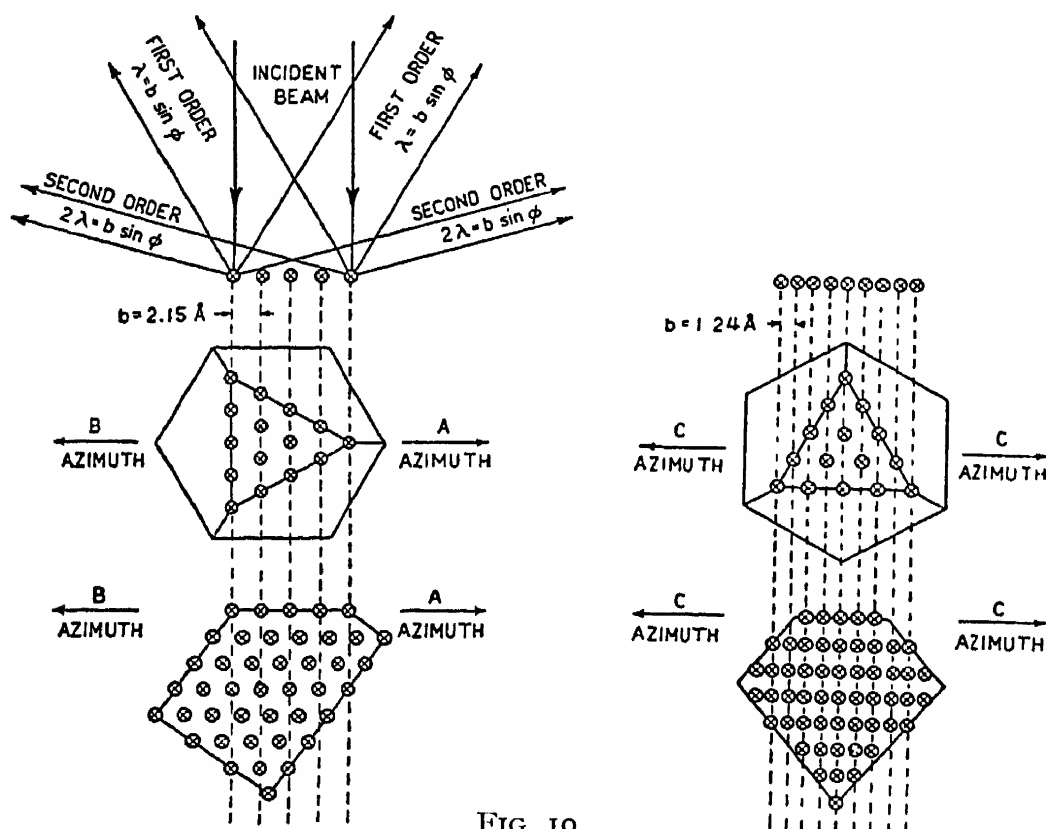


FIG. 10

to receive electrons coming from the crystal at any required angle to the normal, within limits. A back potential of  $\frac{1}{10}$  of the original potential of the electrons was applied between the cylinder and the crystal, so that electrons which had lost more than 10 per cent of their energy were excluded. The crystal could be rotated about the normal to the face used, relative to the plane containing this normal and the Faraday cylinder. In the  $360^\circ$  of motion in azimuth thus obtained, certain positions correspond to specially symmetrical relations of the

<sup>1</sup> C. Davisson and L. H. Germer, *Phys. Rev.* 30, p. 707 (1927).

crystal atoms to the plane containing the cylinder and normal. These positions are indicated in Fig. 10. The C azimuth occurs six times in a revolution, A and B three times each. The difference between the A and B azimuths only comes in

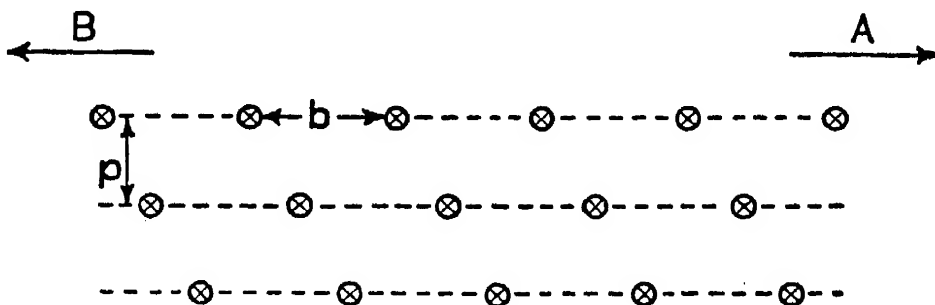


FIG. 11

for the atoms below the surface. The surface layer is identical as viewed from either direction, but the layer below is staggered by  $\frac{1}{3}$  of the spacing of the top layer and thus is placed differently with respect to the latter in the two aspects (see Fig. 11). If

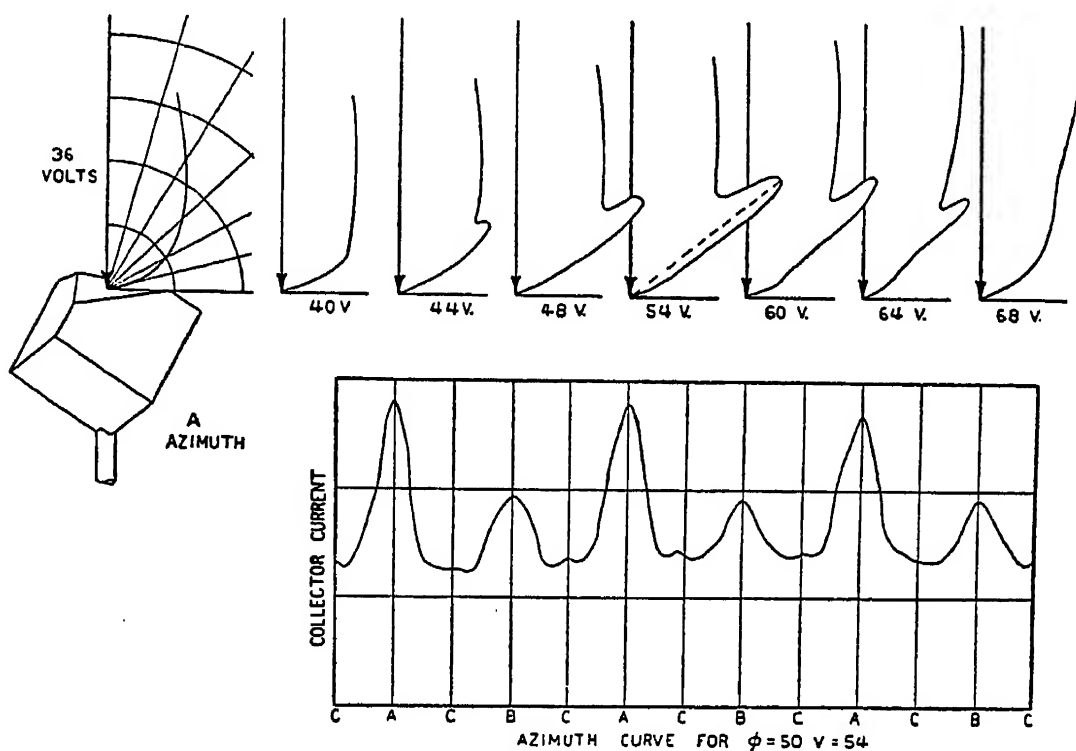


FIG. 12

observations are made in one of these azimuths using electrons of arbitrary voltage and changing the position (co-latitude) of the collector, a curve like that to the left in Fig. 12 will, in general, be obtained. The radius vector indicates the intensity

of scattering in a given direction. This curve shows a steady increase of scattering towards the normal. If, however, a series of such curves are obtained with varying electron speed, it is found that a pronounced spur develops (Fig. 12, to the right). This spur is most marked at a certain voltage, but is visible over a considerable range. The angle of co-latitude of the spur changes at the same time. If the crystal is then rotated in azimuth, with the co-latitude of the Faraday cylinder and the voltage of the rays kept constant, a series of changes occurs as shown in the lower part of Fig. 12. The spur—in this case originally in azimuth A—repeats thrice in a revolution, as it must from the crystal symmetry; it also occurs in a reduced form in the associated azimuth B, again three times.

An exactly similar result occurs if the original observations are made in the B azimuth. Again a spur is found; this time it is best developed at 50 volts energy and  $44^\circ$  co-latitude, but now the spur repeats itself in each B azimuth and with diminished intensity in the three A azimuths. These minor maxima correspond to the spur we first considered, but the voltage and angle are not such as to bring it to its full development. Similar effects occur in the C azimuth, but here the effect repeats six times in a revolution. In the original experiments 24 of these spurs were found: 9 in the A azimuth, 10 in the B and 5 in the C azimuth. The natural interpretation is to regard each of these as analogous to an X-ray diffraction beam reflected from some Bragg plane. For purposes of analysis it is, however, convenient to proceed in a slightly different way. The electrons have very little penetrating power so that only a few layers of the crystal are effective in scattering. The result is a lack of resolving power; it is like using a grating with only half a dozen lines. This explains, to some extent, the diffuseness of the spurs and their occurrence over a wide range of voltage; for, of course, regarded as Laue beams they should occur only with one definite wave-length. Let us take the extreme case and suppose only the top layer of atoms effective. Then we have a plane grating, and for normal incidence we shall get a diffracted beam wherever

$$n\lambda = b \sin \phi, \quad . \quad . \quad . \quad . \quad (2)$$

where  $\phi$  is the angle which the diffracted beam makes with

the normal and  $b$  is the grating constant, in this case the distance between successive rows of atoms running perpendicularly to the azimuth investigated. For the general case this relation will also hold, but there is the extra restriction that the lower layers (separated by the distance  $p$ ) must also be in phase. For the B azimuth (see Fig. 11), this gives

$$p \cos \phi + \frac{b}{3} \sin \phi = n' \lambda$$

Eliminating  $\lambda$  we find

$$\tan \phi = \frac{p}{b} \frac{n}{n' - n/3}.$$

For the A azimuth

$$\tan \phi = \frac{p}{b} \frac{n}{n' + n/3},$$

and in the C azimuth we have simply

$$\tan \phi = pn/b'n'.$$

Calculation shows that  $b = \sqrt{3/8} \cdot a$ ,  $p = a/\sqrt{3}$ ,  $b' = a/\sqrt{8}$ , where  $a$  is the side of the unit face-centred cube. Thus for the A and B azimuths

$$\tan \phi = \sqrt{9/8} \frac{n}{n' \pm n/3}. \quad . \quad . \quad . \quad (3)$$

Davisson's method is to plot  $\lambda$ , or rather  $\sqrt{\frac{150}{P}} \times 10^{-8}$ , against  $\sin \phi$ . For each value of  $n$ , *i.e.* each order of reflection from the plane grating, he draws the straight line  $b/n \cdot \sin \phi = \lambda$ ; the observed beams should all lie on one of these straight lines if they obey the plane law, and if they also obey the space law the values of  $\phi$  should be given by Equation (3). Actually Davisson and Germer found the first requirement satisfied, but not the second (Fig. 13). We shall discuss the reason for the failure in the second case in Chapter XVIII; the first result is strong confirmation of de Broglie's theory, for not merely does it give the right variation of  $\sin \phi$  with  $P$ , namely  $\sqrt{P} \sin \phi$  constant,<sup>1</sup> but the value of the constant checks de Broglie's

<sup>1</sup> That is, the same for all the beams when developed to their maximum. It appears not to be true for the variation with voltage of the position of a single beam.

law,  $\lambda = h/mu$ , absolutely, there being no adjustable constants. Thus for the 54-volt beam illustrated in Fig. 13

$$b \sin \phi = 1.65 \times 10^{-8} \quad \text{while} \quad (150/P)^{\frac{1}{2}} = 1.67,$$

so that the beam is a first-order one. Similarly for the 65-volt beam

$$b \sin \phi = 1.50 \times 10^{-8} \quad \text{and} \quad (150/P)^{\frac{1}{2}} = 1.52.$$

In some of the other cases the discrepancy was greater. The figures show the extent of the agreement graphically; the

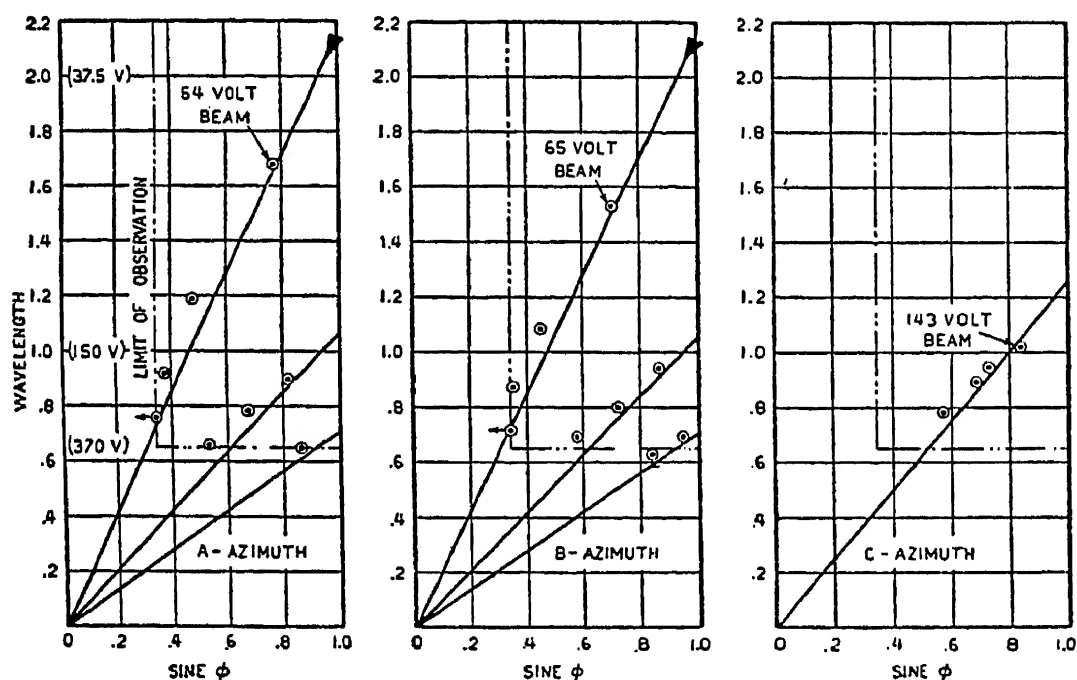


FIG. 13

displacements of the points from the (calculated) lines do not exceed the error to be expected, owing to the relatively large size of the collector and the fact that there was a small error in the cutting of the crystal face. If, however, a series of integers is substituted for  $n'$  in Equation (3) the resulting values of  $\phi$  do not give the positions of the observed spots, though the number is about the same over the whole range; thus, while the surface layer of atoms scatters according to the simple law, other considerations have to be taken into account to explain the behaviour of the lower layers. In addition to the beams here considered, which appear under the best vacuum, Davisson and Germer found others which were apparently

associated with the presence of layers of gas on the surface of the crystal. These will be discussed in Chapter XVIII.

In addition, they found in each azimuth a beam near grazing emergence, shown in Fig. 13 by the wedge-shaped marks. In the A and B azimuths it occurred at 32.5 volts and moved up with increasing voltage.<sup>1</sup> This is exactly the voltage to be expected for a plane-grating beam, and the equivalence in the A and B azimuths also suggests this explanation. The beams increased in intensity at first as the voltage increased, and then decreased again, all the time moving up from the surface. At very small angles of emergence the radiation from the lower layers of atoms will not get through; as the angle increases it begins to do so and weakens the surface beam by interference. This explanation does not account for the initial rise in intensity unless this can be attributed to a change in the scattering for a single atom. It is probable that the beam in the B azimuth is really a space-grating effect. These beams have not been found with a second apparatus. Three space beams which should, theoretically, have occurred in azimuths other than the principal ones were not observed. Their absence may, perhaps, be explained by the considerations discussed on p. 107.

In a more recent paper the same authors have described experiments in which the angle of incidence of the rays was altered. The range used was from 10° to 52° (later 70°). In all cases a beam was found in the direction of specular reflection, and it was this which was chiefly investigated. As the wavelength is varied the intensity of reflection changes, and if the Bragg law were satisfied we should have for maximum intensity

$$\frac{2}{\sqrt{3}}a \cos \phi = n \left( \frac{150}{P} \right)^{\frac{1}{2}},$$

since  $a/\sqrt{3}$  is the spacing of the (111) surface planes. Fig. 14 shows that while the general nature of the effect is as predicted, the exact position of the predicted maxima—shown by the arrows—as a rule does not agree with the most marked maxima

<sup>1</sup> It is not apparent on Fig. 12, which refers to experiments taken before the final heating of the crystals, which was needed to bring out the grazing beams.

on the experimental curve. The possible explanations of this will be discussed in Chapter XVIII.

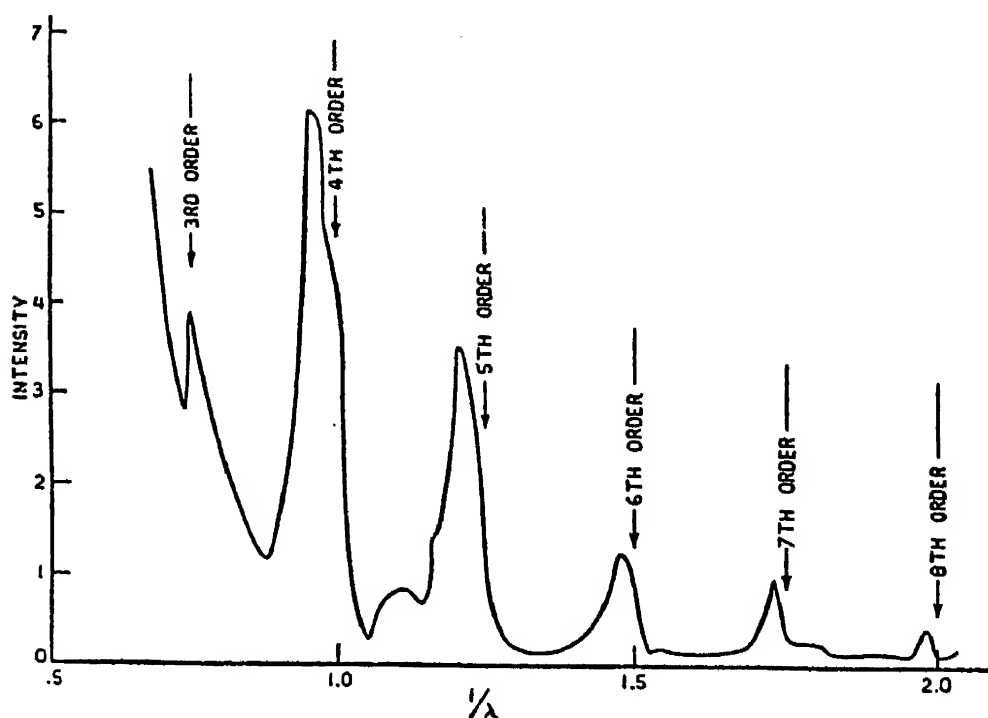


FIG. 14

### Transmission Experiments

The first experiments to indicate a diffraction of electrons by thin films were carried out by the late Mr. A. Reid at Aberdeen. The apparatus was an adaptation of one which had previously been used for measuring the scattering of positive rays in gases. A beam of cathode rays from a gas discharge tube was passed through a fine tube and then deflected by an electrostatic field. The deflected beam passed through a hole 0.25 mm. in diameter in a diaphragm, immediately behind which was mounted a thin film of celluloid. After passing through the film the rays travelled a distance of 20 cm. and then struck a photographic plate so placed as to be normal to the beam. The patterns formed by the impact of the rays on the plate consisted of an intense central spot due to the unscattered rays, surrounded by a fainter region due to rays scattered by the film. In many cases this region was not, as one would naturally expect if the electron is regarded merely as a charged particle, one of uniformly diminishing intensity, but showed one or more rings with the main beam for their

centre (Plate I *a*). At first the rings were not very distinct and we suspected an optical illusion similar to that observed in previous positive-ray experiments.<sup>1</sup> It was found possible, however, to measure the rings photometrically, and they appeared as distinct inflections on the general curve of scattering. In the absence of any certain knowledge as to the crystalline state of celluloid, if any, it seemed natural to regard the rings as analogous to the halos formed by light passing through a cloud of small particles, as in Young's eriometer. The wave-length required was of the right order to fit de Broglie's formula, and the angular diameter of any ring was approximately inversely proportional to the square root of the voltage. In June 1927 a letter appeared in *Nature* describing these experiments,<sup>2</sup> two months after the preliminary account in the same journal of the experiments by Davisson and Germer described above.<sup>3</sup> Some delays were experienced in clearing up certain points of difficulty, and it was not till a year later that a final

TABLE I<sup>4</sup>

Plate	Voltage (P)	D <sub>1</sub> , mm.	D <sub>2</sub> , mm.	D <sub>3</sub> , mm.	D <sub>1</sub> P <sup>1/2</sup> /L	D <sub>2</sub> P <sup>1/2</sup> /L	D <sub>3</sub> P <sup>1/2</sup> /L
March 16 (1)	9,800	12.0	..	..	54.4	..	..
March 19 (2)	10,800	10.6	..	..	57.5	..	..
March 15 (2)	14,800	9.0	18.4	..	54.5	112.0	..
March 15 (3)	19,700	8.2	..	..	57.5	..	..
March 15 (1)	26,000	7.0	14.0	22.5	56.4	112.9	180.8
March 16 (2)	29,500	6.5	13.6	..	58.8	116.8	..
March 19 (1)	35,100	6.25	12.2	19.8	58.0	114.0	186.5
April 17	40,400	5.5	11.5	18.5	55.1	115.8	186.5
Mean	..	..	..	..	56.5	114.4	184.6

account appeared<sup>5</sup> only a day or two before Mr. Reid's tragic death in a motor-cycle accident. The final results showed three rings, for each of which the diameter  $D$  and the voltage  $P$  were connected by the law  $D\sqrt{P} = \text{constant}$ . This is, of course, a necessary result in any diffraction pattern formed by

<sup>1</sup> G. P. Thomson, *Proc. Cambridge Phil. Soc.*, 23, p. 419 (1926).

<sup>2</sup> G. P. Thomson and A. Reid, *Nature*, 119, p. 890 (1927).

<sup>3</sup> Davisson and Germer, *Nature*, 119, pp. 558 ff. (1927).

<sup>4</sup> See A. Reid, *Proc. Roy. Soc. London*, A119, p. 665 (1928).

<sup>5</sup> A. Reid, *Proc. Roy. Soc. London*, A119, p. 663 (1928).

de Broglie waves, since  $\lambda \propto P^{-\frac{1}{2}}$  if relativity is neglected. The quantity  $P$  was determined by measuring the field required to deflect the rays on to the hole in the diaphragm, the dimensions of the apparatus being known.

The ratio of  $D_1 : D_2$  is almost exactly 1 : 2, that of  $D_1 : D_3$  is rather less than 1 : 3, but other plates than those quoted above showed a closer approach to this ratio and it seems probable that the rings are three successive orders. It will, of course, be understood that in these and the following experiments the angle of diffraction is so small, of the order of  $2^\circ$ , that we can write  $\sin \theta = \theta$ . Thus if  $L$  (Fig. 15) is the

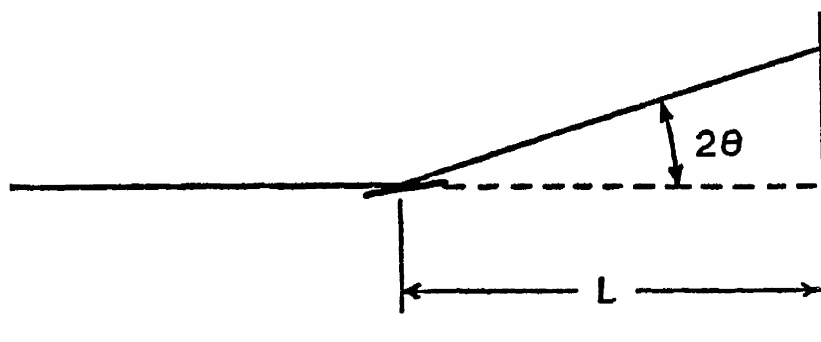


FIG. 15

distance of the plate from the scattering body, and if the effect is regarded as equivalent to reflection from a Bragg plane of spacing  $d$ , we can write

$$\frac{D}{L} = 2 \sin 2\theta = \frac{2N\lambda}{d} \text{ (approximately).} \quad (4)$$

The spacing  $d$ , calculated from the above formula, had a mean value of  $4.46 \times 10^{-8}$ . This is close to the value found for the cross-section of long-chain carbon compounds. These rings were always slightly blurred and it seems possible that they were really double, corresponding to two spacings close together. In one or two plates definite evidence of such doubling was obtained.

The films used had a thickness, as estimated by interference measurements and from measurements of their reflecting power for light, of the order  $3$  to  $5 \times 10^{-6}$  cm. They were made by flowing a drop of an amyl acetate solution of celluloid over the surface of a large dish of water and allowing the amyl

acetate to evaporate. It is advisable to reject the first films formed as they will have picked up any dust particles which there may be on the water, and generally have holes in them.

### Metal Films

The great disadvantage of experiments with celluloid was that its structure was unknown, and so no exact comparison with theory was possible. As soon as it seemed certain that diffraction effects were being obtained with the electrons in celluloid films, attempts were made to obtain films whose

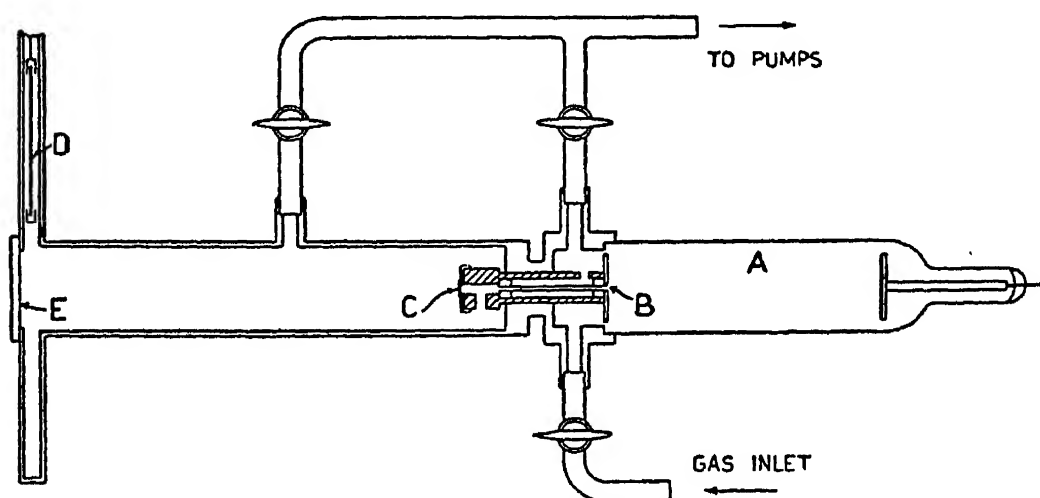


FIG. 16

structure was known, thin enough to give diffraction patterns. After several failures, films of aluminium and of gold were prepared which gave striking patterns. A little later platinum films were made and the results published in a letter to *Nature*<sup>1</sup> which appeared before the account of the experiments just mentioned, which were published in February 1928.<sup>2</sup>

The apparatus used was originally intended as provisional only, but it worked so well that only minor modifications were made in the course of the work to be described. It is shown in Fig. 16. Cathode rays (generated by an induction coil) in the tube A passed through the fine tube B of bore 0.23 mm. and length 6 cm., and struck a film mounted at C. The iron tube shown shaded in Fig. 16 shielded B from magnetic effects. There was also a flat shield of soft iron round the

<sup>1</sup> G. P. Thomson, *Nature*, 120, p. 802 (1927).

<sup>2</sup> G. P. Thomson, *Proc. Roy. Soc. London*, A117, p. 600 ff. (1928).

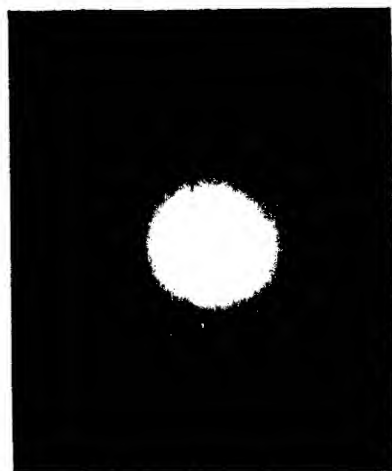
neck between discharge tube and camera. The distance from C to the photographic plate D, when in position, was 32.5 cm. and D could be lowered in two stages by a magnetic release. This enabled two exposures to be taken on each plate, which was an advantage as it was difficult to estimate the best time of exposure to show up the pattern. At E was a willemite screen which could be used to examine the rays while the plate D was still in the upper part of the camera. The camera was exhausted to a low vacuum, the gas coming through the fine tube from A being removed by a three-stage mercury vapour pump. The voltage of the discharge was measured as carefully as possible by means of a spark-gap between 4 cm. aluminium spheres. A preliminary experiment of deflecting the rays by a magnet on their path between C and E showed that they were very nearly homogeneous, the spot on the plate deflecting as a whole except for a very faint tail.

The exposures used were from a few seconds up to a few minutes, depending on the intensity and voltage of the cathode rays used. A few experiments were made with celluloid films, which checked up well with Reid's results and showed that the spark-gap method of measuring potential was reliable.<sup>1</sup> It will be remembered that Reid determined the speed of his rays by the field required to deflect them on to a hole in a diaphragm, his measurements are thus independent of any assumption as to the behaviour of the discharges.

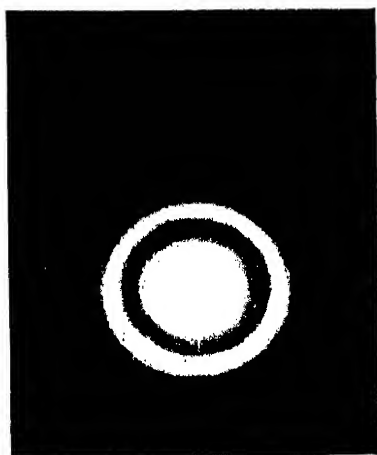
Specimens of the results with gold, aluminium and celluloid are shown in Plate II. It will be seen that in all cases the general effect is that of a series of concentric rings round the spot made by the undeflected beam. In some cases these rings are uniform round the circumference, in others the intensity is more or less concentrated in a series of spots on the circumference. It should be said at once that there can be no doubt that the whole pattern is due to cathode rays which have been deflected by the film. Thus in the absence of the film only the central spot is seen, and if a magnet is brought up between C and E (Fig. 16) the whole pattern is shifted together. In some cases, when bright enough, this can

<sup>1</sup> An error of about 5 per cent in  $\sqrt{P}$  was made in the first measurements owing to neglecting the fall of potential in the leads, valve, etc. This was corrected in a note on p. 661 of the paper in *Proc. Roy. Soc. London*, A119, (1928).

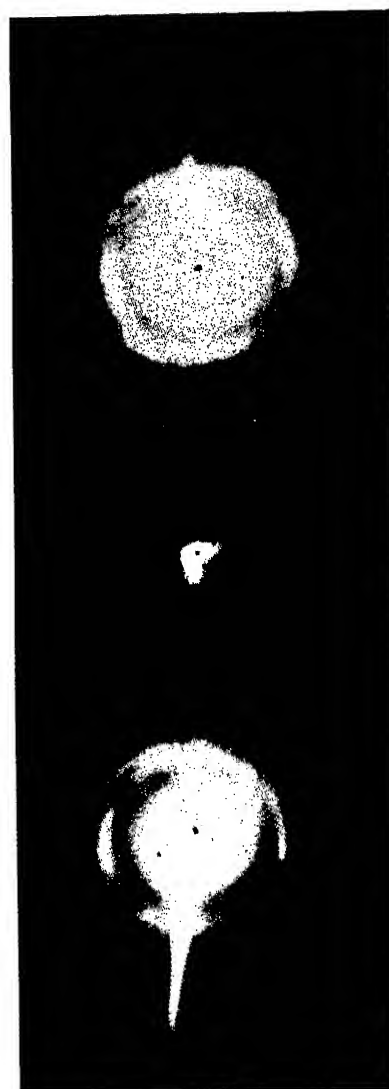
PLATE II  
(Some early photographs)



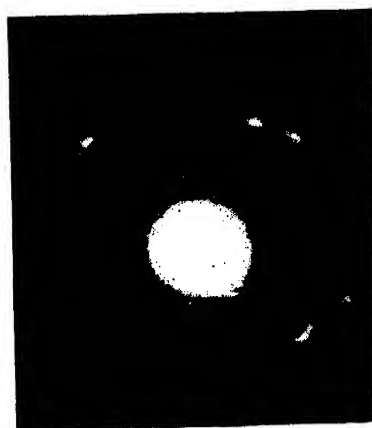
(a) Celluloid



(b) Gold



(c) Platinum ; magnetically deflected patterns



(d) Aluminium



be seen by following the changes in appearance of the willemite screen when a magnet is brought near. In others, when the rings could not be seen on the screen, photographs were taken with a magnetic field between C and D strong enough to move the central spot—which could always be seen—through a considerable distance. In all cases the pattern showed the spot at the centre of the rings, showing that spot and rings had been deflected together. They thus are due to cathode rays of appreciably the same velocity.

A later quantitative investigation <sup>1</sup> showed that the agreement in velocity between the rays forming the rings and those in the central spot was exact to well within the experimental error, which was less than 1 per cent. The films in these experiments had numerous holes, so that the central spot was mostly formed by rays which had gone through without collision. The rings must therefore have been formed by electrons which had undergone elastic collisions only. Plate IIc shows a photograph taken in the course of this research. The two sets of rings were obtained by reversing a magnetic field which deflected the rays between the film and the photographic plate. The spot in the centre is the result of a short exposure without the field and gives the position of the undeflected beam.

The general appearance of the rings immediately recalls that of the Hull-Debye-Scherrer X-ray rings in the case of gold, and a cross between these and a Laue pattern in the case of aluminium. It remains to see if the agreement is exact, and if so, if the value of the wave-length is that predicted by the de Broglie theory. Any diffraction pattern formed in directions making small angles with the original beam must fulfil the condition that its size is proportional to the wave-length causing it (see Equation 4). It is easy to show <sup>2</sup> that if account is taken of relativity,

$$\lambda = \frac{h\sqrt{150/ePm_0}}{(1 + eP/1200m_0c^2)}, \quad . \quad . \quad . \quad (5)$$

<sup>1</sup> *Proc. Roy. Soc. London*, A119, p. 651 ff. (1928).

<sup>2</sup> We have  $\frac{eP}{300} = \frac{m_0c^2}{\sqrt{1 - u^2/c^2}} - m_0c^2$  and  $\lambda = \frac{h\sqrt{1 - u^2/c^2}}{m_0u}$ , eliminating  $u$  and approximating, the result follows. Note that  $h/\sqrt{em_0} = 10^{-8}$ , to the accuracy with which these quantities are known.

where  $P$  as before is the potential through which the electron has been accelerated, measured in volts, and the first power of  $eP/m_0c^2$  is retained. The correcting term never exceeds 3 per cent in these experiments. The extent to which

$$D\sqrt{P}\left(1 + \frac{eP}{1200m_0c^2}\right)$$

is constant for a given ring of a given substance is shown by Table II.<sup>1</sup>

TABLE II

Plate	Spark Gap, mm.	P, volts.	$D_1$ , cm.	$D_1\sqrt{P}\left(1 + \frac{eP}{1200m_0c^2}\right)$
ALUMINIUM				
October 7 (3) . .	5.0	17,500	3.1	415
October 10 (2) . .	9.5	30,500	2.45	434
October 7 (2) . .	10.0	31,800	2.32	418
October 7 (4) . .	13.0	40,000	2.12	430
October 7 (5) . .	14.5	44,000	2.08	445
October 7 (6) . .	16.5	48,600	1.90	430
October 11 (1) . .	16.5	48,600	1.98	446
October 12 (2) . .	20.0	56,500	1.83	446
October 12 (3) . .	20.0	56,500	1.80	438
Mean . .	..	..	..	434
GOLD				
October 13 (1) . .	7.5	24,600	2.50	398
October 12 (4) . .	10.0	31,800	2.15	390
October 12 (5) . .	12.75	39,400	2.00	404
October 12 (6) . .	15.25	45,600	1.86	405
October 12 (7) . .	19.0	54,300	1.63	388
October 17 . .	22.0	61,200	1.61	410
Mean . .	..	..	..	399

The measurements quoted are from the earliest paper,<sup>2</sup> but the result has been confirmed again and again. It holds good for all the metals with which these patterns have been obtained, *i.e.* gold, aluminium, platinum, silver, copper, lead, iron, nickel, tin, and also for several compounds. A slight apparent exception has been shown not to be real.<sup>3</sup> If not

<sup>1</sup> G. P. Thomson, *Proc. Roy. Soc. London*, A117, p. 603 f. (1928).

<sup>2</sup> *Proc. Roy. Soc. London*, A117, p. 600 ff. (1928).

<sup>3</sup> G. P. Thomson, *Proc. Roy. Soc. London*, A119, p. 652 (1928).

due to accidental errors it was probably caused by the rays not being quite homogeneous. We may thus take it that the variation of these patterns with the voltage of the rays is that required if they are caused by the diffraction of de Broglie waves.

GOLD.—The rings obtained with gold obviously resemble the patterns given by powders with X-rays. Gold crystallises in face-centred cubes, for which the spacings are given by

$$d = \frac{a}{\sqrt{h^2 + k^2 + l^2}},$$

where  $hkl$  are all even or all odd (see p. 27). The diameters of the rings become

$$D = \frac{2\lambda L \sqrt{h^2 + k^2 + l^2}}{a}. \quad . \quad . \quad . \quad (6)$$

The relative sizes of the rings in two early photographs with gold films are shown in the first two rows of Table III. The 220 ring is taken as standard. Below are some later measurements; in these the rays were made more uniform in velocity, and hence in wave-length, by placing two or three Leyden jars in parallel with the discharge tube. The increased homogeneity of the rays makes it possible to distinguish the rings corresponding to small spacings. Owing to the relative faintness of the outer rings it is not easy to make them show up well without over-exposing the inner ones, which thus become difficult to measure accurately. All the possible rings are present up to  $\sqrt{27}$ , though  $\sqrt{16}$  is always faint. The rings which should occur at  $\sqrt{32}$  and  $\sqrt{40}$  are masked by rings near them, but traces have been found by photometric measurement. Otherwise all possible rings up to  $\sqrt{60}$  are present, though in several cases two or more rings are too close together to be resolved. In these cases a mean value has been calculated for  $\sqrt{h^2 + k^2 + l^2}$ , weighted to allow for the chances of the rings being formed in a random distribution of crystals. The later plates are a selection from a large number that have been taken for various purposes at different times; there are many others equally good. The agreement with theory is well within the errors of measurement of these rings,

which range in diameter from a little over 1 cm. to about 6 cm.

ALUMINIUM.—Results for aluminium — also a face-centred cubic structure — are shown in Table III. In this case the 'rings' consist of a number of separate spots (see Plate II *d*) but there is no difficulty in measuring the diameters of the circles on which they lie. It will be seen that there is equally good agreement with the theory except for the curious omission of the  $\sqrt{3}$  and probably  $\sqrt{12}$ , its second order. The explanation is as follows. The incomplete nature of the rings shows that comparatively few crystals are present in the area struck by the rays. Konobeievski<sup>1</sup> has shown, by X-ray methods, that in the thinnest aluminium foil the crystals are oriented with their (100) axes perpendicular to the foil. The films used in the above experiments were made by thinning down a piece of the thinnest leaf obtainable, in caustic potash. If the crystals in this case are oriented in the same way no reflection from a (111) plane will be possible, because the Bragg law requires the incidence to be only about one degree from grazing and no (111) planes will be present at so small an angle to the rays. The occurrence on some of the patterns of regular groups of spots is explained in Chapter VI.

INCLINED FILMS.—A few experiments were made with films inclined to the rays, the angle between the film normal and the rays being about 30°. If the crystals of the film are arranged quite at random, no change should be produced by inclining the film, but if the crystals have dominant directions with regard to the plane of the film, changes will be produced in the relative intensities of different parts of the same ring, and the different rings as a whole.

A silver film, prepared by Ironside,<sup>2</sup> showed marked difference in the brightness of different parts of the 200 ring when inclined, though when the film was normal to the rays the ring was of uniform intensity. The brightest parts were at the ends of a diameter parallel to the axis about which the film had been turned. This is what would be expected if there was a tendency for the crystals to be set with one axis normal to the film. The only planes that can reflect the rays are those which make a small angle with them, since the wave-

<sup>1</sup> Konobeievski, *Zeit. für Phys.*, 43, p. 741 (1927).

<sup>2</sup> R. Ironside, *Proc. Roy. Soc. London*, A119, p. 668 (1928).

TABLE III  
RELATIVE DIAMETERS OF RINGS

Column	1	2	3	4	5	6	7	8	9	10	11	12	13	14
Plane indices ( <i>hkl</i> )	(111)	(200)	(220)	(113) (222)	(400)	(331) (420)	(422)	(511) (333)	(440)	(531) (600) (442)	(620)	(533) (622)	(444) (700) (551) (640)	(642) (731) (553)
$\sqrt{h^2+k^2+l^2}$	$\sqrt{3}$	$\sqrt{4}$	$\sqrt{8}$	$\sqrt{11}$ $\sqrt{12}$	$\sqrt{16}$	$\sqrt{19}$ $\sqrt{20}$	$\sqrt{24}$	$\sqrt{27}$	$\sqrt{32}$	$\sqrt{35}$ $\sqrt{36}$	$\sqrt{40}$	$\sqrt{43}$ $\sqrt{44}$	$\sqrt{48}$ $\sqrt{49}$ $\sqrt{51}$ $\sqrt{52}$	$\sqrt{56}$ $\sqrt{59}$
$\sqrt{h^2+k^2+l^2}$ Weighted mean	$\sqrt{3}$	$\sqrt{4}$	$\sqrt{8}$	$\sqrt{11.25}$	$\sqrt{16}$	$\sqrt{19.5}$	$\sqrt{24}$	$\sqrt{27}$	$\sqrt{32}$	$\sqrt{35.4}$	$\sqrt{40}$	$\sqrt{43.5}$	$\sqrt{50}$	$\sqrt{57.8}$
GOLD														
Oct. 12, 1927 (7)	$\sqrt{2.96}$	$\sqrt{4.08}$	$\sqrt{8.00}$	$\sqrt{11.2}$	missing	$\sqrt{19.3}$	..	..	..	..	..	..	..	..
Oct. 17, 1927	$\sqrt{3.02}$	$\sqrt{4.25}$	$\sqrt{8.00}$	$\sqrt{11.7}$	..	$\sqrt{19.9}$	..	..	..	..	..	..	..	..
Dec. 19, 1927 (3)	$\sqrt{2.95}$	$\sqrt{4.08}$	$\sqrt{8.00}$	$\sqrt{11.2}$	..	$\sqrt{19.5}$	$\sqrt{22.7}$	$\sqrt{26.6}$	..	$\sqrt{35.4}$	..	..	..	..
Feb. 25, 1929	$\sqrt{2.96}$	$\sqrt{3.98}$	$\sqrt{8.00}$	$\sqrt{11.0}$	..	$\sqrt{19.5}$	$\sqrt{24.3}$	$\sqrt{27.8}$	..	$\sqrt{34.9}$	..	$\sqrt{43.1}$	..	..
Mar. 13, 1929	$\sqrt{3.06}$	$\sqrt{3.9}$	$\sqrt{8.00}$	$\sqrt{11.0}$	..	$\sqrt{19.5}$	$\sqrt{24.1}$	$\sqrt{27.5}$	..	$\sqrt{35.0}$	..	$\sqrt{42.6}$	$\sqrt{50}$	$\sqrt{56.5}$
Apr. 12, 1929 (3)	..	..	$\sqrt{8.00}$	$\sqrt{11.25}$	$\sqrt{15.7}$	$\sqrt{19.4}$	$\sqrt{24.4}$	$\sqrt{26.7}$	..	$\sqrt{34.7}$	..	$\sqrt{43.5}$	$\sqrt{51.6}$	$\sqrt{58.4}$
ALUMINIUM														
	..	$\sqrt{4.00}$	$\sqrt{8.00}$	$\sqrt{10.9}$	$\sqrt{16.5}$	$\sqrt{20.4}$	..	$\sqrt{27.0}$	..	..	..	..	..	..
	..	$\sqrt{3.98}$	$\sqrt{8.00}$	$\sqrt{11.0}$	$\sqrt{15.7}$	$\sqrt{21.2}$	..	$\sqrt{27.8}$	..	..	..	..	..	..
	..	$\sqrt{4.02}$	$\sqrt{8.00}$	$\sqrt{10.9}$	$\sqrt{15.9}$	$\sqrt{19.4}$	..	$\sqrt{26.8}$	..	$\sqrt{36.0}$	..	..	..	..
	..	$\sqrt{4.00}$	$\sqrt{8.00}$	$\sqrt{10.9}$	$\sqrt{15.4}$	$\sqrt{19.2}$	$\sqrt{23.6}$	$\sqrt{27.4}$	..	$\sqrt{33.0}$	..	..	..	..
PLATINUM														
	$\sqrt{3.00}$	$\sqrt{4.00}$	$\sqrt{8.00}$	$\sqrt{10.9}$	$\sqrt{15.3}$	$\sqrt{18.4}$	$\sqrt{24.0}$	$\sqrt{26.5}$	..	..	..	..	..	..
	$\sqrt{3.07}$	$\sqrt{4.01}$	$\sqrt{8.00}$	$\sqrt{11.3}$	..	..	..	..	..	..	..	..	..	..
	$\sqrt{3.04}$	$\sqrt{4.03}$	$\sqrt{8.00}$	$\sqrt{11.2}$	$\sqrt{16.4}$	$\sqrt{19.0}$	$\sqrt{23.4}$	$\sqrt{27.1}$	..	$\sqrt{35.0}$	..	..	..	..

length is small compared with the spacing, and the only (200) planes which would fulfil this condition would be those whose normals nearly coincided with the line about which the film had been turned. That all the crystals are not placed in this way is shown by the fact that the  $111$  ring appears with the film in the usual position. This ring in the inclined film is brightest on the diameter at right angles to that for the 200 ring, and as the two rings are close together the whole has an elliptical appearance.<sup>1</sup> For an aluminium film which showed, in the normal position, a number of spots on the 200 ring, a pair on the diameter parallel to the axis of turning of the film showed strongly. A few other spots were, however, visible on the ring; the orientation of the crystals with their axes perpendicular to the film is therefore not perfect.

PLATINUM.—Some very thin platinum leaf showed results intermediate between those of gold and aluminium. The rings at first consisted of a large number of spots, but not enough to make them quite continuous. After being laid aside for a few weeks the same film showed continuous arcs extending over about  $60^\circ$ . It is possible that this was a slightly different part of the film, but as several plates were taken in each case, with consistent results, it is more likely that a change had been produced in the film, perhaps caused by strains due to thermal expansion of the pierced aluminium disk on which it was mounted. To produce the later pictures the crystals must have had preferred directions, though the orientation is by no means exact, as shown by the length of the arcs. The pattern showed a clear 4-fold symmetry.

COPPER, NICKEL.—Ironside<sup>2</sup> found with copper films, made by thinning down beaten copper, a tendency to orient with a  $[100]$  axis perpendicular to the film. The  $111$  ring was absent. Most of the other experiments were made on films formed by cathodic spluttering, these showed uniform rings like those of gold. In the great majority of cases the sizes of the rings were in the ratio demanded by the known crystal structure. Nickel was exceptional in showing an hexagonal structure instead of a cubic one.

<sup>1</sup> See G. P. Thomson, *Proc. Roy. Soc. London*, A119, Plate 12A, Fig. 3 (1928).

<sup>2</sup> R. Ironside, *Proc. Roy. Soc. London*, A119, p. 668 f. (1928).

### Absolute Value of the Wave-length

The final stage in the verification of de Broglie's theory is the comparison of the absolute value of the wave-length with that given by experiment. From each ring of each picture a separate wave-length could be deduced and compared with de Broglie's formula. But as the wave-length varies with the speed in the way we have shown, a better method is to assume the theoretical formula and use it to calculate 'a', the size of the unit cube, by means of Equation (6). The mean of all the plates can then be taken and compared with the value found by X-rays.

Where two measurements are given in Table IV, they refer to plates taken with different apparatuses. The table shows agreement within 2 per cent in all cases except in one set of measurements of gold, and in most cases the error is about 1 per cent. This is well within the error of experiment.

TABLE IV  
SIZE OF THE UNIT CUBE,  $a$

Metal	Measurements	
	X-ray	Cathode Ray
Aluminium . . . . .	$4.046 \times 10^{-8}$	$\left. \begin{array}{l} 4.06 \\ 4.00 \end{array} \right\} \times 10^{-8}$
Gold . . . . .	$4.06 \times 10^{-8}$	$\left. \begin{array}{l} 4.18 \\ 3.99 \end{array} \right\} \times 10^{-8}$
Platinum . . . . .	$3.91 \times 10^{-8}$	$\left. \begin{array}{l} 3.88 \\ 3.89 \end{array} \right\} 10^{-8}$
Lead . . . . .	$4.92 \times 10^{-8}$	$4.99 \times 10^{-8}$
Iron . . . . .	$2.87 \times 10^{-8}$	$2.85 \times 10^{-8}$
Silver* . . . . .	$4.079 \times 10^{-8}$	$4.11 \times 10^{-8}$
Copper* . . . . .	$3.60 \times 10^{-8}$	$3.66 \times 10^{-8}$
Tin (white),* spacing of (200) .	$2.91 \times 10^{-8}$	$2.86 \times 10^{-8}$

\* Measurements by Ironside, *loc. cit.*

The agreement is thus entirely satisfactory and we are driven to suppose that the electrons form diffraction patterns just similar to those which would be produced by waves of  $\lambda = h/mv$ . All we have had to assume, in deducing these results, is that each atom acts as a scattering centre and that the

scattered waves are coherent in phase and wave-length with the incident train. This last requirement means that there must be no loss of energy by the scattered electrons, which we have seen is experimentally verified. Besides these elastic collisions there are, no doubt, also inelastic ones. These will cause the continuous background which is always observed between the rings. Since the whole crystal influences the diffracted beam, the scattering in it, if it is regarded as due to a collision of the electron at all, must be considered to be one with the whole crystal. As this is of practically infinite mass there need be no transference of energy. If, on the contrary, the ray were scattered by another free electron energy would be transferred to the latter. If  $\phi$  is the angle of deviation of the ray, the fraction  $\sin^2\phi$  of the original energy is transferred. For the rings considered,  $\phi \sim 0.04$ ; thus the energy given to the free electron would be  $(0.04)^2$  of the original energy. This would be of the order 100 volts. Probably a collision with a bound electron would lead to much the same result if this energy were sufficient to ionise, as would be the case for the outer electrons. Thus the experiment serves to confirm the expectation that, if the scattering is regarded as a collision phenomenon, the collisions must be regarded as being with the crystal, or at least the atoms, rather than with electrons.

### Later Experiments

Muto and Yamaguti <sup>1</sup> have obtained good rings by diffraction of electrons from powders of magnesium oxide and graphite deposited on spider's web. The spacings agree well with those found for X-rays, and the intensities agree fairly.

Ponte <sup>2</sup> has studied powders of the oxides of magnesium and cadmium, and also zinc oxide, which can be prepared as a very thin film by burning a bead of zinc in air. For the first two he was able to verify de Broglie's law to an accuracy of 1 per cent for a range of voltage from about 7000 to 17,000. His most accurate experiments were made with the zinc oxide films, which gave very good rings and enabled the law to be

<sup>1</sup> Muto and Yamaguti, *Proc. Imp. Jap. Acad.* 5, p. 112 (1929).

<sup>2</sup> Ponte, *Compt. Rend.* 188, pp. 244, 909 (1929); *Ann. de Phys.* 13, p. 395 (1930).

established to 3 parts in 1000 from 8000 to 16,000 volts. No abnormality was observed at the energy corresponding to the K ring of zinc which falls in this range. Loria and Klinger<sup>1</sup> have continued the experiments with zinc oxide with about the same accuracy down to 4500 volts. In the course of his experiments on inner potential (p. 159) Tillman verified the law for several crystals using electrons of 4000-6000 volts.

### Reflection

Nishikawa and Kikuchi<sup>2</sup> were the first to show that diffraction patterns could be obtained by allowing electrons to strike the smooth surface of a crystal at glancing incidence. They used a crystal of calcite, and the patterns consisted of black and white lines similar to those previously obtained by Kikuchi with electrons transmitted through mica (see p. 111), and capable of a similar explanation. Emslie,<sup>3</sup> working at Aberdeen, soon afterwards got diffraction patterns from the surface of galena as well as calcite.

REFLECTION APPARATUS.—The form used by the authors is shown diagrammatically in Fig. 17; for experimental details

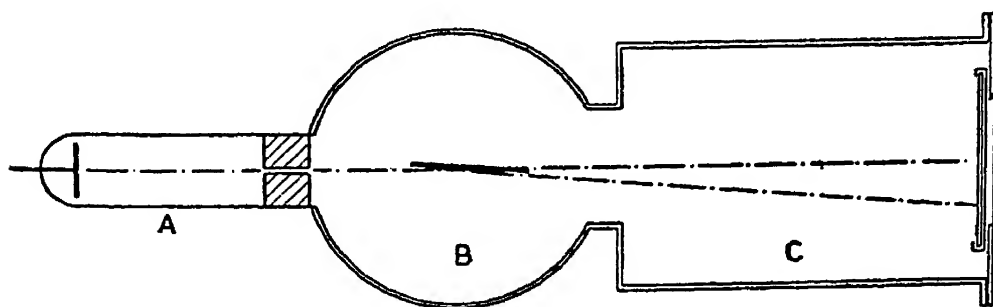


FIG. 17

see Chapter XVI. A is a gas-filled discharge tube from which a fine beam of homogeneous cathode rays passes into the crystal chamber B. The specimen is mounted so that the rays are incident on it at a small glancing angle. It can be adjusted by

<sup>1</sup> Loria and Klinger, *Acad. Polon. Sci. and Litt. Bul.* 1-2A, p. 15 (1937).

<sup>2</sup> Nishikawa and Kikuchi, *Proc. Imp. Jap. Acad.* 4, p. 475 (1928); *Nature*, 121, p. 1019 (1928).

<sup>3</sup> Emslie, *Nature*, 123, p. 977 (1929).

three independent motions without disturbing the vacuum. The angle  $\theta$  (Fig. 18) can be altered by rotation about an axis

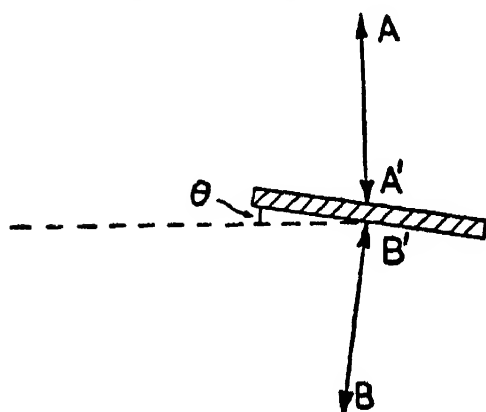


FIG. 18

through the specimen normal to the plane of the figure, the specimen can be moved bodily in the direction  $AA'$ , and it can be rotated about an axis  $BB'$  normal to its surface. After diffraction the electrons pass into the camera  $C$  (Fig. 17) and the pattern can be observed on a fluorescent screen, or a photographic plate can be moved into

place in front of the screen so that the electrons strike its sensitive side.

### Precision Measurements

The most accurate test up to the present of de Broglie's law has been made by von Friesen.<sup>1</sup> He used an etched crystal of galena as diffractor, the surface of this crystal when etched is covered with cubical lumps small enough to allow the electrons to pass through and, for the reason explained on p. 141, to allow the formation simultaneously of spectra of different orders. Von Friesen considered that the range of orders obtained was too great to be accounted for by this alone, and that the axes of different portions of the crystal were slightly inclined to one another, so that the Bragg condition could be nearly satisfied for several orders at once by different parts of the crystal. He used a slit set accurately parallel to a plane in the crystal instead of a pinhole, so that his diffracted pattern was composed of lines like an optical spectrum. The second, third and sometimes the fourth orders of reflection from the cube face (for which the effective spacing  $d$  is given by  $2d = 5.93515 \text{ \AA}$  at  $18^\circ \text{ C.}$ ), were produced on both sides of the direct beam by taking two exposures with the crystal rotated through  $180^\circ$  in between. Great care was taken to maintain the voltage constant by using a valve whose grid potential was governed by that of a condenser. The charge on the condenser was replenished through a photo-electric cell operated

<sup>1</sup> S. von Friesen, Inaugural Dissertation (Uppsala, 1935).

by light reflected from the mirror of a galvanometer. This galvanometer was operated by the current in a circuit in which a fraction of the accelerating voltage obtained by a high tension potentiometer was balanced against the voltage of a standard accumulator. The author expressed his results in terms of the unit of charge  $e$  by combining the value found for the wave-length at a given voltage with Rydberg's constant. From our point of view the interest lies in the verification of de Broglie's law which is shown by the agreement in Table V between the values found for  $e$  for different voltages and orders, and also by the good agreement of the mean value of  $e$  with that of other recent measurements by quite different methods.

TABLE V  
VALUE OF ' $e$ '

Order	2nd	3rd	4th	All Orders
25.8 KV . .	4.7974	4.7964	(4.7931)	4.7963
21.5 KV. . .	4.7957	4.7961	„	4.7959
17.8 KV. . .	4.7964	4.7973	„	4.7968
All voltages . .	4.7965	4.7966	(4.7931)	4.7963

The error of any single wave-length measurement is given as  $\pm 0.1$  per cent, that of the voltage as  $\pm 0.05$  per cent, and the final error in  $e$  as  $\pm 0.10$  per cent.

### De Broglie's Law at High Voltages

In the experiments so far described the relativity correction is small, about  $\frac{1}{2}$  per cent for every 10 KV. of accelerating voltage. The good agreement of von Friesen's results in which it was included is strong evidence in its favour, but measurements at high voltages, where it becomes really large, are important. Kosman and Alichanian<sup>1</sup> have diffracted electrons of as much as 520 KV. energy, but as they had no independent method of measuring the voltage their work affords no check on the relation between wave-length and momentum at high energies.

<sup>1</sup> Kosman and Alichanian, *Naturwiss.* 21, p. 250 (1933).

Hughes<sup>1</sup> has succeeded in getting diffraction patterns with the  $\beta$  rays of a radon source of energies up to 1037 KV. He used a film of gold spluttered on to thin gelatine, and the  $\beta$  rays were focused on to the photographic plate by the magnetic field in a long solenoid. This has the important advantage of increasing the intensity, and the current required to give a clearly focused spot serves as a measure of the momentum of the rays. The solenoid was calibrated by using cathode rays of known energy and therefore known momentum; this enabled Hughes to calculate the current required to focus the principal lines of the  $\beta$ -ray spectrum, and he found that these currents did in fact give a sharply focused central spot. In the reduction of the results, however, the standard values of  $H\rho$  were used, as obtained for the principle  $\beta$ -ray lines by the semicircular focusing method. Since values of  $H\rho$  are proportional to the momentum of the  $\beta$ -ray, Hughes' experiments check de Broglie's law in the simplest form,  $\lambda = h/mu$ , where  $m$  is the relativistic mass, and hence  $mu$  the relativistic momentum. The results from five plates with the apparatus in its final form are shown in Table VI. From one to three rings were measurable on each plate against a dense background, and their relative sizes agreed well with the simple theory.

TABLE VI

$H\rho$	Equivalent Voltage	$D/\sqrt{n}$ Mean	$H\rho D/\sqrt{n}$ Mean
1938	264 KV.	0.523	1013
2980	520 KV.	0.338	1007
4866	1037 KV.	0.207	1006

The value for the cube side of gold found from the mean of these is 3.94 Å, which when compared with the true value of 4.07 Å, gives an error of 3 per cent. Earlier measurements had given a value to 4.14 Å. It appears, then, that the theory holds up to a million volts to better than 5 per cent.

This result is important because the theory given by de Broglie is incomplete since it takes no account of the spin of the electron; it appears that the terms involving spin should

<sup>1</sup> Hughes, *Phil. Mag.* 19, p. 129 (1935). See also Curran, *Phil. Mag.* 24, p. 953 (1937).

become important for speeds near the velocity of light. Thus Equation 5 (p. 15) is incomplete, and it is interesting that it does in fact give the right value for the wave-length. Dirac's theory, which includes spin, gives the same result, but as we shall see (Chapter XX), its predictions in one case conflict with experiment.

### Resolving Power

The sharpness of the patterns formed by the diffraction of electrons is limited by a variety of causes: the finite size of the original beam, the limited extent of the individual crystals, and the lack of homogeneity of the rays. Closely associated with the last cause is a possible limitation in the number of coherent waves forming the train associated with each electron. Observations of the sharpness of the patterns, as measured, for

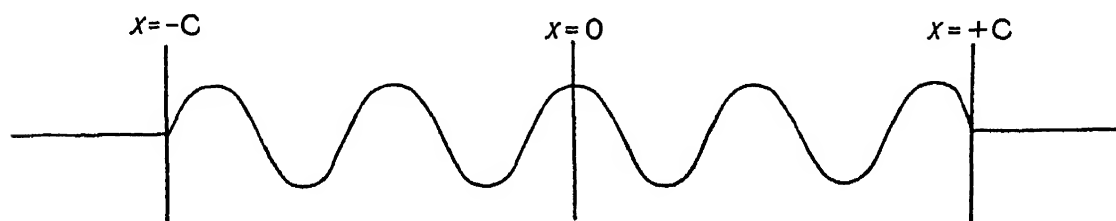


FIG. 19

example, by the closeness of the rings, which can just be seen separate, are of interest as giving information on this last point, especially if the conditions of experiment are chosen so that the width of the rings (due to the size of the beam, the smallness of the crystals and fluctuations in the voltage of the source of electrons) is kept as small as possible. It is then possible to deduce a lower limit for the number of waves in the train of the electrons.

If the beam is considered infinitely fine and the number of elements in the crystals infinite, the width of the rings can be calculated in terms of the number of waves in the train as follows. Consider a train of waves of length  $2C$ , where  $C$  is large compared with  $\lambda$ . Apply Fourier's analysis to a function  $f(x)$  which is equal to  $\cos 2\pi x/\lambda$  from  $x = -C$  to  $x = +C$  and is zero outside these limits (Fig. 19). It can be shown that

$$f(x) = \frac{1}{\pi} \int_0^{\infty} \cos px \left[ \frac{\sin (2\pi/\lambda + p)C}{2\pi/\lambda + p} + \frac{\sin (2\pi/\lambda - p)C}{2\pi/\lambda - p} \right] dp.$$

The coefficients of  $\cos p\kappa$  are small except when  $p$  is nearly equal to  $2\pi/\lambda$ , thus the predominant wave-lengths in the expansion are not very different from  $\lambda$ . For these the second term in the bracket is the important one, and when  $p = 2\pi/\lambda$  it becomes equal to  $C$ . As  $p$  differs more and more from  $2\pi/\lambda$  the second term diminishes and becomes zero when  $p = 2\pi/\lambda \pm \pi/C$ . We shall suppose the effective range of wave-length to correspond with this range of  $p$  and writing the range as  $\lambda \pm \Delta\lambda$  it can easily be seen that  $\Delta\lambda/\lambda = \pm\lambda/2C$ .

In a good photograph the rings corresponding to  $\sqrt{19}$  and  $\sqrt{20}$  of the cubic structure are clearly resolved. This means that the radius of the former ring for  $\lambda + \Delta\lambda$  is less than that of the latter for  $\lambda - \Delta\lambda$ . If we equate them we have

$$\sqrt{19}(\lambda + \Delta\lambda) = \sqrt{20}(\lambda - \Delta\lambda) \text{ whence } 2C/\lambda = \frac{\sqrt{20} + \sqrt{19}}{\sqrt{20} - \sqrt{19}} = 95,$$

so that there must be at least 95 waves in the group. The precision measurements of von Friesen (p. 50) raise this figure to 225. The actual number is probably enormously greater and is determined by the 'uncertainty principle' (Chapter V), but the above calculation is of importance as showing the least number which could explain the observed sharpness of the ring even if all the breadth were ascribed to this cause.

A corresponding calculation can be made of the lateral extension of the waves, for it is obvious that only those atoms of a crystal can produce wavelets capable of coherent interference which are covered by the wave-front of a single electron. In making the calculation a point comes up which will be dealt with more thoroughly later on but can be briefly explained as follows.

Owing to the weak penetrating power of electrons only thin films can be used in transmission, and the best patterns are given by films not much more than  $10^{-6}$  cm. thick. Consider a spot due to reflection from a crystal plane which, since the angles are small, must be nearly normal to the film (Fig. 20). If the thickness  $t$  is  $10^{-6}$  the reflected beam has a breadth  $10^{-6} \sin \theta$ . Such a beam, if left to itself, will spread by diffraction through an angle  $\pm\phi$  given by  $\phi \cdot 10^{-6} \sin \theta = \lambda$ . With usual values of  $\theta$  and  $\lambda$ ,  $\phi$  comes out actually larger than  $\theta$ , so that there is apparently no well-defined beam at all, all the orders

overlapping. The apparent conflict with experiment is removed when we consider the other parallel planes. Waves reflected from such planes (Fig. 21) can be represented each as a single ray, AA' etc., coming from the centre of the plane. This group of rays is the same as would be given by a plane grating at nearly normal incidence and will give sharp spectra if there are a sufficient number of rows of atoms. Applying the usual treatment for the resolving power of a plane grating, the angular distance between the maximum and first minimum for a

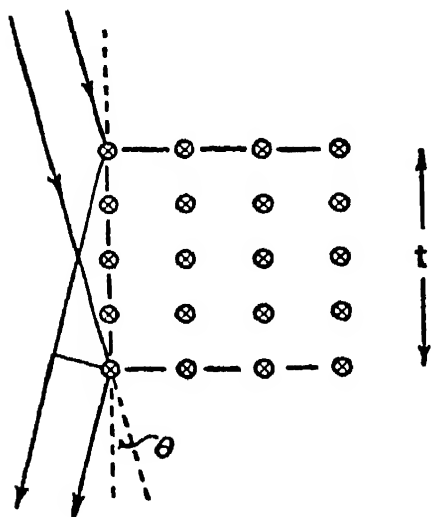


FIG. 20

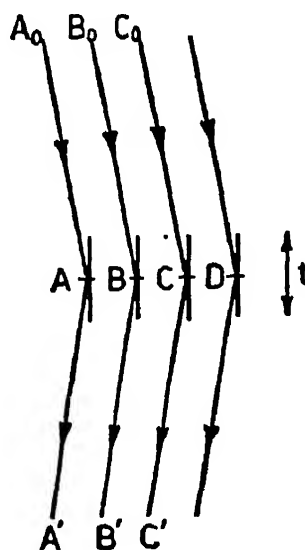


FIG. 21

diffracted beam is  $\delta\theta = \lambda/Nd$ , where  $N$  is the number of planes. Now if  $\sqrt{19}$  and  $\sqrt{20}$  of diameters  $D_{19}$  and  $D_{20}$  are just resolved,  $\delta\theta = (D_{20} - D_{19})/2L = \lambda/d_{20} - \lambda/d_{19} = \lambda(\sqrt{20} - \sqrt{19})/a$ . Therefore the width of the beam, which is approximately  $Nd$ , must be at least  $a/(\sqrt{20} - \sqrt{19}) = 10a$ . Thus the beam must extend over 10 crystal cells or about 40 Å. Von Friesen estimates the resolving power of his crystal in the second order as 150. The value of  $d$  was 2.97 Å and the corresponding width of the beam is 223 Å.

Since the deviation due to a plane grating depends on the angle of incidence, a 'powder' composed of single layers of atoms would give diffractions at all angles. The Bragg setting corresponds to minimum deviation, since the angles with the normal of incident and diffracted rays are equal, and a pattern would be formed in which the rings, in the calculated positions,

would appear as the edges of regions of brightness. In practice the crystals are usually thick enough only to give reflections when set within a few degrees of the Bragg angle, and for this range the deviation, which depends on the cosine of the angle of incidence, is very nearly constant.

## CHAPTER V

### THEORETICAL INTERPRETATION

It is worth while to consider carefully what theoretical deductions may be made from experiments such as those referred to in Chapter IV. A point of importance is the fact that, in the transmission experiments, there would seldom have been more than one electron in the film at once. Thus, since it is almost inconceivable that an electron outside the film should influence the process of diffraction, one must suppose that each individual electron is treated by the film in such a way as to make it much more likely that the electron will fall on or near a ring than in the regions between.

The results of the transmission experiments may be approximately explained by the following assumptions :

(1) Each electron is associated with a wave of approximate wave-length  $h/mu$ , the length of the train being at least 200 waves and the breadth in the wave front at least  $200 \times 10^{-8}$  cm. in certain cases.

(2) Each atom of the crystal is the centre of a wavelet coherent with the original wave, and whose intensity varies with the angle to the original direction of motion of the electron, in a manner which can be calculated from the distribution of charge in the atom (p. 91).

(3) The chance of the electron appearing at any place with its original energy is proportional to the intensity of the composite wave formed by the wavelets.

It should be noticed that the electron is detected by any of a number of processes, such as the charging of a Faraday cylinder, the development of the grain of a photographic plate, or a scintillation on a screen, all of which can be interpreted only as the arrival of a particle with a certain charge and energy.

(4) There is also a chance of the electron losing energy in passing through the crystal. In this case its deflection is governed by other laws of which little is known at present.

It should be emphasised that, at least so far as present knowledge goes, the behaviour of any particular electron must be expressed in terms of probability. For example, in a transmission experiment there is no way of knowing in advance whether any given electron will appear in the central spot or on a ring, and the same difficulty would arise even if the crystal were large and there were only one Laue spot to which diffraction could occur. In addition there is always a probability of inelastic collision. It seems possible, however, at least in theory, to regard each electron as an individual particle fastened in such a way to a wave system obeying Equation (5), p. 15, that it always moves along the wave normal. The expression for the necessary velocity has been given in practically equivalent forms by de Broglie<sup>1</sup> and Schrödinger. The following treatment is from Sommerfeld.<sup>2</sup> We have

$$\frac{\partial \psi}{\partial t} = \frac{h}{4\pi i m} \left( \nabla^2 - \frac{8\pi^2 m}{h^2} F \right) \psi$$

from Equation (6) p. 17. For the conjugate  $\psi^*$  :

$$\frac{\partial \psi^*}{\partial t} = -\frac{h}{4\pi i m} \left( \nabla^2 - \frac{8\pi^2 m}{h^2} F \right) \psi^*.$$

Multiply the first equation by  $\psi^*$ , the second by  $\psi$  and add, thus eliminating  $F$ ,

$$\frac{\partial}{\partial t} (\psi \psi^*) = \frac{h}{4\pi i m} (\psi^* \nabla^2 \psi - \psi \nabla^2 \psi^*).$$

Now, whatever the functions  $\psi$ ,  $\psi^*$ ,

$$\begin{aligned} \psi^* \frac{\partial^2 \psi}{\partial x^2} - \psi \frac{\partial^2 \psi^*}{\partial x^2} &= \frac{\partial}{\partial x} \left( \psi^* \frac{\partial \psi}{\partial x} - \psi \frac{\partial \psi^*}{\partial x} \right), \\ \dots\dots\dots &= \dots\dots\dots \\ \dots\dots\dots &= \dots\dots\dots \end{aligned}$$

Hence

$$\psi^* \nabla^2 \psi - \psi \nabla^2 \psi^* = \text{div} (\psi^* \text{grad } \psi - \psi \text{grad } \psi^*)$$

and

$$\frac{\partial}{\partial t} (\psi \psi^*) + \frac{h}{4\pi i m} \text{div} (\psi \text{grad } \psi^* - \psi^* \text{grad } \psi) = 0.$$

<sup>1</sup> L. de Broglie, *J. phys. radium*, 8, p. 225 (1927).

<sup>2</sup> Sommerfeld, 'Atombau und Spectrallinien' in *Wellenmechanische Ergänzungsband*, 105.

Schrödinger has shown that the quantity  $e(\psi\psi^*)$  behaves like the density of electricity. Hence the above equation may be regarded as expressing that no electricity is created or destroyed, if we take the quantity in parentheses as proportional to a current. We have, in fact, the current density

$$j = \frac{eh}{4\pi im} (\psi \text{ grad } \psi^* - \psi^* \text{ grad } \psi).$$

If the density of a continuous distribution of electricity of one sign is  $\rho$  and the current is  $j$  then the velocity is  $j/\rho$ . In the above case this is

$$w = \frac{eh}{4\pi im} \frac{\psi \text{ grad } \psi^* - \psi^* \text{ grad } \psi}{e\psi\psi^*} = \frac{-h}{2\pi im} \text{IM}[\text{grad } \log \psi],$$

where IM signifies 'the imaginary part of'. Sommerfeld and Schrödinger appear to prefer to deal rather with the above expression for the current than with the velocity, but de Broglie uses an expression equivalent to the above for  $w$ . It should be noticed that if we turn back to Chapter I and substitute for our original wave expression  $\psi = a_{xyz} \sin (nt - \phi_{xyz})$  the complex form  $\psi = a_{xyz} e^{i(nt - \phi)}$ , then

$$\begin{aligned} \text{IM}[\text{grad } \log \psi] &= \text{IM}[\text{grad } \log a_{xyz} + i \text{ grad } (nt - \phi)] \\ &= -i \text{ grad } \phi. \end{aligned}$$

Thus

$$w = \frac{h}{2\pi m} \text{ grad } \phi.$$

The phase velocity

$$v = \frac{n}{\text{grad } \phi} = \frac{2\pi mc^2}{h(\text{grad } \phi)} = \frac{c^2}{w}$$

and  $vw = c^2$ . This is the extended form of the relation which holds for monochromatic plane waves in the form  $Vu = c^2$ , where  $V$  is the *wave* velocity and  $u$  that of the corresponding particle.

So far we have been dealing in differential equations regarded as expressing the behaviour of a continuous distribution of electricity. To bring this into line with the experimentally observed discontinuity of electric charge it is usual to reinterpret  $\psi\psi^*$  as the probability (per unit volume) of the presence of an electron near an assigned place. The continuity equation

then tells us that, if we have a dense swarm of electrons distributed according to this law, they will continue to be distributed according to it if they move with the velocity  $w$  found above. The swarm indeed need not even be dense, if the state of motion is steady and continues for a sufficiently long time. It follows that all the results of our experiments can be stated in the form, that an electron moves along the normal to a certain wave  $\psi$  with velocity  $w$ , where  $\psi$  is determined as a solution of Equation (4), p. 15 (which of course includes (5) as a special case), with the value of  $F$  appropriate to the crystal used. This apparently replaces probability by certainty; but the change is apparent only, for we do not know along which wave normal any given electron has started, and normals originally close together may and will ultimately

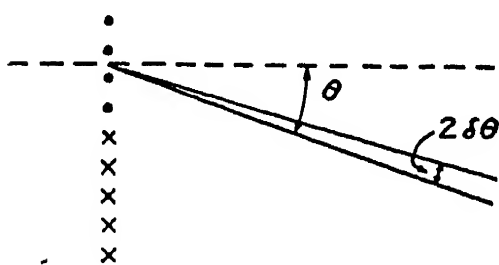


FIG. 22

diverge widely. Nevertheless, the above view seems to us helpful in enabling one to form a mental picture of what is taking place. On this view, then, one regards each electron as accompanied by a wave which guides it. The electron is obliged,

by the law of its existence, to move always along the normal to this wave at the speed given by the above expression. The form of the wave is governed by the nature of the expression for  $F$  which described the field in which it moves; thus the presence of an atom will influence the motion of the electron even though the particular wave normal along which the electron is moving may pass the atom at a considerable distance. However, the effect of a distant atom will, in general, be less than that of one near the line of motion. To illustrate this, consider electrons incident normally on a plane grating consisting of a rather small number of atoms (Fig. 22). The electrons will be diffracted, but since the resolving power is limited the diffracted beam will be wide, and the electron may, with about equal probability, be at any angle from  $\theta - \delta\theta$  to  $\theta + \delta\theta$ . The atoms have deflected it through an angle of the order of  $\theta$ . Now add an equal number of atoms ( $\times$  in Fig. 22) at one end of the grating. Apart from a doubling of the intensity (if the electron beam is sup-

posed to extend over the whole of the new grating) the effect of the doubled resolving power is to diminish  $\delta\theta$  to  $\frac{1}{2}\delta\theta$ . We may say that the effect of the added atoms on those electrons which passed through the original part of the grating has been to deflect them through an angle,  $\frac{1}{2}\delta\theta$ , small compared with the angle  $\theta$  through which they were deflected by the original set of atoms close at hand.

It seems necessary to suppose a separate wave system for each electron, not only because the diffraction takes place under conditions when only one electron is present in the film at a time, but also because it would be perfectly possible to detect the electrons separately and so each must be regarded as an individual. But this view raises difficulties concerned with the length of the train of waves. A monochromatic train extends to infinity in both directions and is a physical impossibility. It is difficult to see, for example, how the length of an approximately uniform train for an electron in a diffraction experiment could exceed the distance between the cathode and the photographic plate. But if the train is not monochromatic it can be analysed into Fourier components of different wave-lengths and these waves will have an appreciable intensity over a finite range. To each wave-length corresponds a velocity by the formula  $\lambda = h/mu$ . Which are we to take as the velocity of the electron?

Without further information the velocity must be regarded as indeterminate, and this view is in agreement with the 'uncertainty principle' due to Heisenberg, which has had great influence on physics in recent years. This principle asserts that between any coordinate  $q$  of a particle and its canonically conjugate momentum  $p$  the relation exists that, if  $\Delta q$  is the uncertainty with which the first can be measured and  $\Delta p$  that for the second, then  $\Delta p \Delta q \sim h/2\pi$ . This statement was originally deduced from a detailed consideration of the errors involved in measurements owing to the interaction of the means of detection (light quantum or electron) with the object to be investigated. On the wave theory it appears as a natural consequence of the above considerations concerning finite wave trains. Thus we can only be perfectly certain of the velocity of an electron when it is associated with an infinite wave train, and then its position is quite indeterminate; for

we cannot proceed to determine the position without cutting the train. If the train is of length  $l$ , that is the uncertainty of position. The corresponding uncertainty of momentum can be found as follows. Let there be  $N$  waves in the train, then the result on p. 54 shows that the wave-length ranges from  $\lambda - \Delta\lambda$  to  $\lambda + \Delta\lambda$ , where  $N = l/\Delta\lambda$ . Hence  $\Delta\lambda = \lambda^2/l$ . But  $\lambda = h/p$ , therefore

$$\Delta p = -\frac{h\Delta\lambda}{\lambda^2} = -\frac{h}{l}, \quad \text{or} \quad \Delta p \Delta q = h,$$

the sign having no significance. Here we have assumed a distribution of waves with constant intensity over a range  $\lambda - \Delta\lambda$  to  $\lambda + \Delta\lambda$ , thus  $\Delta\lambda$  is the maximum uncertainty from the mean. The probable error will be less. In the particular

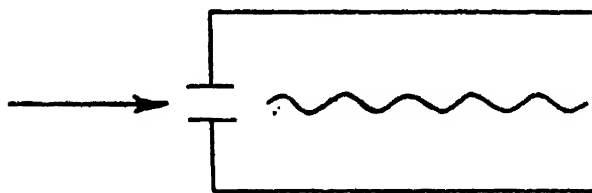


FIG. 23

case of a distribution of intensity following the error law it can be shown that  $\Delta p \Delta q = h/2\pi$ . In all cases it will be of this order.

Thus we can only determine the momentum of a particle accurately if we have a long train of waves available, which makes the position uncertain, and conversely.

To take a concrete case: let us suppose that a stream of electrons is allowed to enter a chamber through a valve open for only a very short time, as in Fig. 23. Such a valve might, for example, consist of a condenser across which a sufficient potential could be placed to drive the electrons to the sides and so exclude them from the vessel. Then the train of waves allowed to enter is of finite length and, however homogeneous the incident beam of electrons, those inside will show a variation in momentum or an 'uncertainty', the more pronounced the shorter the time during which the valve was open. By the ordinary view one would attribute this variation to a disturbing force exerted by the mechanism of the valve, but the argument shows that whatever this mechanism may be, there is an irreducible minimum of uncertainty for any given length of wave train.

A similar uncertainty attaches to the position in the wave-front, with which is correlated sideways velocity. In fact if

we have an infinite plane wave, whose direction can be determined with perfect exactness, the position in the wave-front is quite indefinite. By contracting the wave-front the position can be made more certain, but the direction then becomes uncertain, for the waves will spread by diffraction. If the wave-front is reduced to a point the direction becomes completely undermined. The nature of the relation between the two uncertainties can easily be seen. If a plane wave of width  $d$  be admitted through a slit (Fig. 24) there will be appreciable diffraction up to an angle  $\lambda/d$  on either side. The original momentum was  $p$ ; the sideways component of the diffracted momentum is thus anything between

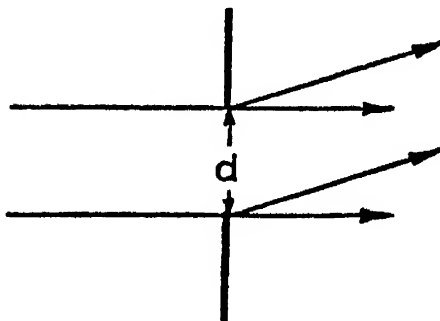


FIG. 24

$\pm \lambda p/d$ . But  $\lambda = h/p$ , so this becomes  $\pm h/d$  and the uncertainty of position is  $\pm d/2$  in the same sideways direction, so that the product of the two uncertainties for this direction is  $h/2$ .

Another pair of canonically conjugate quantities are time and energy. Thus if the energy of a system is to be known very exactly the experiment must extend over a considerable time. Suppose the system whose energy is required is a photo-electron. Its energy will be known if the energy level from which it comes is known and also the frequency of the light which ejected it. [We may suppose the electron to come from a gas molecule in a good vacuum and so get rid of the additional uncertainty caused by collisions.] But if the time is restricted to an interval  $t$  there will only be  $t\nu$  waves of light incident on the atom, and the frequency will be uncertain by a fraction of the order  $1/t\nu$  giving an uncertainty of energy  $h\nu/t\nu = h/t$  and the result follows as before. One cannot say that a given particle has a definite energy at a given time, any more than one can say that it has a definite frequency. Thus the conservation of energy only has a meaning if sufficient time is available for observation.

This 'uncertainty' principle has been regarded as destroying the basis for the idea of determinism in physics. If the world is subject to an irreducible uncertainty it is impossible to say that definite effects follow definite causes, because we

do not know with sufficient certainty either the causes or the effects. While this is undoubtedly true, as far as it goes, it may be pointed out that exact laws are not excluded by the fact that they are unverifiable. It seems to be purely a matter of convenience. There is no object in discussing exact laws which cannot be verified, if the inexact laws will explain the observations with convenience; but conversely, there should be no objecting to postulating laws and quantities which afford a convenient and graphic mode of expression, merely because they are not observable without introducing uncertainties. Such an objection would apply equally to the introduction of the electric and magnetic vectors as separate quantities in general electrodynamic theory, for the only quantity that can be really observed, viz. the force on a charged particle, is compounded from them. It seems, then, quite legitimate to keep to the idea of a particle moving with definite velocity, even in the case of short wave-trains where this velocity cannot be accurately measured. It is of interest to consider what this velocity actually turns out to be. Darwin has investigated a number of cases of the propagation of groups of waves corresponding to free electrons.<sup>1</sup> The simplest case is that of one dimension and no external forces.

Darwin takes the equation

$$\frac{1}{2}(h/2\pi i)^2 \frac{\partial^2 \psi}{\partial x^2} = -\frac{h}{2\pi i} \frac{\partial \psi}{\partial t}$$

(the change of sign from our Equation 6, p. 17, is merely a change from  $\psi$  to  $\psi^*$ ) and assumes a solution of the type

$$\psi(x, t) = \int e^{\frac{i2\pi}{h}(px - p^2t/2m)} \phi(p) dp,$$

where  $\phi(p)$  is to be determined to fit the initial conditions. This expression is equivalent to taking the sum of a number of waves corresponding to momenta  $p$ . Notice that, as the relativity mass is not used, the wave velocity,  $p/2m$ , is quite different from the value given by the general theory. The change is equivalent to taking out the high frequency  $m_0c^2/h$

<sup>1</sup> C. G. Darwin, *Proc. Roy. Soc. London*, A117, p. 258 (1927).

from all the vibrations and, as it were, observing the heterodyne waves instead of the original train. It does not, however, affect questions of wave-length or of the motion of the particles.

For the wave at  $t=0$  Darwin assumes

$$f(x) = \exp \left[ -\frac{1}{2\sigma^2}(x - x_0)^2 + i\frac{2\pi}{h}mv(x - x_0) \right].$$

This is a group centred round  $x = x_0$  with an intensity  $\rho = e^{-(x-x_0)^2/2\sigma^2}$  so that  $\sigma$  represents the uncertainty with which the electron is situated at  $x_0$ . The independent quantity  $v$  determines the wave-length, but for the moment we will not attribute any other physical significance to it. To determine  $\phi(p)$  we have at  $t=0$

$$\int e^{i\frac{2\pi}{h}px} \phi(p) dp = f(x) = \exp \left[ -\frac{1}{2\sigma^2}(x - x_0)^2 + i\frac{2\pi}{h}mv(x - x_0) \right],$$

of which the solution is

$$\phi(p) = \frac{\sigma}{h} \sqrt{2\pi} \exp \left[ -\frac{1}{2} \left( \frac{2\pi\sigma}{h} \right)^2 (p - mv)^2 - i\frac{2\pi}{h}px_0 \right];$$

substitute in the equation for  $\psi$  and integrate :

$$\psi(x, t) = \frac{\sigma}{\left( \sigma^2 + \frac{i\hbar t}{2\pi m} \right)^{\frac{1}{2}}} \exp \left[ -\frac{\frac{1}{2}(x - x_0 - vt)^2}{\sigma^2 + \frac{i\hbar t}{2\pi m}} + i\frac{2\pi}{h}mv(x - x_0 - \frac{1}{2}vt) \right].$$

To find the intensity, *i.e.* the probability of an electron at any given place, we multiply by the conjugate and find

$$\rho(x, t) = \frac{\sigma}{[\sigma^2 + (\hbar t/2\pi m)^2]^{\frac{1}{2}}} \exp \left[ -\frac{(x - x_0 - vt)^2}{\sigma^2 + (\hbar t/2\pi m)^2} \right];$$

thus the electron at time  $t$  is most likely to be at  $x_0 + vt$  and the uncertainty is  $\sqrt{\sigma^2 + (\hbar t/2\pi m)^2}$ . We may now regard  $v$  as a kind of most probable velocity.

It should be noticed that the use of the imaginary in this work differs from that in ordinary wave theory where we end by taking the real part. Here we are rather concerned on the one hand with the modulus of the complex quantity which gives us the electric density, and on the other with the argument

which gives the velocity. A graph, for example, of the real part of  $f(x)$  would have no physical significance. The uncertainty  $[\sigma^2 + (ht/2\pi\sigma m)^2]^{\frac{1}{2}}$  may be regarded as compounded, by the method of squares, of the two independent uncertainties  $\pm\sigma$  and  $\pm ht/2\pi\sigma m$ ; the latter corresponds to an uncertainty  $h/2\pi\sigma$  in momentum and the product of this with the uncertainty of initial position is  $h/2\pi$ , in agreement with Heisenberg.

Now consider the above from the point of view of our definition of velocity :

$$\begin{aligned} w &= \frac{h}{2\pi m} \text{IM}[\text{grad log } \psi] \\ &= v + \frac{h^2 t}{4\pi^2 m^2} \frac{x - x_0 - vt}{\sigma^4 + \frac{h^2 t^2}{4\pi^2 m^2}} \\ &= v + \frac{(x - x_0 - vt)t}{t^2 + T^2}, \end{aligned}$$

where

$$\sigma^2 2\pi m / h = T.$$

If  $x$  is the coordinate of the electron particle,  $w = dx/dt$ . Let  $y = x - vt$ , then

$$\frac{dy}{dt} = \frac{t(y - x_0)}{t^2 + T^2},$$

which gives

$$x = x_0 + vt + C\sqrt{t^2 + T^2}.$$

The constant of integration  $C$  is determined by the initial conditions. If the value of  $x$  for the particle at  $t = 0$  was really  $x = x_0 + \xi$ , then the value at any later time is

$$x = x_0 + \xi\sqrt{1 + (t/T)^2}.$$

Initially the velocity is  $v$  in all cases ; it then changes and when  $t$  is large

$$x = x_0 + vt + \frac{\xi t}{T},$$

giving a velocity  $v + \frac{\xi}{T}$ .

This change of the velocity presumably implies a spontaneous change in the energy of the electron, for the energy is regarded

as associated with the particle rather than with the waves. At first sight this seems inadmissible, but the whole idea of the uncertainty principle implies an ignoring of the conservation of energy where, as here, the time of observation is limited.

The irregular disturbance spreads because the groups of which it may be regarded as composed move at different rates. The speed with which it is necessary to move in order to keep always with waves of the same wave-length is the group velocity for this wave-length. This, by the original de Broglie theory, is the speed  $u$  of the particle for which  $\lambda = h/mu$ ; thus the particle has, always, a speed appropriate to the group of waves with which it is for the moment moving. As the waves spread out the particle tends to a fixed velocity and so moves with a certain group of waves. Which group, of the many possible, is chosen must be regarded as determined by the chance of the initial position of the particle with respect to the wave.

Such a train of waves will, in general, contain a very large number of waves. Thus, suppose an electron released initially photo-electrically with a train of, say, 1000 waves. There is an uncertainty of 0.1 per cent in wave-length and the same in group velocity; thus when the whole has gone, say, 10 cm. it will have spread over 1 mm., but for an electron of only 150 volts energy this is  $10^7$  waves. Had the initial train been assumed shorter, the spread would have been still greater. In the above example the  $10^7$  waves range over a difference of 0.1 per cent in wave-length; if the train had been shorter, though the spread would have been greater, the range of wave-lengths covered would have been greater also. The length of the train with a wave-length within 0.1 per cent of the wave-length corresponding to a 150-volt electron, would have been the same. It should be remembered that the idea of a group comprising an infinitesimal range of wave-lengths is an idealisation which, like that of a monochromatic wave, requires in strictness an infinite length of train. Thus the group idea will give useful results only after the waves have spread to such an extent that the apparent wave-length changes relatively slowly along the train.

The above theoretical work, including the equations in Chapter II, does not apply in a magnetic field. In this case

the current vector depends not only on  $\psi$  but also on the magnetic field. The field acts like a crystalline medium for the electron waves in that the ray, or path of energy, is no longer normal to the wave front. Thus it would be impossible to obtain an expression for the velocity determined only by the wave. This case was considered by de Broglie<sup>1</sup> at an early stage of the theory, but it does not seem worth while to consider it in detail here, for the assumption that the wave can be expressed by a single quantity  $\psi$  neglects that property of the electron which was expressed as its spin on the orbit theory. Since the spin is intimately connected with the magnetic properties of the electron it is not surprising that some such difficulty as the above should arise. The solution of it involves the use of more complicated expressions for the waves and is discussed in Chapter XX.

### Problems involving More than One Electron

There are two classes of 'many-electron' problems. One which can be treated by representing a stream of electrons as a solution of a wave equation with only three variables; the other in which the wave equation itself must involve  $3n$  independent variables, as in the case of a complicated atom. The former method is equivalent to ignoring the mutual action between the electrons or, at most, to representing it by its average effect on the potential. There is no essential difference from the case of one electron. If, indeed, as is commonly done, the initial beam of electrons is represented by a monochromatic wave, this is an idealisation even for a single electron; but however the electron was originally produced and whatever its original wave-train, by the time it has gone even a fraction of a millimetre there will be a train of an immense number of waves over which the change in wave-length is quite negligible. The assumption of a monochromatic wave is thus justified for all practical purposes; and if there are many electrons the only difference is an increase in the effective amplitude of the wave, as long as the Coulomb and Ampère forces between the electrons are negligible. Each electron has its own wave system which determines the chance of its being at any

<sup>1</sup> L. de Broglie, *Ondes et mouvements* (Paris, 1926), p. 31.

assigned place. The assumption of a single wave for the whole beam is merely a convenient way of superposing the essentially independent effects of the separate electrons.

When, however, the importance of the mutual interactions makes it necessary to use a many-dimensioned wave equation, the definition of velocity which we have used so far breaks down. This case occurs especially with the electrons which form part of an atom. In these cases the conception of velocity loses most of its value as there is no practical means of measuring it, even approximately. Schrödinger has shown, however, that it is possible, even in this case, to devise a consistent definition. Thus, if the density associated with electron  $\sigma$  is defined by

$$\rho_{\sigma} = \int \dots \int \psi \psi^* \tau_1 \tau_2 \dots \tau_{\sigma-1} \tau_{\sigma+1} \dots \tau_N,$$

where the quantities  $\tau_1$ , etc., are the elements of space associated with the various electrons, and if we define a quantity

$$\iota_{\sigma} = \int \dots \int \frac{h}{4\pi im} (\psi \text{ grad } \psi^* - \psi^* \text{ grad } \psi) \tau_1 \tau_2 \dots \tau_{\sigma-1} \tau_{\sigma+1} \dots \tau_N,$$

then 
$$\frac{\partial \rho_{\sigma}}{\partial t} + \text{div } \iota_{\sigma} = 0.$$

Thus if  $\rho_{\sigma}$  is regarded as measuring the probability of the presence of the electron,  $\iota_{\sigma}/\rho$  may be taken for its velocity.

## CHAPTER VI

### EXTENDED THEORY OF DIFFRACTION

#### Reciprocal Lattice

THE conditions of diffraction can be put into a specially convenient form by making use of Ewald's 'reciprocal lattice', which is defined as follows: Let the unit cell of the crystal be determined by three vectors  $\alpha_1, \alpha_2, \alpha_3$  representing the edges

which meet in the origin  $O$ , so that any lattice point is given by  $\mathbf{r} = \nu_1 \alpha_1 + \nu_2 \alpha_2 + \nu_3 \alpha_3$ , where  $\nu_1, \nu_2, \nu_3$  are integers. Draw from  $O$  three vectors  $\beta_1, \beta_2, \beta_3$  such that  $\beta_2 = [\alpha_2 \alpha_3]/v$ , etc.,<sup>1</sup> where  $v$  is the volume of the unit cell of the crystal;

$$v = (\alpha_1 [\alpha_2 \alpha_3]) = (\alpha_2 [\alpha_3 \alpha_1]) = (\alpha_3 [\alpha_1 \alpha_2]).$$

Treat these vectors as the edges of the unit cell of a new lattice and imagine this reciprocal lattice extended to infinity. [If the axes are rectangular, the vectors  $\beta$  are parallel to  $\alpha$  and  $|\beta_1| = 1/|\alpha_1|$ , etc., thus the spacings of the reciprocal lattice are

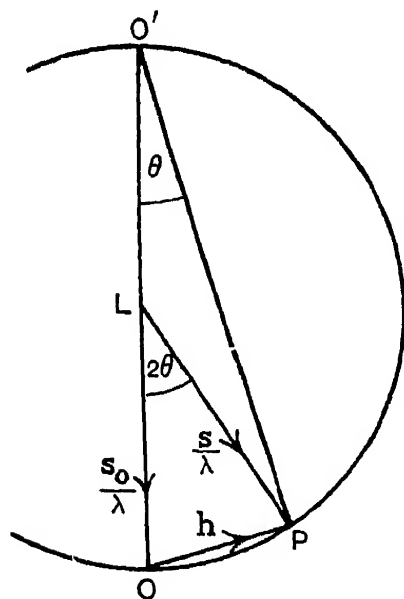


FIG. 25

large where those of the original lattice are small and *vice versa*.] Any point of the reciprocal lattice can be connected to the origin by a vector

$$\mathbf{h} = A_1 \beta_1 + A_2 \beta_2 + A_3 \beta_3.$$

The connection between the reciprocal lattice and diffraction can be seen as follows. From  $O$  draw  $OL = 1/\lambda$  in a direction

<sup>1</sup> The brackets  $[ ]$  are used to denote 'vector product', *i.e.* a vector normal to the plane of the multiplied vectors and of magnitude equal to the area of the parallelogram of which they are edges. The brackets  $( )$  denote scalar product, *i.e.* the product of the absolute magnitudes of the two vectors and the cosine of the angle between them.

opposed to that of the incident electrons. With centre L describe a sphere (the Ewald sphere) through O. We will prove that if this sphere passes through any point P of the reciprocal lattice, the direction LP will be that of a diffracted beam satisfying the Laue (and Bragg) conditions. Let  $\mathbf{s}_0$  be unit vector along the incident ray,  $\mathbf{s}$  unit vector in the direction of diffraction, then the path difference between wavelets scattered at the origin and at the lattice point  $\mathbf{r}$  is the difference between the projections of  $\mathbf{r}$  on the directions of  $\mathbf{s}_0$  and  $\mathbf{s}$ , *i.e.*  $(\mathbf{r} \cdot \overline{\mathbf{s} - \mathbf{s}_0})$ . Hence the Laue conditions require that  $(\mathbf{r} \cdot \overline{\mathbf{s} - \mathbf{s}_0})/\lambda$  is integral for all  $\mathbf{r}$ .

But 
$$\frac{\mathbf{s} - \mathbf{s}_0}{\lambda} = \mathbf{OP} = \mathbf{h} = \sum_3 \mathbf{A}_i \boldsymbol{\beta}_i$$

and 
$$\frac{1}{\lambda} (\mathbf{r} \cdot \overline{\mathbf{s} - \mathbf{s}_0}) = (\mathbf{r} \cdot \mathbf{h}) = A_1 \nu_1 + A_2 \nu_2 + A_3 \nu_3,$$

since  $(\boldsymbol{\alpha}_a \boldsymbol{\beta}_b)$  is zero if the suffices are different, as the vectors are perpendicular, and is unity if the suffices are equal. Now  $\sum_3 A_i \nu_i$  is integral for all integral values of  $\nu$  if, and only if, the A's are integral, *i.e.* if, and only if, P is a point of the reciprocal lattice.

The connection of this construction with Bragg's theorem is readily apparent. Produce OL to O', the other end of the diameter, and let  $\angle \text{OO}'\text{P} = \theta$ , then

$$\text{OP} = 2\text{OL} \sin \angle \frac{\text{OLP}}{2} = \frac{2 \sin \theta}{\lambda}.$$

Thus the deviation  $2\theta$  is that which would result from reflection from a plane  $\perp \text{OP}$  of spacing  $d = 1/\text{OP}$ . It remains to show that a plane of this spacing occurs in this direction in the crystal itself. The normal from the origin to the first net plane of indices  $(hkl)$  has the property that the projection on its direction of either of the three intercepts  $\alpha_1/h$ ,  $\alpha_2/k$ ,  $\alpha_3/l$  is equal to the length  $d$ . Let the normal be represented in direction by the vector  $\sum_3 \mathbf{A}_i \boldsymbol{\beta}_i$  of length  $p$ , where the A's cannot yet be assumed to be integral. Then the projections are

$$\left( \frac{\alpha_i}{h} \cdot \frac{\sum_3 \mathbf{A}_i \boldsymbol{\beta}_i}{p} \right) = \frac{A_i}{hp},$$

and the similar expressions  $A_2/kp$  and  $A_3/lp$ ; these are equal to one another and to  $d$  if  $A_1 = h$ ,  $A_2 = k$ ,  $A_3 = l$  and  $p = 1/d$ . Hence the direction of the normal is that of  $\sum_3 h\beta_1$ , and the length OP

of this vector of the reciprocal lattice is  $1/d$  as required. It follows that the pattern obtained on a distant screen will be the projection from L of those points P of the reciprocal lattice lying on the sphere. Clearly it is only in exceptional cases that a point will lie actually on the sphere, but the rigorous conditions are relaxed in various ways. Firstly, the wave-length will not be exactly fixed, and hence the radius of the sphere will be slightly indeterminate, so that instead of a true surface we have a volume bounded by spheres touching at O. In practice this uncertainty is due to fluctuations in the voltage used to accelerate the electrons, and to losses of energy between the region where the electrons were generated and the crystal. But even apart from this there would be a slight uncertainty in wave-length since no finite wave-train can be strictly monochromatic, and if analysed by Fourier's series must give a range of wave-lengths and not only a single value of it. Again, the crystal is not really an infinitely extended perfect lattice. Real crystals have imperfections so that different parts of them are orientated in slightly different directions, and this implies a rotation of the reciprocal lattice with regard to LO. Further, the penetrating power of electrons is so small that, however large the specimen, the effective volume of the crystal is always fairly strictly limited in at least one direction, and the present assumption of an infinitely extended lattice often needs serious modification.

### Case of a Finite Crystal

For a finite crystal the points of the reciprocal lattice must be replaced by more or less extended regions of form determined by the size and shape of the crystal. This is best seen by applying Fourier analysis. If we start with the case of an infinite crystal, any function of position such as the electrostatic potential  $V$  of the charges forming the atoms of the crystal can be expressed as a three-dimensional Fourier series. The axes of the crystal represent the fundamental periods,

and integral submultiples of them give the higher terms of harmonics.

When the crystal is finite,  $V$  is zero outside it, but remains periodic inside except quite close to the surface, where the conditions are presumably somewhat different from those well inside. Neglecting this difference,  $V$  can still be expressed by Fourier's theorem, but we now need an integral instead of a sum. In other words, instead of a discrete series of harmonics there is a continuous distribution.

If  $xyz$  are coordinates of any point in the crystal with the crystal axes as axes of coordinates, and if  $x' = x/a$ , etc. (p. 21), then  $\mathbf{r} = x'\alpha_1 + y'\alpha_2 + z'\alpha_3$ . Suppose that the wavelet scattered from the infinitesimal region  $dx'dy'dz'$  round any point  $(x'y'z')$ , not necessarily a lattice point, is proportional to  $Vdx'dy'dz'$  (we shall show in Chapter VII that this is approximately true if  $V$  is the potential inside the scattering matter). As before, the path difference between the wavelet scattered in the direction  $\mathbf{s}$  from  $(x'y'z')$  and that from the origin is  $(\mathbf{r} \cdot \mathbf{s} - \mathbf{s}_0)$  and  $\mathbf{s} - \mathbf{s}_0/\lambda = \text{OP}$  (see Fig. 25). As before, we write  $\text{OP} = \mathbf{h} = \sum_3 A_i \beta_i$ , but the  $A$ 's are no longer to be considered integral, so that  $\mathbf{P}$  is now not a point of the reciprocal lattice.

The amplitude  $S$  of the wave scattered by the whole crystal in the direction of  $\mathbf{s}$  is

$$S = \iiint V e^{2\pi i(\mathbf{r} \cdot \mathbf{h})} dx' dy' dz',$$

where the integration is taken over the whole volume of the crystal. Now  $(\mathbf{r} \cdot \mathbf{h}) = x'A_1 + y'A_2 + z'A_3$  because of the relations between the vectors  $(\alpha_1, \alpha_2, \alpha_3)$ ,  $(\beta_1, \beta_2, \beta_3)$ .

$V$  has now to be expressed as a Fourier integral. In fact

$$V = \iiint_{-\infty}^{\infty} C_{(pqr)} e^{2\pi i(px' + qy' + rz')} dp dq dr,$$

the coefficients  $C_{(pqr)}$  are in general complex, and  $C_{(-p, -q, -r)}$  is the conjugate complex of  $C_{(pqr)}$ ; this ensures that  $V$  shall be real. Hence

$$S = \iiint_{-\infty}^{\infty} \left[ \iiint_{-\infty}^{\infty} C_{(pqr)} e^{2\pi i(px' + qy' + rz')} dp dq dr \right] e^{2\pi i(x'A_1 + y'A_2 + z'A_3)} dx' dy' dz'$$

where the limits of integration with respect to  $x'y'z'$  are extended to cover all space, since the Fourier expression for  $V$  is valid even outside the crystal where  $V=0$ . In an integral like this the only terms that matter are those for which the exponent vanishes, which it does when  $p = -A_1$ ,  $q = -A_2$ ,  $r = -A_3$ , and  $S$  is then proportional to  $C(pqr)$ , where  $pqr$  have the above values. Thus the amplitude of the wave scattered in the direction LP (Fig. 25), where  $OP = \sum_3 A_i \beta_i$ , is proportional to the Fourier coefficient  $C_{(-A_1-A_2-A_3)}$  in the expansion of  $V$ , and the intensity to its modulus squared.

In order to see how the Fourier components depend on the outward form of the crystal, we will first return to the case when the crystal is infinite.  $V$  is then strictly periodic and the only values of  $pqr$  which occur in its expansion are those for which  $px' + qy' + rz'$  changes by integers as  $x'y'z'$  move from one lattice point to the next, *i.e.* change by unity. Hence  $p = m_1$ ,  $q = m_2$ ,  $r = m_3$ , where  $m_1 m_2 m_3$  are any integers positive or negative. The quantities  $A$  which determine the direction of the scattered wave are  $-m_1$ ,  $-m_2$ ,  $-m_3$  and are now integral;  $P$  is thus a point of the reciprocal lattice as was shown above. Incidentally it should be noticed that the intensity of the wave scattered along LP is proportional to  $|C_{(-A_1-A_2-A_3)}|^2$ . Thus the point  $A_1 A_2 A_3$  of the reciprocal lattice not only determines the direction of the reflected beam whose indices  $hkl$  are equal to  $A_1 A_2 A_3$ , but the intensity of this reflection is proportional to the modulus squared of the Fourier component of  $V$  with the same indices, for

$$|C_{(-A_1-A_2-A_3)}|^2 = |C_{(A_1 A_2 A_3)}|^2.$$

The corresponding result has been used by Sir William Bragg in the case of X-rays, where the scattering depends on the electron density, to calculate the distribution of this density in the cell of a crystal; he added together Fourier components of magnitudes determined by the measured intensities of reflection by the various planes.

When the crystal is finite other values of  $pqr$  are associated with appreciable values of  $C_{(pqr)}$ . In fact as long as the difference between  $px' + qy' + rz'$  and  $-m_1 x' - m_2 y' - m_3 z'$  is small over the whole body of the crystal, the Fourier terms con-

taining  $pqr$  will fit the periodicity of the crystal well enough, and there will not be much difference in the values of the corresponding coefficients  $C_{(pqr)}$ . The permissible range of  $p$  on each of the integral values which allows this to happen is inversely as the range of  $x'$ , *i.e.* as the number of cells of the crystal in the direction in which  $x'$  is measured. Hence the region round each point of the reciprocal lattice will be extended in the direction of each axis to an extent inversely proportional to the extension of the crystal parallel to the corresponding axis. Thus, for example, to a crystal in the form of a flat plate will correspond an elongation of the points of the reciprocal lattice normal to the plate. Any of these extended regions cut by the sphere will give rise to diffracted beams whose intensity will in general diminish with the distance of the region of intersection from the point, since  $|C_{(pqr)}|^2$  in general diminishes as  $pqr$  recedes from the values  $m_1, m_2, m_3$ . Thus to a perfectly periodic infinite structure corresponds a geometrical point in the reciprocal lattice, and any deviation from perfect periodicity, such as is inevitably involved in a limitation of size, is reflected in the size of the region of intensity round each reciprocal lattice point, which grows larger the greater the divergence from perfect periodicity. While the above rough argument shows the general character of the phenomenon, the exact calculation in the case of a crystal of any arbitrary shape is difficult and laborious.

Von Laue<sup>1</sup> has shown that the integrals determining the distribution of intensity in the neighbourhood of a reciprocal lattice point can be reduced to the sum of contributions from the various edges of the crystal. The distribution round each point of the reciprocal lattice is the same and, corresponding to each face of the crystal, the region of appreciable intensity is extended by a protrusion normal to the face. The region has a centre of symmetry at the reciprocal lattice point and, if the shape of the crystal has a centre of symmetry, planes of zero intensity pass through the reciprocal lattice point. Von Laue has worked out the case of the octahedron in full.

For the octahedron the region of intensity round each point of the reciprocal lattice has eight protruding horns,

<sup>1</sup> Von Laue, *Ann. d. Phys.* 26, p. 55 (1936).

each normal to one face of the octahedron. When the sphere passes near, but not through, a lattice point it may intersect some of the horns, and to the projections of these intersections on to the plane of the photographic plate corresponds a group of spots. Laue<sup>1</sup> has explained in this way results obtained by Kirchner and Lassen,<sup>2</sup> Brück<sup>3</sup> and one of the authors.<sup>4</sup>

When an etched surface of a single crystal of a metal is used to diffract electrons at grazing incidence, it is found in general that a pattern of spots appears which is regular if the direction of the electrons is an important zone axis. It represents the section of the reciprocal lattice of the crystal by the Ewald sphere, which for the wave-lengths used is nearly a plane. In these experiments films of metals were used. The first authors deposited their films on rock-salt, while we deposited ours on an etched single crystal of copper. Some of the patterns showed the unusual features that some or all of the spots were replaced by a group of two or four spots centred at the place where the normal spot should have been. Plate VIII *b* shows a plate taken by us of cobalt deposited on the (110) face of the copper crystal. In these conditions the cobalt conforms to the copper in forming a face-centred cubic lattice which follows the orientation of the underlying metal. Von Laue shows that the pattern can be explained in detail by supposing that the free surface of the cobalt is covered with projections bounded by (111) faces and forming parts of octahedra. When the sphere passes at some distance from a point of the reciprocal lattice it intersects the horns; four of these were equally inclined to the direction of the incident electrons, which was parallel to a cube edge; when the sphere passes close to the point it goes through the central region and only one point results. From the size of this central region Von Laue estimates the length of the edges of the octahedra as  $1.3 \times 10^{-6}$  cm. Fig. 26 from Von Laue's paper<sup>1</sup> shows the calculated positions of the spots which can be compared with the experiment. The absence of groups round the 'forbidden' points of the reciprocal lattice, *e.g.* 520 between 420

<sup>1</sup> Von Laue, *Ann. d. Phys.* 29, p. 211 (1937).

<sup>2</sup> Kirchner and Lassen, *Ann. d. Phys.* 24, p. 113 (1935).

<sup>3</sup> Brück, *Ann. d. Phys.* 26, p. 233 (1936).

<sup>4</sup> Cochran, *Proc. London Phys. Soc.* 48, p. 723 (1936).

and 620, is interesting.<sup>1</sup> Though the structure factor vanishes *at* these points, it has a finite value a little distance away and one would expect the region of intensity to have the horns but no central region. Von Laue considers that the absence of anything corresponding to this indicates that the surface of the crystal is not formed by *complete* face-centred cubes, but

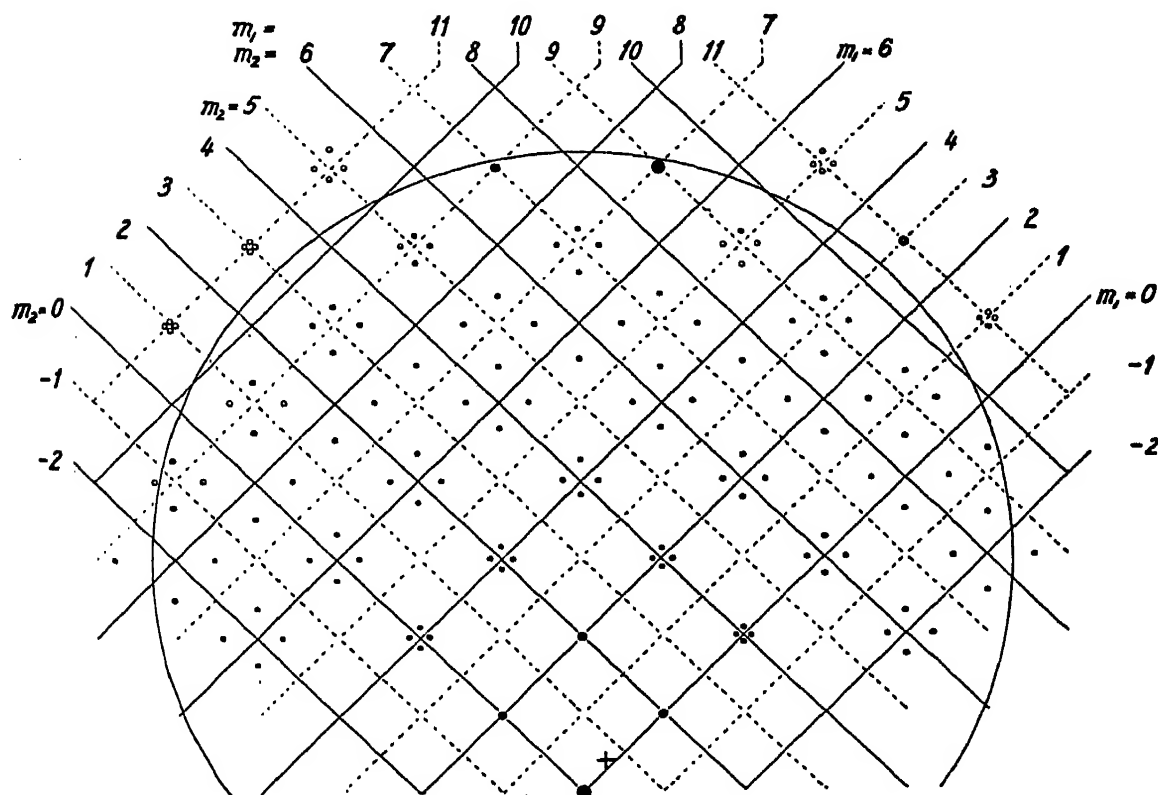


FIG. 26

by the corners of the oblique cells forming the true lattice (p. 27) of the crystal, which would give a much smoother surface. For the true lattice, which contains only one atom per cell, the question of 'forbidden' spectra does not arise; they would correspond to fractional indices. The experiments by the other authors, in some of which the metal films were stripped off and examined by transmission, can be explained on similar lines.<sup>2</sup>

The intensity scattered by a crystal which takes the form of a parallelepiped formed of unit cells can be calculated by

<sup>1</sup> These spots may be recognised in Fig. 26 from the numbers at the edges of the diagram;  $m_1$ ,  $m_2$  are used in place of the usual symbols  $h$ ,  $k$ .

<sup>2</sup> Cf., also, a recent paper by Menzer (*Zeit. für Krist. A*, 99, p. 410, 1938); also recent papers by Kirchner and others in the *Ann. d. Phys.* 1938.

elementary methods. If there are  $N_1$ ,  $N_2$ ,  $N_3$  cells respectively along the axes, and if the path differences between waves scattered from the origin and from the ends of the axes are, as before,  $A_1\lambda$ ,  $A_2\lambda$ ,  $A_3\lambda$ , the intensity due to one scattering point in each cell is proportional to <sup>1</sup>

$$\frac{\sin^2 (\pi N_1 A_1)}{\sin^2 \pi A_1} \cdot \frac{\sin^2 (\pi N_2 A_2)}{\sin^2 \pi A_2} \cdot \frac{\sin^2 (\pi N_3 A_3)}{\sin^2 \pi A_3}.$$

Each factor is the well-known expression for the resultant of  $N$  vibrations with a phase difference of  $2\pi A$  between each. When there is more than one scattering point per cell the above expression is to be multiplied by the structure factor. The extension of the region of intensity of each point of the reciprocal lattice parallel to the  $\beta_1$  axis, for example, can be found by considering the first factor. It is a maximum when  $A_1$  is integral, *i.e.* at the lattice point. If  $A_1 = \text{integer} + p$ , the factor becomes  $\sin^2 \pi N_1 p / \sin^2 \pi p$ ; this vanishes first when  $p = \pm 1/N_1$  and has a subsidiary maximum of magnitude  $4N_1^2/9\pi^2$  near  $p = \pm 3/2N_1$ , if  $N_1$  is fairly large.

If we have a powder composed of equal crystals such that

$$\frac{|\beta_1|}{N_1} = \frac{|\beta_2|}{N_2} = \frac{|\beta_3|}{N_3} = \frac{1}{Na},$$

the region round the point can be taken as roughly spherical and the angular half-width of the diffracted rings is  $\lambda/Na$ , so that the size of the crystals can be found by measuring the width of the rings.

For thin plates the regions of intensity are lines normal to the plate through the points of the reciprocal lattice. For extremely thin plates the lines may have appreciable intensity, except perhaps for a few points, all the way from one reciprocal lattice point to the next, and the crystal will behave as a cross-grating.

### Numerical Values

The above theory is very closely similar to the corresponding theory for X-rays, but in practice the experimental results for electron diffraction differ in important respects from those

<sup>1</sup> See for example *Conduction of Electricity through Gases*, vol. ii, p. 265.

for X-rays. This is explained by the relative magnitudes of the quantities involved. There are two important differences: firstly, the wave-length of the electrons most commonly used is small compared with the distance apart of the atoms, instead of being of the same order of magnitude as it is with X-rays; secondly, the interaction between electrons and the atoms of the crystal is much greater than that between X-rays and atoms so that much thinner layers are effective. It is found in practice that films of most substances thicker than a small multiple of  $10^{-5}$  cm. give only diffuse scattering without regular diffraction. The wave-length of 40,000-volt electrons is  $0.6 \times 10^{-9}$  cm., while the (111) spacing of gold is  $2.35 \times 10^{-8}$ , hence the Bragg angle is only  $0.73^\circ$ . Even for the 600 reflection it is only  $2.5^\circ$ , and reflections for this and smaller spacings are generally fairly weak. In other words, the radius  $1/\lambda$  of the sphere in Fig. 25 is  $1.67 \times 10^9$ , while the cube corners of the reciprocal lattice of gold are  $5.0 \times 10^7$  apart. For many purposes the part of the sphere with which we are concerned can be treated as a plane. Since the angles are so small, a very slight distortion of the crystal is enough to allow reflections from several planes to occur simultaneously. In fact, if it were permissible to treat the sphere as a plane, and if the crystal were set with OL as a zone axis, reflections would occur corresponding to all the points of the reciprocal lattice corresponding to net planes through the axis, which would lie on the plane through O normal to it. Thus the distortion required to bring one of them, say P, into action is merely the distortion required to move P from the plane to the sphere.

Distortion of this kind is probably mainly responsible<sup>1</sup> for the patterns shown by very thin films of mica which were first observed by Kikuchi (Plate III a). Here the pattern is what would be given by a single layer of crystal cells in the cleavage plane, which are arranged in a pseudohexagonal lattice. Actually the mica, though thin ( $\sim 10^{-6}$  cm.), had many more than one layer of cells, but a slight bending of the film would bring out an extended pattern.

Even if the mica kept perfectly flat some such pattern might still appear, for owing to the thinness of the crystal

<sup>1</sup> W. L. Bragg, *Nature*, 124, p. 125 (1929); Darbyshire and Cooper, *Proc. Roy. Soc.* 152, p. 104 (1935).

the lattice points are extended. This extension is shown in Fig. 27, which is drawn to scale for a crystal of mica  $10^{-6}$  cm. thick, for electrons of 40,000 volts energy, for a spacing in the plane of the crystal of  $5.17 \text{ \AA}$ , and for a spacing between successive cleavage planes of  $20 \text{ \AA}$ .

If the sphere *just* passes through the region of intensity round the lattice point Q, this point and all points such as P inside it will give rise to diffracted spots. Assuming that the crystal plane is normal to the rays, the angular width of the region containing the spots can readily be found. Let the sphere cut the region of intensity at Q'. The half angular width is  $OQ \cdot \lambda$ , since  $1/\lambda$  is the radius of the sphere; but  $OQ^2 = QQ' \cdot 2/\lambda$ , hence the half width is  $\sqrt{2\lambda QQ'}$ . The value  $QQ'$  is given by the calculation on p. 78 as  $1/N_1 a = 1/t$ , where  $t$  is the thickness of film. Hence the half width is  $\sqrt{2\lambda/t}$ . If the crystal is tilted there will in general be one point in which a plane of the reciprocal lattice touches the sphere. The projection of this point will be surrounded by a wide region in which each point of the reciprocal lattice in the plane will give a diffracted spot.

FIG. 27

Kikuchi found that flakes of mica, which were too thick to give the cross-grating effect, showed a pattern containing, in addition to certain black and white lines (see below, p. 111), a number of spots arranged on concentric circles (Plate III *b*). These he explained as Laue spots, for which all three conditions were approximately satisfied, some tolerance being provided by the inhomogeneity of the rays and by the thinness of the specimen (as explained above). The spots would form part of the cross-grating pattern, but only those are preserved which also nearly satisfy the third Laue condition. This condition is equivalent to saying that the spots lie on one of a series of cones, with any identity-period of the crystal as axis. This identity-period can be regarded as the *c* axis of the crystal, for we can draw the unit cell in an infinite variety of ways

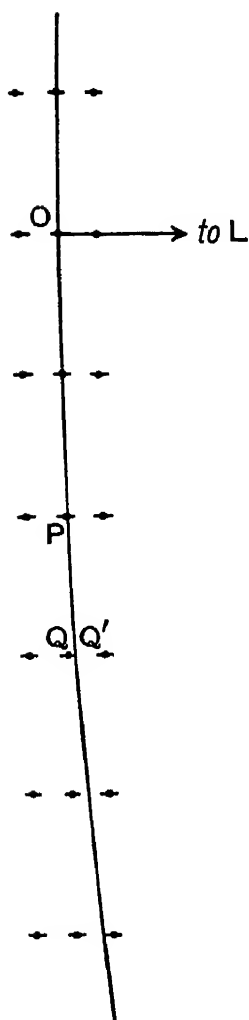
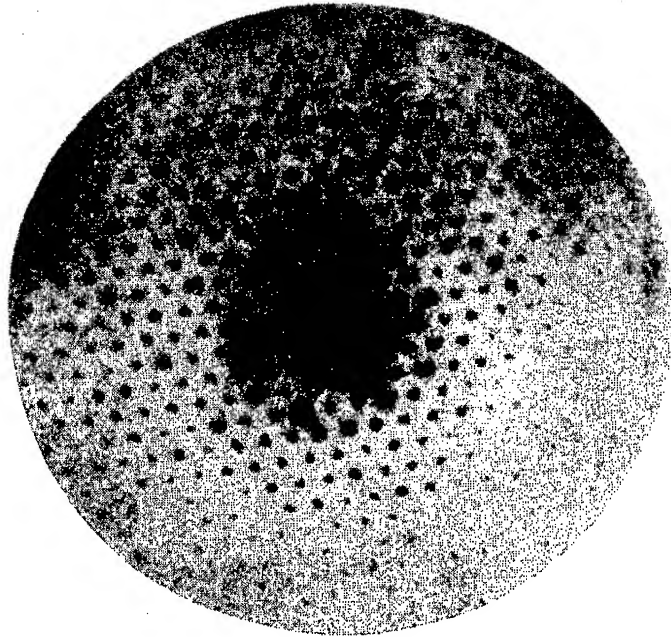


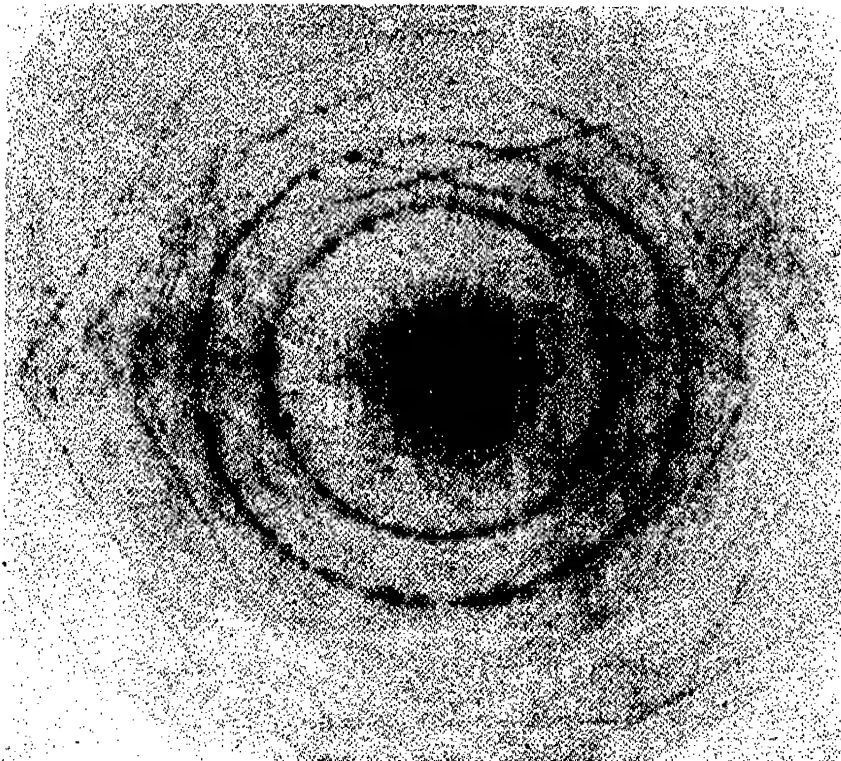
FIG. 27

### PLATE III

(These illustrations are 'negatives')



(a) Mica, thin sheet. (*Kikuchi.*) Taken from *Phys. Zeits.* 31, Pl. XXIV. (1930)



(b) Mica, medium thickness. (*Kikuchi.*) Taken from *Jap. Journ. Phys.* 5, Pl. VI. (1928)



(cf. Fig. 5) — though naturally ways which are crystallographically simple will in general give the most strongly marked results. In practice the  $c$  axis is taken at a small angle  $\phi$  to the incident electrons, and the atoms in the  $a, b$  plane determine the cross-grating spectrum. The cones intersect the photographic plate in ellipses, which are practically circles, and any cross-grating spot which would lie near one of the circles, will appear as a Laue spot, owing to the tolerance mentioned above.

We can calculate as follows the positions and widths of the circular regions in which the spots lie, and which are often known as 'Laue zones'. The condition for interference between two lattice points at the ends of a ' $c$ ' axis is  $c(\cos \phi - \cos \psi) = n\lambda$ , where  $\psi$  is the angle which the diffracted ray makes with the axis, and  $n$  is the order of the zone. Since  $\phi$  and  $\psi$  are small we have  $c(\psi^2 - \phi^2) = 2n\lambda$ .

If the tolerance is due to a limitation of the crystal to  $N$  cells in the  $c$  direction, the range  $\pm\Delta\psi$ , over which the zone extends, is given by

$$Nc(\cos \phi - \cos \overline{\psi \pm \Delta\psi}) = \lambda(Nn \pm 1),$$

whence

$$\Delta\psi = \lambda/Nc \sin \psi,$$

except when  $\psi = 0$ , in which case

$$\Delta\psi = \sqrt{\frac{2\lambda}{Nc}}.$$

The last expression agrees with that found on p. 80, which refers to the case when  $\phi = \psi = 0$ , and, of course,  $n = 0$ . The zone of zero order for which  $\phi = \psi$  will always pass through the undeflected spot. Such a circle was observed by Kikuchi.

It sometimes happens that the crystals in a polycrystalline specimen are large enough and few enough to give rise to a number of discrete spots rather than continuous Debye-Scherrer rings. In such cases it is often noticeable that pairs of spots occur at opposite ends of diameters, and sometimes groups of spots are seen on the same circle showing a symmetry characteristic of the crystal. The reason is that some piece of crystal has a zone axis, or at least a single plane, nearly

parallel to the incident electrons, and one or more pairs of points of the reciprocal lattice, on opposite sides of  $O$ , lie nearly on the sphere. An instance of this can be seen in the pattern of aluminium on Plate II *d*.

A more developed form of this pattern has been obtained by Trillat and Hirsch<sup>1</sup> from commercial platinum leaf, which sometimes gives single crystals large enough to cover the whole cross-section of the electron beam. The regular arrangement of spots which result is exactly analogous to that given by very thin mica.

In the course of work with thin flakes of graphite and molybdenite Finch and Wilman<sup>2</sup> have observed a large number of spots whose position does not agree either with that of regular Laue spots, or with that of the spots of a cross-grating pattern. Both these crystals show very easy cleavage parallel to the  $(hko)$  plane and have a layer structure. The flakes used were very thin; some of the principal pieces were probably of the order of 40 Å, and the small detached fragments were probably only two or three cells in thickness. At first the extra spots were attributed to 'forbidden' planes, and to planes of fractional indices, but it seems more likely that they are really due to small pieces inclined at random angles to the incident beam. With such thin flakes the points of the reciprocal lattice will be so drawn out in the ' $l$ ' direction that the regions of intensity will form practically continuous lines from one point to the next. Whatever the setting of the crystal fragment, the Ewald sphere will cut these lines, and diffracted spots will appear on the plate. The distribution of intensity along the lines will not be uniform; some spots will therefore be brighter than others, and as all are faint because the area of the fragment is less than the cross-section of the electron beam, one would not expect to find a complete pattern from any one fragment. In the experiments with molybdenite, where the flakes were much distorted, a number of spots were observed at small angles. These are best thought of as due to glancing reflections from fragments set with their cleavage planes at small angles to the beam. As the fragments are so

<sup>1</sup> Trillat and Hirsch, *Jour. de Phys.* 3, p. 185 (1932).

<sup>2</sup> Finch and Wilman, *Proc. Roy. Soc.* 155, p. 345 (1936); *Trans. Farad. Soc.* 32, p. 1539 (1936).

thin, the reflection will follow the optical law, and its intensity will not be vastly affected by the fact that Bragg's law is not obeyed.

In the course of experiments with cadmium iodide crystals, which also occur in thin flakes and give good cross-grating patterns, Finch and Wilman<sup>1</sup> have observed patterns containing groups of spots which they attribute to diffractions with fractional indices. It seems to the authors that these spots could be explained on the lines of the last paragraph except that it would be necessary to suppose that the reflecting surfaces were the sides of hexagonal prisms instead of their bases.

### Subsidiary Rings

Finch and Wilman found also that a powder of graphite crystals, formed by drying a colloidal suspension on a fine-meshed nickel gauze or on thin collidon, gave continuous rings near some, but not all, of the normal rings. Since we are now dealing with crystals whose directions are distributed continuously, the above explanation cannot apply. It seems probable<sup>2</sup> that these rings are due to the subsidiary maxima well known in the theory of optical gratings. We have seen (p. 78) that the intensity of diffraction from a crystal in the form of a parallelepiped with edges parallel to the cell axes is given by the product of three factors of the form

$$\frac{\sin^2 (\pi NA)}{\sin^2 \pi A},$$

If the crystal is in thin flakes only the factor corresponding to the axis of the reciprocal lattice normal to the flake need be considered, and the distribution of intensity in a line through each point of the lattice parallel to this direction is given by the above expression. This is the well-known expression for the resultant of  $N$  simple harmonic oscillations with a phase difference between each of  $2\pi A$ . It has its greatest value  $N^2$  when  $A = m$ , an integer; it vanishes when  $A = m \pm 1/N$ , and then has a secondary maximum which, when  $N$  is large, occurs

<sup>1</sup> Finch and Wilman, *Trans. Farad. Soc.* 33, p. 1435 (1937).

<sup>2</sup> This view has been accepted by Finch and Wilman. See *Ergebnisse der Exakt. Naturwiss.* 16, p. 363 (1937).

near  $A = m \pm 3/2N$  and has an intensity of about  $4N^2/9\pi^2$ , or about  $4\frac{1}{2}$  per cent of the main maximum. In the case of graphite the cleavage plane is normal to the  $c$  axis, whose length is  $6.79 \times 10^{-8}$  and  $|\beta_3| = \frac{1}{c}$ . If  $P$  (Fig. 28) is any point  $hkl$  of the reciprocal lattice and  $P''PP'$  is drawn parallel to  $|\beta_3|$  so that  $P''P = P'P = 3|\beta_3|/2N$ ,  $P'$ ,  $P''$  will be the secondary maxima

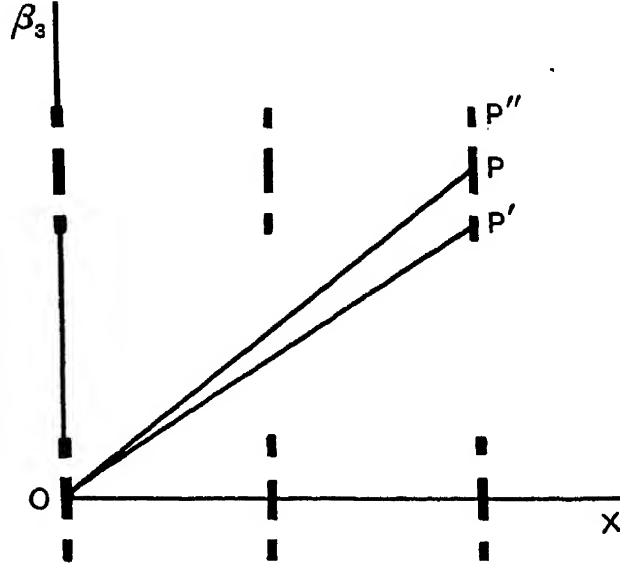


FIG. 28

of intensity. The radii of the rings corresponding to the main and subsidiary maxima are proportional to  $OP$ ,  $OP'$ ,  $OP''$  and the spacing  $d = 1/OP$ . Now

$$\cos \widehat{OPP'} = \frac{l|\beta_3|}{OP} = \frac{ld}{c},$$

hence

$$\frac{OP - OP'}{OP} = \frac{PP' \cos \widehat{OPP'}}{OP} = \frac{3ld^2}{2Nc^2} = \frac{3ld^2}{2tc},$$

where  $t$  is the thickness of the flake. This gives the separation between the main and subsidiary rings as a fraction of the radius of the main ring. Notice that rings for which  $l=0$  will not have subsidiaries. Finch and Wilman found that a certain film gave subsidiaries, corresponding to spacings 2.079 and 1.961, on the two sides of the 101 ring of spacing 2.027, and another pair 1.961 and 1.462 bracketing the 103 ring of spacing 1.541. The 102 ring is not well placed for observing

subsidiaries and is faint. No subsidiaries were seen near the strong 110 ring for which  $l=0$ . According to the above formula the thickness of the flakes comes out at 30 Å in each case, corresponding to between 4 and 5 cells thickness; probably fragments of both thicknesses were present.<sup>1</sup> The crystals in this film, although continuously arranged, had a tendency to orientate with their  $c$  axes normal to the film. When the film was inclined, the 101 ring and its subsidiaries each broke into four arcs. The two subsidiaries showed the greatest intensity when the film was inclined to about 12° and 24° respectively. The angles P'OX, P''OX, when P is the point 101, are 11.7° and 22.7°, and show an excellent agreement. This seems to be the first time that subsidiary diffraction maxima have been observed, except in optics.<sup>2</sup>

<sup>1</sup> For values of  $N$  as small as this the maxima will not occur quite where we have supposed. Actually there are two equivalent layers in each cell of graphite, so we have to deal with 8-10 in all. For 8 layers the phase difference for the subsidiary maxima shifts from 270° to 280°.

<sup>2</sup> Cf. also Cochrane, *Proc. Phys. Soc.* 48, p. 731 (1936).

## CHAPTER VII

### CONSIDERATION OF INTENSITIES OF DIFFRACTION

#### Atomic Scattering Curve

THE intensities of the rings in a diffraction pattern depend among other factors on the intensity of scattering by the individual atoms, and from measurements of the relative intensities of the rings it is possible to calculate the way in which the scattering for the individual atoms varies with angle. The distribution of intensity when X-rays are diffracted by a polycrystalline aggregate or powder has been thoroughly investigated, and it has been found that the total radiation in a cone of semi-apex angle  $2\theta$ , *i.e.* for planes at a glancing angle  $\theta$ , is given by

$$R = kF^2\lambda^3 \frac{1 + \cos^2 2\theta}{2 \sin 2\theta} \cos \theta \cdot \frac{pV}{2},$$

where  $V$  is the volume of the crystal,  $p$  is the number of equivalent planes giving the reflection and is obtained by permuting the crystal indices and their signs,  $\lambda$  the wave-length,  $k$  a factor corresponding to the X-ray scattering of a single electron, and  $F$  a factor which represents the number of electrons to which each crystal cell is equivalent in scattering<sup>1</sup> power.  $F$  varies with  $\theta$  because the scattered waves due to the several electrons will not be exactly in phase except when  $\theta = 0$ , and at other angles will interfere so that the combined amplitude is less than the sum of the separate amplitudes of the several electrons. When  $\theta$  is small, as in the present experiments, we may write for the *linear* density,  $D$ , of scattered electrons on any ring  $D = k'E^2 p/\theta^2$ , where  $k'$  is a constant for any single photograph and  $E$  is the factor for electrons corresponding to  $F$  for X-rays. Since  $p$  is an easily calculable integer, a measurement of  $D$  for various rings will enable us to compare the

<sup>1</sup> For an elementary substance with one atom per cell,  $F$  will be replaced by  $f$ , the scattering factor for a single atom.

values of  $E$  for the angles  $\theta$  to which the different rings correspond.

Experiments to find  $E$  have been made<sup>1</sup> with films of gold prepared by spluttering on cellulose acetate and dissolving the latter away. These films show no sign of preferred orientation of the crystals which would vitiate the results. The intensity was determined by photometry of the photographic plates, two exposures being made on each and the results combined in such

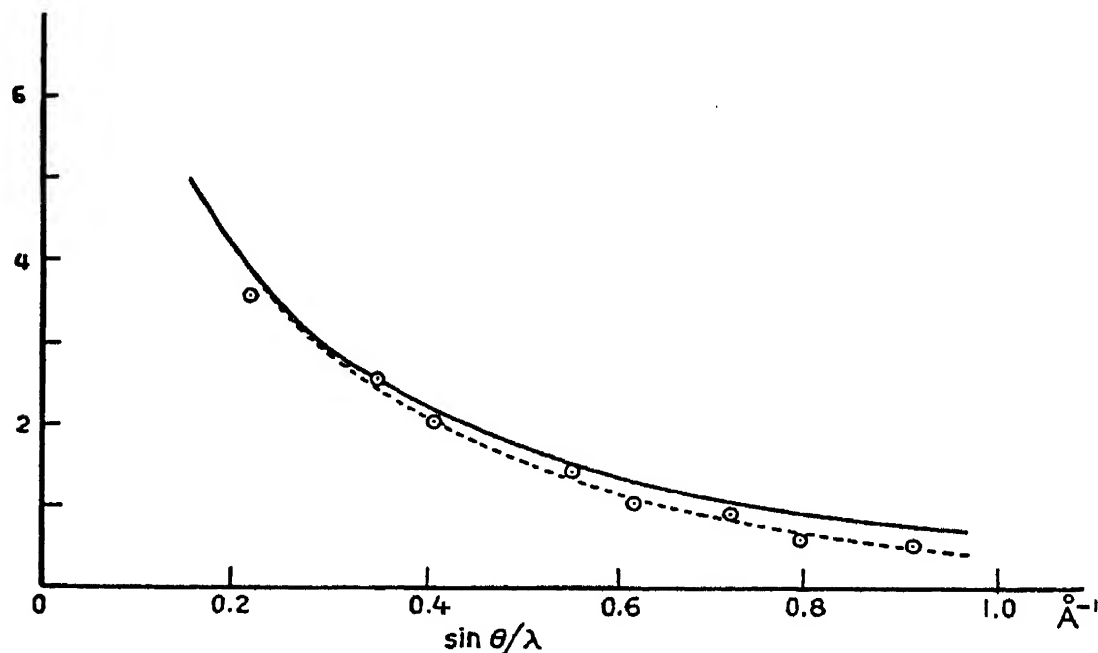


FIG. 29

a way as to eliminate the characteristics of the plate (see p. 244). Experiments with different voltages showed that  $E$  can be regarded as a function of  $\sin \theta/\lambda$ . The points in Fig. 29 show the values found for  $E$  in arbitrary units plotted against  $\sin \theta/\lambda$ . The variation with angle of atomic scattering is more rapid for electrons than for X-rays.

Similar experiments have been made by Mark and Wierl<sup>2</sup> for gold, silver and aluminium. The curve for gold is close to that given above, and those for silver and aluminium are progressively steeper with decreasing atomic number.

However, a recent paper by Ornstein and others<sup>3</sup> indicates results rather different from the above, the curve for silver

<sup>1</sup> G. P. Thomson, *Proc. Roy. Soc.* 125, p. 352 (1929).

<sup>2</sup> Mark and Wierl, *Zeit. für Phys.* 60, p. 741 (1930).

<sup>3</sup> Ornstein, Brinkmann, Hauer and Tol, *Physica*, 5, p. 693 (1938).

being considerably less steep. The rings were very sharp and it is probable that the crystals were larger than those in the author's experiment (*l.c.*).

### Theory of Atomic Scattering

To determine theoretically the scattering factor for a single atom it is necessary to know the equation of propagation of the waves. For electrons of speed small compared with that of light the equation is

$$\nabla^2\psi + \frac{8\pi^2m}{h^2}(E - V)\psi = 0,$$

where  $E$  is the energy of an electron assumed constant and  $V$  is the potential energy (expressed as a function of the co-ordinates  $(xyz)$  which the electron would have at any point of space).

The problem of the scattering of material waves was first solved by Born, but the method which follows is a modification of his work to suit this problem given by Mott.<sup>1</sup> He assumes that the wave inside the atom is not much disturbed by the scattering, and that the above wave equation applies with fixed  $V$ ; the reaction of the electrons on the charges in the atom is thus neglected.<sup>2</sup> It can then be shown that each point in the atom scatters a wavelet of amplitude

$$\frac{2\pi m}{R h^2} V(xyz) dx dy dz$$

at a distance  $R$  from the centre of the atom, the amplitude of the wave at  $(xyz)$  being taken as unity. If  $V$  is greater than zero the wavelet starts with the same phase as that of the whole wave at  $(xyz)$ : if  $V$  is less than zero it starts with opposite phase. The proof is as follows. It is a known result in the theory of differential equations that the most general solution of

$$(\nabla^2 + k^2)\psi = f(xyz)$$

is

$$\psi(xyz) = G(xyz) + \frac{1}{4\pi} \iiint \frac{e^{ik|\mathbf{r}-\mathbf{r}'|}}{|\mathbf{r}-\mathbf{r}'|} f(x'y'z') dx' dy' dz',$$

<sup>1</sup> Mott, *Proc. Roy. Soc.* 127, p. 658 (1930).

<sup>2</sup> Henneberg (*Zeit. für Phys.* 83, p. 555, 1933) shows that the distortion of the incident electron-wave by the atom may become important for heavy atoms.

where  $\mathbf{r}, \mathbf{r}'$  are the vectors from the origin to  $(xyz)$ ,  $(x'y'z')$  and  $G(xyz)$  is the general solution of  $(\nabla^2 + k^2)G = 0$ .

Schrödinger's equation is of the above type, and  $k^2 = 8\pi^2 mE/h^2$  so that  $2\pi/k$  is the wave-length of the electron waves at a great distance from the atom.

Therefore any solution must satisfy the "integral equation",

$$\psi(xyz) = G(xyz) + \frac{1}{4\pi} \iiint \frac{e^{ik|\mathbf{r}-\mathbf{r}'|}}{|\mathbf{r}-\mathbf{r}'|} \cdot \frac{8\pi^2 m}{h^2} \cdot V(x'y'z') \psi(x'y'z') dx' dy' dz',$$

where the integration extends over the region for which  $V$  is appreciable, *i.e.* the volume of the atom.

Now the solution which describes the scattering will consist of two parts, an incident wave and a scattered wave. For large  $\mathbf{r}$ , the integral on the right tends to  $AR^{-1}e^{ikR}$ , where  $A$  depends on the direction only. The integral therefore represents the scattered wave, and  $G$  must be chosen to represent an incident wave. Let  $G = e^{ikz}$ . This is a wave of unit intensity, corresponding to unit volume density of incident electrons. The form of the integral shows that, as we have said, the scattered wave is made up by the interference of wavelets scattered by each element of volume, each being of amplitude

$$(2\pi m/h^2) V(xyz) \psi(xyz) dx dy dz / R.$$

If the scattering is small, it is sufficient to take for  $\psi$  the part due to the incident wave. The wavelets start with the phase of  $\psi$  and will interfere with one another. To calculate this interference, we assume that the atom has spherical symmetry. Wavelets from a shell between  $r$  and  $r + dr$  will combine to form a wave with phase equal to that of a wavelet scattered from the origin, as can be seen by combining in pairs the wavelets from portions of the shell at the opposite ends of diameters. If A, B (Fig. 30) are two such scattering portions, and if AB makes an angle  $\theta'$  with the bisector of the angle between the incident and scattered rays, then the phase difference between the wavelets is

$$\frac{2\pi}{\lambda} (NB - AM) =$$

$$\frac{2\pi}{\lambda} \cdot AB \cdot \left[ \cos\left(\frac{\pi}{2} - \frac{\phi}{2} - \theta'\right) + \cos\left(\frac{\pi}{2} - \frac{\phi}{2} + \theta'\right) \right] = \frac{4\pi}{\lambda} \cdot AB \cdot \cos \theta' \sin \frac{\phi}{2},$$

where  $\phi$  is the angle of scattering.

The resultant amplitude of the wavelets is diminished because of this phase difference by a factor

$$\cos \left[ \frac{4\pi r}{\lambda} \cos \theta' \sin \phi/2 \right].$$

The mean value of this factor for all pairs of points AB is

$$\int_0^{\pi/2} \cos \left[ \frac{4\pi r}{\lambda} \cos \theta' \sin \phi/2 \right] \sin \theta' d\theta' = \frac{\sin \mu r}{\mu r},$$

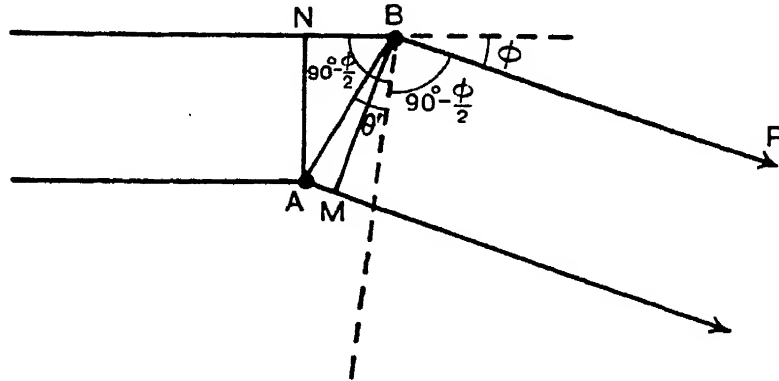


FIG. 30

where 
$$\mu = \frac{4\pi}{\lambda} \sin \phi/2.$$

Hence the resultant amplitude for the whole atom is

$$\begin{aligned} \frac{8\pi^2 m}{h^2 R} \int_0^\infty \frac{\sin \mu r}{\mu r} \cdot V(r) \cdot r^2 dr &= -\frac{8\pi^2 m}{h^2 R} \left[ \frac{\cos \mu r}{\mu^2} \cdot V(r) \cdot r \right]_0^\infty \\ &\quad + \frac{8\pi^2 m}{h^2 R} \int_0^\infty \frac{\cos \mu r}{\mu^2} \frac{d}{dr} \{V(r) \cdot r\} dr. \end{aligned}$$

But  $V(r) \cdot r$  tends to zero at infinity for a neutral atom, and to  $Ze^2$  at the origin where  $Ze$  is the nuclear charge. Hence the amplitude is

$$\begin{aligned} \frac{8\pi^2 m}{h^2 R} \left\{ \frac{Ze^2}{\mu^2} + \frac{1}{\mu^2} \left[ \frac{\sin \mu r}{\mu} \frac{d}{dr} \{V(r) \cdot r\} \right]_0^\infty - \frac{1}{\mu^2} \int_0^\infty \frac{\sin \mu r}{\mu} \frac{d^2}{dr^2} \{V(r) \cdot r dr\} \right\} \\ = \frac{8\pi^2 m}{h^2 R \mu^2} \left[ Ze^2 - \int_0^\infty \frac{\sin \mu r}{\mu r} \frac{d}{dr} \left( r^2 \frac{dV(r)}{dr} \right) dr \right] \\ = \frac{8\pi^2 m e^2}{h^2 R \mu^2} \left[ Z - \int_0^\infty \frac{\sin \mu r}{\mu r} \sigma dr \right], \end{aligned}$$

where  $\sigma dr$  is the total electronic charge between  $r$  and  $r + dr$ .

Now X-rays are scattered by the electronic charges in an atom, and the amplitude of the resultant wave is also changed by interference. The expression  $\int_0^\infty \frac{\sin \mu r}{\mu r} \sigma dr$  gives the factor by which the amplitude exceeds that due to a single electron, and is denoted by  $f$ . Hence the amplitude of the electronic wave is

$$\frac{8\pi^2 m e^2}{h^2 R \mu^2} [Z - f] = \frac{e^2 \operatorname{cosec}^2 \phi/2}{R \cdot 2m u^2} [Z - f].$$

It will be noticed that the above result is equivalent to saying that each element of charge  $d\rho$  in the atom scatters a wavelet of amplitude  $e \operatorname{cosec}^2 \phi/2 \cdot d\rho / 2m u^2 R$ . By the usual interpretation the intensity of scattering is taken as proportional to the square of the corresponding wave amplitude, and the chance of an electron being scattered in a small solid angle  $\delta\omega$  is

$$\frac{n e^4 \operatorname{cosec}^4 \phi/2}{4m^2 u^4} [Z - f]^2 \delta\omega,$$

assuming that there are  $n$  independent atoms in unit cross-section of the incident beam. This may be compared with the classical formula for scattering by a fixed charge, namely

$$\frac{e^4 \operatorname{cosec}^4 \phi/2}{4m^2 u^4} \delta\omega.$$

The form of the function  $f$  can be calculated with fair approximation for a heavy atom such as gold, and Fig. 29, p. 87, shows the extent of the agreement in the case of gold, the points being the experimental results and the full line  $(Z - f) \operatorname{cosec}^2 \phi/2$  in arbitrary units adjusted to fit at

$$\left( \sin \frac{\phi}{2} \right) / \lambda = 0.35.$$

The dotted line shows the result of applying a correction for the heat motion of the atoms in the gold crystals.

On the other hand, Ornstein's results for silver and copper show a marked divergence from what is predicted by Mott's theory, the slope of the curve plotted as in Fig. 29 being less steep. We consider that this difference is probably due to the

size of the crystals used and indicates an interesting limitation of the theory as so far expressed. On p. 86 we have taken the expression commonly used in X-ray calculations, according to which the intensity of a reflection is proportional to the square of  $F$ , and this is in agreement with the theory indicated on p. 74, which makes the intensity proportional to the square

TABLE VII

 $\{E(\theta)\}^2$  CALCULATED FROM HARTREE FIELDS

To obtain cross-sections in absolute units multiply by  $5.66 \times 10^{-20}$

$\frac{\sin \theta}{\lambda} \times 10^{-8}$ :	0.1	0.2	0.3	0.4	0.5	0.6	0.7	0.8	0.9	1	1.1
$\sqrt{\text{Volts.}} \sin \theta$ :	1.22	2.45	3.67	4.90	6.12	7.35	8.57	9.80	11.02	12.25	13.47
Li	6,400	900	275	112	64	36	24	15	10	7	5
Be	12,100	2,760	655	225	108	61	37	23	17	12	8
B	22,500	4,220	1180	425	196	100	59	35	24	17	13
C	19,600	5,610	1780	655	295	148	88	53	35	25	18
N	14,400	4,900	1960	860	415	222	123	74	48	32	23
O	8,100	4,550	2080	1020	540	295	172	104	67	45	31
F	14,400	4,900	2560	1240	645	361	210	130	85	56	40
Ne	4,900	3,900	2180	1220	700	420	256	156	106	72	49
Na	18,200	4,900	2280	1290	772	470	289	188	126	85	59
Mg	22,500	7,200	2820	1890	830	515	327	220	149	100	70
Al	40,000	10,200	3400	1600	900	558	361	237	164	114	83
Si	70,000	13,200	4150	1830	1000	610	400	275	188	130	94
P	67,600	15,600	5300	2220	1160	675	436	289	204	144	104
S	57,600	17,400	6130	2600	1340	770	480	324	222	160	116
Cl	57,600	20,300	7410	3130	1520	850	530	346	243	173	125
A	48,400	18,200	7100	3380	1660	930	580	380	268	193	142

of the Fourier component of  $V$ . But, in the dynamical theory discussed in Chap. XIX, the quantity most nearly corresponding to the intensity of reflection is proportional to the first power of the Fourier component. The discrepancy is due to the neglect, on our present theory, of the weakening of the primary beam due to its interaction with the atoms, while the dynamical theory refers to a crystal of unbounded extent, at least in certain directions. The truth will thus lie between the two in such a way that the theory which we have given is

a good approximation for small crystals, while for large ones the dynamical theory must be used. Preliminary calculations which have been made by Dr. M. Blackman indicate that a quantitative explanation of both sets of results will be possible on these lines.

TABLE VIII  
 $\{E(\theta)\}^2$  CALCULATED FROM THE THOMAS-FERMI FIELD

$\frac{\sqrt{\text{Volts. sin } \theta}}{Z^{1/3}}$	$\frac{\{E(\theta)\}^2}{Z^{2/3}}$
0.0	$2160.0 \times 10^{-18} \text{ cm.}^2$
0.062	2120.0
0.104	2010.0
0.208	1460.0
0.41	678.0
0.62	344.0
0.83	202.0
1.04	122.0
1.25	79.0
1.46	54.0
1.66	44.0
1.87	29.6
2.08	18.7
3.12	6.43
4.16	2.52
6.25	0.61
10.4	0.089
12.5	0.046
14.6	0.026
16.7	0.016
18.7	0.010
20.8	0.0064
25.0	0.0032
31.2	0.0013

Bragg <sup>1</sup> proposes to denote by  $E(\theta)$  the quantity

$$\frac{e^2}{2mu^2} (Z-f) \frac{1}{\sin^2 \theta} = \frac{e^2 m}{2h^2} (Z-f) \frac{\lambda^2}{\sin^2 \theta},$$

where  $2\theta = \phi$ , and this is plotted for aluminium in Fig. 31. (p. 97). If a beam containing  $N$  electrons per sq. cm. falls upon an atom, the number of electrons scattered through  $2\theta$  in a solid angle  $d\omega$  is  $N\{E(\theta)\}^2 d\omega$ .

<sup>1</sup> *The Crystalline State*, I, p. 255.

Mott and Massey<sup>1</sup> have given a table of the quantity  $\{E(\theta)\}^2$  for the elements from lithium to argon, calculated using Hartree atomic fields. For elements of higher atomic number, the Thomas-Fermi atomic model may be used and it may be shown<sup>1</sup> that, for this model,  $\{E(\theta)\}^2 Z^{-\frac{2}{3}}$  is a function of  $Z^{-\frac{1}{3}} \sqrt{P} \sin \theta$  only. A table can therefore be provided which enables  $\{E(\theta)\}^2$  to be found for the elements of higher atomic number. The two tables are reproduced above (Tables VII and VIII). It should be remembered that the deviation  $\phi = 2\theta$ .

### Structure Factor

In general when the unit cell contains more than one atom, the intensity of the diffracted beams depends not on the atom form factors only but also on the structure factor. This has been defined (p. 26) as the intensity scattered in a particular direction by the material in a unit cell. It is found by adding the amplitudes of the wavelets scattered from the individual atoms in the cell, having due regard to phase, and squaring the result. The expression can be put in the simplest form by the use of complex quantities, but in this case they are only a mathematical convenience, not an essential part of the theory. Suppose that a typical atom in the cell has coordinates  $x_p, y_p, z_p$ , then for scattering in the direction corresponding to the indices  $hkl$  the path difference between the wavelet scattered by this atom and that scattered by a (possibly imaginary) atom at the origin is

$$\left(\frac{x_p}{a}h + \frac{y_p}{b}k + \frac{z_p}{c}l\right)\lambda = (x_p'h + y_p'k + z_p'l)\lambda,$$

the amplitude  $E_p$  of the wavelet being the atomic form factor discussed above. The resultant for the whole cell can be expressed in amplitude and phase by

$$\sum_p E_p e^{2\pi i(x_p'h + y_p'k + z_p'l)},$$

where the summation is taken over all the atoms in the cell. The intensity is the (modulus)<sup>2</sup> of this and is

$$\left\{ \sum_p E_p \cos 2\pi(x_p'h + y_p'k + z_p'l) \right\}^2 + \left\{ \sum_p E_p \sin 2\pi(x_p'h + y_p'k + z_p'l) \right\}^2.$$

<sup>1</sup> Mott and Massey, *Theory of Atomic Collisions*. On p. 120 of their book will be found also a table of  $\{E(\theta)\}^2$  for H and He. There are four obvious errors in the second column of this table.

$E_p$  is of course a function of the direction of scattering and hence of  $hkl$ . Since  $E_p$  diminishes rapidly as the angle of diffraction increases, the structure factor will tend to diminish as  $hkl$  increases. In many cases all that is needed is to see whether a given reflection exists or is forbidden by the structure of the unit cell, for this purpose it is not necessary to know the values of  $E$ . Even when numerical values are required rough values of  $E$  are often enough.

### Intensities for Compound Crystals

In order to test this theory accurately it is necessary to know the values of the quantities  $E$ . This involves knowing the corresponding quantities  $f$ . Instead of calculating these from first principles, they can often be found from measurements of the intensities of X-ray reflections, for these depend on  $f$  in exactly the same way that the electron reflections depend on  $E$ .

Shirai<sup>1</sup> has used the measurements of James and Brindley to calculate in this way the relative intensities of electron reflections from the different planes of potassium chloride, and has compared the results with measurements of the intensities of the rings in powder photographs of this compound. He finds reasonably good agreement; no correction was made for temperature. Yearian<sup>2</sup> on the other hand finds marked differences for zinc oxide, the reflections from planes parallel, or nearly parallel, to the basal plane being too strong. Care was taken to exclude the possibility of a preferential orientation of the crystals in the powder, and it does not seem likely that the discrepancy can be explained in this way, which in any case would be more likely to give the opposite effect. Yearian makes a good case for supposing that the discrepancy is due to the nucleus of the zinc atoms being displaced with respect to the electron cloud. The above theory assumes spherical symmetry for the atoms; since the nucleus plays no part in X-ray scattering its displacement would not affect the values found for  $f$ , so that the values calculated for  $E$  would be incorrect.

<sup>1</sup> Shirai, *Phys. Math. Soc. Jap. Proc.* 15, p. 420 (1933).

<sup>2</sup> Yearian, *Phys. Rev.* 48, p. 631 (1935).

The degree of distortion required, however, is so large as to involve energy changes of an amount which seems improbable. Professor Lark-Horovitz, under whose supervision the work was done, has informed us that the results can probably be best explained by a distortion of the valence shells of electrons. Such a distortion would produce only a comparatively small effect on  $f$ , but a large one on  $E$ , which depends on  $Z - f$ , especially at small values of  $\sin \theta/\lambda$ .

For another possible cause of abnormal intensities see p. 132.

The intensities of the rings due to a powder scattered on to a massive supporting block and examined by "reflection" have been measured by Laschkarew and Tashaban.<sup>1</sup> Absorption plays an important part. For MgO they found that the intensity of diffraction involves a factor  $1 - a/2\theta$ , where  $\theta$  is the Bragg angle for the ring considered, and  $a$  is the glancing angle of the primary beam on the supporting surface. This formula is similar to that which holds in the corresponding X-ray case.

### Absolute Intensity of Scattering

The above experiments do not enable us to check the value, predicted by the theory, for the absolute intensity of scattering, but theory and experiment agree so well as far as the variation with angle is concerned that it seems reasonable to trust the theory for the absolute magnitude. The most important point that appears is the very large values of the scattering of electronic waves as compared with X-rays. When the numbers are inserted the formulae become

$$\text{for electrons} \quad A'/A = \frac{1}{r} \cdot 2.38 \times 10^{-10} (Z - f) \left( \frac{\lambda \times 10^8}{\sin \theta} \right)^2 = E/r,$$

$$\text{for X-rays} \quad A'/A = \frac{1}{r} 2.82 \times 10^{-13} f,$$

where  $A'$  is the amplitude at distance  $r$  of the wavelet scattered by an atom acted on by a plane wave of amplitude  $A$ . W. L. Bragg (*l.c.*) has calculated these expressions for aluminium and they are shown in Fig. 31. The abscissae are values of  $\sin \theta/\lambda \times 10^{-8}$

<sup>1</sup> Laschkarew and Tashaban, *Phys. Zeit. Sowjet.* 6, p. 205 (1934).

and so reflections from a definite crystal plane occur at the same abscissa whatever the wave-length. It will be seen that there is a factor of the order  $10^4$  between the amplitudes of scattering for the two kinds of wave for the same reflection. It is of course in agreement with observation that a very thin

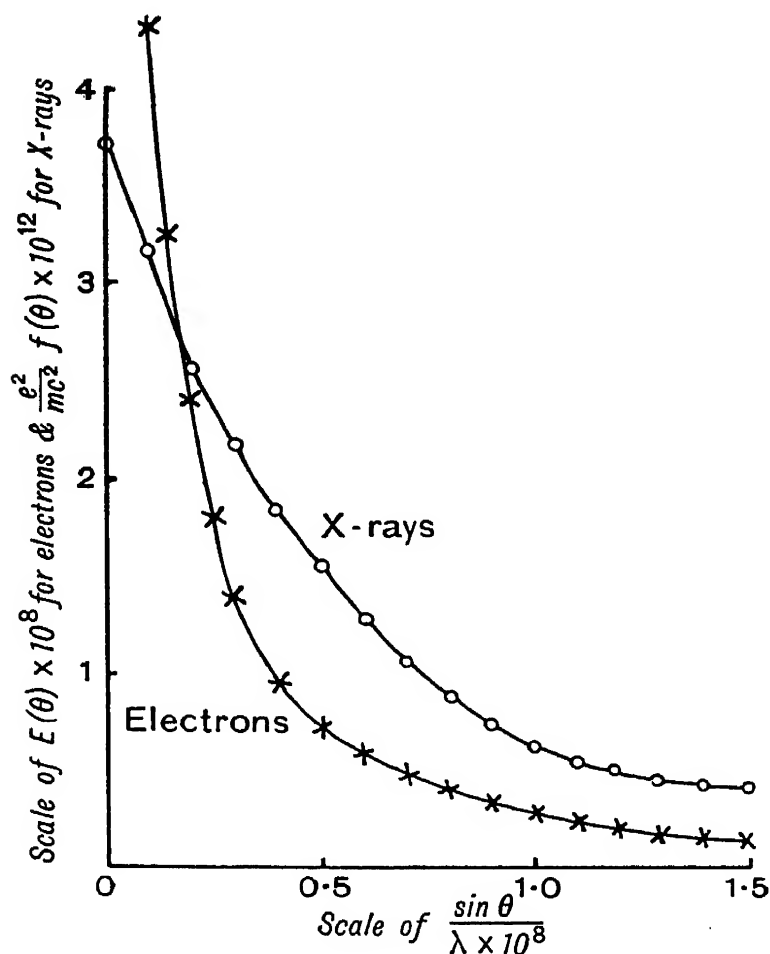


FIG. 31

sheet of material is sufficient to scatter electrons strongly though it would produce very little effect on X-rays.

As Bragg points out, the intensity of scattering by a single plane of atoms normal to the incident rays can be calculated by considering the Fresnel zones. The area of the first Fresnel zone calculated for a distance  $r$  is  $\pi r \lambda$ , and the amplitude due to the atoms in it is reduced in the ratio  $2/\pi$  since the wavelets range in phase over the angle  $\pi$ . If there are  $N$  atoms per unit area the effect of the zone is therefore to give an amplitude  $A'N\pi r \lambda 2/\pi$  and that of the whole wave is half this or  $A'N r \lambda = ANE\lambda$ . For aluminium at the small angle of deviation corre-

sponding to the (111) reflection this is about  $0.025\text{\AA}$ . Twenty atom planes scattering in phase would, if the law held, give an amplitude half the original, and this takes account of one only of the many diffracted beams which would be produced by such a thin sheet. In fact Kirchner<sup>1</sup> has found for a sheet of mica  $9 \times 10^{-6}$  cm. thick that the *intensity* (amplitude squared) of the 060 diffraction is about 0.7 per cent of the incident beam. This is much less than the above theory suggests, but even so when all the diffractions are considered it is enough to account for a very considerable weakening of the primary beam. Kirchner in fact finds that the fraction of the electrons which passes undeflected through a sheet of mica depends considerably on whether the mica is in a position to give strong reflections or not. The discrepancy with theory is explained when we consider that the beam diffracted in any particular direction by the first plane of atoms will be again diffracted by the succeeding planes, and the amplitude will not grow as rapidly as the above calculation would imply. Indeed, it is obvious from energy considerations that, however many scattering planes there may be, the sum of the intensities in all the diffracted beams cannot exceed that of the original beam. The proper consideration of the way in which the energy of the beam is transferred from one to another of the possible diffracted beams requires a more thoroughgoing dynamical theory of the interaction between electron and crystal than has been given so far; it will be dealt with in Chapter XIX. For the moment we will anticipate the results by saying that, in general, the waves settle into a steady state in which the directions, and in most cases the relative intensities, are given very nearly by the purely kinematical considerations of the previous chapter, modified when necessary by the refraction of the electrons when entering or leaving the crystal.

One exceptional case should, however, be mentioned here. If the surface of the crystal is flat and the rays, instead of being nearly normal to it, strike at a small glancing angle, the scattering effect of the surface layer becomes much enhanced. Consider the wavelets scattered by a plane of atoms in the direction of optical reflection. If P is a point distant  $r$  from B the half width of the effective first Fresnel zone will be

<sup>1</sup> Kirchner, *Ann. d. Phys.* 13, p. 38 (1932).

AB, where A is determined by the consideration that the wavelet from it arrives at P half a period behind that from B. The wavelet from A has a start on that from B equal to the time taken by the waves to go the distance  $AB \cos \theta$ . Hence the required condition is that  $AP - BP - AB \cos \theta = \lambda/2$ . A simple calculation shows that this holds when  $AB = \sqrt{\lambda r} / \sin \theta$ , the zone is thus increased in length by the factor  $1/\sin \theta$ , and the number of atoms contained in it is increased in the same proportion since the dimension perpendicular to the plane of the figure is unchanged. For a glancing angle of the order of  $2^\circ$  the amplitude of the wave reflected by a single plane of atoms is therefore nearly 30 times as large as that of a wave diffracted by a plane

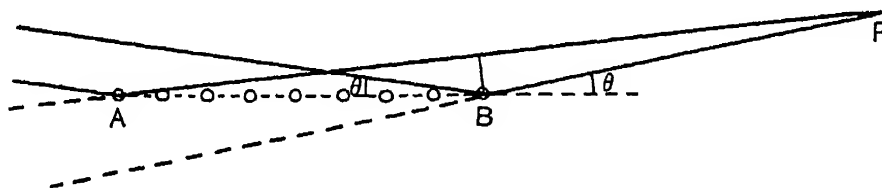


FIG. 32

of atoms set normally to the incident electrons, the deviation, and hence the value of  $E$ , being supposed the same. This gives an amplitude comparable with that of the original wave, and the hypothesis on which Bragg's law is based that successive planes of atoms reflect nearly equal amplitudes becomes quite untenable. Only the top two or three layers at the most will be effective and these with rapidly diminishing intensity. Harding<sup>1</sup> has shown how to deal with this case which will be discussed further in Chapter XIX. It should be noticed that it only arises when the surface of the crystal is flat to atomic dimensions, which as a rule only happens when a natural or cleavage surface of a crystal is used to reflect the electrons.

### Limitation of Effective Penetration caused by Inelastic Collisions

In considering the thickness of material effective in diffraction we must take account of both possible types of interaction between electrons and atoms, namely elastic and inelastic scattering. Only the former can give rise to inter-

<sup>1</sup> Harding, *Phil. Mag.* 23, p. 271 (1937).

ference in directions related in a definite way to that of the original beam, as are the effects we have considered so far. Once the electron has made an inelastic collision it has lost all memory of its original direction, and must be regarded as starting afresh from the atom with which the inelastic collision took place. It has produced a change in an atom which is theoretically, at least, observable, and in certain cases even practically so, *e.g.* if the atom is one of silver in a photographic emulsion or forms part of a phosphorescent centre. Hence from the point of view of Chapter V the 'experiment', which started with the emission of the electron, has ended, the wave-packet of the electron has served its purpose in guiding the electron to its destination, and passes out of the picture. The electron of course still exists, but if we want to consider its future history we must do so by supposing a wave to spread from the place of collision as centre. Any interference pattern which such a wave can cause by being scattered in the crystal will be related in some definite way to the axes of the crystal, but not at all to the original direction of motion of the electron. In general the inelastically scattered electrons will help to form the very considerable 'background', which exists in patterns even from quite thin specimens.

Now we can calculate roughly the distance which an electron can penetrate a solid without making an inelastic collision, and so becoming incapable of interfering. Smith<sup>1</sup> finds that the number of primary ions made by an electron of 4500 volts energy (the fastest he used) in argon at 1 mm. pressure is about 0.9 pair per cm. For fast electrons the chance of ionisation is roughly inversely as the energy, and for 30,000 volts would be 0.13 per cm. Now there are  $3.55 \times 10^{16}$  atoms per c.c. in the gas, while in an ordinary solid of about the same atomic number as argon there are about  $0.6 \times 10^{23}$  atoms per c.c. (*e.g.* iron has  $0.84 \times 10^{23}$ , copper  $0.85 \times 10^{23}$ , aluminium  $0.6 \times 10^{23}$ , NaCl  $0.45 \times 10^{23}$ ). Hence the mean free path for ionisation in a solid is

$$\frac{3.55 \times 10^{16}}{0.13 \times 0.6 \times 10^{23}}, \text{ or } 4 \times 10^{-6} \text{ cm. approximately.}$$

In addition, there are to be considered the inelastic collisions

<sup>1</sup> Smith, *Phys. Rev.* 36, p. 1293 (1930).

which result in excitation of the atoms without ionisation. The inclusion of these collisions will, of course, decrease the effective free path.

The above calculation is in agreement with the general experience that films of heavy metals more than about  $10^{-6}$  cm. thick give patterns with rather heavy backgrounds, and also with the experiments of Kirchner,<sup>1</sup> who finds that  $\mu^{-1}$  for mica is about  $2.8 \times 10^{-6}$  cm. for electrons of 30,000 volts energy. In this work  $\mu$  was the absorption coefficient measured by the diminution of intensity in the primary beam.

It follows that crystals as thick as  $10^{-5}$  cm. or more would destroy the capacity for interference of most of the electrons passing through them, and we must attribute most of the intensity of the rings to crystals thinner than this.

It follows also that in all cases when diffraction patterns are formed by transmission either through films or through protrusions on a solid surface, the pattern is determined rather by the atoms in the plane normal or nearly normal to the incident beam acting as a cross grating, than by true Bragg reflections.<sup>2</sup> For consider the wavelets from a line of length  $t$  of atoms with which the incident electrons make a small angle  $\phi$ . The phase difference in a direction  $\psi$  between the wavelets from the ends of the line is

$$\frac{2\pi t}{\lambda} (\cos \phi - \cos \psi) = \frac{\pi t}{\lambda} (\psi^2 - \phi^2).$$

If  $t = 4 \times 10^{-6}$ ,  $\phi = 1/30$ ,  $\lambda = 0.5 \times 10^{-9}$ , the phase difference is less than  $2\pi$  for all values of  $\psi$  between  $\pm 3.7 \times 10^{-3}$  radians, corresponding to a ring 3 mms. thick on a plate 40 cms. away. The rings due to large crystals are in fact considerably finer than this, and part of their width is due to other causes.

Besides the losses due to inelastic scattering there is another reason why thin crystals, of the order of  $10^{-6}$  cm., will give more intense diffraction patterns than thicker ones. For

<sup>1</sup> Kirchner, *Ann. d. Phys.* 13, p. 38 (1932). In Kirchner's experiments the absorption coefficient was found from the loss in intensity in the main beam after passing through films of mica. With the thickness used ( $\sim 10^{-5}$  cm.) the main beam only retained a few per cent of its original strength, and though Kirchner showed that the elastically scattered beams also had intensities of this order of magnitude, it seems probable that the main loss of intensity from the main beam was caused by the inelastic scattering.

<sup>2</sup> Cf. p. 55.

the thick crystals reflection will only occur over a narrow range of angle of incidence ( $\sim 10^\circ$ ), and in a random assembly few will be at the correct angle. But for a two-dimensional grating at nearly normal incidence the deviation is proportional to the cosine of the angle of incidence, and so will be constant to 1 per cent over a range of  $\pm 8^\circ$ . It is true that such a grating will never give the 100 per cent reflection which can theoretically be given by a large crystal at the Bragg angle, but, since a single layer of atoms will diffract several per cent of the rays, one  $10^{-6}$  cm. thick would probably diffract a very large fraction. Hence the much greater range of angle for the thin crystal will far more than compensate for the better diffracting power of the thick crystal when set at the most favourable angle.

It will have been noticed that the E functions depend on the quantity  $\sin\theta/\lambda$ , which is constant for any Bragg reflection. Thus, as the wave-length is altered, all the quantities involving elastic collisions are the same, provided we always consider reflection by the same Bragg planes. Suppose, in particular, that we consider reflection by planes parallel to the crystal surface. The effective depth of penetration, as measured by the number of atom-layers used in diffraction, will remain the same, the greater penetrating power of the faster electrons being balanced by their greater obliquity. For electrons of more than about 200 volts the chance of an inelastic collision per unit path is roughly inversely as the energy, *i.e.* varies as  $\lambda^2$ , while the length of path, keeping  $\sin\theta/\lambda$  constant, is inversely as  $\lambda$  for equal depth of penetration below the surface. Thus the mean depth before an inelastic collision occurs will be proportional to  $\lambda$ . Hence slow electrons will be more affected by inelastic collisions than fast ones. But if electrons which have lost energy are not recorded, as in the experiments of Davisson and Germer, there will be little to choose between slow and fast electrons as regards the relative effectiveness of the various layers of atoms. There is, however, one important difference. While for fast electrons the surface will have to be extremely perfect to count as smooth, moderate roughness will not make much difference to the slow electrons, as they strike the surface at a much bigger glancing angle.

### Size of Central Maximum and Background Scattering

White<sup>1</sup> has investigated the intensities in the patterns formed by transmission through thin gold foil of thickness  $\sim 150$  Å. The diffraction rings in such cases are superimposed on a strong background which decreases in intensity with the distance from the central spot. The intensities of the different regions were measured photometrically. If  $2\pi r.f(r)dr$  is the total number of electrons striking the photographic plate at a distance between  $r$  and  $r+dr$  from the centre,  $r.f(r)$  was

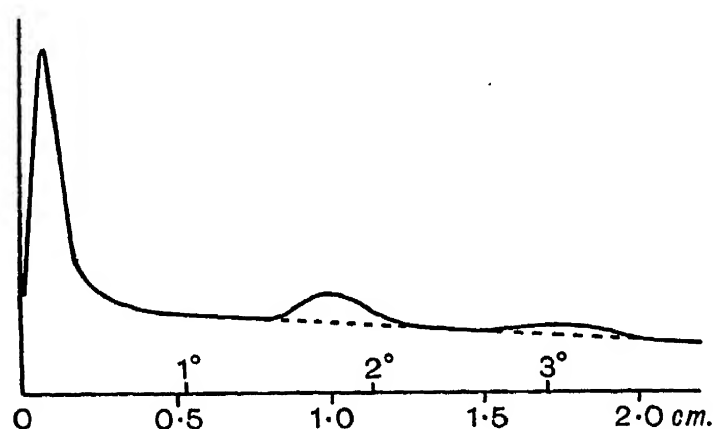


FIG. 33

found to be practically constant over the plate except in the immediate neighbourhood of the central spot (Fig. 33). Kirchner<sup>2</sup> has measured  $f(r)$  in the course of his investigations into the passage of electrons through thin films of mica. Only one curve is given for  $f(r)$ , but it shows the same general character as White's.

It is generally assumed that the background is mainly due to inelastic scattering. Some diffuse elastic scattering must indeed occur due to the thermal agitation of the atoms in the crystals, but since the main elastic scattering, as shown by the intensity of the rings, is a comparatively small fraction of the whole, the thermal effect is not likely to be very important. Theoretical investigations of inelastic scattering of electrons have been made for single atoms. If one assumes that the

<sup>1</sup> White, *Phil. Mag.* 9, p. 641 (1930).

<sup>2</sup> Kirchner, *Ann. d. Phys.* 13, p. 38 (1932).

scattering by thin foils is single, then the results of this theory as developed by Bethe <sup>1</sup> and by Morse <sup>2</sup> may be applied directly to the present problem.

Morse has given explicit formulae (based on the Thomas-Fermi atomic model) which are valid for angles of scattering greater than  $\Delta E/2E$ , where  $\Delta E$  is the energy loss of an electron of energy  $E$ . One would certainly expect the theory to hold from  $1^\circ$  upwards, which would cover the experimental investigations of White. The theory indicates that  $f(r)$  should fall off as  $1/r^3$  in the case of gold, whereas White's experiments indicate  $1/r$ . Bethe's theory is valid down to smaller angles, and can be used to obtain information about the region below  $1^\circ$ . It indicates a large increase of  $f(r)$  with decreasing  $r$ , reaching a constant value near  $r=0$ , and showing little variation for angles of less than a few minutes of arc. At larger angles, the general tendency of the  $f(r)$  curve is again such as to suggest a more rapid falling off of  $f(r)$  with  $r$  than is indicated by experiment. Thus for hydrogen, for which exact calculations are possible,  $f(r)$  should fall off as  $1/r^2$  in the region above a few minutes of arc. In comparing this result with that of Morse it should be remembered that the latter is only valid for heavy atoms.

As regards the absolute magnitude of the scattering, a preliminary calculation, for the results of which, as for other help in this section, we are indebted to Dr. Blackman, indicates that the mean free path for all inelastic collisions in gold should be of the order 40 Å. This is less than would be expected from the experiments, but it would be considerably increased if the very small angle scattering (of the order of a few minutes of arc) were ignored. Some results of White's are of interest in this connection (Table IX): they refer to gold films of about 200 Å thickness and electrons of about 30 kv., the distance between plate and film being 32.7 cm. For the central maximum White found an approximately Gaussian distribution over about 2 mm. on either side after allowing for the natural width of the beam. For 30 kv. the parameter ' $a$ ' in the expression  $y = y_0 \exp(-x^2/a^2)$  was 0.80 mm. for a film 140 Å thick, and 1.18 mm. for one of 250 Å.

<sup>1</sup> Bethe, *Ann. d. Phys.* 5, p. 325 (1930).

<sup>2</sup> Morse, *Phys. Zeit.* 33, p. 444 (1932).

There has recently been some controversy<sup>1</sup> as to whether the electrons forming the central spot have lost any appreciable amount of velocity. Experiments have been made to see if any change in the diameter and width of the rings due to test specimens is caused by placing a thin foil in the path of the electrons before they reach the specimen. It is, however, agreed that the loss in velocity suffered by 45 kv. electrons in traversing without appreciable deflection a film of aluminium or mica

TABLE IX  
RELATIVE INTENSITIES

Central Maximum . . . . .	60
Rings : (111) . . . . .	7.1
(200) . . . . .	2.4
(220) . . . . .	1.3
(311 and 222) . . . . .	2.7
Background within 2 cm. of centre .	180
Total background, order of . . .	300

$10^{-4}$  cm. thick does not exceed 1 per cent. Such a film is of course considerably thicker than those used for diffraction.

It is noticeable<sup>2</sup> that when the relative intensity of the background is increased by lowering the voltage, or by taking a thicker film, the sharpness of the rings does not greatly change, but they gradually lose contrast with the background. The background in reflection pictures is usually darker than in transmission. It depends greatly on the state of the surface, and cannot be easily treated theoretically.

One may conclude that there is a definite discrepancy between theory and experiment in the case of transmission patterns, but further measurements are needed with films prepared and treated in various ways. It is possible that atoms which do not form part of any regular crystal lattice may play an important part.

<sup>1</sup> Trillat and Hautot, *Ann. d. Phys.* 30, p. 165 (1937), 31, p. 583 (1938); Kirchner, *Ann. d. Phys.* 30, p. 683 (1937).

<sup>2</sup> Thomson, *Proc. Roy. Soc.* A125, p. 352 (1929); Cochrane, *ibid.* A166, p. 228 (1938).

## CHAPTER VIII

### SOME SECONDARY EFFECTS

#### Refractive Index

IN the interior of a solid the potential varies from place to place, and if the solid is crystalline the variation is periodic ; it is this periodic variation which produces the diffraction of electrons passing through the crystal, and as we have seen, the intensities of the different diffracted beams depend on the amplitudes of the corresponding Fourier components of the potential. But besides this periodic variation, the potential inside a solid differs from that outside by a constant term, which we may think of as being the zero order term in the Fourier expansion. To a first approximation the effect of the solid on the electrons is got by adding the separate effects of this constant term and that of the periodic terms. The latter we have already studied, it remains to consider the effect on the electrons of suddenly entering a region in which the potential is different from that of free space ; in practice positive to it. We have already seen (p. 19) that a region of varying potential acts on the waves like a medium of variable refractive index ; when the electrons are accelerated their wave-length is shortened, and on crossing a discontinuity of potential there occurs a refraction following Snell's law with a refractive index equal to the ratio of the wave-lengths on the two sides of the boundary.

When account is taken of relativity, the wave-length of an electron accelerated through a potential  $P$  is

$$\lambda = h / \sqrt{2em_0P(1 + eP/2m_0c^2)} ;$$

if it passes into a region in which the potential increases by  $\Phi$  the new value of  $\lambda$ , namely  $\lambda'$ , is got by writing  $P + \Phi$  in the above expression instead of  $P$ . Hence the refractive index

$$\mu = \frac{\lambda}{\lambda'} = \frac{\sqrt{2em_0P + \Phi \cdot (1 + e \cdot P + \Phi/2m_0c^2)}}{\sqrt{2em_0P(1 + eP/2m_0c^2)}}$$

and

$$\mu^2 = \left(1 + \frac{\Phi}{P}\right) \left[ \frac{1 + e(P + \Phi)/2m_0c^2}{1 + eP/2m_0c^2} \right].$$

Since  $2m_0c^2/e \sim 10^6$  volts, the factor in the square bracket is nearly unity except for very fast electrons and, to the first order of small quantities,

$$\mu^2 - 1 = \frac{\Phi}{P} \left(1 + \frac{Pe}{2m_0c^2}\right),$$

where for 40,000 volt electrons, the bracket differs from unity by about  $1/25$ . As we shall see,  $\Phi$  for most substances is of the order of 10 volts, so that  $\mu^2 - 1$  is small for fast electrons. Nevertheless the refraction effects may be important. Consider the case (Fig. 34 *a*) in which the electrons incident on a surface

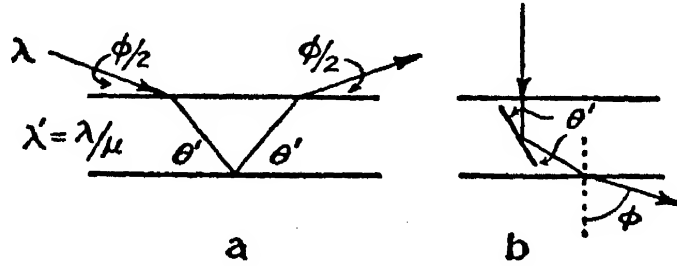


FIG. 34

are refracted from Bragg planes parallel to the surface. If  $2d\sin\theta = n\lambda$ , then  $2\theta$  is the deviation which would occur in the absence of refraction. Let  $\phi$  be the observed deviation, and  $\theta'$  the glancing angle inside the crystal. Then, by Snell's law,  $\cos \phi/2 = \mu \cos \theta'$  and  $2d \sin \theta' = n\lambda' = n\lambda/\mu$ .

Thus

$$\frac{\cos \phi/2}{\mu} = \sqrt{1 - \frac{n^2\lambda^2}{4d^2\mu^2}}$$

and

$$\sin^2 \phi/2 = 1 - \mu^2 + \frac{n^2\lambda^2}{4d^2} = 1 - \mu^2 + \sin^2 \theta.$$

Now for 40,000 volt electrons and for the 200 reflection from gold,  $\sin^2\theta$  is  $2.3 \times 10^{-4}$ , while for  $\Phi = 10$  volts,  $1 - \mu^2 = -2.6 \times 10^{-4}$ , so that these two quantities are comparable. Under these conditions, indeed, the reflection could not occur, since  $\sin^2 \phi/2$  is slightly negative. In fact no reflection is possible for which

$$\frac{n^2\lambda^2}{4d^2} < \frac{\Phi}{P} (1 + Pe/2m_0c^2).$$

It may be noticed that the *relative* change in angle is almost independent of the voltage  $P$ , for

$$\frac{\sin^2 \phi/2}{\sin^2 \theta} = 1 + \frac{1 - \mu^2}{\sin^2 \theta} = 1 - \Phi \frac{8em_0 d^2}{m^2 h^2}$$

neglecting the relativity correction.

On the other hand, for normal incidence on a flat plate the effect is very small (Fig. 34 *b*). We have  $2d \sin \theta' = n\lambda' = n\lambda/\mu$  and  $\mu \sin 2\theta' = \sin \phi$ . Hence  $\sin \phi = 2\mu \sin \theta' \cos \theta = n\lambda/d \cos \theta'$  which, when  $\theta'$  is small, is very nearly indeed equal to  $2\theta$ . Thus in this case the effects of refraction cancel, which, together with the small ratio of  $\Phi/P$ , explains why it is not necessary to take account of refraction in considering transmission through thin films. For other angles of incidence the effect in general is of the order  $\Phi/P$  or  $\sim 0.02^\circ$ , which can usually be neglected.

Returning to the case of Fig. 34 *a*, the effect of refraction is to draw the diffracted beam towards the refracting surface. If  $\eta'$ ,  $\eta$  are the distances of a diffracted spot on the photographic plate from the line in which the plane of the refracting surface cuts it (the 'shadow edge') with and without refraction,  $\eta'^2 = \eta^2 - L^2(\mu^2 - 1)$  where  $L$  is the distance of the plate.

Hence

$$\eta - \eta' = \frac{L^2(\mu^2 - 1)}{\eta + \eta'},$$

so that for spots far out, for which  $\eta - \eta'$  is small, the displacement due to refraction is inversely as the distance from the shadow edge. It should be noticed that the crystal will have to be set at a different angle to the incident beam if refraction occurs from what would otherwise be necessary. The actual change in the position of the diffracted spot as measured from the incident beam is twice that when the position is measured from the shadow edge, but the change as a fraction of the coordinate measured is the same in the two cases.

If we wish to consider the influence of refraction on the reflection from a crystal plane which is not parallel to the free surface we must decide how the crystal is to be supposed to be set in the two cases, since an adjustment which would give a reflection in the absence of refraction will not do so if this is appreciable. The most useful supposition is that the reflecting

planes in the two cases are parallel. Now the angle of Bragg reflection in the crystal is only altered in the ratio  $\mu : 1$  which produces a negligible effect so that  $\theta$  and  $\theta'$  can be taken as equal. Let the incident beam meet the plate in C (Fig. 35) and let P be the position in which a reflection would occur from the plane AB if there were no refraction. Owing to refraction the direction of the incident beam in the crystal is displaced to  $C_1$  where  $XC_1^2 - XC^2 = (\mu^2 - 1)L^2$ .

The reflecting plane must be shifted to  $A_1B_1$ , parallel to AB, and the direction of the reflected beam in the crystal is

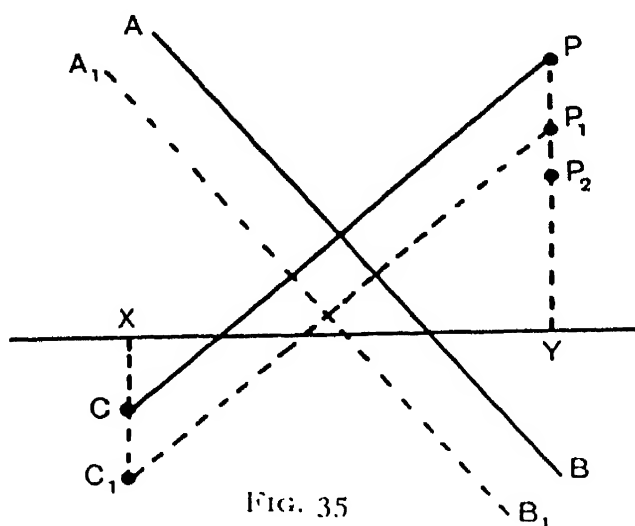


FIG. 35

$P_1$  where  $C_1P_1$  is parallel to  $CP$  and approximately equal to it. This beam is refracted on leaving the crystal and its direction is displaced from  $P_1$  to  $P_2$  in a direction normal to the surface to an extent given by

$$YP_1^2 - YP_2^2 = (\mu^2 - 1)L^2.$$

Writing  $\frac{XC}{L} = a, \frac{PY}{L} = y, \frac{P_2Y}{L} = y_2$

and using the fact that  $PP_1 = CC_1$ , it can easily be shown that

$$\begin{aligned} y_2^2 &= y^2 - 2(y + a)\{\sqrt{a^2 + \mu^2 - 1} - a\} \\ &= (y + a)^2 + a^2 - 2(y + a)\sqrt{a^2 + \mu^2 - 1}. \end{aligned}$$

This may be used to determine the change to be expected on account of refraction in the shape of rings due to a polycrystalline substance or liquid bounded by a smooth surface.

Each point of the circle would be drawn towards the shadow of the free surface and the nearer that the point originally was to the surface the greater would be the displacement. As a

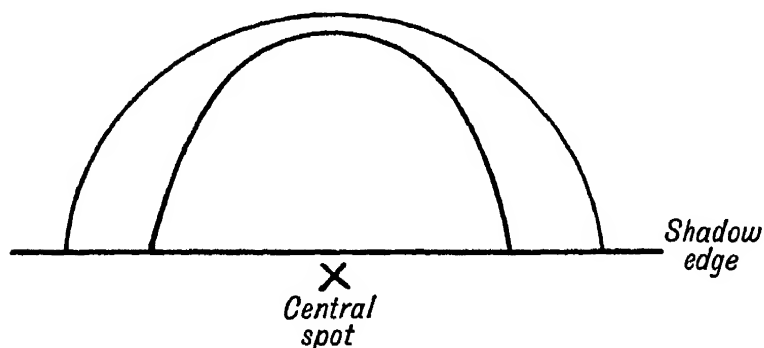


FIG. 36

result a ring originally circular would be altered to a shape like the letter U (Fig. 36).

### Single Refraction

The deviation due to a single refraction only may readily be calculated. If  $\alpha$ ,  $\alpha'$  be the angles which the ray makes with the surface inside and outside the material (Fig. 37),

$$\mu = \frac{\cos \alpha'}{\cos \alpha},$$

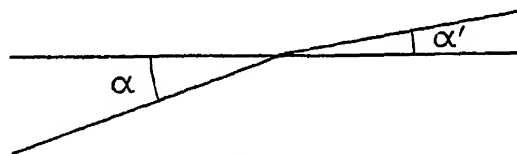


FIG. 37

and hence 
$$\mu^2 = \frac{1 - \sin^2 \alpha'}{1 - \sin^2 \alpha} = 1 - \alpha'^2 + \alpha^2,$$

when the angles are small, which is the only case which matters.

Hence 
$$\alpha - \alpha' = \frac{\mu^2 - 1}{\alpha + \alpha'},$$

which is clearly equivalent to the result given above (p. 108), showing that the important effect of the refractive index is the bending of the rays, rather than the change in the Bragg angle due to the change in wave-length. Since the effect of the refractive index diminishes as the angles with the surface increase there will be a value of  $\alpha$  above which it is inappreciable.

In most reflection experiments the glancing angles between

the paths of the electrons and the apparent surface are of the order of  $2^\circ$ . If a particular part of the surface makes an angle  $\beta$  with the apparent surface, the value of  $\alpha'$  is  $\beta \pm 2^\circ$ . If  $\beta$  is large, *i.e.* if the surface is rough, the effect of refraction can be neglected. An estimate can be made as follows of the magnitude of  $\beta$  above which this holds.

For a deviation of 0.5 mm. on a plate 40 cm. away  $\alpha - \alpha' = 1.25 \times 10^{-3}$ ; taking  $\mu^2 - 1 = 3 \times 10^{-4}$  we get  $\alpha \doteq \alpha' = 0.12 \text{ rad.} = 6.9^\circ$ . While a shift of 0.5 mm. would be fairly easily detectable on a pattern of sharp rings or spots, and would cause an appreciable broadening of the rings if there were also unrefracted electrons present, many of the patterns in which refraction might occur are diffuse, and then the angles would have to be considerably smaller to give a noticeable effect, so that the above criterion must be used with caution. In any case it refers to an arrangement in which only one refraction is effective.

### Kikuchi Lines

In the course of experiments on the diffraction of electrons passing through thin films of mica, Kikuchi<sup>1</sup> discovered an important effect which has since borne his name. Using different thicknesses of mica he found three types of pattern. The first, due to the thinnest films, consisted of a pattern of spots which we have already discussed (p. 79), the second from rather thicker films consisted of spots arranged on circles and satisfying the three Laue conditions (p. 80), together with pairs of black and white lines (Plate III *b*), the third from the thickest films consisting of lines only (IV *a*). It is with these lines that we are now concerned. The most convenient way of describing their positions is in terms of the theory which Kikuchi originally brought forward to explain them, since this has been found to represent correctly not only the patterns observed by him but also a great variety obtained in later experiments. He supposes that the electrons entering the crystal are first scattered diffusely, and that then those of them which make the Bragg angle with any net plane of the crystal are reflected from that plane. He also makes the reasonable

<sup>1</sup> S. Kikuchi, *Proc. Imp. Acad. Japan*, 4, pp. 271, 354 (1928); *Jap. Jour. Phys.* 5, p. 83 (1928).

assumption that the intensity of the electrons after the first scattering steadily diminishes as the angle which their direction makes with the original beam increases. Suppose  $AB$ ,  $A'B'$  (Fig. 38) represent net planes. Some of the diffusely scattered electrons which would have emerged in the direction  $P$  are reflected into the direction  $Q$  if  $\theta$  satisfied the Bragg condition for the plane  $AB$ . On the other hand some which would have gone to  $Q$  are reflected by  $A'B'$  to  $P$ . But it is clear that the electrons in the former group have suffered a smaller deviation

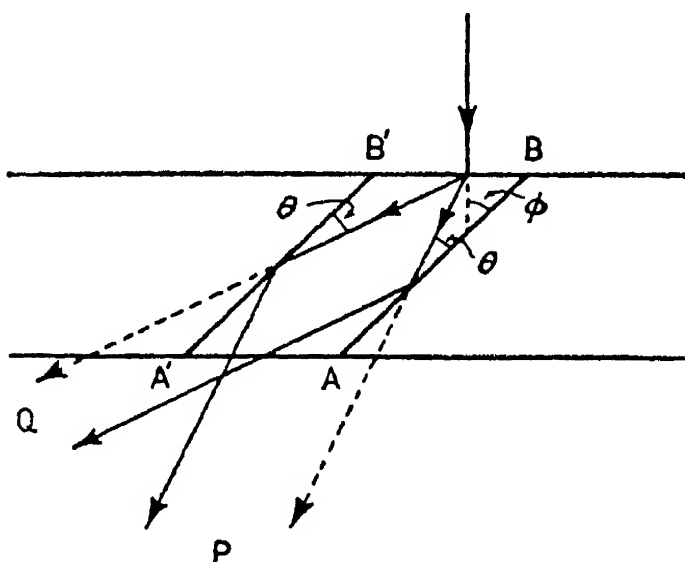
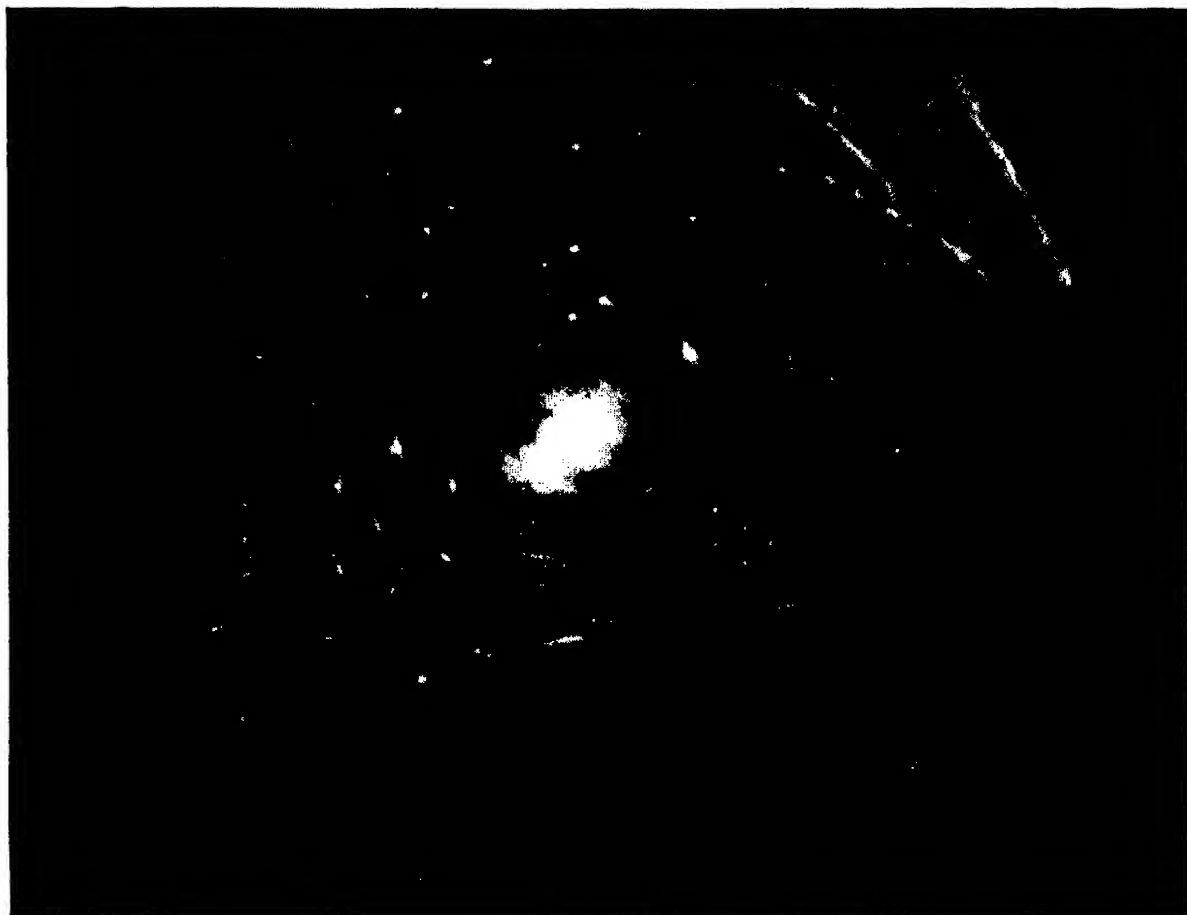


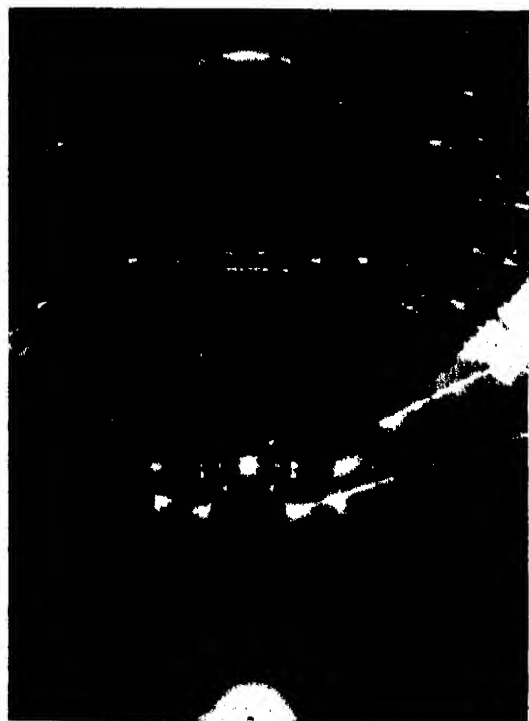
FIG. 38

at the first scattering, and hence are more numerous, than those in the latter, so on the whole  $Q$  gains electrons and  $P$  loses. For electrons initially scattered in all directions, the reflected directions form cones with the normal to  $AB$  as axis, and with semi-vertical angles  $\pi/2 - \theta$  on either side of it. These cones intersect the photographic plate in hyperbolae which in practice are nearly straight lines (the angles in Fig. 38 are for clearness drawn much too large). The angle between  $P$  and  $Q$  is  $2\theta$ , and the distance between the black and white lines on the plate is  $S = 2L\theta = LN\lambda/d$  where  $d$  is the spacing of the planes. If there is more than one order,  $N$ , of reflection, there will be several pairs of black and white lines. Such are in fact observed. The intersection with the plate of the net plane causing the lines is midway between them, and Kikuchi found that he could determine the orientation of the crystal from this fact, different pairs of lines giving consistent results. Table X

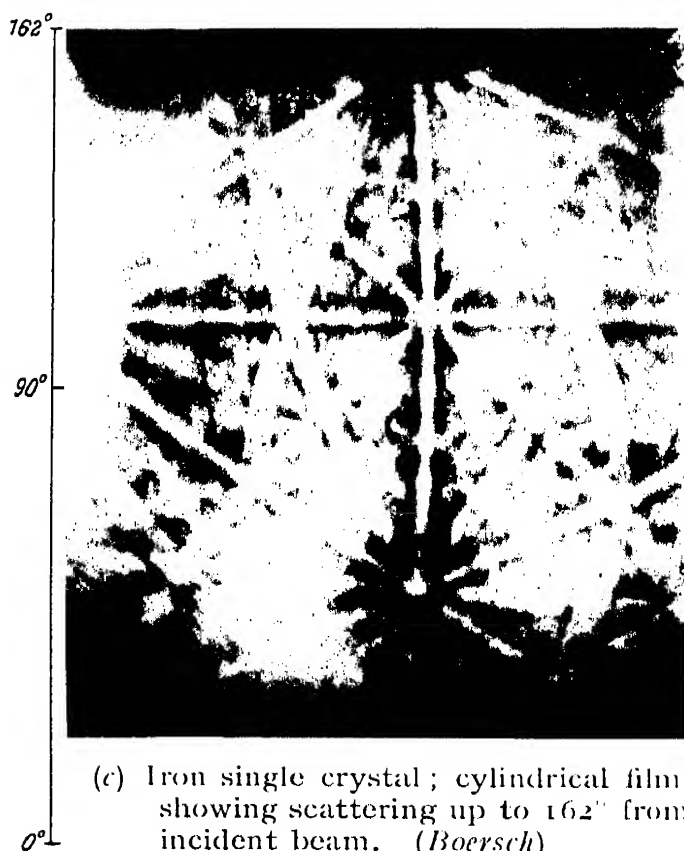
# PLATE IV



(a) Mica, thick sheet. (*Finch*)



(b) Fluorite cube face, beam approximately parallel to cube edge. (*Finch*)



(c) Iron single crystal ; cylindrical film, showing scattering up to  $162^\circ$  from incident beam. (*Boersch*)



from Kikuchi's paper shows the values of the various spacings  $d$ , calculated from the distance apart of the lines. The agreement with the values known from the X-ray analysis of mica is admirable. Shortly afterwards Nishikawa and Kikuchi<sup>1</sup> showed that similar lines were produced by reflection from the face of a calcite crystal and that their positions could be determined in the same way. Later experimenters have obtained them from a number of ionic crystals both with natural faces and after

TABLE X  
KIKUCHI'S CALCULATIONS OF  $d$

Indices of Planes	$d$ in Å		Indices of Planes	$d$ in Å	
	Cathode Rays	X-rays		Cathode Rays	X-rays
(010)	9.00	8.98	(331)	1.50	1.94
(100)	5.16	5.13	(061)	1.48	1.48
(120)	3.43	3.39	(331)	1.47	1.47
(130)	2.57	2.58	(161)	1.43	1.43
(131)	2.60	2.59	(261)	1.31	1.30
(201)	2.55	2.58	(171)	1.22	1.24
(132)	2.57	2.53	(353)	1.21	1.23
(201)	2.49	2.52	(425)	1.23	1.22
(203)	2.50	2.49	(193)	0.97	0.97
(231)	1.95	1.96	(391)	0.88	0.86
(051)	1.78	1.79	..	..	..

etching. One of the authors<sup>2</sup> has shown that they are also produced by single crystals of metals.

According to the above theory the line receiving an excess<sup>3</sup> of electrons should always be the more distant from the original direction of the beam. This is found to be the case. When a plane is parallel to the original beam the theory predicts no effect, since the reflection to the two sides should be equal. Actually a band of enhancement is produced, whose edges are approximately where the lines would be if the initial beam was otherwise directed.

<sup>1</sup> Nishikawa and Kikuchi, *Proc. Imp. Acad. Jap.* 4, p. 475 (1928).

<sup>2</sup> Cochrane, *Nature*, 138, p. 202 (1936).

<sup>3</sup> There is an unfortunate confusion in nomenclature. Kikuchi calls a line 'black' when it receives an excess of electrons, it is so on the negative and Plate III *a, b* are negatives. Other writers call a line 'black' when it is so on a positive. It seems better to refer to the lines as 'enhanced' and 'weakened', since even the latter have a considerable background intensity and the existence of this background is probably essential to their production.

Besides these symmetrical bands it is frequently found that the background in the region between a pair of Kikuchi lines is of different intensity from that outside, thus producing the appearance of a band, though the lines bounding it are of different intensities. For specimens examined by reflection, the region between the lines always receives an excess of electrons, and this applies also to the true symmetrical bands. In transmission, as Boersch<sup>1</sup> has shown, the region receives an excess of electrons when the mica is thin, but usually it is in defect for thicker films. Cases are known (p. 302) where a symmetrical band changes from excess to defect along its length. Boersch<sup>1</sup> has found that if the electrons before reaching a thin film of mica are made diffuse by passing through a layer of zinc oxide, the bands show a defect of electrons instead of an excess. It would seem therefore that what matters is the extent to which the initial beam of electrons has been diffused before the Bragg reflections occur.

The bands formed by reflection, both symmetrical and otherwise, extend to very large angles even with fast electrons.<sup>2</sup> Plate IV *c* taken from Boersch's paper shows bands due to a single crystal of iron. The film was bent into a cylinder, with its axis normal to the incident beam and parallel to the surface of the crystal, and the scale shows the azimuth angles reckoned from the direction of the beam. Possible explanations of these phenomena are discussed in Chapter XIX. It should be noticed that apart from considerations of intensity the position of the lines and bands is independent of the original direction of the beam, though they depend on its wave-length. If the crystal is rotated they move as if rigidly attached to it.

### Nature of the Primary Scattering

Nothing has been said so far as to the nature of the primary scattering postulated by Kikuchi. Measurements of the distance between the lines of a pair show that, if the theory is to be accepted, the wave-length of the scattered electrons is nearly the same as that of the original beam, so they cannot have lost much energy. On the other hand no measurements yet

<sup>1</sup> Boersch, *Phys. Zeit.* 38, p. 1000 (1937).

<sup>2</sup> Meibonn and Rupp, *Zeit. für. Phys.* 82, p. 690 (1933).

made would have detected an energy change of 100 volts, and it is probable that the majority of inelastic collisions involve energy changes of less than this. It is therefore quite possible that the primary scattering is inelastic. The question will be discussed further in connection with the dynamical theory of crystal diffraction in Chapter XIX.

### Intersections of Kikuchi Lines

When two Kikuchi lines intersect, especially if they do so at a small angle, it is often found that they are, as it were, repelled from the point of intersection, the two halves of different lines joining up to form a figure resembling the two branches of a hyperbola (Fig. 39 and Plate VI *b*). Shinohara<sup>1</sup> has explained

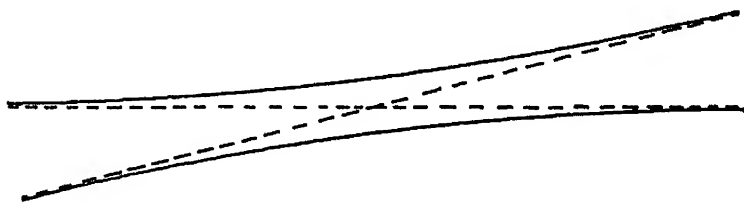


FIG. 39

this by pointing out that there is a peculiar relation between the two directions of the diffusely scattered electrons which would be reflected to the point of intersection by the planes causing the two lines. In fact if  $\mathbf{h}$ ,  $\mathbf{h}'$  are the vectors to the points of the reciprocal lattice corresponding to the two lines,  $\mathbf{s}$  the unit vector in the direction of the intersection, and  $\mathbf{s}_0$ ,  $\mathbf{s}'_0$  the vectors corresponding to the diffusely scattered electrons before reflection,  $\mathbf{s} - \mathbf{s}_0 = \lambda \mathbf{h}$  and  $\mathbf{s} - \mathbf{s}'_0 = \lambda \mathbf{h}'$ . Hence  $\mathbf{s}_0 - \mathbf{s}'_0 = \lambda(\mathbf{h}' - \mathbf{h})$  so that  $\mathbf{s}_0$ ,  $\mathbf{s}'_0$  satisfy the Bragg condition for the plane whose indices are the difference of those corresponding to the two planes corresponding to the two Kikuchi lines. Thus  $\mathbf{s}_0$ ,  $\mathbf{s}'_0$  have each simultaneously two possibilities of reflection and one may expect each reflection to be weakened. This will be especially marked if  $\mathbf{h}' - \mathbf{h}$  corresponds to a strong reflection, as will usually be the case if its indices are small. If the Kikuchi lines make a small angle, *i.e.* correspond to planes which are nearly parallel, this will usually be the case. The effect is analogous to the "Aufhellung" observed with

<sup>1</sup> Shinohara, *Sci. Pap. Inst. Phys. and Chem. Res.* 20, p. 40 (1932).

X-rays. Shinohara<sup>1</sup> has also observed short enhanced lines close to strong Kikuchi lines. He explains these as portions of weak Kikuchi lines brought into prominence by the proximity of the stronger line.

### Interference between Kikuchi Lines and Laue Spots

The intensity of the Laue spot, due to the surface plane of a crystal, depends on the azimuth of the crystal. If the azimuth is such as to make several Kikuchi lines pass through or near the spot the intensity of the latter is in general diminished.<sup>2</sup> This does not necessarily imply any dynamic connection between the wave systems causing the two kinds of patterns, but simply means that when several lines pass through a Laue spot the crystal is in a very special setting. In any case the line due to the surface plane itself must pass through the spot, if the crystal is set at the Bragg angle to the rays. Any extra lines imply that the emergent ray could have been reflected from more than one plane. If the crystal is rotated about an axis normal to the plane of incidence, one would expect the strongest reflections to occur at deviations equal to twice the Bragg angles of the various orders, and this is what happens in most azimuths. If, however, the azimuth is one of the special ones, Kikuchi and Nakagawa<sup>3</sup> have found that the maxima of one or more of the orders are doubled, owing presumably to the interference effect discussed in the preceding paragraph. They have also found a related abnormality. With many crystals a spot occurs at an angle corresponding to specular reflection by the surface plane, even when the Bragg condition is not satisfied. This is caused by the slight penetration of the electrons at glancing incidence, which results in only a few planes being effective in scattering the electrons. The abnormality occurs when the specularly reflected spot coincides with a Kikuchi line due to some oblique plane. The intensity of reflection is then increased beyond that due to the sum of that due to spot and line taken separately. As a result, the rotation photograph shows an

<sup>1</sup> Shinohara, *Sci. Pap. Inst. Phys. and Chem. Res.* 20, p. 40 (1932).

<sup>2</sup> Beeching, *Phil. Mag.* 20, p. 841 (1935).

<sup>3</sup> Kikuchi and Nakagawa, *Sci. Pap. Inst. Phys. and Chem. Res.* 21, p. 256 (1933).

extra maximum of intensity (see Plate X *c*). We have here an interference between surface and body reflections, and no detailed explanation has been given as yet.

### Parabola $\epsilon$ and Circles

Shinohara<sup>1</sup> was the first to observe, in addition to the straight lines, parabolic curves which appeared to be envelopes of the lines, and they have been since found by many experimenters. Later Emslie<sup>2</sup> by reflection from stibnite found in certain positions two enhanced circles with the direction of a strong zone axis as centre. Similar circles have been found by Tillman<sup>3</sup> with zinc blende, by Finch<sup>4</sup> and others with fluorite, and by Shinohara<sup>5</sup> with zinc blende and mica, but they are rarer than the parabola $\epsilon$  which always occur with them. Parabola $\epsilon$  and a circle may be seen in Plate IV *b*.

### Envelopes of Kikuchi Lines

When a number of Kikuchi lines making small angles with each other are present, they may touch a curve which can be regarded as their envelope, though with the restriction that, since only a discrete series of lines are present, they can only touch the envelope at a limited number of points. But owing partly to the interference effect described above, the 'envelope' often appears surprisingly clearly on the plate. There is often a region of diminished electronic intensity between the envelope and the visible portion of the lines which should touch it. Shinohara has shown that this is explicable in the same way as other instances of the interference of Kikuchi lines. The 'interfering plane',  $h' - h$ , is in many cases the surface plane of the crystal. The forms and positions of the envelopes can be calculated for a cubic crystal as follows :

Let  $\{l_1 m_1 n_1\} \{l_2 m_2 n_2\} \{l_3 m_3 n_3\}$  be the direction cosines with respect to the crystal axes of three mutually perpendicular zone axes, and let  $\{l_3 m_3 n_3\}$  be sufficiently near the direction of

<sup>1</sup> Shinohara, *Sci. Pap. Inst. Phys. and Chem. Res.* 20, p. 39 (1932).

<sup>2</sup> Emslie, *Phys. Rev.* 45, p. 43 (1934).

<sup>3</sup> Tillman, *Phil. Mag.* 19, p. 485 (1935), and *Trans. Farad. Soc.* 31, p. 1109.

<sup>4</sup> Finch, Quarrel and Wilman, *Trans. Farad. Soc.* 31, p. 1051 (1935).

<sup>5</sup> Shinohara, *Phys. Rev.* 47, p. 730 (1935).

the original beam to intersect the photographic plate. Take this intersection as origin and the projections of  $\{l_1 m_1 n_1\}$   $\{l_2 m_2 n_2\}$  on the plate as  $Ox$ ,  $Oy$  (Fig. 40). Let any net plane of Miller indices  $(hkl)$  intersect the plate in AB. Assuming that  $L$ ,

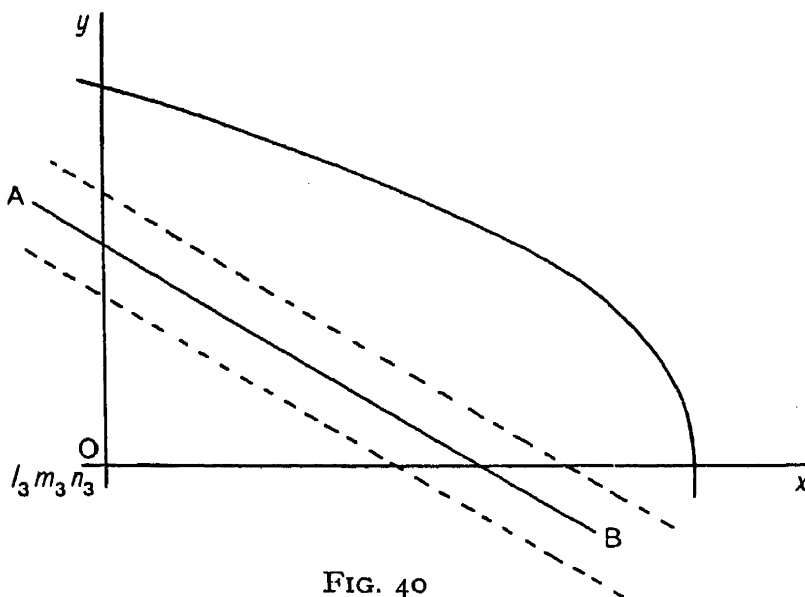


FIG. 40

the distance from the crystal to the plate, is large compared with distances on the plate, the perpendicular from  $O$  on  $AB$  is

$$\frac{L(hl_3 + km_3 + ln_3)}{\sqrt{h^2 + k^2 + l^2}},$$

which we will write

$$\frac{L\Sigma(hl_3)}{\sqrt{h^2 + k^2 + l^2}}.$$

The equation of  $AB$  is

$$\frac{L\Sigma(hl_3)}{\sqrt{h^2 + k^2 + l^2}} = \frac{x\Sigma(hl_2) + y\Sigma(hl_1)}{\sqrt{h^2 + k^2 + l^2}}$$

and those of the Kikuchi lines of order  $n$  are

$$\frac{L\Sigma(hl_3)}{\sqrt{h^2 + k^2 + l^2}} \pm \frac{L\lambda n}{2a} \sqrt{h^2 + k^2 + l^2} = \frac{x\Sigma(hl_2) + y\Sigma(hl_1)}{\sqrt{h^2 + k^2 + l^2}}$$

or 
$$L\Sigma(hl_3) \pm \frac{L\lambda n}{2a} (h^2 + k^2 + l^2) = x\Sigma(hl_2) + y\Sigma(hl_1),$$

where  $a$  is the cube edge, the enhanced line having that sign which brings it farther from the direction of the original beam.

In practice  $x, y, L\lambda n/2a$ , are small compared to  $L$  and hence  $\Sigma(hl_3)$  is small for all lines which actually appear on the plate. For many it will be zero,  $(hkl)$  belonging to the zone of  $\{l_3m_3n_3\}$ . The envelopes actually observed correspond to groups of lines for which  $\Sigma(hl_3)$  is constant. In choosing the one-dimensional series of planes, whose Kikuchi lines are to form the envelope, another relation between  $hkl$  must be taken. This could be any arbitrary function, thus giving rise to a great variety of envelopes, but it seems that for all those actually observed the increments  $\Delta h, \Delta k, \Delta l$  from plane to plane are in a constant ratio, which is of course one of integers, and usually of simple ones. Since  $\Sigma(hl_3)$  is to be constant,  $\Delta h, \Delta k, \Delta l$  is orthogonal to  $l_3, m_3, n_3$ , and we will take the ratio of these increments to be that of  $l_1:m_1:n_1$ , which, since  $\{l_1m_1n_1\}$  is a zone axis, is necessarily integral. To find the envelope we differentiate and find

$$\Sigma\left\{Ll_3 - xl_2 - yl_1, \pm \frac{L\lambda n}{a}h\right\}\Delta h = 0$$

or substituting for  $\Delta h$ , etc.

$$\Sigma\left(-yl_1 \pm \frac{L\lambda n}{a}h\right)l_1 = 0,$$

the other terms vanishing because of the orthogonal relations.

Hence 
$$y = \pm \frac{L\lambda n}{a}\Sigma(hl_1).$$

But we can write

$$h^2 + k^2 + l^2 = [\Sigma(hl_1)]^2 + [\Sigma(hl_2)]^2 + [\Sigma(hl_3)]^2 = [\Sigma(hl_1)]^2 + B^2 + C^2,$$

say. Hence the equation of the envelope is

$$LC \pm \frac{L\lambda n}{2a} \left[ \frac{a^2}{L^2\lambda^2n^2}y^2 + B^2 + C^2 \right] = \pm \frac{a}{L\lambda n}y^2 + Bx$$

or 
$$LC \pm \frac{L\lambda n}{2a}[B^2 + C^2] - Bx = \pm y^2 \frac{a}{2L\lambda n},$$

which is a parabola with the projection of the zone axis  $\{l_1m_1n_1\}$  as axis. This is found in fact to fit the observed parabolae with reasonable accuracy. In theory, there is a doubly infinite set of these parabolae for varying values of  $B$  and  $C$  besides other such sets corresponding to the choice of other zone axes

as  $\{l_1 m_1 n_1\}$ . In practice only a few values of  $C$  are possible on a plate of ordinary dimensions. Envelopes of both enhanced and weakened lines are found, though the former are usually more conspicuous. By varying  $B$  we get, as the envelopes of the parabolae,

$$LC \pm \frac{L\lambda n}{2a} C^2 = \frac{a}{2L\lambda n} (x^2 + y^2),$$

which is a circle round the projection of the zone axis  $\{l_3 m_3 n_3\}$ . Shinohara and Finch explain the circles in this way, and their radii are given roughly by assigning to  $C$  the smallest values, other than zero, compatible with the known values of  $\{l_3 m_3 n_3\}$ . There is however an important difference between the circles and the parabolae, in that while the lines, if unaffected by interference, would actually touch the parabolae they would not actually touch the circles except for special values of  $a/L\lambda$ . As Shinohara points out, the circles are the boundaries inside which lines belonging to a certain group of planes cannot lie. His argument can be put into our notation as follows. The perpendicular from  $O$  on the Kikuchi line is

$$\frac{L\Sigma(hl_3)}{\sqrt{h^2 + k^2 + l^2}} \pm \frac{L\lambda n}{2a} \sqrt{h^2 + k^2 + l^2} = \frac{LCd}{a} \pm \frac{L\lambda n}{2d},$$

where  $d$  is the spacing corresponding to  $hkl$ . If  $hkl$  vary so that  $C$  is constant, but  $d$  varies, the minimum for this expression occurs when  $d^2 = \lambda na/2C$ , and is  $L\sqrt{2n\lambda C/a}$ , which is the radius of the above circle if the small second term on the left-hand side is neglected. In some cases<sup>1</sup> the 'circles' are really polygons, sometimes made partly of enhanced and partly of weakened lines. In such cases the above explanation probably is correct. In other cases the circles are, apparently at least, quite continuous and separated from the nearest lines by a small gap. Emslie's circles were of this kind, and he suggested an alternative explanation.

### Linear Diffraction

If a wave travels along a line of atoms giving rise to wavelets as it passes over the successive atoms, these wavelets will

<sup>1</sup> Finch, *l.c.*, also Shinohara, *l.c.*

reinforce over certain cones round the line of atoms as axis. The semi-vertical angles  $\phi$  (Fig. 41) are given by

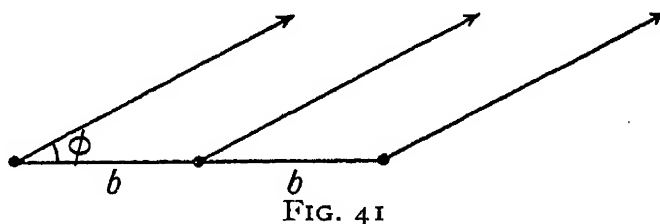
$$b/\lambda' - (b \cos \phi)\lambda = \text{an integer } n,$$

where  $b$  is the spacing along the line of atoms,  $\lambda'$  is the wavelength in the space between the atoms, and  $\lambda$  that outside. Writing  $\lambda = \lambda' \sqrt{1 + \Phi/P}$  the above equation reduces to

$$\sin^2 \phi = \frac{2n\lambda}{b} \left( \cos \phi + \frac{n\lambda}{2b} \right) - \frac{\Phi}{P},$$

which is exact.

In a cubic crystal the distance between lattice points in the direction of the zone axis  $\{HKL\}$  is  $a\sqrt{H^2 + K^2 + L^2}$ . The distance between atoms may be less, if there is more than one atom per cell. Taking  $\{HKL\}$  as the direction  $\{l_3 m_3 n_3\}$ , the square of the angular radius of the circle considered as an envelope is



$$\frac{x^2 + y^2}{L^2} = 2\lambda n \left( \frac{C}{a} \pm \frac{\lambda n C^2}{2a^2} \right).$$

But 
$$\frac{C}{a} = \frac{\Sigma(hl_3)}{a} = \frac{\Sigma hH}{a\sqrt{H^2 + K^2 + L^2}} = \frac{\Sigma hH}{b}.$$

Since  $C$  is to be as small as possible, write  $\Sigma hH = 1$ .

Then 
$$(x^2 + y^2)/L^2 = \frac{2n\lambda}{b} \left( 1 + \frac{n\lambda}{2b} \right),$$

which agrees with the exact expression if  $\Phi$  is neglected, and  $\cos \phi$  is put equal to 1. Emslie considered that the disturbance from an inelastic collision was confined to a 'potential tube' along a row of atoms. This supposition is not however necessary in order to get the result. If an atom is acting as a virtual source of waves, the wavelets scattered by all the atoms near it will not in general combine exactly in any direction, as the path differences between them will vary according to a complicated law. Only along a line of atoms radiating from the

original atom will there be a simple phase relation, and reinforcement will occur in the directions given above.

By introducing the term in  $\Phi$ , a much better fit can be got between the observed and calculated radii, the difference being of the order 0.5 mm. with  $L = 20$  cm. The value of  $\Phi$  required is more than the usual inner potential. Tillman (*l.c.*) finds that for zinc blende it varies from 16.5 to 32 volts for different azimuths, the usual value being 12.6. He has shown that these differences can be adequately accounted for by the potential distribution in a simple model of the crystal. On the other view, the difference between observed and calculated radii is an interference effect of the same character as that seen at the intersection of two lines. At present it seems impossible to decide definitely between the two views.

It is perhaps worth mentioning that in the case of transmission, where refraction does not come in, the circles are identical in position with the loci of intensification of the spots of the cross-grating discussed on p. 80. In his earliest experiments Kikuchi described these loci as rings, and on some of his illustrations they can clearly be seen to be continuous (Plate III *b*). They could be explained on purely geometrical grounds if any appreciable part of the mica were an imperfect crystal, so that only a small region in each cleavage plane scattered in phase, thus causing the points of the reciprocal lattice to be extended parallel to this plane. For mica this is perhaps possible, but the corresponding explanation in the reflection cases seems untenable, since it implies that the crystal is more perfect along the beam than perpendicular to it, and the circles appear for several azimuths.

### Refraction of Kikuchi Lines

In dealing with the refraction of Kikuchi lines it must be remembered that the direction of the incident beam is immaterial, but the refraction of the electrons on leaving the crystal occurs as before. As long as we are dealing with single crystals, for which alone Kikuchi lines are important, the change in the direction of diffraction measured from the free surface is the same for a line as for a spot. Hence for a line parallel to the free surface the relation on p. 110 remains valid. In the case

of oblique lines, each point is drawn in towards the surface according to the same law, so that the line becomes a hyperbola.

### Effect of Crystal Size on the Dimensions of the Lattice

This is perhaps the most suitable place to mention work by Finch<sup>1</sup> and others, having for its primary object the investigation of a possible change in the dimensions of the lattice of a crystal when the size of the crystal is very small. Crystals of alkali halides were deposited by evaporation on thin films of gold or celluloid, and zinc oxide was deposited as smoke. These specimens gave sharp diffraction rings by transmission, and the diameters could be measured to about 1 part in 1000. They agree excellently with theory as far as the relative sizes of the rings of any one substance were concerned, and are perhaps the most accurate test so far made, but the voltage was not measurable with sufficient accuracy to give absolute values. The main part of the research was a comparison of the lattice constants of various specimens with those of gold, the two sets of rings appearing on the same plate, either because the films were composite, or by the use of the double shutter method (p. 229). The size of the crystals could be estimated from the sharpness of the rings (p. 78) and is recorded in Table XI, taken from Finch and Fordham's paper; 'small', 'medium', 'large' refer to crystals of about 40, 60, and 100 Å or more, respectively. There is a clear tendency for the electron diffraction values to be high. The crystals in the gold foils used were relatively large, so that if the effect is due to crystal size, small ionic crystals must have a larger lattice spacing than the large ones used for the X-ray determinations. This is in the reverse direction to the surface effect predicted on theoretical grounds by Lennard-Jones.<sup>2</sup> There does not seem to be any marked correlation between the magnitude of the discrepancy and the size of the crystals, and it seems equally possible that the discrepancy is due, either to an error in the X-ray value for gold, or to some second order effect modifying the theory

<sup>1</sup> Finch and Wilman, *Jour. Chem. Soc.* p. 751 (1934); Finch and Fordham, *Proc. Phys. Soc.* 48, p. 85 (1936).

<sup>2</sup> Lennard-Jones, *Zeit. für Krist.* 75, p. 215 (1930).

of electron diffraction differently for conductors and non-conductors.

TABLE XI.  
CRYSTAL SIZE AND LATTICE DIMENSIONS

Substance	Crystal Size	$a$ (Å) referred by Electron Diffraction to the Value $a_{Au}=4.070$	$a$ (Å) by X-rays	Difference (Å)
LiF .	Medium	$4.027 \pm 0.005$	$4.020 \pm 0.002$	$+0.007$
LiCl .	Large	$5.136 \pm 0.003$	$5.143 \pm 0.006$	$-0.007$
LiBr .	Large	$5.495 \pm 0.008$	$5.489 \pm 0.006$	$+0.006$
LiI .	Medium	$6.019 \pm 0.005$	$6.000 \pm 0.007$	$+0.019$
NaF .	Small	$4.641 \pm 0.004$	$4.619 \pm 0.002$	$+0.022$
NaCl .	Medium	$5.669 \pm 0.005$	$5.6280$	$+0.041$
NaBr .	Large	$5.963 \pm 0.005$	$5.962 \pm 0.002$	$+0.001$
NaI .	Large	$6.469 \pm 0.005$	$6.462 \pm 0.006$	$+0.007$
KF .	Small	$5.356 \pm 0.010$	$5.36$	?
KCl .	Medium	$6.319 \pm 0.005$	$6.277 \pm 0.002$	$+0.042$
KBr .	Large	$6.630 \pm 0.004$	$6.586 \pm 0.002$	$+0.044$
KI .	Medium	$7.078 \pm 0.008$	$7.052 \pm 0.003$	$+0.026$
Graphite	Large	$2.458 \pm 0.005$	$2.45 \pm 0.03$	?
ZnO .	Large	$\begin{cases} a = 3.258 \pm 0.005 \\ c = 5.239 \pm 0.005 \end{cases}$	$\begin{cases} 3.2426 \\ 5.1948 \end{cases}$	$\begin{cases} +0.015 \\ +0.044 \end{cases}$

NOTE.—The X-ray values are taken in most cases from the 1931 supplement to the *Strukturbericht* of the *Zeitschrift für Kristallographie*.

### Temperature Effect

We should expect the effect of temperature on the diffraction of fast electrons to be of the same character as for X-rays, namely a diminution in the intensities of the diffracted beams, which is more marked for the larger angles of diffraction. Kakesita<sup>2</sup> has confirmed this in the case of pyrites and gold foil, over the range from room temperature to 320° C. For slow electrons the effect is complicated by changes in the gas layers on the surface with rise of temperature, but Lasch-

<sup>1</sup> Finch and Wilman (*Ergeb. exakt. Naturwiss.* 16, p. 353, 1937) have recalculated the third and last columns of this table assuming Trzebiatowski's X-ray value of 'a' for graphite (2.456) as standard. The electron diffraction values are thus all reduced by one part in a thousand and the positive differences become correspondingly smaller.

<sup>2</sup> Kakesita, *Mem. Coll. Sci. Kyoto Univ.* 17, p. 32 (1934).

Laschkarew and Kusmin,<sup>1</sup> using graphite, have found a variation in intensity which agrees with the Debye law for X-rays (see p. 280). The effect of temperature on the diffraction of fast electrons by a gold foil has also been studied experimentally by Coster and van Zanten.<sup>2</sup> According to their results, the ratio of the intensities of the  $\sqrt{3}$  and  $\sqrt{8}$  rings at 250° C is about 10 per cent greater than at 18° C. For the  $\sqrt{4}$  and  $\sqrt{11}$  rings the value is about 7 per cent. From these values, and assuming the Debye law, they calculate the characteristic temperature of gold to be 160° C. Specific heat measurements give from 163° to 186°.

Boersch<sup>3</sup> has found that the intensity of Kikuchi lines and bands does not vary much over a wide range of temperature for a number of crystals.

<sup>1</sup> Laschkarew and Kusmin, *Phys. Zeit. Sowjet.* 6, p. 211 (1934).

<sup>2</sup> Coster and van Zanten, *Physica* 6, p. 17 (1939).

<sup>3</sup> Boersch, *Phys. Zeit.* 38, p. 1000 (1937).

## CHAPTER IX

### THE PRINCIPAL TYPES OF DIFFRACTION PATTERN AND THEIR INTERPRETATION

THE experiments described in Chapter IV served to establish de Broglie's law and to justify the ideas concerning the relation between waves and particles explained in Chapter V. The further development of electron diffraction is concerned chiefly with the study of surface layers, for which the wave properties of electrons provide a very useful tool. X-rays have afforded a means of determining the structure of a large number of crystalline or semi-crystalline solids, but their great power of penetration makes them unsuited to the study of effects which depend on the peculiarities of a few atomic layers near the surface. For this purpose electronic waves are much more convenient. If we were limited to specimens in the form of films thin enough to be transparent to electrons, the usefulness of the method would be much restricted, and a large proportion of the work has been done by the reflection method described on p. 49.

#### Types of Diffraction Pattern

The principal<sup>1</sup> types of diffraction pattern formed by reflection or transmission can be classified as follows :

##### A. TRANSMISSION PATTERNS

(a) Continuous rings due to a powder of small crystals (Plates I, II *b*). The rings may be sharp or diffuse.

(b) Rings formed of a large number of spots, formed when the crystals are not sufficiently numerous to give (a) but yet are small enough for many to be covered by the electron beam.

(c) Patterns consisting of arcs of circles indicating that the

<sup>1</sup> We have already discussed certain exceptional types of patterns in Chapter VI.

small crystals are not arranged at random, but have certain preferred directions (Plate V *a*).

(*d*) Cross-grating patterns such as those found by Kikuchi for thin films of mica (Plate III *a*). These are always due to single crystals.

(*e*) Patterns of spots and Kikuchi lines, the latter being relatively more prominent the thicker the crystal. These also are always due to single crystals, and if the Kikuchi lines are sharp the crystals cannot be appreciably bent (Plates III *b*, IV *a*).

(*f*) Patterns formed by rotating the specimen during exposure (Plate V *c*).

(*g*) Patterns of spots and diffuse patches, found by Finch from anthracene (Plate IX *a*).

(*h*) Composite patterns due to two or more of the above superposed.

## B. REFLECTION PATTERNS

(*a*) Continuous arcs extending over nearly a semicircle, the rest being blocked out by the shadow of the solid specimen. The arcs may be sharp ( $a_1$ ) or diffuse ( $a_2$ ) (Plate V *d*, *e*).

(*b*) Arcs formed of a large number of spots, bearing the same relation to B(*a*) that A(*b*) does to A(*a*).

(*c*) Patterns of relatively short arcs, or arcs of uneven intensity, indicating orientation of small crystals (Plate V *f*).

(*d*) Cross-grating patterns of spots, with, ( $d_1$ ), or without ( $d_2$ ), Kikuchi lines (Plate VI *a*, *d*).

(*e*) As (*d*), but with the spots elongated into lines normal to the plane of the specimen. Two cases are found in one of which ( $e_1$ ), the elongation, is only in the direction of smaller deviation, in the other, ( $e_2$ ), it is symmetrical (Plate VII *a*).

(*f*) Patterns of spots and Kikuchi lines. These are given by single crystals with smooth surfaces (Plates IV *b*, VI *b*).

(*g*) Patterns of rather diffuse lines parallel to the surface of the specimen, and often having more intense spots on them. This pattern is associated with a layer of grease or similar organic substance (Plates VIII *d*, *e*; X *b*).

(*h*) Rotation patterns, sometimes used for the measurement of inner potential (p. 158) (Plate X *c*).

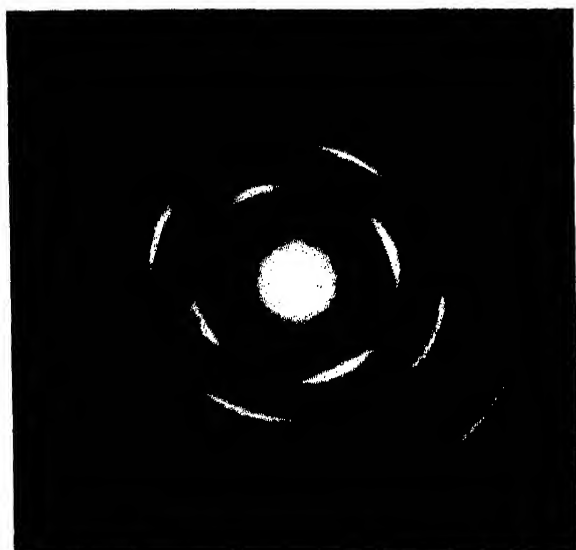
(*i*) Composite patterns due to more than one of the above superposed.

### Interpretation of Transmission Patterns

We have already discussed most of the cases of transmission patterns, but something more may be said in connection with the orientation of crystals. In transmission, orientation of the crystals does not necessarily cause 'arcing', A(c). If a zone axis of the crystals is always nearly parallel to the incident rays only those rings will appear which correspond to planes through the zone axis, and if the crystals are disposed at random round the zone axis, the rings which do appear will be of uniform intensity round the circumference. Since the normal to the film is the most probable preferred direction, this is a common case when films are used normal to the rays. If the orientation of the zone axis is only partial, all possible rings will appear but the intensities will be abnormal. For this reason great care must be taken in making deductions from the intensities of the rings if there is any reason to suspect orientation. The best test is to incline the specimen so that the axis of symmetry of the orientation is no longer parallel to the incident rays. If there is orientation the rings will then break up into arcs, pattern A(c). As the specimen is tilted, any plane that becomes nearly parallel to the incident rays will give rise to two spots (or arcs if the orientation is not perfect) at opposite ends of a diameter. The necessary degree of tilt measures the angle between the plane and the normal to the film, and the diameter is perpendicular to the position of the plane when reflection occurs. Any plane parallel to the axis of orientation will always give a pair of spots, and the diameter joining them is perpendicular to the projection of the axis of orientation on the photographic plate.

In general each ring will reduce to four arcs situated at the extremities of diameters, as can be seen from Fig. 42. Here ABCD represents an approximately plane portion of the Ewald sphere, LO is the direction of the incident electrons, OP is the normal to the film and we suppose that the (*hkl*) planes of all the crystals lie in the film, but that the crystals are otherwise at random. Then we can take P as the point (*hkl*) of the reciprocal lattice for all the crystals, and the other points (*A*<sub>1</sub>*A*<sub>2</sub>*A*<sub>3</sub>) lie on circles with centres on OP, and in planes normal to it. Any such circle will cut the Ewald sphere in the

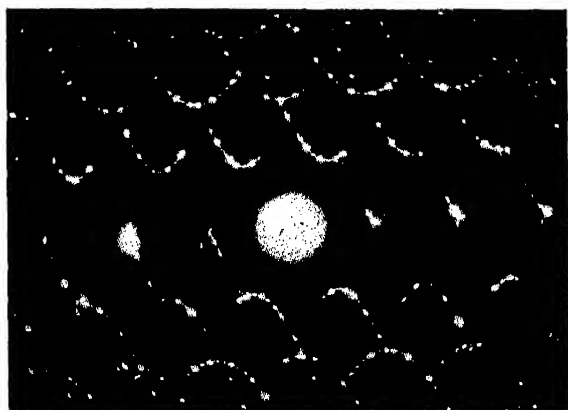
# PLATE V



(a) Beaten gold foil. (*Trillat and Oke-tani*). Taken from *Journ. de Phys.* 8, p. 66 (1937)



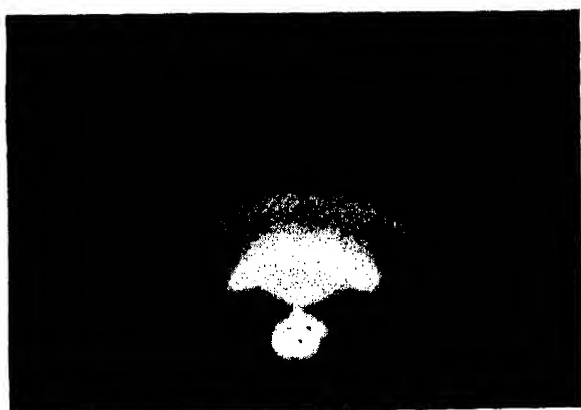
(b) Cadmium iodide, inclined film, (001) orientation. (*Kirchner*)



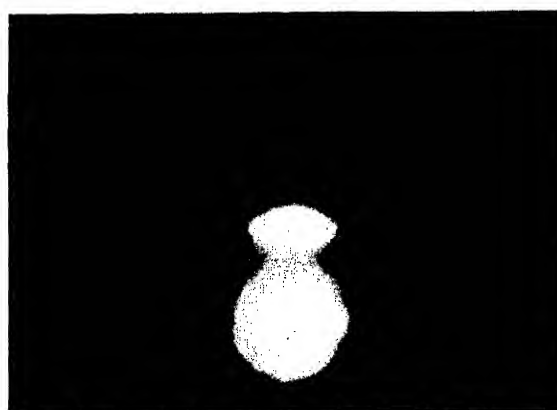
(c) Molybdenite, inclined film, rotated during exposure. (*Finch*)



(d) Spluttered platinum ; normal pattern



(e) Platinum spluttered in oxygen at low voltage ; probably mainly di-oxide



(f) Spluttered platinum, (111) orientation





$\angle \text{SOP}$  is the angle between the vectors of the reciprocal lattice corresponding to  $hkl$  and  $A_1A_2A_3$ . Hence

$$\begin{aligned}\cos \phi \sin \delta &= \frac{(h\beta_1 + k\beta_2 + l\beta_3) \cdot (A_1\beta_1 + A_2\beta_2 + A_3\beta_3)}{\text{OP} \cdot \text{OS}} \\ &= \{hA_1|\beta_1|^2 + kA_2|\beta_2|^2 + lA_3|\beta_3|^2\}d_1d_2,\end{aligned}$$

where  $d_1, d_2$  are the spacings corresponding to the planes  $hkl, A_1A_2A_3$  respectively. If the axes are cubic this reduces to

$$\cos \phi \sin \delta = \frac{hA_1 + kA_2 + lA_3}{\sqrt{h^2 + k^2 + l^2} \sqrt{A_1^2 + A_2^2 + A_3^2}}$$

When  $\phi$  and  $\delta$  are measured, this relation gives a check on the value assumed for the direction of preferred orientation, and on the assignment of indices to the rings.<sup>1</sup>

Sometimes not only is there a preferred direction for some zone axis, but there is a preferred orientation round the zone axis. This is an approach to the case of a single crystal, and the pattern  $A(c)$  of arcs which is formed can be regarded as derived from the cross grating pattern of the net plane, normal to the rays, by a small rotation about this normal. If the orientation is loose, additional arcs may appear at other distances from the centre, usually corresponding to reflections from planes whose normals would not be greatly inclined, in a perfect single crystal, to the net plane causing the main pattern.

### Width of Rings

If it can be assumed that the crystals in the film are approximately cubical in external form, and of about the same size, it is possible to determine this size from the width of the rings (p. 78). Taking account of the divergence of the rays, Brill<sup>2</sup> has shown that the half-breadth of the line in radians is  $0.94 \lambda \sec \theta / \Lambda + b$ , where  $\Lambda$  is the mean edge of each cube,  $\theta$  the Bragg angle and  $b$  the width due to the finite width of the electron beam. This is the same formula as for X-rays, and he assumes that a certain parameter has the value found for X-rays. It is also assumed that the electrons are monochromatic. In

<sup>1</sup> Cf. Kirchner, *Zeit. für Phys.* 76, p. 576 (1932).

<sup>2</sup> Brill, *Zeit. für Krist.* 87, p. 275 (1934).

practice it is best to determine  $b$  by experiment on a film with large crystals; this allows to some extent for the part of broadening which is due to the beam not being quite monochromatic. It may be mentioned that in the case of films which give spots, the size of a spot is often less than the geometric width of the beam, as calculated from the sizes of the diaphragms. This is because the very small crystal which gives the spot acts as an extra diaphragm, and limits the beam. It is found in practice that the width of rings, as long as they are clearly visible, does not depend much on the thickness of the film.

If the individual crystals are very much smaller in one direction than in another, one would expect the breadth of the rings to vary. Thus Fig. 44 shows the reciprocal lattice for

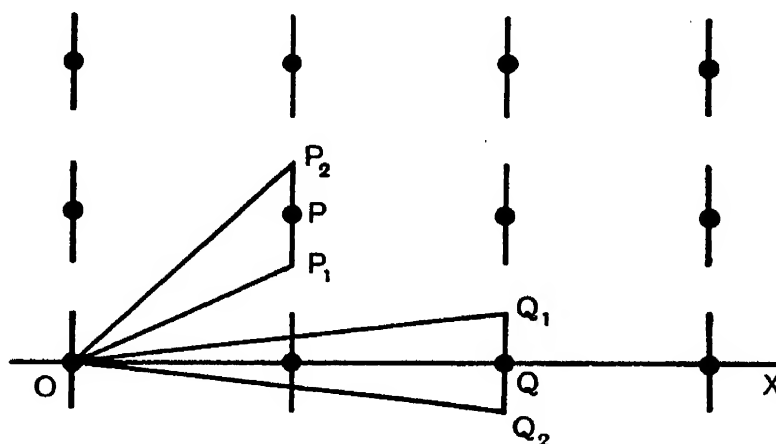


FIG. 44

a crystal formed of plates parallel to  $OX$ . The width of the ring corresponding to a point  $P$  is given by the difference in the radii  $OP_1$ ,  $OP_2$  from  $O$  to the ends of the region of appreciable intensity. Clearly this will vary with the position of  $P$ , being least when  $P$  is at  $Q$  on  $OX$ . In this case we have to take the difference between  $OQ$  and  $OQ_1$ , giving a ring sharp on the inside and slightly diffuse on the outside. It will be greatest for points for which  $OP$  is perpendicular to  $OX$  and here the rings will be diffuse but symmetrical. It is not uncommon to find patterns in which some rings are sharper than others, but as far as we know, no independent confirmation of the corresponding shape of the crystallites has been made.

Several cases are recorded in which the relative intensities of the rings of a pattern did not agree with that calculated

from the atomic and structure form factors even though there was no orientation.<sup>1</sup> It seems probable that these discrepancies can sometimes be accounted for by supposing the crystals much more extended in some directions than in others, forming plates or needles. In such cases not only will the rings differ in sharpness, but their intensities may be influenced. This will happen if the width due to the small size of the crystals is greater than that due to the spread of the beam.<sup>2</sup>

Thus Trendelenburg and Wieland<sup>3</sup> have shown that in many cases of crystals of the layer lattice type, such as aluminium silicate, there is a marked difference between the relative intensities of the rings as found by electrons and X-rays, while substances such as quartz which have no tendency to form thin sheets do not show much difference. The extreme case is that when the crystals reduce to planes of atoms.

### Rings due to Assemblies of Cross Gratings

Von Laue (*l.c.*) has examined the spectra which would be produced by a medley of cross gratings arranged at random. He finds that rings would be produced with sharp inner edges. The positions of the edges are those of the rings due to three-dimensional crystals two of whose axes can be taken as the axes of the plane grating, only those rings being present for which the index corresponding to the third axis is zero. Thus if the grating were formed by the atoms in the  $xy$  plane of a crystal, the  $(hko)$  rings should appear. Since the analysis applies strictly only to a single plane of atoms, the structure factors, which refer to a complete cell, may be modified, and 'forbidden' rings might appear. Thus the atomic layer parallel to the cube face of a face-centred cubic structure should give all rings  $(hko)$ , for which  $h+k$  is even. This might explain a ring observed by Quarrell<sup>4</sup> in an evaporated film of cobalt, corresponding to the  $(110)$  spacing of a face-centred cubic structure. Von Laue finds that the distribution of

<sup>1</sup> E.g. Darbyshire and Cooper, *Trans. Farad. Soc.* 30, p. 1038 (1934). See also p. 95.

<sup>2</sup> Cf. the analysis of von Laue, *Zeit. für Krist.* 82, p. 127 (1932), Fig. 2.

<sup>3</sup> Trendelenburg and Wieland, *Wiss. Veröff. Siemens-Konzern*, 13, p. 31 (1934).

<sup>4</sup> Quarrell, *Proc. Phys. Soc.* 49, p. 279 (1937).

intensity inside the ring depends on whether the plane gratings are transparent or opaque. In the first case the intensity is a maximum at the ring and steadily decreases outside. For opaque gratings the intensity slowly increases up to an angle of deviation  $\chi$ , given by  $\sin \frac{1}{2}\chi = \sqrt{\sin \theta}$ , where  $\theta$  is the Bragg angle corresponding to the ring. This would usually be outside the range of the plate. The above analysis, however, does not take account of the atomic form factor, which would cause a decrease with increasing deviation and make both kinds of grating behave in qualitatively the same way. While

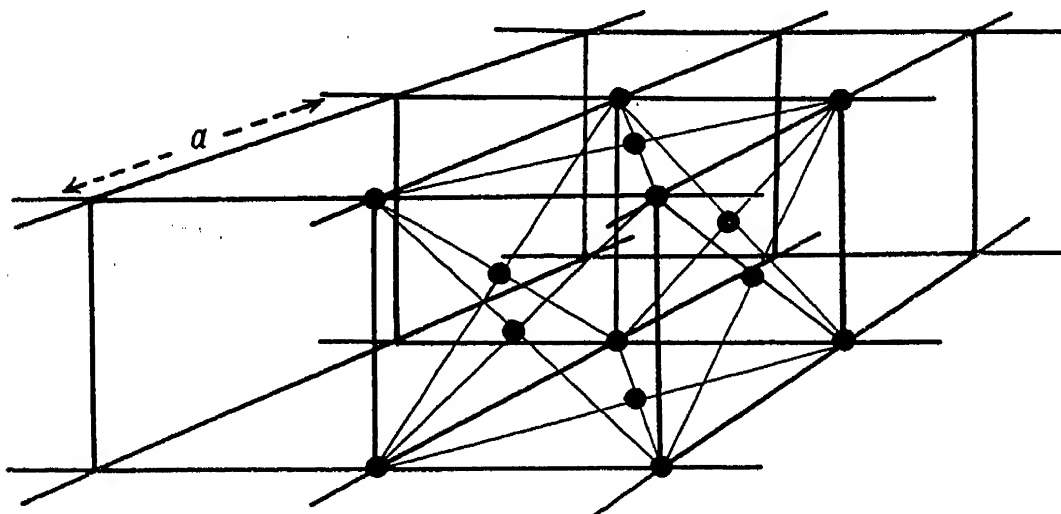


FIG. 45

it is very unlikely that a single atom plane could exist by itself, and doubtful if even a layer of complete cells would be stable for most crystal forms, layers of foreign atoms on the surfaces of solids are well known to occur. Further, a crystal probably need not always consist of complete cells. For example, a face-centred cubic crystal, bounded by cube faces, might well have complete layers of atoms on a pair of opposite faces.

Thus in the structure illustrated in Fig. 45 there are, for each cube, 8 corner atoms each shared by 4 cubes or 2 per cube, 4 atoms on the surface between cubes, each shared by 2 giving again 2 per cube, and one atom on the top and bottom surface not shared with any other cube. This makes 6 in all against 4 in the material in bulk, so that we have here the equivalent of  $1\frac{1}{2}$  cells of thickness. The extra  $\frac{1}{2}$  cell behaves for many purposes like a cross grating, but there is the complication

that the wavelets from it have a definite phase relation to those from the rest of the structure. When the main structure gives no diffracted intensity, the intensity due to the whole is that due to the cross grating, but where the main structure gives a diffracted beam we must add *amplitudes*, and the resulting intensity may be greater or less than before. This, also, may account for some abnormal intensities.

### Bands

Cross gratings due to incomplete crystal cells may account for the bands of intensity observed by Finch and others,<sup>1</sup> in patterns formed by transmission through thin films of metals. They were first attributed to gas in the interstices of the metal structure. Quarrell, in his latter paper, finds a prominent and persistent band associated with the simultaneous presence of rings corresponding to close-packed hexagonal and to face centred cubic structures, these he finds with films of cobalt, nickel, copper, platinum, palladium, gold and silver, prepared by evaporation, by electrolysis and by chemical methods. The band extends from the (100) ring of the hexagonal to the (200) of the cubic structure. He considers it due to a progressive change from the hexagonal to the cubic structure caused by a buckling of the basal plane of the hexagonal lattice to form the (110) plane of the cubic lattice. Apart from a difficulty in seeing how the superposed layers of atoms would behave, it is not clear how a gradual transition in structure can account for a band with sharp edges. An optical grating whose spacing gradually varies from  $d_1$  at one end to  $d_2$  at the other would, it is true, give bands instead of spectral lines. To find the distribution of intensity in the band one must express the spacing of the grating as a function of a coordinate measured across. It will be roughly periodic, with a period ranging from  $d_1$  to  $d_2$ . If this function is now analysed in a Fourier's series, each term of the series can be regarded as a grating which will give a small contribution to the diffracted intensity. But the terms in the series are not limited to the range  $d_1 \rightarrow d_2$ , they extend from  $0 \rightarrow \infty$ . Only if the change

<sup>1</sup> Finch, Quarrell and Wilman, *Trans. Farad. Soc.* p. 1051 (1935), and Quarrell, *l.c.*

is very gradual can the terms outside the former range be neglected. In the case of a wide band this implies a great number of lines in the grating, or in the case we are actually considering, very many crystal planes. It seems doubtful if electrons could penetrate deep enough to bring out the full diffraction pattern of such a structure. A similar objection applies to the explanation in terms of occluded gas.

On the other hand, a system of cross gratings due to incomplete cells gives a band with one sharp edge, bounded by a normal ring as observed. In Quarrell's case a layer parallel to the basal plane of the hexagon would serve, and he found in fact that the crystals were orientated with this plane parallel to the surface of the films, so that its area was probably large in many of the crystals. The other edge would not be sharp, and one would have to suppose that the apparent limitation of the band by the strong (200) ring was an optical effect due to contrast. If, as is possible, there was an alternation of structure between the hexagonal and cubic, each dividing layer would have the properties of a cross grating, and the intensity would be enhanced if the alternations were numerous. As is well known, the (001) plane of the hexagonal closest packing is identical with the (111) plane of the face-centred cubic structure, the difference between the two structures being due to the different ways in which successive layers are superposed in the two cases.

Burgers<sup>1</sup> has reported a pattern which he attributes to a structure of cross gratings. The specimen was a thin film of nickel-iron, which had been etched in nitric acid. In addition to spots due to the nickel-iron, rings were observed which showed a sharp inner edge but were diffuse to the outside. The structure responsible for them could not be identified with certainty, but the cross grating was probably caused by a layer of foreign atoms on the surface of the metal, perhaps forming an oxide. Steinheil<sup>2</sup> has tried to reproduce the conditions of von Laue's theory by using a powder of small and thin flakes of mica. He finds a pattern which contains the cross-grating rings and also faint rings corresponding to space-grating interferences. The relative intensities of the cross-grating rings,

<sup>1</sup> Burgers, *Zeit. für Krist.* A94, p. 301 (1936).

<sup>2</sup> Steinheil, *Zeit. für Phys.* 89, p. 50 (1934).

which of course would also occur in a space-grating pattern, lie between the values to be expected on von Laue's theory and those found in a separate experiment with X-rays, which might be expected to give roughly the intensities for a space grating. The rings were not particularly sharp on the inner edges, but Steinheil attributes this to the breadth of the primary beam. (See also Plate X *a*.)

### **Determination of Crystal Axes and Chemical Identification**

Unless the crystal has a high degree of symmetry, it is not an easy matter to determine the crystal axes from the ring pattern. A cubic crystal can be recognised at once, since the diameters of all the rings are proportional to the square roots of integers, and the hexagonal and tetragonal systems can generally be identified by using the nomographs published by Hull and Davey.<sup>1</sup> In many cases one is more interested in the chemical composition of an unknown structure than in its crystalline form, and it is better to start from the chemical end, by comparing the pattern of the unknown substance with that to be expected from the structure as determined by X-rays, of the most probable compounds. If X-ray determinations are not available, it is often possible to take a comparison pattern by electron diffraction. Thus many salts give good patterns when powdered and sprinkled on to a thin film of cellulose acetate or similar substance, and then examined by transmission. Sometimes a powder sprinkled on a polished copper specimen will give good rings, the diffuse rings of the copper not causing much confusion. The problem of identifying a substance whose diffraction pattern is known is similar to the corresponding problem in spectroscopy, and the process is essentially a tentative one.

### **Rotation Photographs**

Some very beautiful effects are obtained by rotating thin flakes of single crystals such as mica or molybdenite. An example is shown in Plate V *c* taken from a paper by Finch and

<sup>1</sup> Hull and Davey, *Phys. Rev.* 17, p. 549 (1921).

Wilman.<sup>1</sup> The spots, of what would otherwise be a cross-grating pattern, are drawn out into hyperbolae which are beaded, at points corresponding probably to other main, and subsidiary, diffraction maxima. Finch and Wilman show that the pattern due to a pure two-dimensional grating rotated about any axis, consists of a number of conics with centres on the line formed by the projection of the axis of rotation on the photographic plate. If, as in most of the experiments, the axis of rotation is perpendicular to the direction of the beam the conics are hyperbolae or straight lines, the angle between the asymptotes being twice the angle of inclination of the cross grating to the axis of rotation. If the axis of rotation is in the plane of the grating, or what is nearly the same thing, if the crystal is bent about an axis in its plane, the hyperbolae become portions of straight lines normal to the axis.

### Interpretation of Reflection Patterns

In discussing reflection patterns it is often convenient to make use of a representation introduced by Kirchner and Raether.<sup>2</sup>

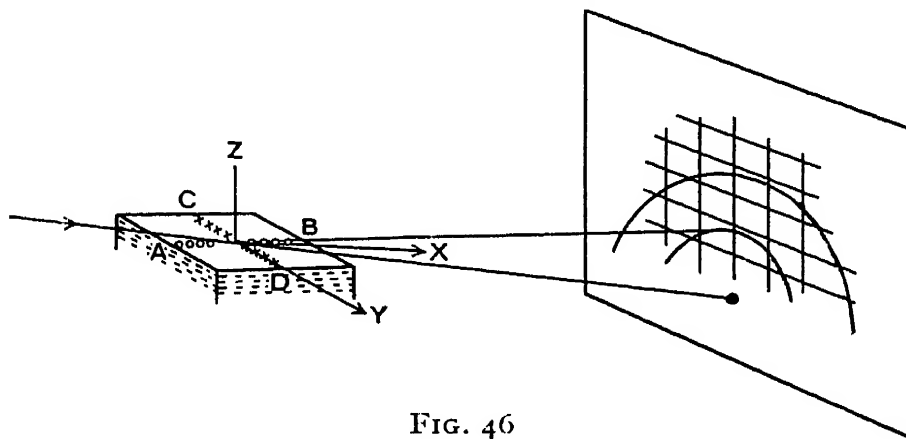


FIG. 46

Suppose that the surface of the crystal is a net plane, and that a row of atoms AB is nearly in the direction of the incident electrons, and another row CD normal to it (Fig. 46). The condition that the wavelets from any line of atoms shall be in phase is that the diffracted ray shall lie on one of a series of cones with the line of atoms as axis. For atoms in the line CD, the

<sup>1</sup> Finch and Wilman, *Trans. Farad. Soc.* 23, p. 1539 (1936).

<sup>2</sup> *Phys. Zeit.* 30, p. 510 (1932).

cones cut the photographic plate approximately in vertical lines, for the atoms in AB we get circles with the point in which AB cuts the plate as centre, and for atoms in successive planes we get horizontal lines. Only if all three intersect in a point is a true Laue spot formed. But if the penetration normal to the surface is slight, the horizontal lines, which then depend on the interference of wavelets from a short line of atoms only, are ill defined and become broad bands, and any intersection of the vertical lines and circles inside the band will give a spot. If the dimensions in the surface are limited, the vertical lines and the circles also become diffuse, but it can readily be seen that, for equal extensions in the two directions, the circles broaden much more than the lines. For a constant direction of the incident beam the path difference for wavelets from A and B depends on  $AB \cos \phi$ , where  $\phi$  is the angle between AB and the diffracted beam. The variation of this with  $\phi$  is  $AB \sin \phi \cdot \delta\phi$ . Now  $\phi$  is small, but the corresponding angle  $\chi$  for the atoms in the line CD is nearly  $\pi/2$ , hence for a given variation of path,  $\delta\phi$  is larger than  $\delta\chi$ , if  $AB = CD$ . It follows that the angular half-width, measured to a place where interference has reduced the amplitude to a given fraction of its maximum value, is greater for the circles than for the lines.

### Ring Patterns

There is an obvious resemblance between the ring patterns obtained with the 'reflection' type of arrangement, and those found by transmission. Measurement shows that the sizes of the rings are identical in the two cases.<sup>1</sup> It follows that no appreciable refraction of the electrons takes place. We have seen that refraction is appreciable if, and only if, the electrons pass through the surface at a small angle, say less than  $5^\circ$ . Since the glancing angle of the electrons to the apparent surface of the specimen is often less than this, we conclude that the effective surface is a rough one, and that the electrons pass through excrescences on the surface as in Fig. 47, the process being really much more of the character of transmission, than of reflection as one would naturally have supposed. The difference from the true transmission patterns is thus very

<sup>1</sup> G. P. Thomson, *Proc. Roy. Soc. A* 128, p. 649 (1930).

slight, but one or two small points should be noticed. In the first place the beam of electrons, though narrow, has a finite cross section and since the specimen is presented to it at a very

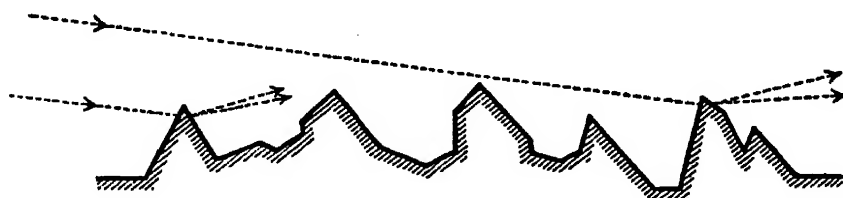


FIG. 47

small angle, often less than  $1^\circ$ , a considerable length of the specimen, as measured along the beam, is irradiated. This causes an uncertainty in the distance from specimen to plate and, since the size of the rings is proportional to this distance, there is a corresponding broadening of the rings. The effect can be diminished by using a small specimen, but this is not always convenient for reasons of intensity.

We have seen that an electron cannot penetrate more than a small multiple of  $10^{-6}$  without a large probability of an inelastic collision. Hence only those parts of the projections will be effective for diffraction which are thinner than this. Unfortunately an electron can penetrate a much greater distance ( $\sim 10^{-3}$  cm.) before it loses so much energy that it ceases to effect the photographic plate. Reflection photographs always show a heavy background of these inelastically scattered electrons which sometimes makes it difficult to see the rings. Much depends on the shape of the projections. If they are sharp, and not more than  $\sim 5 \times 10^{-6}$  at the base, the patterns should be good and the background slight. On the other hand, a number of round-topped lumps  $10^{-5} - 10^{-3}$  cm. thick will give much back-

ground and little diffraction. If the projections are sharp, the distance 'a' (Fig. 48), which is effective for diffraction,

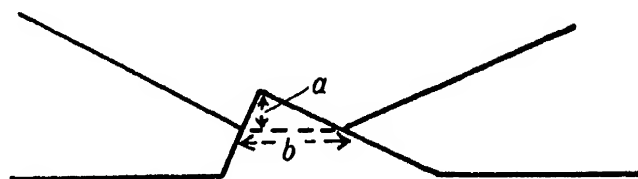


FIG. 48

will be of the same order of magnitude as 'b' which we have placed at  $5 \times 10^{-6}$ , so that some hundreds of atoms are available in the direction of the normal to the apparent surface. This is enough to give rings as sharp as are commonly observed. If, on the other hand, the projections are

round-topped, 'a' is much less than 'b' and the resolving power for this direction is affected. Round each point of the reciprocal lattice the region of intensity is drawn out normal to the apparent surface, and the intersections of the regions with the sphere, when the lattice is rotated to correspond to the random orientation of the crystals, are drawn out in the same direction. This extension has more effect in broadening the rings in the middle of the arc than near the shadow of the specimen, where the extension is nearly tangential to the ring. It is often found that rings in reflection patterns are sharper near the shadow. There is often a tendency for rings in reflection patterns to be most intense near the centre line of the plate. This is probably because the reflecting planes are likely to be larger if nearly parallel to the apparent surface. Owing to the above effects, the widths of reflection rings do not give a satisfactory means of determining the size of the diffracting crystals.

### Arc Patterns

In reflection patterns, any orientation of the crystals will cause the rings to form arcs of varying intensity, except in the very special case when the axis of orientation is along the incident beam, and this can at once be detected by rotating the specimen. Usually the axis of orientation is normal to the apparent surface of the specimen. When the orientation is strong the rings break into short separated arcs, when it is weak there may only be just perceptible changes of intensity round the circumference.

When the arcs are well marked, it is easy to determine the nature of the orientation. Any ring with an arc on the normal to the apparent surface must be due to a plane lying in this surface, and this determines the orientation, if it is of the simple type in which one crystal plane tends to lie in the surface. A series of checks is given by measuring the angles between the radii to the arcs on the various rings, Fig. 49. The arcs C, D are due to reflection from planes normal to the radii and intersecting the plane of the figure in the dotted lines, the angles between the planes are thus equal to the angles between the radii. If the indices of two rings are  $h_1h_2h_3$ ,

$h'_1 h'_2 h'_3$ , and the axes are cubic, possible angles between the arcs are given by

$$\cos \psi = \frac{\sum_3 (\pm h h')}{\sqrt{h_1^2 + h_2^2 + h_3^2} \sqrt{h_1'^2 + h_2'^2 + h_3'^2}},$$

where  $\sum_3 (\pm h h')$  is the sum of three products of the form  $h_p h'_q$ , where  $p, q$  each take the value 1, 2, 3, but in any order, and the  $h$ 's and  $h'$ 's can each have either sign. This applies also to the arcs on a single ring, but the  $h$ 's and  $h'$ 's are now the same set of integers.

It is not uncommon to find patterns in which two types of orientation occur simultaneously, so that it is worth measuring up the angles to see if they all check up with the apparent direction of orientation.

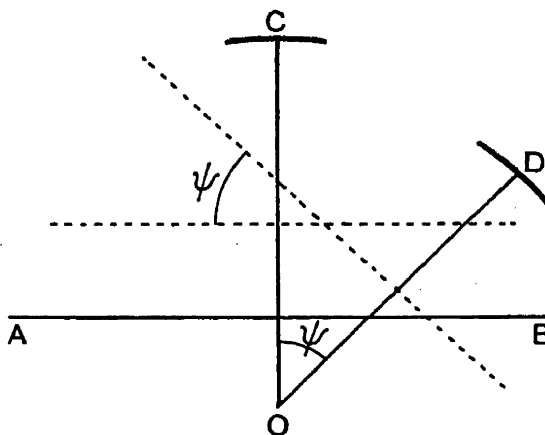


FIG. 49

### Cross-grating Patterns

Single crystals of metals, when etched, give typical cross-grating patterns when examined by the reflection method.<sup>1</sup> These patterns, like the ring patterns, are really caused by electrons passing through projections on the surface. The extended pattern may be explained either by a distortion of the crystal, or by the considerations of limited resolving power which we have already discussed. Some effect due to the latter must certainly be present. From p. 80 the half angular width of the zero order zone is  $\sqrt{2\lambda/t}$ . Taking for  $t$  the maximum possible value  $4 \times 10^{-6}$ , and putting  $\lambda = 0.6 \times 10^{-9}$ , the half angular width is 0.017, which for most metals is of the order of the deviation corresponding to the inmost spots. Probably, moreover, most of the diffracted intensity comes from parts of the specimen much less than  $4 \times 10^{-6}$  cm. thick. The best test for distortion of the crystal is given by the Kikuchi lines. If there are sharp Kikuchi

<sup>1</sup> G. P. Thomson, *Proc. Roy. Soc.* 133, p. 1 (1931).

lines, the crystal must be nearly perfect, at least as regards orientation, for the position of the lines is directly determined by the orientation of the crystal. If the lines are absent, it is a fair presumption that the crystal is distorted, though there remains the possibility that the projections giving rise to the diffraction may be too thin to produce the lines. Diffuse lines imply some distortion, but if the line is visible at all the distortion cannot be very serious. With the metals lines are weak and diffuse and often absent, with ionic crystals, some of which when etched give good cross-grating patterns, they are often strong and sharp. This is what one would expect since the softness of single crystals of metals makes them very liable to distortion.

With the exceptions noted below, p. 144, cross-grating patterns show no sign of refraction, and the observed positions of the spots agree well with the geometrical theory. The orientation of a crystal of known structure, corresponding to an observed pattern, can be found without much difficulty. As we have seen, the pattern is the projection of those points of the reciprocal lattice which lie on the sphere, which for this purpose can be treated as a plane.<sup>1</sup> If  $h_1k_1l_1$ ,  $h_2k_2l_2$ , are the indices of any two spots of the pattern, the line joining them is parallel and proportional to the vector

$$(h_1 - h_2)\beta_1 + (k_1 - k_2)\beta_2 + (l_1 - l_2)\beta_3.$$

Its length, in fact, is equal to the radius of the ring which would correspond to the reflection  $h_1 - h_2$ ,  $k_1 - k_2$ ,  $l_1 - l_2$ . By choosing two spots fairly close together, the distance can be measured with sufficient accuracy to determine the equivalent reflecting plane, and hence the values of  $h_1 - h_2$ ,  $k_1 - k_2$ ,  $l_1 - l_2$ , apart from signs which are arbitrary, and the assignment of the indices to particular axes which will also be arbitrary if two or more of the axes of the crystal are equivalent. If this process is repeated for a second pair of spots, two directions in the reciprocal lattice are fixed, and hence the attitude of the crystal. The two directions are parallel to  $OP$ ,  $OP'$ , where  $P$ ,  $P'$  are the points whose indices are the differences of

<sup>1</sup> Von Laue (*Zeit. für Krist.* 84, p. 1, 1933) has shown that, in the case of some patterns of one of the authors, better agreement can be reached by taking account of the curvature of the sphere.

those of the pairs of points, say  $A_1A_2A_3$ ,  $B_1B_2B_3$ . When the incident beam is nearly normal to an important net plane, the pattern will be regular and the spots close together. Any point with indices  $pA_1 + qB_1$ ,  $pA_2 + qB_2$ ,  $pA_3 + qB_3$ , where  $p$  and  $q$  are integers, lies in the plane of the reciprocal lattice determined by the origin and  $A_1A_2A_3$ ,  $B_1B_2B_3$ , and will give a point of the pattern if the curvature of the sphere can be neglected. For the vector from the origin to it is  $p.OP + q.OP'$ , which clearly lies in the plane  $OPP'$ . The approximate direction of the incident beam has indices proportional to  $A_2B_3 - B_2A_3$ ,  $A_3B_1 - B_3A_1$ ,  $A_1B_2 - B_1A_2$ , if the axes are rectangular.

If the crystal has been cut at random, the pattern will probably consist of a few points only, apparently irregularly spaced, but the same procedure can be followed. The assignment of indices to the spots can be checked by measuring the angles between the lines joining various pairs of spots, and comparing them with the calculated angles between planes having indices equal to the differences of those assumed for the pairs.

In analysing a pattern the stronger spots are to be preferred, as weak spots may be due to a small piece of crystal orientated differently from the rest, because of twinning or some other reason. Even if really due to the main crystal, a faint spot may correspond to a point of the reciprocal lattice some way off the sphere. If the intensities of the spots are to be considered it will be necessary to go to a second approximation and take account of the curvature of the sphere. This has been done in one case by von Laue,<sup>1</sup> who finds that the further the lattice points are off the sphere the weaker appears the corresponding spot.

Individual spots tend to be strongest for the irregular patterns, probably because there are fewer of them to divide the diffracted electrons, and for purposes of exhibition to an audience a crystal cut irregularly is therefore to be preferred.

### Cross-grating Patterns with Elongated Spots

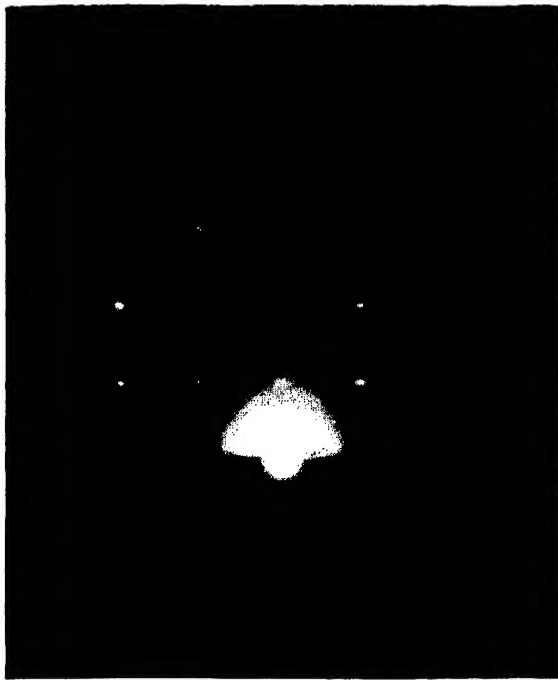
It is not uncommon to find patterns in which the spots of a cross grating are elongated, in a direction normal to the

<sup>1</sup> Von Laue, *l.c.*

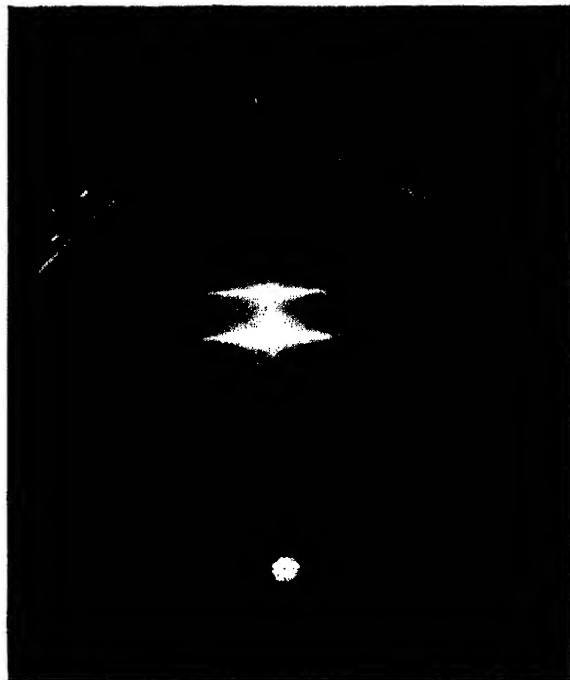
apparent surface of the specimen, sometimes to such an extent that the pattern can be best described as formed of a number of parallel lines of uneven intensity, the regions of greater intensity representing the spots of the cross grating. An example is shown in Plate VII *a* from a paper by Jenkins<sup>1</sup>; it is due to a layer of oxide on the surface of molten lead. We should expect an extension of the spots in a direction normal to the surface, for the reasons explained on p. 138, if the depth of penetration of the electrons normal to the apparent surface of the specimen were very limited, or if the specimen consisted in a thin surface layer. In fact, the effect generally occurs when one would have expected the surface to have no very marked projections; etched surfaces usually do not show it. While patterns of this kind are often associated with single crystals, this is not necessarily always so, in fact the example illustrated is a case in point. Here the crystals were all rather strictly orientated with one axis normal to the surface, but otherwise were at random. A pattern of this kind can be looked at from two points of view. It may be considered as formed by the superposition of all the possible cross-grating patterns formed when a crystal is rotated about the fixed axis, each spot being then extended because of the low resolving power normal on the surface. Alternatively, we may think of it as an arc pattern with short arcs, corresponding to a strong orientation of one axis of the crystal, each arc being then spread out along the normal to the surface for the same reason as before. The second explanation is perhaps to be preferred, for when this pattern is formed from an aggregate of crystals there is no need to suppose the resolving power limited in the direction of the electronic beam. If the crystals are at random round an axis, whose direction can vary by a few degrees in any direction, each crystal plane can be found in the correct position for a Bragg reflection. In Fig. 50, OA is the axis of orientation and the spots of the reciprocal lattice are extended normal to the surface of the specimen, *i.e.* approximately parallel to OA. If the lattice is rotated about OA., which itself wobbles about within the small cone, each of the short lines will become in succession tangential to the fixed Ewald sphere.

<sup>1</sup> Jenkins, *Proc. Phys. Soc.* 47, p. 109 (1935).

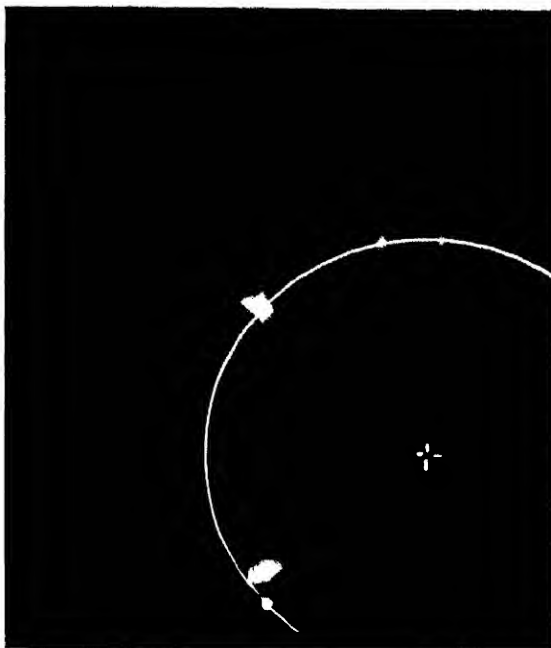
# PLATE VI



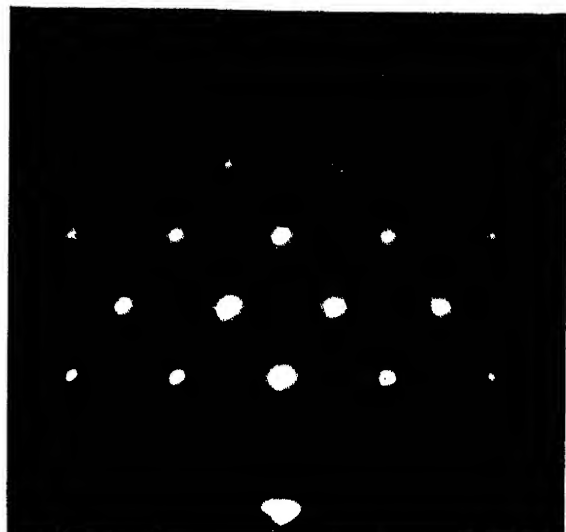
(a) Etched silver crystal, cube face, beam parallel to cube edge



(b) Diamond, natural (111) face



(c) Rock-salt, cleavage face ; circle with centre + superimposed



(d) Etched zinc blende, (110) face, beam parallel to cube-face diagonal. (1 inch)



While the cross-grating patterns due to etched crystals show no refractive effects, the patterns of the type *e*, which we are now considering, sometimes do so. Thus Jenkins<sup>1</sup> was able to find the inner potentials of a number of oxides, by measuring the displacements of the centres of the elongated spots from their calculated positions. In some experiments with single crystals of zinc blende and rock-salt, Raether<sup>2</sup> observed extended patterns of rather elongated spots. On measurement, he found that the centres of the spots were displaced, owing to refraction, towards the surface of the crystal. No Kikuchi lines appear on the published patterns

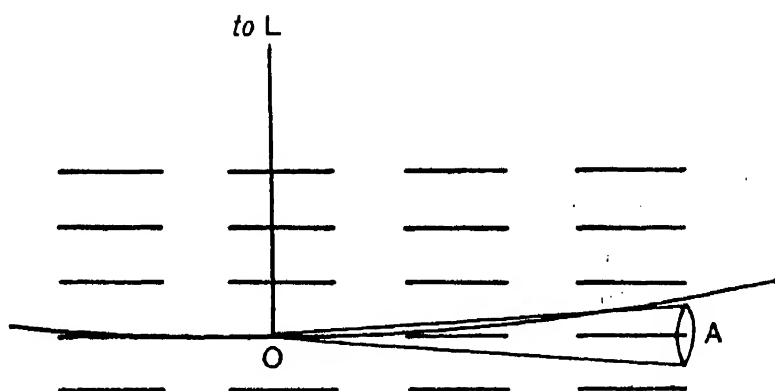


FIG. 50

due to the zinc blende, nor on those due to pyrites, which was also studied. The crystals were therefore imperfect, and the large number of spots, which appear at once, can be explained by supposing that pieces of the surface were set at different angles to give the different spots. If we suppose that the separate pieces did not project appreciably above the mean surface, the rays would pass through the surface at small glancing angles, and be refracted. Raether himself explains the large number of spots visible at once as an example of the strong interaction between the possible diffracted rays in the crystal. Some details of his explanation are not clear, but he apparently had in mind something similar to the effect discussed on p. 300. We prefer an explanation in terms of imperfections in the crystal, partly because the magnitude of the dynamical effect seems insufficient, but mainly because

<sup>1</sup> Jenkins, *l.c.*

<sup>2</sup> Raether, *Zeit. für Phys.* 78, p. 527 (1932).

other experimenters<sup>1</sup> under apparently similar conditions,<sup>2</sup> have not found nearly such a wide array of spots as Raether.

Patterns of the type we have called  $e_1$  are sometimes found in which the spots of a cross grating are elongated unsymmetrically towards the shadow edge; such a case was observed by French for a polished crystal of chromium. In these patterns the main spot corresponds to the cross-grating effect without refraction, and the extension is due to refraction. The two are probably due to different parts of the specimens, the first to projections, the second to portions that are nearly flat. Since the effect of refraction depends on the angle of emergence, one cannot say how much of the length of the extension is due to variations in this angle, and how much to poor resolving power in the flatter parts of the specimen.

Associated with patterns of the type  $e_1$  and  $e_2$  it is not uncommon to see a rather diffuse streak stretching from the shadow edge nearly normal to the surface. This is probably due to an optical reflection of electrons from nearly flat parts of the specimen, the top layer of atoms giving an appreciable effect by itself, so that Bragg's law need not be satisfied. Since the surface will usually have a slight curvature, reflection over a range of angles will occur.

### Patterns of Spots and Lines

A crystal with a smooth surface, *e.g.* a cleavage face of rock-salt, gives a pattern in which the most prominent feature is usually the Kikuchi lines, which can be very sharp and strong if the crystal is perfect, in the sense that the orientation of every part is accurately the same. Plate VI *b* from a diamond shows the sharpness of some of the lines. For certain settings of the crystal Laue spots appear, of which those in the plane of symmetry are generally the easiest to find. These centre-line spots persist over a considerable range of angle of incidence; in the case of diamond, indeed, they never entirely disappear.

<sup>1</sup> Kikuchi and Nakagawa, *Sci. Pap. Inst. Phys. Chem. Res.* 21, p. 30 (1933); Tillman, *Phil. Mag.* 18, p. 656 (1934).

<sup>2</sup> In Raether's patterns from rock-salt, Kikuchi lines appear, showing that part at least of the crystal was perfect as regards orientation. It may be that the spot pattern was due to small fragments loosely oriented, or that the surface was split up, so that the interference condition, in the direction of the incident beam, was relaxed.

Here again we are dealing with an effect due to the limited depth of penetration of the electrons, too few planes being effective to make the reflection fully selective. For a quantitative discussion see Chapter XIX. The position of the spots is affected by refraction at the smooth surface of the crystal, and can be used to calculate the inner potential (p. 155).

If refraction is neglected the following considerations apply to the positions of the spots and lines. Fig. 51 represents the

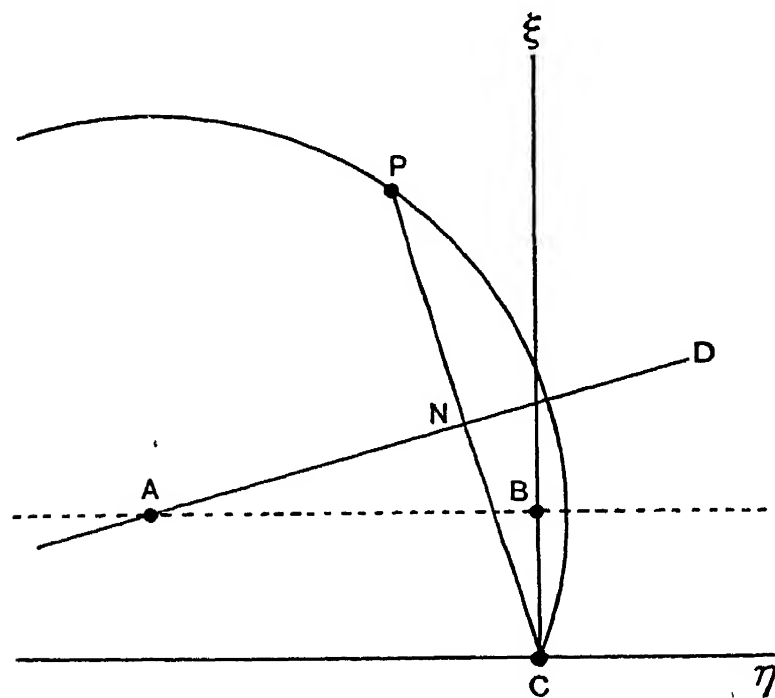


FIG. 51

plane of the photographic plate, and C the point in which the incident beam from the crystal at O would strike it.<sup>1</sup> AB is the intersection of the plate with the plane of the crystal, which lies below AB. For a Bragg reflection to occur, some plane must make a small angle with the incident beam; let it intersect the plate in AD. Then the reflection must occur at P, where AD bisects CP at right angles, to make the angles of incidence and reflection equal. Since OAB and OAD are crystal planes, OA is a zone axis. If there are several spots they are probably due to other planes through OA, since all such planes do at least lie near OC, while other planes are distributed at random through space. Since  $AP = AC$  all

<sup>1</sup> The point O cannot, of course, be shown in Fig. 51.

reflections from these planes will lie on the circle with centre A and radius AC.

If the crystal is cubic with a cube face as free surface, simple relations hold between the coordinates  $(\xi\eta)$  of spots with respect to axes  $C\xi, C\eta$  as drawn. Let  $(hkl)$  be a plane giving a Bragg reflection, and let the third index refer to the axis normal to the surface of the crystal. The perpendicular distance of the corresponding point of the reciprocal lattice from the plane through the origin parallel to the surface of the crystal is  $l/a$ , where  $a$  is the cube side. Since CO is nearly parallel to the crystal surface, the  $\xi$  coordinate of P, which is the projection of the point of the reciprocal lattice on the photographic plate, is very nearly  $\lambda L/a$ , where  $L = OC$ . Taking  $\lambda L/a$  as the unit for measurement on the plate we write  $\xi = l$ . In these units  $CP^2 = h^2 + k^2 + l^2$ , hence  $\eta^2 = h^2 + k^2$ . Hence we must look for points on the circle for which  $\xi^2$  and  $\eta^2$  are integral. If  $\eta^2$  is also the sum of squares, and the numbers so found, together with  $\xi$ , correspond to a structure factor which does not vanish, a spot will be observed. Plate VI c shows a case in point in which the three points have coordinates (9.90, 0), (12.1, 3.99), (12.15, 5.98).

In these patterns the points are sharp because the regions of intensity are only extended normal to the surface of the crystal. For any fixed position of the crystal these lines will intersect the Ewald sphere in points which will only become diffuse if different parts of the crystal are differently orientated.

Kikuchi lines are to be expected corresponding to any plane through OA (Fig. 51); the white and black members of each pair lie on opposite sides of A and equidistant from it. The separation of the lines is equal to the radius of the ring in a 'powder' pattern which would correspond to reflection from the plane in question. In analysing a pattern of Kikuchi lines it is best to start by choosing pairs close together, the separation of these will determine the corresponding planes without ambiguity. The direction of the plane is the line midway between the pair, and when two such planes have been drawn, the orientation of the crystal is determined. If the free surface of the crystal is known, one plane is sufficient. Indices can be assigned to other Kikuchi lines whose separation is too great for the corresponding spacing to be determined without ambiguity,

or for which one of the pair is invisible, by measuring the angles to known lines. The correct indices are such as to make these agree with the calculated values of the angles between the corresponding planes. Besides the lines, bands are often observed bounded where lines might be expected on the theory given on p. 112 (cf. Plate IV *b*). For a discussion of these see Chapter XIX.

When a crystal is set at a symmetrical azimuth it not infrequently happens that a small group of spots appears near the direction of the undeviated beam (cf. Kikuchi and Nakagawa, *l.c.*). They often lie on a circle, which can be regarded as the Laue zone of zero order with regard to that line of lattice points in the surface of the crystal which is nearly parallel to the incident beam. The depth of penetration of the electrons is small enough for the interference due to successive planes parallel to the surface of the crystal to be unimportant, and the other interference conditions are nearly satisfied.

A sharp spot in the plane of incidence is often observed, with a deviation equal to twice the Bragg angle for reflection from the surface planes. Its origin is discussed on p. 299.

### Extra Rings and Spots

A number of experimenters have recorded rings or spots which could not be explained on the simple theory by the supposed structure of their specimens, indeed it is almost a rarity for a prolonged research to end without some unexplained diffraction being found. There is no doubt that in the great majority of cases these are due to impurities. A layer less than 100 Å thick is enough to give strong diffractions even at normal incidence, and this is only about twice the length of many common organic molecules. Extreme cleanness is required in preparing and handling the specimens, and even so, as we shall see, there is a good chance of contamination by vapours when the specimen seems safe in the camera. Again, when chemical changes are possible, it will often happen that a small amount of a compound is formed, so little that only one or two of the strongest rings appear. In such a case it is usually impossible to identify the compound, and the rings have to be classed as of unknown origin. In our opinion

the geometrical theory of diffraction given above accounts for all the diffractions which can be assigned with certainty to substances with known structures, with the possible exception of one or two cases discussed in Chapter XIX which may require the dynamical theory to explain them. The numerous cases of 'forbidden' reflections, reflections of fractional order, and surface effects, which have been reported by many experimenters can mostly be explained as due either to impurities, or in some cases to pieces of crystal thin enough to give cross-grating diffractions at oblique incidence.

Darbyshire and Cooper<sup>1</sup> have observed 'forbidden' spots in the spectra of what appeared to be single crystals of cadmium and zinc. They give reasons for supposing that the crystals were really aggregates and suggest that the 'forbidden' spots were due to successive diffractions by two crystals of the aggregate. The same explanation probably covers the 'forbidden' spots found by Raether<sup>2</sup> in patterns from a crystal of pyrites. No Kikuchi lines appeared, so the crystal was presumably imperfect, the different regions oriented at small angles to each other acting as separate diffracting crystals. For the same reason the relative intensities of the normal spots was different from what would be expected from their structure factors. As can readily be seen from a consideration of the reciprocal lattice construction an explanation of this kind can only apply to certain types of 'forbidden' spots. If  $h_1k_1l_1$ ,  $h_2k_2l_2$  are permitted reflections  $h_1 \pm h_2$ ,  $k_1 \pm k_2$ ,  $l_1 \pm l_2$  can appear by successive diffraction in two approximately parallel crystals.

It is important to notice two sets of experiments which refer to common forms of contamination. It had been observed that while films of celluloid and similar substances gave diffuse rings<sup>3</sup> when first formed they often developed on keeping brilliant patterns of sharp rings, or of spots.<sup>4</sup> This was said to be due to a slow crystallisation, but Mark and Trillat<sup>5</sup> showed that the supposed structure did not agree with that found by X-rays, and was surprisingly the same for a number

<sup>1</sup> Darbyshire and Cooper, *Proc. Roy. Soc.* 152, p. 104 (1935).

<sup>2</sup> Raether, *l.c.*

<sup>3</sup> Reid, *Proc. Roy. Soc.* A119, p. 663 (1928).

<sup>4</sup> Taylor Jones, *Phil. Mag.* 16, pp. 793, 953 (1933) ; 18, p. 291 (1934).

<sup>5</sup> Mark and Trillat, *Ergebnisse d. techn. Röntgenkunde*, 4, p. 70 (1934).

of compounds. Further work by Motz, Trillat and Mark<sup>1</sup> proved that the sharp patterns were due to an impurity which could be washed off in ether, and that the pattern disappeared after heavy electron bombardment, though the film remained intact. They were able to reproduce the pattern by deliberately contaminating a film with various long chain compounds such as paraffin, or with beeswax. Similar patterns had been observed with metal films and could be imitated in the same way. The reason that many long chain compounds give much the same pattern, when a film is examined by electrons at normal incidence, is that the carbon chains are set normal to the surface, and packed close together into a structure which does not depend much on the length of the chain. Since the layer, which is not more than one or two molecules thick, is probably generally formed by spreading over the surface, it is most likely to appear when there is no great affinity between the ends of the long molecules and the surface over which they have to slide. In this way the above authors explain the greater effectiveness of the paraffins as compared with the fatty acids, and certain differences in the susceptibility to contamination of films of various substances. The strongest spacings observed are at about 4.14, 3.67, 2.92 and 2.50 Å; the spot pattern corresponds to a rectangular network in the plane of the film, with sides 4.8 and 7.2 Å.

Aylmer, Finch and Fordham have pointed out how easily thin films of certain metals can be contaminated with mercury so as to give extra rings. In the case of gold, even standing for an hour in their camera evacuated by a mercury pump with a liquid-air trap was enough to produce faint extra rings. Specimens obtained by thinning commercial gold-leaf gave the same extra rings. Here there was apparently no chance for the specimen to have been contaminated during treatment, and the mercury must have been present in the original leaf. Silver shows a very similar result though less strongly, copper and palladium only when deliberately exposed to mercury. Gold and silver are capable of forming a great variety of

<sup>1</sup> Trillat and Motz, *Compt. rend.* 200, pp. 1299, 1466 (1935); Mark and Motz, *Sitz. Akad. Wiss. Wien*, 144, p. 587 (1935); Motz and Trillat, *Zeit. für Krist.* 91, p. 248 (1935). Cf. also Lark-Horovitz, Yearian and Howe, *Phys. Rev.* 48, p. 101 (1935).

patterns when amalgamated, but rings at 4.44 and 2.56 Å are generally present. When the films are heated the rings due to the amalgam are often strengthened, and may appear even when not visible before. The authors explain this interesting result by supposing that the metallic parts become incapable of diffraction, either by melting or evaporation.

### Depth of Penetration of Electrons

In interpreting the results of electron diffraction by the reflection method it is very important to know roughly the depth to which the electrons can penetrate, while retaining their power to form an interference pattern. Closely allied with this is the thickness of the minimum layer which can be detected by the method. The answer to these questions depends greatly on the state of the surface. If the surface is flat, the depth normal to the surface to which the electrons penetrate will be very small owing to the small glancing angles involved; if it is rough, the depth below the summits of the projections may be at least as large as the distance which electrons can travel in the material without losing the power of interference. This distance is estimated in the calculation on p. 100 as approximately 400 Å for 30,000-volt electrons.

Experimental data from transmission experiments may be considered in relation to this question. For mica, Darbyshire<sup>1</sup> finds that films up to 2700 Å thickness give patterns containing spots. Beyond this thickness only Kikuchi lines are found. The detailed results are given in Table XII.

For a denser substance, such as gold, the thickness which will give a pattern arising from elastically scattered electrons is much less than in the case of mica. One of the authors<sup>2</sup> found that with 32,000-volt electrons, gold films thicker than 500 Å gave no pattern. We may expect that projections of this order of thickness will give a similar result in reflection experiments. Such a conclusion is confirmed by the results obtained on depositing, by electrolysis, known thicknesses of nickel over the surface of a copper single crystal.<sup>3</sup> It appears

<sup>1</sup> Darbyshire, *Zeit. für Krist.* A86, p. 313 (1933). (The voltage of the electrons is not stated but was probably  $\sim 30,000$ .)

<sup>2</sup> Cochrane, *Proc. Roy. Soc.* A166, p. 228 (1938).

<sup>3</sup> Cochrane, *Proc. Phys. Soc.* 48, p. 723 (1936), and unpublished results.

that the minimum thickness to give a detectable pattern with 30,000-volt electrons is of the order of 10–12 Å; with a thickness of 200 Å the pattern from the deposit and the base are of about equal intensity; the effect of the base is obliterated by a deposit of  $\sim 400$  Å. In these experiments we are not, of course, dealing with smooth surfaces.

From Harding's interpretation of Beeching's experiments (see p. 297) it appears that two or three atomic layers produce

TABLE XII

DARBYSHIRE'S RESULTS FOR TRANSMISSION THROUGH MICA

Thickness (Å)	Central Spot on Fluorescent Screen	Nature of Pattern
1760	Clearly visible	Cross-grating of spots; faint Kikuchi lines
2160	Fairly visible	Spots lying on rings; Kikuchi lines
2580	Weak	A few spots; well-defined Kikuchi lines
2730	Very weak	" " "
3560	Invisible	Only Kikuchi lines
4460	Invisible	"
7600	Invisible	"

an appreciable effect on a *smooth* surface by extending the range of strong reflection. Finch and Wilman<sup>1</sup> have performed an ingenious experiment to find the thickness required to obliterate the effect of a smooth surface. A quantity of an alcohol-ether solution of  $C_{32}H_{66}$ , sufficient to give, on drying, a monomolecular layer, was spread over the surface. The resulting paraffin gave a "grease" pattern indicating that the long-chain molecules were standing up on end. Also there was no sign of the pattern from the substrate. Now the length of the  $C_{32}H_{66}$  chain is 43 Å<sup>2</sup> so that a layer of this thickness is more than sufficient to obliterate the substrate effect. This point is also dealt with by Schoon.<sup>3</sup> He compares the reflection patterns from a crystal of cetyl palmitate

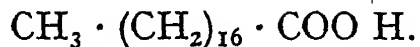


<sup>1</sup> Finch and Wilman, *Trans. Farad Soc.* 33, p. 337 (1937).

<sup>2</sup> The distance between alternate  $CH_2$  units is 2.54 Å (cf. p. 198).

<sup>3</sup> Schoon. Reported in *Nature*, 142, p. 263 (1938).

154 THEORY AND PRACTICE OF ELECTRON DIFFRACTION  
and from a crystal of stearic acid



For 25,000-volt electrons the patterns are the same, so that the penetration in this case must be less than 20 Å; for 40,000-volt electrons the patterns differ, so that the penetration is now greater than 20 Å, this being the length of the stearic acid chain.

## CHAPTER X

### THE MEASUREMENT OF INNER POTENTIAL

#### Theory

SINCE the inner potential,  $\Phi$ , of a crystal causes a displacement of the diffracted electrons, this displacement can be used to measure  $\Phi$ . When fast electrons are used a necessary condition is that the electrons should make small angles with the surface of the crystal, otherwise the effect is negligibly small. It is therefore necessary to use smooth surfaces, and since we are dealing throughout with angles of the order of a degree, the accuracy required is considerable. The only surfaces which have been successfully used are natural or cleavage surfaces; the polished surfaces of metals give diffuse rings with no signs of refraction, presumably because the angles which the electrons make with the actual surface are increased by its waviness or irregularity beyond the value ( $\sim 5^\circ$ ) which would give a detectable effect. Some polished crystals, especially gems, give sharp patterns, and it is possible that they could be used (see p. 194).

While all the electrons diffracted by a smooth crystal are affected by refraction, in practice those in the plane of incidence are generally used. Both the Bragg reflections<sup>1</sup> from the planes parallel to the surface, and the Kikuchi<sup>2</sup> lines due to the same planes have been employed. If  $\phi$  is taken as the observed angle of deviation in reflection, or twice the angle between the rays forming the Kikuchi line and the surface of the crystal as the case may be, the same theory applies in both cases.

From p. 107, we have

$$\sin^2 \phi/2 = 1 - \mu^2 + \frac{n^2 \lambda^2}{4d^2}$$

and

$$\mu^2 - 1 = \frac{\Phi}{P} (1 + Pe/2m_0c^2),$$

<sup>1</sup> Yamaguti, *Proc. Phys. Math. Soc. Jap.* 12, p. 203 (1930).

<sup>2</sup> Shinohara, *Sci. Pap. Inst. Phys. Chem. Tokyo*, 18, p. 315 (1932).

while  $\lambda = h/\sqrt{2em_0 P(1 + Pe/2m_0c^2)} = h/\sqrt{2em_0 P_r}$ ,

where  $P_r = P(1 + Pe/2m_0c^2)$ .

Hence  $P_r \sin^2 \phi/2 = \frac{n^2 h^2}{8em_0 d^2} - \Phi \left( \frac{P_r}{P} \right)^2$ .

If  $V$ ,  $V_r$ ,  $E$  are the values of  $P$ ,  $P_r$ ,  $\Phi$  in volts and  $d$  is measured in Ångströms, we get the working equations

$$V_r \sin^2 \phi/2 = \frac{n^2}{d^2} \times 37.5 - E(V_r/V)^2 \quad \text{and} \quad V_r = V(1 + V10^{-6}).$$

Usually it is possible to observe several orders, and if  $\sin^2 \phi/2$  is plotted against  $n^2$  the results for constant  $E$  should be a

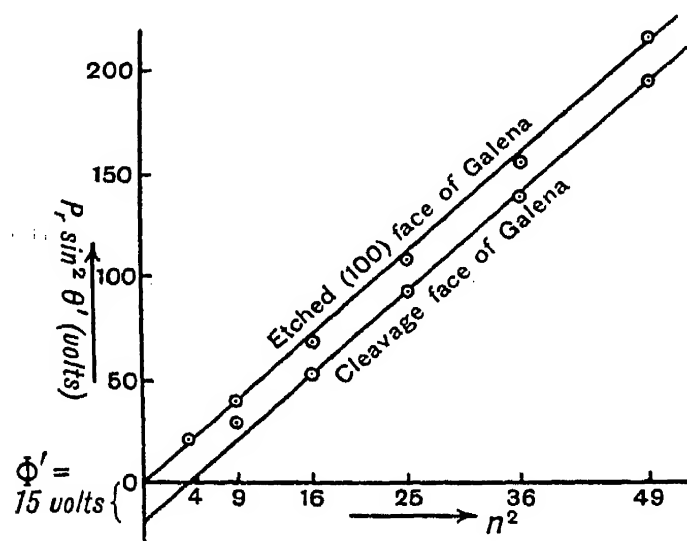


FIG. 52

straight line, whose intercept on  $n^2 = 0$  gives  $E(V_r/V)^2$ . The slope of the line enables ' $d$ ' to be found, or if this is known from X-ray measurements, gives a check on the measurement of  $V$ . Fig. 52 shows an example for galena taken from Tillman's paper. In this case it was also possible to get diffraction without refraction by etching the surface of the crystal, giving a cross-grating pattern by transmission through the projections and the plates taken from the etched specimens gave a check on the value assumed for ' $d$ '. It will be noticed that the point corresponding to the third order lies off the line, the value of  $E$  corresponding to it being too small. This is an instance of a general principle first established by

Yamaguti<sup>1</sup> for molybdenite, zincblende, graphite and talc, and it is found that, if the inner potential is graphed as a function of  $n$ , it increases with  $n$ , reaching an asymptotic value after the first few orders.<sup>2</sup>

A theory of this variation has been given by Laschkarew<sup>3</sup> on the supposition that  $\mu$  is a function of the depth below the surface with a period equal to the spacing of the planes. If

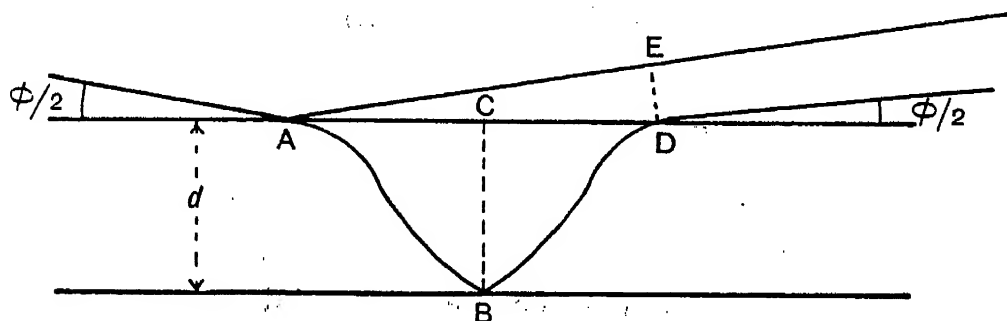


FIG. 53

$z$  is measured normal, and  $x$  parallel to the surface, the equivalent path of an electron moving along AB (Fig. 53) is

$$\lambda_0 \int_A^B \frac{ds}{\lambda},$$

where  $\lambda_0$  is the wave-length *in vacuo* and  $\lambda$  the variable wave-length in the crystal. If the angle between the path and the surface at any point is  $\alpha$ , this becomes

$$\lambda_0 \int_0^d \frac{dz}{\lambda \sin \alpha} = \int_0^d \frac{\mu^2 dz}{\sqrt{\mu^2 - \cos^2 \phi/2}}$$

since  $\mu \cos \alpha = \cos \phi/2 = \text{constant}$ . The distance AC is

$$\int_0^d \frac{dx}{dz} \cdot dz = \int_0^d \cot \alpha dz = \int_0^d \frac{\cos \phi/2 \cdot dz}{\sqrt{\mu^2 - \cos^2 \phi/2}}.$$

The condition for the Bragg reflection is that the equivalent path along AB + BD is  $n\lambda + AE$  or

$$2 \int_0^d \frac{\mu^2 dz}{\sqrt{\mu^2 - \cos^2 \phi/2}} - 2 \int_0^d \frac{\cos^2 \phi/2 \cdot dz}{\sqrt{\mu^2 - \cos^2 \phi/2}} = n\lambda.$$

<sup>1</sup> Yamaguti, *Proc. Phys. Math. Soc. Jap.* 16, p. 95 (1934).

<sup>2</sup> Cf. Kikuchi and Nakagawa, *Zeit. für Phys.* 88, p. 757 (1934).

<sup>3</sup> *Zeit. für Phys.* 86, p. 797 (1933); 89, p. 820 (1934).

Therefore

$$2 \int_0^d \sqrt{\mu^2 - \cos^2 \phi/2} \cdot dz = 2 \int_0^d \sqrt{(\mu^2 - 1) + \sin^2 \phi/2} \cdot dz = n\lambda.$$

If  $\mu^2 - 1$  is small compared with  $\sin^2 \phi/2$ , *i.e.* for large orders, this can readily be shown to be equivalent to

$$\sin^2 \phi/2 = 1 - \mu_0^2 + \frac{n^2 \lambda^2}{4d^2},$$

where 
$$\mu_0^2 - 1 = \frac{1}{d} \int_0^d (\mu^2 - 1) dz,$$

thus the effective inner potential for large orders is the mean potential over the crystal, which is what we have defined as the inner potential. The effective potential for small orders will be less. A simple model in which the potential is taken as zero over part of the spacing, and equal to a constant over the rest is found to give reasonably good agreement in most cases.<sup>1</sup>

### Experimental Details

In the case of some crystals, such as mica and molybdenite, curved flakes can be used to get the variation in glancing angle required to give many orders of reflection. In other cases the crystal must be rotated, unless the Kikuchi lines are used. An important source of error is uncertainty in the direction of the undeviated beam, and it is therefore desirable to use reflections to both sides.<sup>2</sup> A typical rotation photograph is shown in Plate Xc. When Kikuchi lines are used, their position has to be measured from the line of intersection of the crystal surface with the photographic plate. Shinohara determined this line by observations of the parts of oblique lines which were little affected by refraction. Tillman<sup>3</sup> set the crystal so that a Bragg spot due to the surface planes

<sup>1</sup> Yamaguti, *Proc. Phys. Math. Soc. Jap.* 17, p. 58 (1934), but cf. 18, p. 372 (1936); Miyake, *Sci. Pap. Ins. Phys. Chem. Tokyo*, 26, p. 216 (1935).

<sup>2</sup> In using the rotation method it is necessary to choose an azimuth in which the results are as free as possible from interference with oblique Kikuchi lines. Kikuchi and Nakagawa, *Sci. Pap. Inst. Chem. Phys. Res.* 21, p. 256 (1933); see also Chapter XIX.

<sup>3</sup> Tillman, *Phil. Mag.* 18, p. 656 (1934).

appeared at its brightest on the line. In this setting the shadow edge is midway between the undeviated and diffracted spots. The only measurements for metals with fast electrons are due to Darbyshire,<sup>1</sup> who prepared cleavage surfaces of zinc, antimony, bismuth and tellurium. The two last, however, gave no result, in the case of bismuth the surface is apparently traversed with furrows, while tellurium undergoes a rapid surface change even *in vacuo*.

### Variation of $\Phi$ with the Energy of the Rays

Most of the measurements have been made with cathode rays in the range 25-70 kv., but Tillman has made a number of experiments with 5 kv. electrons, using an Evershed and Vignolles dynamo, and a hot cathode discharge tube. The diffracted beams were rather weak, and it was necessary to increase the intensity by magnetic focusing. As will be seen from Table XIII, the results agree very well with those at higher voltages. As a result of experiments at really low voltages ( $\sim 200$  volts) values have been assigned to the inner potential of various substances, but the theory is still so uncertain that it is doubtful if much weight can be attached to these determinations, especially as in some cases two values have to be assumed. Laschkarew<sup>2</sup> finds 18-20 volts for graphite, and Davisson and Germer got the best fit for their experiments on nickel by taking  $E = 18$  volts.

### Pyrites

Very remarkable results have been obtained by Yamaguti<sup>3</sup> from a study of pyrites. Different specimens give potentials varying from 4.9 to 11.2 volts for the (100) face, and from 5.8 to 2.7 volts for the (111) face, while the specimen which gave the highest value in the first case gave the lowest in the second. Different experiments on the same specimen and face showed a rather wider variation than usual, but the variation of  $E$  with the order of the reflection was about

<sup>1</sup> Darbyshire, *Phil. Mag.* 16, p. 761 (1933).

<sup>2</sup> Laschkarew, *Trans. Farad. Soc.* p. 1081 (1935).

<sup>3</sup> Yamaguti, *Proc. Phys. Math. Soc. Jap.* 17, p. 58 (1935).

normal. Yamaguti considers that these variations must be due to impurities on the surface together with an abnormal variation of potential in the crystal itself, but it is not clear why this particular substance should show these peculiarities.

TABLE XIII  
INNER POTENTIALS OF VARIOUS SUBSTANCES IN VOLTS

Substance	Yamaguti	Shinohara	Kikuchi and Nagakawa	Miyake	Dixit	Tillman		Jenkins	Beeching	Uyeda	Mean
Rock-salt NaCl	7.7	6.3	..	..	..	H. 7.1	L. 6.0	..	..	..	6.8
Zincblende Zns	12.7	..	12.2	12.18	(2.6)	12.2	12.1	..	..	..	12.3
Galena PbS	..	..	..	..	12.5	13.7	13.1	..	..	..	13.1
Pyrates FeS <sub>2</sub>	11.2	} ..	} ..	} ..	} 5.1	} 3.7	} ..	} ..	} ..	} ..	} 5.0
Stibnite Sb <sub>2</sub> S <sub>3</sub>	-4.9										
Fluorspar CaF <sub>2</sub>	11.9	..	..	..	..	14.3	14.3	..	..	..	13.5
Calcite CaCO <sub>3</sub>	..	..	..	..	..	11.6	13.3	..	..	..	12.5
Gypsum	12.4	13.8	..	..	..	12.5	12.5	..	..	..	12.8
Mica KH <sub>2</sub> Al <sub>3</sub> (SiO <sub>4</sub> ) <sub>3</sub>	9.1	..	..	..	..	7.7	8.5	..	..	..	8.4
Molybdenite MoS <sub>2</sub>	10.6	10.4	..	..	..	..	..	..	..	..	10.5
Graphite C	17.1	..	..	..	..	..	..	..	..	19.5	18.3
Diamond C	11.5	..	..	..	..	..	..	10.7	..	13.0	11.7
Talc (OH) <sub>2</sub> Mg <sub>3</sub> (Si <sub>4</sub> O <sub>10</sub> )	..	..	..	..	..	..	..	..	20.8	..	20.8
Haematite Fe <sub>2</sub> O <sub>3</sub>	12.0	..	..	..	..	..	..	..	..	..	12.0
PbO artificial	..	..	..	..	12.6	..	..	..	..	..	12.6
ZnO	..	..	..	..	..	..	..	12.3	..	..	12.3
SnO	..	..	..	..	..	..	..	12.3	..	..	12.3
	..	..	..	..	..	..	..	14.2	..	..	14.2

Long-chain organic compounds	..	..	..	..	..	1.3	} Murison
Various organic mixtures	..	..	..	..	..	3.1-7.2	
Zinc	..	..	..	..	..	15.5	} Darbyshire
Antimony	..	..	..	..	..	20.0	
C <sub>30</sub> H <sub>62</sub>	..	..	..	..	..	6.0	} Thiessen and Schoon
C <sub>31</sub> H <sub>64</sub>	..	..	..	..	..	7.1	
Stearic Acid	..	..	..	..	..	6.3	

Notes.—Some measurements by Raether, for which readings are not given, and some by one of the authors, are excluded as probably less accurate. Dixit's measurements were made visually on the fluorescent screen. They were not corrected for relativity. The measurements by Tillman marked H refer to electrons of average energy 30,000 volts, they have been corrected for relativity in accordance with the formula in the text. Those marked L refer to electrons of about 5000 volts.

References.—In addition to those given above: Yamaguti, *Proc. Phys. Math. Soc. Jap.* 14, pp. 1, 57 (1932); Dixit, *Phil. Mag.* 16, p. 980 (1933), 17, p. 732 (1934); Jenkins, *Proc. Phys. Soc.* 47, p. 109 (1935); Beeching, *Phil. Mag.* 20, p. 841 (1935); Uyeda, *Proc. Phys. Math. Soc. Jap.* 20, p. 280 (1938); Thiessen and Schoon, *Zeit. für Phys. Chem.* (B) 36, p. 195 (1937).

### Calculation of Inner Potential

If the structure of the crystal were known, and if it were possible to calculate the electronic distribution of the atoms, it would clearly be possible to find the potential at any point and hence the mean value. Unfortunately the second requirement is difficult to fulfil. The peripheral parts of the atoms are the most important, and the distribution here is the least known, and is liable to be modified by chemical combination. Calculations based on the Hartree distribution have not been successful. Others, in which the electronic distribution is deduced from the X-ray '*f*' curves for the atoms, give better results, but the method involves summing a series of rather large positive and negative terms which nearly balance, and so is inaccurate. Calculations by Shinohara and by Dixit show a certain measure of agreement with experiment, but can hardly be relied upon as yet to correct either the experiments or theories. Perhaps the best is that of Laschkarew (*l.c.*), who finds 8.4 volts for rock-salt.

## CHAPTER XI

### STUDY OF THE GROWTH OF CRYSTALS

#### Growth in Thin Films

THE method of electron diffraction is well suited to the study of the growth of crystals, since the top layers of a crystal can be studied without interference from the rest. Among the earliest of the diffraction patterns were some taken with films made from beaten foils.<sup>1</sup> These patterns confirmed the conclusion formed from experiments with X-rays that the crystals of such films are orientated, one crystal plane tending to lie in the plane of the film. This is shown by an abnormal distribution of intensity among the rings, those being strongest, in transmission patterns, which correspond to reflections from planes normal to the plane of the film, and also by the changes which occur when the films are tilted.<sup>2</sup> Sometimes the rings are broken into arcs showing an additional kind of orientation in which a second zone axis of the crystal tends to point in a certain direction. This is known to occur with rolled metal sheet; it is also found with beaten films when examined by electron diffraction<sup>2</sup> (cp. Plate Va). The area examined is very small, and the necessary dissymmetry may be supplied by the direction of a glancing blow. In some cases one or two crystals cover the whole area.

Interesting changes occur in the orientation of the crystals in thin films under the action of heat. Thus Trillat and Oketani<sup>3</sup> find that a beaten film of pure gold, heated *in vacuo* or in air, begins to grow large crystals when the temperature exceeds about 650° C. These crystals increase in size till one covers the whole area exposed to the electrons. Such crystals are usually orientated with an important zone axis normal to the film. If the gold is alloyed, the growth of large crystals starts at a lower temperature, about 350° when the film is

<sup>1</sup> G. P. Thomson, *Proc. Roy. Soc.* 117, p. 600 (1928).

<sup>2</sup> *Ibid.* 119, p. 651 (1928).

<sup>3</sup> Trillat and Oketani, *Jour. de Phys.* 8, p. 59 (1937).

heated *in vacuo*; at temperatures over  $500^{\circ}$  the effect is reversed,<sup>1</sup> and uniform rings due to numbers of disorientated crystals appear. These films, even before treatment, usually show pronounced orientation of the arc type (Plate V *a*), which Trillat and Hirsch<sup>1</sup> interpret as meaning that the crystals are deformed. On this view the first recrystallisation would imply a straightening out of the lattice; on the view suggested above, one particular crystal, out of a number disposed with axes roughly parallel, must grow at the expense of the rest.

An interesting modification occurs in certain parts of the films, usually the thinnest, at temperatures above about  $550^{\circ}$  C. (for pure gold). Rings appear, often with spots on them, which correspond to an hexagonal structure of side  $5.28 \text{ \AA}$  orientated with the *c* axis normal to the film. The dimensions of this structure do not seem to bear any simple relation to those of ordinary gold.

When a gold alloy containing 1 per cent Cu and 1.5 per cent Ag is heated in air, rings appear<sup>2</sup> which agree with those found by one of the authors<sup>3</sup> on heated copper. The oxide is unstable, decomposing at room temperature in the course of years, and rapidly when heated *in vacuo*.

A curious effect is reported by Preston and Bircumshaw,<sup>4</sup> who find that while a gold foil will recrystallise at about  $450^{\circ}$  when heated in air, it will not do so in hydrogen or *in vacuo* up to  $700^{\circ}$ , although no sign of oxide or any rings belonging to a foreign structure appear. They do not state the composition of their foils, which may have been different from those used by Trillat. Finch and Fordham<sup>5</sup> agree in finding no recrystallisation of pure evaporated gold films heated up to  $550^{\circ}$  *in vacuo*, at which temperature they collapsed. Platinum and palladium also showed no recrystallisation.

### Growth on Substrates

An important group of researches concerns the growth of crystals deposited in various ways on substrates. It is found,

<sup>1</sup> Trillat and Hirsch, *Jour. de Phys.* 3, p. 185 (1932).

<sup>2</sup> Trillat, Oketani and Miyake, *Jour. de Phys.* 8, p. 354 (1937).

<sup>3</sup> G. P. Thomson, *Proc. Roy. Soc.* 128, p. 649 (1930); Murison, *Phil. Mag.* 17, p. 96 (1934).

<sup>4</sup> Preston and Bircumshaw, *Phil. Mag.* 21, p. 713 (1936).

<sup>5</sup> Finch and Fordham, *Soc. Chem. Ind.* 56, p. 632 (1937).

in many cases, that the crystals are orientated with some particular crystal plane parallel to the surface of the substrate. When the substrate is a crystal of a structure at all similar to that of the deposited substance, the crystals of the latter often grow in a special relationship to the structure of the substrate, which determines not only the direction of a plane, but of the lines of atoms in the plane, and therefore the complete orientation of the deposited crystals.

### Evaporated and Sputtered Layers

Kirchner<sup>1</sup> has studied the deposits formed by evaporating substances on to a thin film of celluloid or other material and examining the specimens by transmission. A number of metals gave results similar to those earlier found by one of the authors,<sup>2</sup> namely rings, often rather diffuse, corresponding to the normal crystal structure, but Kirchner noticed the interesting fact that the thicker layers gave sharper rings, and hence presumably were composed of larger crystals than the thinner. Bismuth showed orientation with the (111) plane parallel to the film. A number of experiments were made using inorganic compounds, which showed as a rule the following features. Very thin layers ( $\sim 10^{-7}$  cm.) gave diffuse rings when first formed, but on standing for a few hours, or less if warmed, the rings sharpened and the crystal became more or less strongly orientated, shown by the abnormal relative intensities of the rings, and by the rings breaking up when the film was inclined. Thicker films show sharper rings, and orientation from the beginning. Cadmium iodide, which has a layer lattice, shows the effect very well (Plate V *b*). It orientates with the basal hexagonal plane parallel to the surface. Calomel,  $\text{Hg}_2\text{Cl}_2$ , is exceptional in orientating with an axis, the tetragonal, *in* the surface.

As a result of investigations by several authors<sup>3</sup> on films prepared at liquid air temperatures, it appears that in general such films show more or less diffuse rings indicating small crystals. On warming up to room temperature or above, the

<sup>1</sup> Kirchner, *Zeit. für Phys.* 76, p. 576 (1932).

<sup>2</sup> G. P. Thomson, *Proc. Roy. Soc.* 125, p. 352 (1929).

<sup>3</sup> Gen, Zelmanoff and Schalnikoff, *Phys. Zeit. Sowjet.* 4, p. 825 (1933) (studied Cd, Hg, Ni and Fe). Hass, *Ann. d. Phys.* 31, p. 245 (1938) (studied Ag and Sb). Ogawa, *Tohoku Univ. Sci. Rep.* 26, p. 92 (1937) (studied Ni).

rings grow sharper, showing that the crystals are increasing in size. In the case of nickel the crystal form also changes, and with it the magnetic properties. In these experiments care has to be taken to prevent impurities condensing on the surface; thus Hass found that, unless he used a carefully constructed shield, a layer of impurity estimated at 1000 Å thick formed on the specimen quite obliterating the pattern. It is possible that the main effect may be due to gas molecules being deposited simultaneously with the metal, and breaking up the regularity of the lattice. Gas is necessarily present when the films are formed by spluttering, and is difficult to avoid in the case of evaporation. On the other hand, it may be that a necessary part of the mechanism of growing crystals of any considerable size is a free mobility of atoms over the surface already formed, and this may be impossible at low temperatures.

Quarrell<sup>1</sup> has found that various metals which normally crystallise in the face-centred cubic form take up an orientation with the (110) planes parallel to the surface, when evaporated on to a 'cellulosic' substrate, and that in addition rings appear characteristic of the hexagonal close packed structure of the same density as the ordinary close packed cubic form. One of the authors<sup>2</sup> had found that nickel spluttered on to rock-salt assumed the hexagonal structure. Lassen<sup>3</sup> and Brück<sup>4</sup> have examined the structures of thin metal films evaporated *in vacuo* on to the cube face of rock-salt, and find that they depend greatly on the temperature of the rock-salt during the deposition. At low temperatures the metal crystals are in random orientation; above a certain critical temperature there is complete orientation, a plane of the metal being parallel to the cube face of the salt, and a line of atoms in the metal parallel to a line in the salt. At temperatures in between there is partial orientation. In some cases, *e.g.* gold and aluminium, there were two types of single crystal orientation. One, at lower temperatures, with the (111) plane parallel to the cube face, and the cube face diagonal of the metal parallel to that of the salt, the other, at higher temperatures, with the (100) plane parallel to the cube face, and the

<sup>1</sup> Quarrell, *Proc. Phys. Soc.* 49, p. 279.

<sup>2</sup> G. P. Thomson, *Proc. Roy. Soc. A* 125, p. 352 (1929).

<sup>3</sup> Lassen, *Phys. Zeit.* 35, p. 172 (1934); Lassen and Brück, *Ann. d. Phys.* 22, p. 65 (1935).

<sup>4</sup> Brück, *Ann. d. Phys.* 26, p. 233 (1936).

cube edges of the two structures parallel. This last was the final state at high temperatures for all the face-centred cubic metals, including nickel. The body-centred metals, iron and chromium, could have either a (110) plane parallel to the cube face of the salt, the cube edges of the two being parallel, or the cube faces of the two structures could be parallel, but with cube face diagonal parallel to cube edge. When quartz and molybdenum bases were used, the temperatures for

TABLE XIV  
ORIENTATION AND TEMPERATURE (DEGREES C.)

Metal	Plane	Rock-salt (Brück)	Mica (Rüdiger)	Calcite (Rüdiger)	Fluorite (Rüdiger)	Quartz (Rüdiger)
Ag	111	..	150	470	> 500	..
	100	150	..	510	..	..
	110	..	..	..	..	..
Au	111	..	450	360	380	560* Max
	100	400	..	470*	..	..
	110	..	..	510	..	..
Pd	111	..	470	400	400	540* Max
	100	250	..	420*	..	..
	110	..	..	490	..	..

orientation were higher and, as might be expected, single crystals were never formed. Gold showed a (111) orientation on quartz at 480° C., changing to (100) at 700° C. Aluminium gives (100) at low temperatures and (110) at higher.

Lassen and Brück's work has been further extended by Rüdiger,<sup>1</sup> who evaporated each of the metals gold, silver and palladium on to the cleavage faces of mica, calcite and fluorite, on to polished quartz and on to the *natural* face of quartz. The deposits were examined by the reflection method and in some cases by transmission. Again a notable feature of the results was the dependence of the orientation on temperature as shown in Table XIV. An asterisk indicates that the orientation was only of the fibre type.

As regards the *complete* orientation of the deposits, usually more than one type of orientation was present. This is illus-

<sup>1</sup> Rüdiger, *Ann. d. Phys.* 30, p. 505 (1937).

trated in Fig. 54, which shows three different types of orientation, designated 1, 2 and 3, for a (111) gold plane on a mica cleavage plane. Generally, silver and palladium behave in the same way as gold.

The results of Lassen, Brück and Rüdiger may be compared with those found earlier by Murison, Stuart and one of the authors,<sup>1</sup> and by Dixit.<sup>2</sup> The former examined films of platinum, prepared (for experiments on catalysis) by spluttering on to blanks of molybdenum, quartz and glass. Where the conditions were such that the films became heated while being made they were generally found to be orientated, the preferred face being (100), (111) or (110) in the great majority of cases. Dixit worked with evaporated films mostly on polished molybdenum blanks. Silver, aluminium and zinc each showed several types of orientation after heat treatment. Dixit found that in all

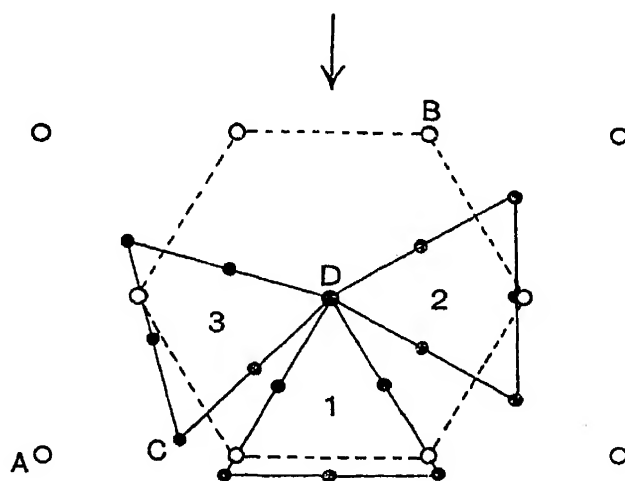


FIG. 54

cases the orientation first produced was that in which the most densely packed plane of atoms was parallel to the surface; at higher temperatures other planes took its place. In fact the area occupied per atom in each plane was proportional, for any given metal, to the absolute temperature at which orientation on that plane was most prominent. Dixit explained this by supposing a layer of atoms on the surface to act as a two-dimensional gas. It will be seen that Dixit's law is followed, at least qualitatively, by Brück's result.

Some experiments which afford an instructive insight into the mechanism of crystal growth have been made by Burgers and Dippel<sup>3</sup> on the formation by evaporation of crystals of calcium fluoride (cubic). Previous work by Coper, Frommer and Zocher,<sup>4</sup> using X-rays, had indicated that the crystals had

<sup>1</sup> Thomson, Murison and Stuart, *Proc. Phys. Soc.* 45, p. 381 (1933).

<sup>2</sup> Dixit, *Phil. Mag.* 16, p. 1049 (1933).

<sup>3</sup> Burgers and Dippel, *Physica*, 1, p. 549 (1934).

<sup>4</sup> Coper, Frommer and Zocher, *Zeit. für Elektrochem.* 37, p. 571 (1931).

a laminar structure parallel to the (111) planes, and that the inclination of these planes to the underlayer varied with the angle of incidence of the vapour beam. Burgers and Dippel found that films of less than about  $10^{-5}$  cm. thick showed random orientation. Above this thickness they showed (111) orientation, but the direction of the (111) axis was influenced by the direction of the vapour beam. Three disks were arranged so that the vapour came normally on to the centre one, and at angles of  $65^\circ$  to the normal on those to the right and left. The centre disk showed orientation with the (111) axis normal to the plane; in the other two this zone axis made an angle of  $10^\circ$  with the normal in a direction towards the vapour beam. Experiments on the absorption of iodine by these films make it very probable that the (111) planes form the most prominent boundary planes of the crystallites which compose the films, and which are therefore in the form of flat plates.<sup>1</sup> A rather similar result has been found by Beeching<sup>2</sup> for aluminium deposited by evaporation on glass. In this case the cube face was the plane of orientation, and when the incident vapour came at  $45^\circ$  to the surface the cube faces of the deposited metal made average angles of about  $15^\circ$  with the surface.

When substances naturally crystallise in flat plates, as do cadmium iodide and probably bismuth, it is easy to see that when crystals of considerable size form in thin films those whose planes lie in the surface will be favoured, since they can grow indefinitely while the others cannot. It is less easy to see how the orientation occurs in the case of substances, like most metals and calcium fluoride, which crystallise in the cubic system and so have several crystallographically equivalent directions. But it seems likely that even with these substances orientation on non-crystalline substrates is associated with the formation of flat plates, though which of the several equivalent directions are chosen for extended growth must depend on the supply of material. There is good reason to suppose<sup>3</sup> that in many cases crystals grow by atoms arriving on a face, moving over it till they come to the edge and then prolonging the face. If we postulate this, as suggested by

<sup>1</sup> Burgers and van Amstel, *Physica*, 3, p. 1057 (1936), have found a similar effect for evaporated layers of barium.

<sup>2</sup> Beeching, *Phil. Mag.* 22, p. 938 (1936).

<sup>3</sup> Volmer, *Trans. Farad. Soc.* 28, p. 359 (1932).

Burgers and Dippel, we can explain most of the facts. The influence of the direction of the vapour stream in evaporated films is immediately evident. Planes normal to the stream will receive more atoms per unit area than the others and so grow faster. However, planes parallel to the surface have the advantage that they can grow in both directions, and one would expect the maximum rate of growth to occur for planes between these two directions, if they are not the same. It should be remembered that the surface of the substrate is probably, as a rule, wavy rather than truly flat on the scale with which we are concerned (films of  $10^{-6}$ - $10^{-5}$  cm. thickness). The question as to which type of face will appear is more difficult; partly, no doubt, it is an inherent property of the substance, but it seems partly to depend on still undetermined conditions. Why, for example, did Quarrell's films tend to give (110) orientations for the face-centred cubic metals, and also an appreciable amount of the hexagonal modification? Dixit and Brück only got this orientation when the substrate was strongly heated, but this cannot have happened with Quarrell's substrates, since they were organic. Perhaps the substrate even when non-crystalline has a specific effect in certain cases, but none of the experimenters so far have found any.

Films made by spluttering rarely show orientation, except after heating to temperatures comparable with, though very considerably smaller than, the melting-points of the metals. At the pressure at which spluttering is usually done the free path of atoms is small, and the metal probably arrives at the surface from all directions at random. When the orientation is produced by heating, the important factor is the ability of a crystal to grow along the surface but not normal to it, because the available material is confined to a thin film. Suppose, for example, that the temperature favours the growth of cubes, then those cubes which happen to start with a cube face nearly parallel to the surface can grow indefinitely in this direction, while others will be limited. After a time a large proportion of the material will be in the form of crystals with the favoured orientation.

In connection with the question of growth by heating some experiments of Andrade and Martindale<sup>1</sup> are important.

<sup>1</sup> Andrade and Martindale, *Phil. Trans.* 234, p. 69 (1935).

They studied by microscopic methods films of gold spluttered on quartz. They found that a first stage in the formation of crystals from (apparently) amorphous films was the appearance of 'spherulites', detected by double refraction; these are apparently tiny crystals with spikes protruding in all directions. Later, crystals of triangular form appear, with a (111) face parallel to the surface, and parts of the films become very thin, forming 'windows'. The electron diffraction experiments indicate that gold films when first formed are never amorphous, though the crystal size is often small enough to give diffuse rings ( $\sim 2 \times 10^{-7}$  cm. cube side). No sign appears of the spherulites in the work we have been considering, but the appearance of the flat crystals with (111) orientation is in good agreement with what has been found at the lowest temperature, and with the view suggested above.

### Crystals Grown Electrolytically

Finch and Sun<sup>1</sup> have shown that metals electrolytically deposited on a neutral base, such as a polished disk of the same or of a different metal, give as a rule a random arrangement in thin films, but an orientation with a plane parallel to the surface if the deposit is thick. The plane chosen for orientation depends on the current density, which was of the order of 0.01 amp. per sq. cm., and on the composition of the bath, as well as on the metal.<sup>2</sup> If, instead of a neutral base, an oriented layer of metal crystals is taken, in practice one formed as above, the fresh deposit at first is determined by the oriented layer, but after a certain thickness there is a reversion to the form of orientation characteristic of the metal being deposited. At intermediate thicknesses the arrangement may be almost random. To take an example: iron deposited on a substrate of gold in the (100) orientation showed first a (100) orientation but for thick films a (111), which is what iron shows when deposited under the same conditions on a neutral base.

When single crystals are used as bases it is possible to draw more exact conclusions as to the relations between the atoms in

<sup>1</sup> Finch and Sun, *Trans. Farad. Soc.* 32, p. 852 (1936).

<sup>2</sup> Cf. Finch and Williams, *Trans. Farad. Soc.* 33, p. 564 (1937).

the two crystals. Cases have long been known in which one ionic crystal when grown on the surface of another takes up a definite orientation with respect to the substrate, *e.g.* KCl on mica. Wood<sup>1</sup> showed by means of X-rays that the structure of one metal can be continued in that of another electrodeposited on it. One of the authors<sup>2</sup> found that silver deposited electrolytically on a single crystal of copper was orientated in conformity with the copper, and Farnsworth<sup>3</sup> evaporated silver on to a gold crystal with a similar result. The work of one of the authors<sup>4</sup> and of Finch and Sun (*l.c.*) goes into greater detail.

The former used a single crystal of copper cut to either the (110) or (111) face and etched. The etching, as we shall see, brings out faces other than the apparent surface of the crystal. Copper itself could be deposited in conformity with the original structure up to a thickness of 40,000 Å, and probably indefinitely, provided the current density did not exceed a few milliamps. per sq. cm. Large current densities gave a random distribution of small copper crystals. Nickel, whose cube side is 3.517 Å against 3.608 for copper, when deposited with a current density of 0.3 mA./cm.<sup>2</sup> or more, gave a random distribution of crystals, but the rings due to them passed through the spots due to the copper, so that apparently the spacing of the nickel had increased to that of copper. Measurement of the patterns confirmed this spacing, which also applies to the deposits with lower current densities. At 0.025 mA./cm.<sup>2</sup> a deposit 60 Å thick merely continued the structure of the copper, the pattern being unchanged. Thicker deposits gave a curious pattern including the original spots, extra spots regularly arranged, and lines joining them (Plate VIII c). It was shown that this pattern could be explained by a deposit of nickel on (111) copper faces exposed by the etching, if it were supposed that frequent twinning of the deposit on the (111) face occurred. The twin crystals explain the extra spots, while the atoms in the plane of twinning, which are abnormally situated, will scatter electrons with a different phase relationship to those in the main structure. A number of such twinning planes can account for the lines connecting

<sup>1</sup> W. A. Wood, *Proc. Phys. Soc.* 43, p. 138 (1931).

<sup>2</sup> G. P. Thomson, *Proc. Roy. Soc.* 133, p. 1 (1931).

<sup>3</sup> Farnsworth, *Phys. Rev.* 43, p. 900 (1933).

<sup>4</sup> Cochrane, *Proc. Phys. Soc.* 48, p. 723 (1936).

the spots. Frequent twinning of this kind might be caused by the slight strain in the deposit caused by its conforming in dimensions to the copper. Silver has a face-centred cubic structure with side  $4.06 \text{ \AA}$ ; when deposited very slowly (15 *micro*-amps. per sq. cm.) it gave a pattern of spots similar to that of the copper, but with the usual silver spacing, showing that the silver was deposited conformably with the copper in orientation but not in spacing (Plate VII c). More rapidly formed deposits were at random. Current densities of a few microamps. per sq. cm. gave deposits of cobalt in conformity with the copper;

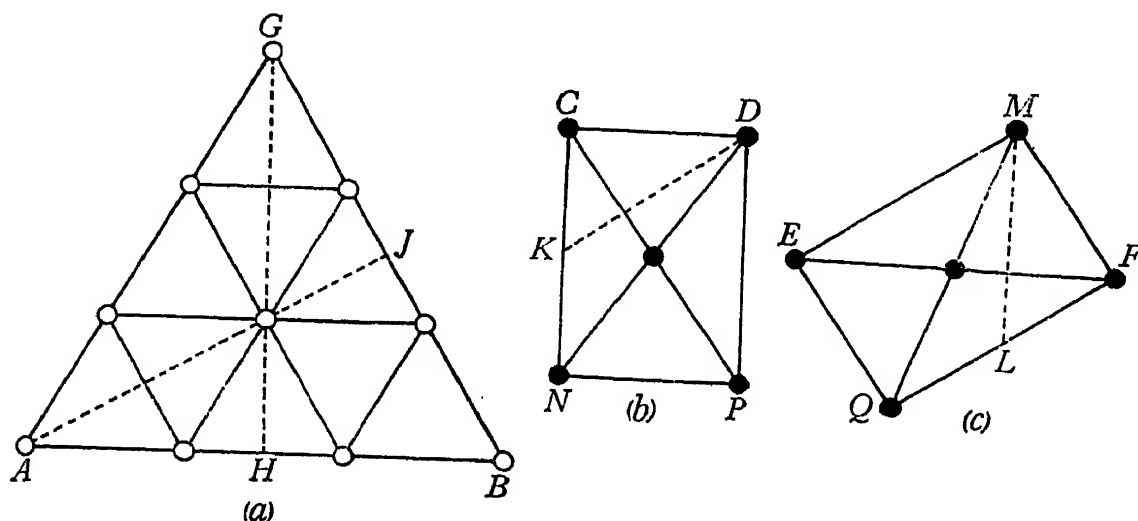
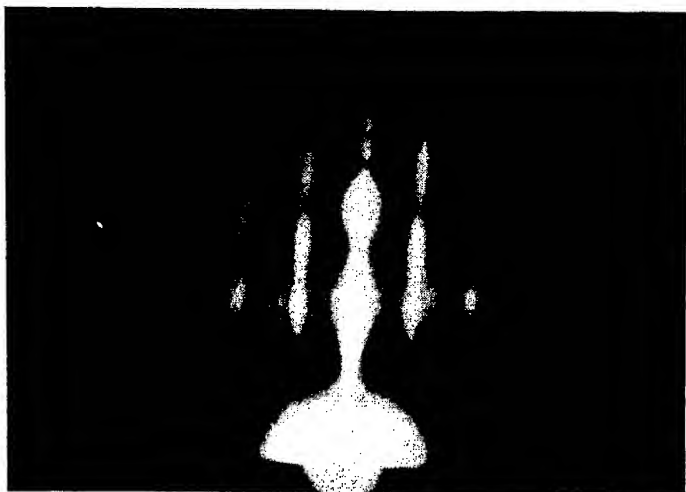


FIG. 55

the patterns showed the features discussed on p. 76, which prove that the small cobalt crystals were bounded by octahedral faces. Larger current densities gave rings of cubic and hexagonal cobalt. It was not found possible to use small current densities with chromium (body-centred cubic). Nevertheless deposits made at  $0.2 \text{ A./cm.}^2$  for a few seconds showed spots due to chromium, in which the chromium had formed orientated crystals. This metal is deposited simultaneously in two different orientations. In both, the  $(110)$  planes of chromium are parallel to the  $(111)$  planes of copper. The arrangements of the atoms in the common plane in the two cases are shown in Fig. 55, in which (a) shows the atoms in the copper plane and (b), (c) those in the chromium plane, in the two relative orientations observed. The figures are drawn to scale, and the dotted lines show the trace of other planes normal to the ones illustrated. The hexagonal metals,

## PLATE VII



(a) Oriented PbO on molten lead. (*Jenkins.*) Taken from *Proc. Phys. Soc.* 47, p. 114 (1935)



(b) Cobalt deposit on copper single crystal, (110) face, beam parallel to cube edge



(c) Thin silver deposit on copper single crystal, (110) face, beam parallel to cube-face diagonal. Spots are due to copper, short arcs due to silver



zinc and cadmium, did not yield orientated deposits even at low current densities.

Finch and Sun's specimens were made by electroplating on to thinned pieces of beaten leaf which gave patterns of arcs, usually short ones, and were nearly single crystals; the composite films were examined by transmission. Table XV shows the results; the 'first direction' gives the crystal

TABLE XV  
FINCH AND SUN'S RESULTS ON ORIENTATION

Substrate	Substrate Orientation	Deposit	Orientation Observed	
			First Direction	Second Direction
Pt	(110)	Cu	(110) <sub>Pt</sub>    (110) <sub>Cu</sub>	(110) <sub>Pt</sub>    (110) <sub>Cu</sub>
		Ni	(110) <sub>Pt</sub>    (110) <sub>Ni</sub>	(110) <sub>Pt</sub>    (110) <sub>Ni</sub>
		Co	(110) <sub>Pt</sub>    (110) <sub>Co</sub>	(110) <sub>Pt</sub>    (110) <sub>Co</sub>
Pd	(100)	Cu	(100) <sub>Pd</sub>    (100) <sub>Cu</sub>	(001) <sub>Pd</sub>    (001) <sub>Cu</sub>
		Fe	(100) <sub>Pd</sub>    (100) <sub>Fe</sub>	(011) <sub>Pd</sub>    (001) <sub>Fe</sub>
Au	(100)	Fe	(100) <sub>Au</sub>    (100) <sub>Fe</sub>	(011) <sub>Au</sub>    (001) <sub>Fe</sub>
		Co	(100) <sub>Au</sub>    (100) <sub>Co</sub>	(001) <sub>Au</sub>    (001) <sub>Co</sub>
		Ni	(100) <sub>Au</sub>    (100) <sub>Ni</sub>	(011) <sub>Au</sub>    (001) <sub>Ni</sub>

plane of the deposit which is parallel to the surface plane of the substrate, the 'second direction' gives two other parallel planes in deposit and substrate, so that the orientation is completely specified.<sup>1</sup>

### Discussion

The simplest form of orientation is that in which a definite plane of the growing crystal is parallel to the surface of the substrate, but the crystals are arranged at random about the normal to the surface. This occurs under suitable conditions with both evaporated and electrolytically deposited films, and we have seen reason to suppose that it may be accounted for by considering the way in which material is supplied to the

<sup>1</sup> In some cases a curious structure of the central spot was observed, and extra arcs were found which are explained as due to the diffraction by the second constituent of the specimen of beams already diffracted by the first. Rather similar effects were observed by Kirchner (*l.c.*) with cadmium iodide on mica.

growing crystal, combined with a tendency for some particular crystal form to predominate.

Complete orientation, in which the new crystal has its axes completely determined by those of the substrate, has long been known in the case of certain ionic crystals grown from solution, *e.g.* sodium nitrate on calcite. In the experiments we have been describing the effect has been observed in many cases of metals deposited both by evaporation and by electrolysis. In general the effect occurs most readily when the metal and substrate have a similarity of structure, but in some of Rüdiger experiments there is no resemblance. It certainly occurs in many cases where there is not even an approximate fit between the atoms of crystal and substrate. In one of Finch and Sun's experiments, alone, does the orientation seem to have been determined by a fit of this kind. They found an orientation of iron on gold which seems to depend on the accident that the cube side for gold is very nearly  $\sqrt{2}$  times that for iron. This makes alternate iron atoms in the cube face fit the gold atoms, when the orientation is as Finch and Sun found it.

The orientated crystals give sharp spots and are certainly of considerable size, though it is not of course necessary to suppose that they extend over the whole surface of the substrate. Brück and Rüdiger find that in many cases the orientation is such as to make the sum of the distances between nearest atoms of the crystal and substrate a minimum, reckoned over the first cell. We are inclined to doubt if a law of this kind can explain the results. Since the periodicities are in most cases incommensurable, the relative positions of the atoms of crystal and substrate will change irregularly as the crystal grows, and what might be a favourable arrangement for the first few atoms would probably be an unfavourable one later on. Nor does it seem probable that any movement of the crystal as a whole over the surface of the substrate can account for the orientation. In general, with incommensurable periods, the difference in the energies between different orientations will at most be of the order of the energy of attachment of a few atoms, and this seems inadequate to orientate crystals containing many thousands of atoms to an accuracy of a degree or less. A possible explanation is that the growth is determined by special lines

of atoms in the substrate, such for example as the edge of a crack, or the internal angle at the bottom of a step on the surface, for it is unlikely that the surface is ideally flat. Such a line of atoms would be a zone axis of the substrate, usually a simple one. If the atoms of the growing crystal formed up along this line, the crystal would grow so as to make them also a zone axis, and we should have two zone axes of the two crystals coinciding. If also two planes coincide, for the reasons discussed above, we have complete orientation of the type actually found.

In almost all cases so far observed an important line of atoms in the substrate surface does in fact coincide with one in the growing crystal, the only exception being case 3 (Fig. 54) of the orientation on mica found by Rüdiger. The evidence here seems to consist in the pattern repeating at intervals of  $15^\circ$ . It seems possible that the orientation may have been slightly different from what was supposed. Actually the arrangement drawn in Rüdiger (Fig. 54) gives angles of  $12^\circ$  and  $18^\circ$ , inside a period of  $30^\circ$ , while an arrangement giving parallel lines of gold atoms CD and mica atoms AB can be drawn to give angles of  $19^\circ 8'$  and  $10^\circ 52'$ .

The existence of a minimum temperature for complete orientation as found by Brück and Rüdiger may be due to the presence of a gas layer, especially along the critical lines, which requires a high temperature to remove it. Alternatively, the mobility of the atoms on the surface may be too small at low temperature to allow them to find the directing cracks or steps, so that they simply join on to whatever other atoms may be near them irrespective of orientation.

Finch and Quarrell<sup>1</sup> have reported a case in which aluminium (cube side  $4.05 \text{ \AA}$ ), when evaporated on to platinum (cube side  $3.91 \text{ \AA}$ ), gave a tetragonal structure, with two axes equal to  $3.91$ , and one to  $4.05$ . In a similar way a thin layer of oxide formed on zinc gave a hexagonal structure different from the oxide in bulk, its basic plane having the dimensions of that of zinc. While several extra rings were found in the case of aluminium, others which would have been expected from the structure suggested did not occur; some of the extra rings possibly arise from the platinum underlayer, since the

<sup>1</sup> Finch and Quarrell, *Proc. Roy. Soc.* 141, p. 400 (1933).

aluminium film is very thin. It does not seem certain that the divergence of the main rings from the normal dimensions exceeds the possible experimental error. In the case of the zinc oxide also some rings are missing, and the evidence does not seem sufficient to fix the structure with complete certainty. While a definite proof of 'pseudomorphism' of this kind would perhaps favour Brück's hypothesis, it would not be decisive. In this connection, too, we may recall the results of one of the authors (p. 171) in which it was found that the lattice of a nickel deposit suffered a small change in dimensions so as to conform exactly with the copper lattice. This appears to be an exceptional case. The evidence at present available is insufficient to decide between the two views. Further experiments with crystals other than cubic would be very helpful.

The experiments of Finch and Sun (*l.c.*) show that the orientation can change from one corresponding to the substrate for thin films to one characteristic of the metal and bath for thick. The thickness required depends, among other things, on the size of the crystals in the substrate,<sup>1</sup> for submicroscopic crystals it is of the order 1000 Å, for larger crystals it may be as much as 20,000 Å. The change may be explained as follows. When the crystals have grown to some distance from the substrate they will interfere with one another, the resulting distortion will produce fresh nuclei or growing points, and the growth of the crystals which start from these will be largely governed by the supply of material. As the ions come up normal to the general surface, a plane in this surface will receive more material per unit area than one inclined to it. Hence if the conditions of the bath favour the growth of some particular form, say the cubic, crystals with a cube face parallel to the surface will grow into plates and expand at the expense of the others. This assumes, what we have postulated throughout, that atoms arriving at the surface of a crystal tend to move over the surface to the edges, and there form up as an extension to the surface. It is of course not necessary to suppose that all the atoms do so, but merely that there is a tendency in this direction.

<sup>1</sup> Cf. Finch and Williams, *Trans. Farad. Soc.* 33, p. 564 (1937).

## CHAPTER XII

### OXIDES

#### Oxides of Copper

ONE of the authors<sup>1</sup> examined an oxidised copper surface using the reflection method, and found that the lattice spacings deduced from the electron diffraction pattern did not agree with the known X-ray structures of either CuO or Cu<sub>2</sub>O. This point has been further investigated by Murison.<sup>2</sup> When copper is heated in an oxygas flame he finds Cu<sub>2</sub>O formed. But if it is heated at 400° C. in a furnace tube through which air is blown, the unknown pattern appears and he concludes that this is another crystalline form of cupric oxide (CuO'). It is apparently only formed as a surface film. Darbyshire<sup>3</sup> and Smith<sup>4</sup> also found Cu<sub>2</sub>O on a copper surface heated in a flame, the film being stripped off and examined by transmitted electrons. Miyake<sup>5</sup> confirms these results and finds that further heating of the unknown structure (CuO') transforms it into ordinary CuO (tenorite). Bronze, copper-nickel and copper-magnesium alloys give similar effects, but Miyake finds that with other alloys, such as brass, oxides of the alloying elements may be formed.

#### Oxides of Aluminium

Some experiments were made by Otty<sup>6</sup> at Aberdeen on aluminium oxide. He took a rectangular loop of copper wire, dipped it into molten aluminium and immediately withdrew it. This gave a film on the loop which contained transparent portions suitable for electron diffraction. The patterns obtained consisted of very diffuse rings. Better specimens were prepared

<sup>1</sup> Thomson, *Proc. Roy. Soc. A* 128, p. 641 (1930).

<sup>2</sup> Murison, *Phil. Mag.* 17, p. 96 (1934).

<sup>3</sup> Darbyshire, *Trans. Farad. Soc.* 27, p. 675 (1931).

<sup>4</sup> Smith, *J. Am. Chem. Soc.* 58, p. 173 (1936).

<sup>5</sup> Miyake, *Sci. Pap. Inst. Phys. Chem. Res. Tokyo*, 29, p. 167 (1936).

<sup>6</sup> Otty, unpublished observations made in 1929.

by stripping the naturally occurring oxide film from a piece of aluminium foil, using Sutton's method (etching away the aluminium with HCl gas). The patterns showed two diffuse rings which might possibly have arisen by a broadening of the rings to be expected from the X-ray structure of  $\gamma$ -Al<sub>2</sub>O<sub>3</sub>. It is evident therefore that the oxide consisted of very small crystal grains, which might explain the protective nature of the oxide coating.

Steinheil<sup>1</sup> also used a 'stripping' method and obtained transmission patterns of aluminium oxides. He states that at room temperature the oxide formed is a cubic face-centred structure which he names  $\epsilon$ -Al<sub>2</sub>O<sub>3</sub> (lattice constant  $a = 5.35$  Å). When the oxide is produced by holding aluminium leaf in a small flame it conforms to the X-ray structure of  $\gamma$ -Al<sub>2</sub>O<sub>3</sub> (face-centred cubic,  $a = 7.90$  Å), the agreement being fairly good. (He finds  $a = 7.77$  Å.) Belwe<sup>2</sup> also obtained in this way  $\gamma$ -Al<sub>2</sub>O<sub>3</sub> (with  $a = 7.73$  Å). When the oxide is formed by anodic oxidation, the crystal grains are very small and indeed by reflection Belwe gets no pattern at all, but only by transmission. Preston and Bircumshaw<sup>3</sup> found a so-called 'amorphous' film on aluminium giving a pattern of two diffuse rings, but at high temperatures  $\gamma$ -Al<sub>2</sub>O<sub>3</sub> of normal grain size was obtained. The film on molten aluminium is also  $\gamma$ -Al<sub>2</sub>O<sub>3</sub>.<sup>4</sup> Beeching<sup>5</sup> obtained patterns from thin aluminium films on glass which indicated the presence of a form of  $\gamma$ -Al<sub>2</sub>O<sub>3</sub> (face-centred cubic,  $a = 7.82$  Å); on heating to 250° C. the structure 'contracted', giving  $a = 5.53$  Å.

### Oxides and Hydroxides of Iron

Using the reflection method, Cates<sup>6</sup> examined rust on iron and steel and identified it as  $\gamma$ -FeOOH, with the crystal structure of the mineral form Rubinglimmer. On heating, the rust changed to  $\gamma$ -Fe<sub>2</sub>O<sub>3</sub> (the magnetic form of this oxide).

<sup>1</sup> Steinheil, *Ann. d. Phys.* 19, p. 465 (1934).

<sup>2</sup> Belwe, *Zeit. für Phys.* 100, p. 192 (1936).

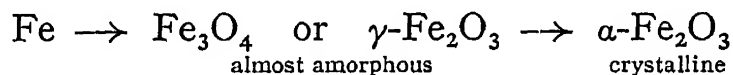
<sup>3</sup> Preston and Bircumshaw, *Phil. Mag.* 22, p. 654 (1936).

<sup>4</sup> Darbyshire and Cooper, *Trans. Farad. Soc.* 30, p. 1037 (1934).

<sup>5</sup> Beeching, *Phil. Mag.* 22, p. 938 (1936).

<sup>6</sup> Cates, *Trans. Farad. Soc.* 29, p. 817 (1933).

Smith<sup>1</sup> worked with the transmission method, 'stripping' when necessary by an electrolytic procedure. He found that a piece of polished iron, heated in air until interference colours showed, was covered with  $\text{Fe}_3\text{O}_4$ . The stripped film, on being heated to  $600^\circ\text{C}$ ., changed to  $\gamma\text{-Fe}_2\text{O}_3$ . He also studied the brownish film which forms on the surface of a solution of ferrous ammonium sulphate when exposed to ammonia. It proved to be  $\gamma\text{-FeOOH}$  and when heated changed to  $\gamma\text{-Fe}_2\text{O}_3$  as in Cates's observations. Nelson<sup>2</sup> examined the surface of iron which had been left exposed to air and found the pattern to agree with the structure of  $\text{Fe}_3\text{O}_4$  or  $\gamma\text{-Fe}_2\text{O}_3$  (they are difficult to distinguish). The process of oxidation of the surface of iron when heated appears to be rather complicated. By a careful study, using electron diffraction, Miyake<sup>3</sup> concludes that, *as far as the surface is concerned* the effect above  $250^\circ\text{C}$ . can be represented thus :



( $\alpha\text{-Fe}_2\text{O}_3$  is the non-magnetic  $\text{Fe}_2\text{O}_3$ ). The  $\alpha\text{-Fe}_2\text{O}_3$  only exists as a thin layer  $<0.002\text{ mm}$ . and underneath he finds crystalline  $\text{Fe}_3\text{O}_4$ . On heated stainless steels he obtains  $\text{FeCr}_2\text{O}_4$  co-existing with  $\text{Cr}_2\text{O}_3$  or with a solid solution of  $\text{Cr}_2\text{O}_3$  and  $\alpha\text{-Fe}_2\text{O}_3$ . According to some reflection experiments made by one of the authors,<sup>4</sup> the naturally occurring film on stainless steel is possibly  $\text{FeCr}_2\text{O}_4$  (cubic ;  $a = 8.1\text{ \AA}$ ). Iitake, Miyake and Imori<sup>5</sup> find that the film on iron passivated in dichromate is  $\gamma\text{-Fe}_2\text{O}_3$ . They stripped and examined the coating by transmission.

### Other Oxides

Various other metallic oxides have been investigated by electron diffraction and the oxides identified through the known X-ray structures of bulk materials. The particular oxide obtained (when several are possible) depends largely on the

<sup>1</sup> Smith, *J. Am. Chem. Soc.* 58, p. 173 (1936).

<sup>2</sup> Nelson, *J. Chem. Phys.* 5, p. 252 (1937).

<sup>3</sup> Miyake, *Sci. Pap. Inst. Phys. Chem. Res. Tokyo*, 31, p. 161 (1937).

<sup>4</sup> Thomson, unpublished observation.

<sup>5</sup> Iitake, Miyake and Imori, *Nature*, 139, p. 156 (1937).

method of preparation. Jenkins<sup>1</sup> has shown from reflection photographs that the scums on molten metals, Pb, Zn and Sn, are PbO (litharge), ZnO and SnO (tetragonal). The scum on molten bismuth could not be identified, there being no X-ray data on bismuth oxides. An interesting feature is that the scums consist of electron-optically flat crystals, resting on their (001) faces, and the inner potentials of the oxides can thus be determined. The structure of MgO, formed on exposing magnesium to the air, is found by Finch and Quarrell<sup>2</sup> to be hexagonal, whereas the normal MgO lattice is cubic, and here, as in the case of ZnO,<sup>3</sup> some kind of 'pseudomorphism' is suggested. In the case of nickel the only oxide which has been observed is NiO and agreement is found with the X-ray structure.<sup>4</sup>

Films of oxides can often be obtained by withdrawing a copper, tungsten, nickel or quartz loop from molten metal. Otty studied zinc oxide films in this way. He used a copper wire loop (1 cm.  $\times$  0.3 cm.), cleaned in HCl and dipped into ZnCl solution, which acts as a flux. The scum on the molten zinc was removed and the wire loop dipped in and withdrawn. The diffraction patterns indicated that the oxide had the usual X-ray structure of ZnO (hexagonal) with the micro-crystals oriented so that their *c* axes were normal to the plane of the film. In this way, too, Darbyshire and Cooper<sup>5</sup> were able to study (amongst other oxides) the oxide of bismuth (Bi<sub>2</sub>O<sub>3</sub>). Two distinct patterns were obtained on different occasions. The pattern usually occurring was extremely complicated and represented a body-centred tetragonal lattice having  $a = 10.85 \text{ \AA}$ ,  $c = 11.28 \text{ \AA}$ . In a few cases, however, the pattern corresponded to a face-centred *cubic* lattice with  $a = 5.43 \text{ \AA}$ . This latter value is related in the expected way to the known structure of Y<sub>2</sub>O<sub>3</sub>.<sup>6</sup>

Hopkins,<sup>7</sup> using the reflection method, examined protective coatings on the surface of magnesium and magnesium alloys.

<sup>1</sup> Jenkins, *Proc. Phys. Soc.* 47, p. 109 (1935).

<sup>2</sup> Finch and Quarrell, *Proc. Phys. Soc.* 46, p. 148 (1934).

<sup>3</sup> Cf. p. 175.

<sup>4</sup> Davisson and Germer, *Phys. Rev.* 40, p. 124 (1932); Smith, *l.c.*; Darbyshire, *l.c.*; Preston, *Phil. Mag.* 17, p. 466 (1934).

<sup>5</sup> Darbyshire and Cooper, *Trans. Farad. Soc.* 30, p. 1037 (1934).

<sup>6</sup> Jenkins, however (*l.c.*), deduces a different structure for bismuth oxide.

<sup>7</sup> Hopkins, *J. Inst. of Metals*, 57, p. 227 (1935).

These protective films had been formed by boiling in a solution of dichromate or similar oxidising substances. The coating could not be identified but it was noticed that the diffraction rings were very diffuse, indicating small crystal grains and, as in other cases, it was suggested that perhaps the protective quality was attributable to this fact.

### Growth of Oxide Layers

Although the identification of oxide coatings and films by electron diffraction is of great interest, the method of investigation goes further than this, since it enables us to determine how

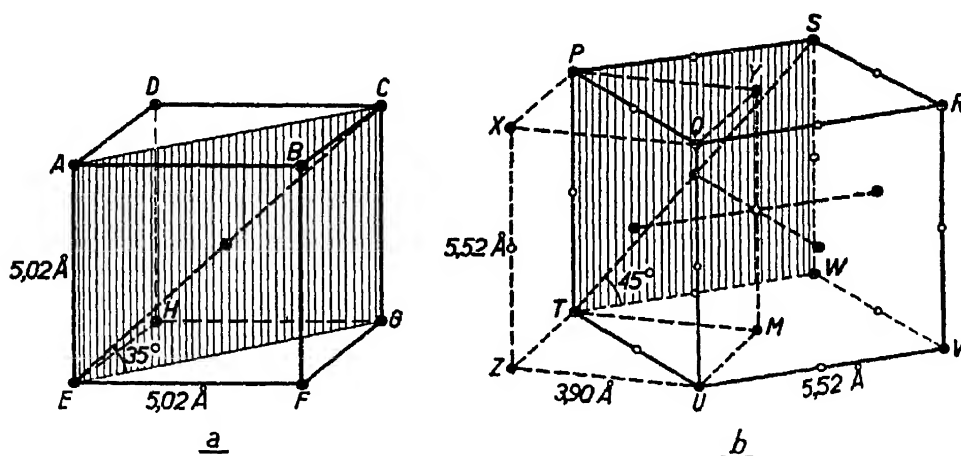


FIG. 56

the oxide lattice grows on the metal lattice. One of the authors<sup>1</sup> investigated the oxide on a copper single crystal from this point of view and found that the oxide layer was also oriented as a single crystal in such a way that the Cu atoms in the oxide lattice are similarly placed to those in the copper lattice but further apart. However, Yamaguti,<sup>2</sup> who heated a copper crystal up to a very high temperature (1000° C.), found two other types of orientation of the oxide lattice on the copper.

Burgers and van Amstel<sup>3</sup> investigated the formation of barium oxide on barium. The formation of the oxide is shown to occur through an expansion of the barium (body-centred cubic) lattice (a) into a tetragonal lattice (b) in which the oxygen atoms (represented by circles in Fig. 56) are placed.

<sup>1</sup> Thomson, *Proc. Roy. Soc. A* 133, p. 1 (1931).

<sup>2</sup> Yamaguti, *Proc. Phys.-Math. Soc. Jap.* 20, p. 230 (1938).

<sup>3</sup> Burgers and van Amstel, *Physica*, 3, p. 1057 (1936).

The tetragonal lattice XPYQUZTM is also equivalent to a new cubic lattice PSRQUTWV (see Fig. 56). Using X-rays, Mehl, M'Candless and Rhines<sup>1</sup> had found a similar type of growth for iron oxide FeO on iron. Nelson<sup>2</sup> also studied iron oxide. Using electron diffraction he showed that the oxide film formed on iron at room temperature in dry air is  $\text{Fe}_3\text{O}_4$  and grows so that the  $(\sqrt{2}, 1, 0)$  direction in the oxide is parallel to the (111) direction in iron. This does not completely define the orientation. It is, however, consistent with the view that the (cubic)  $\text{Fe}_3\text{O}_4$  is oriented on the iron lattice in the same way as (cubic) FeO orients on iron.

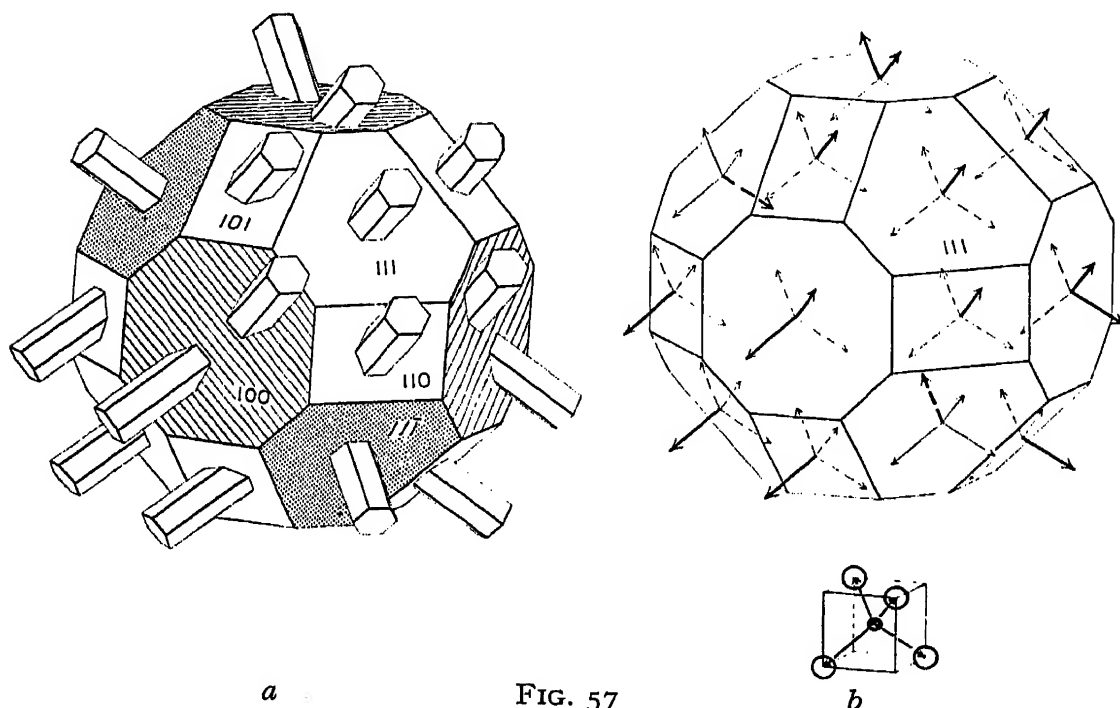


FIG. 57

Yamaguti<sup>3</sup> and Aminoff and Broomé<sup>4</sup> investigated the formation of ZnO on zinc blende and Miyake<sup>5</sup> investigated antimony oxides on stibnite. In these cases single crystal orientation of the oxide was observed.

The formation of the (hexagonal) zinc oxide on various faces of the zinc blende (cubic) is illustrated in Fig. 57 *a* taken from Aminoff and Broomé's paper. In the blende each zinc ion is surrounded by four tetrahedrally placed sulphur ions.

<sup>1</sup> Mehl, M'Candless and Rhines, *Nature*, 134, p. 1009 (1934).

<sup>2</sup> Nelson, *J. Chem. Phys.* 5, p. 252 (1937).

<sup>3</sup> Yamaguti, *Proc. Phys.-Math. Soc. Jap.* 17, p. 443 (1935).

<sup>4</sup> Aminoff and Broomé, *Kungl. Svenska Vetensk. Hand.* vol. 16 (1938).

<sup>5</sup> Miyake, *Sci. Pap. Inst. Phys. Chem. Res. Tokyo*, 34, p. 565 (1938).

The S ions round a zinc are first replaced by oxygen ions and the oxide crystal then grows as a hexagonal lattice, the  $c$  axis of the latter being normal to a tetrahedral face and the other axes being tetrahedral edges (Fig. 58). The distance Zn–O has also to be 16 per cent less than Zn–S. Fig. 57 *b* shows the

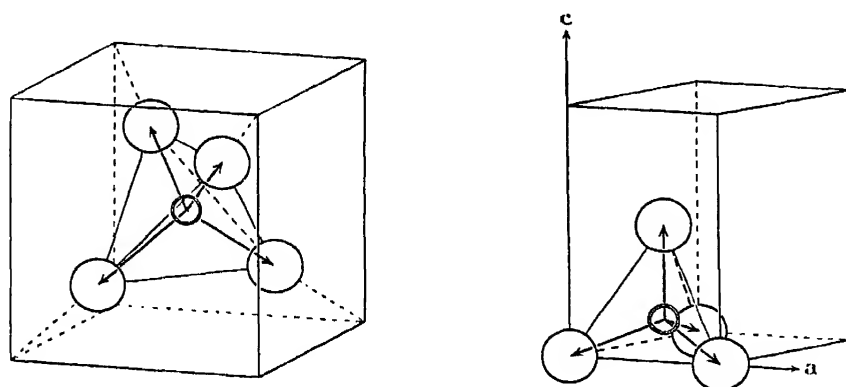


FIG. 58

directions of the three  $\text{Zn} \rightarrow \text{S}$  vectors on various faces of the blende and should be compared with Fig. 57 *a*.

The growth of  $\text{Sb}_2\text{O}_3$  on stibnite ( $\text{Sb}_2\text{S}_3$ ), according to Miyake, is illustrated in Fig. 59. It is seen that the lattice points of the oxide fit almost exactly on to those of the stibnite if we confine ourselves to a few unit cells. Actually there is a

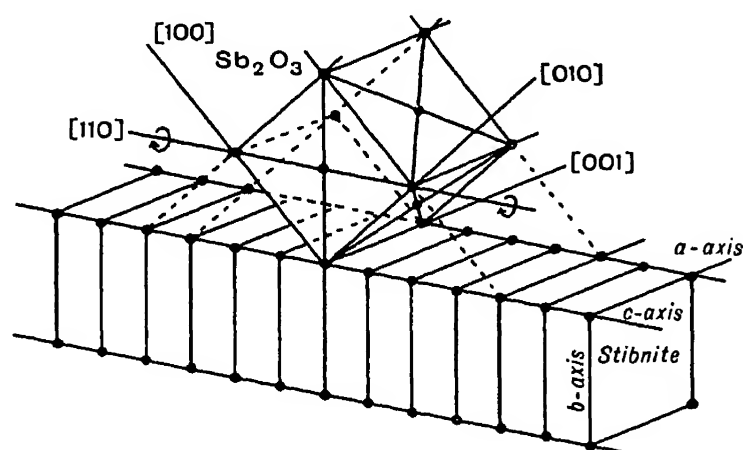


FIG. 59

difference of about 1 per cent between the cube edge of the oxide and the  $a$  axis of the stibnite. This should be compared with the discussion on p. 174 regarding Brück's laws.

While more results are desirable, especially from single crystals, before general conclusions may be drawn, the influence of the metal lattice in determining the orientation of the oxide

lattice is clearly demonstrated. In this connection, too, the observations of Jenkins<sup>1</sup> are of interest. While on molten metal (lead for example) the oxide grains are oriented with (001) planes parallel to the surface but otherwise at random, yet, on cooling slowly, the metal underneath solidifies as a large crystal and the oxide grains are pulled about so that they now orient on the solid metal as a single crystal.

It may be noted that the oxide films, obtained by withdrawing loops or gauzes from the molten metal, are often oriented as a fibrous structure. This affects the intensities of the diffraction rings, and may cause some to be missing altogether, so that care has to be taken in determining the crystal structure. Probably some such effect was present in Bragg and Darbyshire's films of zinc oxide<sup>2</sup> which appeared not to have the normal lattice structure. This fibrous type of orientation may also occur in surface layers of oxides and in general does not indicate any special connection with the underlying metal lattice, being rather a characteristic of the oxide itself.

<sup>1</sup> Jenkins, *l.c.*

<sup>2</sup> Bragg and Darbyshire, *Trans. Farad. Soc.* 28, p. 522 (1932).

## CHAPTER XIII

### POLISH

*General.*—It is an everyday experience that many surfaces — especially metallic ones — acquire a uniform, mirror-like appearance when they are rubbed with a suitably chosen, fine-grained powder. The polishing powder is usually mixed with water or other liquid and applied on a cloth pad ; but sometimes a good polished surface can be achieved using dry chamois leather or thick-piled cloth alone, provided the rubbing is continued for a sufficiently long time. Newton <sup>1</sup> believed that such polishing action merely consisted in levelling the surface by removing projections and this view was probably fairly general, until the end of last century. Rayleigh,<sup>2</sup> however, pointed out that grinding action seemed different from polishing. Beilby <sup>3</sup> also began to form a new hypothesis based on microscopical observations and his final conclusions were presented in 1921.<sup>4</sup> According to Beilby, polishing causes the surface material to flow, and the resulting polished surface is a glass-like amorphous layer — often referred to now as the Beilby layer. In this layer the atoms or molecules are arranged like those of a liquid. Beilby's ideas did not, however, gain general acceptance amongst metallographers and further investigation seemed desirable, using other methods.

In 1928 Knauer and Stern <sup>5</sup> studied the variation in reflecting power of polished surfaces (glass, steel and speculum) for molecular rays ( $H_2$  and He). They only found appreciable specular reflexion when the incidence was nearly grazing — at a glancing angle of more than  $10^{-3}$  radians the reflection was negligible. From this fact and the de Broglie wave-length of the rays ( $\sim 1 \text{ \AA}$ ) they deduced that the polished surfaces were

<sup>1</sup> Newton, *Opticks*; also Hooke, *Micrographia Obs.* II, 'Of the edge of a razor'.

<sup>2</sup> Rayleigh, *Nature*, 64, p. 385.

<sup>3</sup> Beilby, *Rep. Brit. Ass.* p. 604 (1901).

<sup>4</sup> Beilby, *Aggregation and Flow of Solids*. London: Macmillan.

<sup>5</sup> Knauer and Stern, *Zeit. für Phys.* 53, p. 779 (1929).

by no means plane but subject to an unevenness of 100–1000 Å. These molecular ray results yield no information as to the arrangement of the atoms in the surface. For the direct study of the actual atomic arrangement in the polish layer electron diffraction is, at present, the only method available, since X-rays are unsuitable owing to the thinness of the layer and the great penetrating power of these rays. The electrons do not penetrate more than about 500 Å into a solid before being inelastically scattered and so, by allowing the beam to fall on the polished surface at a small angle, the diffraction pattern will be formed only by atoms near the surface. Although Beilby did not consider that any distinction was to be drawn between the polish layer on metals and that on non-metals, electron diffraction results have shown that the two may be quite different in character. It will be convenient, therefore, to deal separately with polish on metals and on non-metals.

### Polish on Metals

Using the electron diffraction camera, French<sup>1</sup> examined the polish layer on copper, silver, chromium and gold. He found in each case a pattern of two diffuse haloes (Plate VIII *a*). The unpolished metal gave a pattern of sharp rings<sup>2</sup> and, as was shown by examination at different stages of polishing, these gradually became diffuse and finally yielded the characteristic polish pattern. There are two immediately obvious interpretations of the halo pattern. Since the effect of small grain size is to cause the rings to be broadened it may be supposed that the polish layer consists of very small grains. This view is, to some extent, supported by the actual radii of the haloes, when one takes into account the radii and intensities of the sharp rings in the normal polycrystalline patterns. For copper, however, the first halo is too small. An alternative interpretation is that the atoms are not arranged as in a lattice but are simply packed together as in a liquid with a limiting distance of approach,  $s_0$ , which is taken to be the same as in the crystalline state. The pattern to be expected from such a structure is

<sup>1</sup> French, *Proc. Roy. Soc. A*140, p. 637 (1933).

<sup>2</sup> Spots in the case of chromium, which had large crystal grains.

given approximately by the Wierl<sup>1</sup> formula (cf. p. 250) :

$$I = 2E^2 \left( 1 + \frac{\sin \chi}{\chi} \right),$$

where  $I$  = intensity of diffracted electrons in a direction  $\phi$ ,

$E$  = atomic scattering factor,

and  $\chi = 4\pi s_0 \frac{\sin \phi/2}{\lambda}$ .

If  $E$  is constant broad maxima occur when  $\chi = 7.725, 14.066$ , etc. From the radii of the haloes, and using the above formula, French calculates  $s_0$  and finds fair agreement with the value of  $s_0$  in the crystalline state as given by X-rays, except in the case of iron and silver. The procedure usually adopted, however, is first to calculate the Bragg spacings corresponding to the radii of the haloes. The spacing  $d$  is defined by the equation  $d = \lambda/2 \sin (\phi/2)$ , and therefore

$$d = \frac{2\pi s_0}{\chi}.$$

Substituting the above values of  $\chi$ , we find for the first and second haloes,  $d_1 = 0.81 s_0$  and  $d_2 = 0.45 s_0$ . The effect of allowing for  $E$  is to alter these values to  $0.89 s_0$  and  $0.48 s_0$ ,<sup>2</sup> but when visual observations are made on the plates it is problematical whether there is any necessity to make allowance for  $E$  (cf. p. 252). In preference to the Ehrenfest gas formula, the Prins formula for the scattering by a monatomic close-packed liquid should really be used.<sup>3</sup> Again neglecting  $E$  one gets from the Prins curve  $d_1 = 0.79 s_0$  and  $d_2 = 0.44 s_0$ . These more exact expressions only differ slightly, however, from the Ehrenfest values.

The two views — small grain size and liquid-like packing — are extremely difficult to distinguish. If  $E$  is assumed constant, it is easy to show that, for body-centred and face-centred cubic metals, the first diffuse ring given by the Wierl formula is practically of the same radius as the first ring in the normal polycrystalline pattern. This latter is always a very strong ring, and, when broadening occurs, will be the main contributor

<sup>1</sup> Actually this formula was originally given by Ehrenfest.

<sup>2</sup> Cf. Darbyshire and Dixit, *Phil. Mag.* 18, p. 961 (1933).

<sup>3</sup> Cf. Raether, *Zeit. für Phys.* 86, p. 82 (1933).

to the first diffuse halo. Similar considerations may be applied to the second halo. It appears to us that the distinction between the two views is not very important. In a liquid the inter-atomic forces are still fairly appreciable and the atoms will tend to congregate into small groups each of which resembles a small crystal grain. These groups will disperse and reform as time proceeds, but, at any instant, such a liquid will not differ essentially from a conglomerate of small crystal grains.

French also showed that the haloes were circular and therefore there was no effect due to refraction. As is explained on p. 110, refraction comes into play when the electrons enter and leave a surface at a small angle and causes the rings to be U-shaped. The polished surface of a metal must therefore have at least a few small projections through which the electrons pass. This agrees with Knauer and Stern's results.

Raether,<sup>1</sup> working independently, obtained similar patterns to French, using polished surfaces of iron, copper, nickel, silver, gold, and cadmium. He showed that the results did not depend on the polishing material, and that burnishing gave the same effect as polishing. The haloes from copper, iron and nickel were too small to agree quite satisfactorily with either theory.<sup>2</sup> Other investigations have been made by Miwa<sup>3</sup> and Darbyshire and Dixit.<sup>4</sup> The latter show that bismuth and antimony, which are not close-packed in the crystalline state, give a halo pattern when polished whose dimensions indicate a close-packing arrangement in the polish layer. This may be said to be evidence in favour of the liquid-like view. The Bragg spacings of the two polish halves are as follows:—<sup>5</sup>

Bi	Sb	Zn	Te	Cd	Au	Ag	Pb	Mo	Cu	Cr
2.24	2.25	2.40	2.30	2.37	2.34	2.27	2.40	2.38	2.28	2.24 Å
1.25	1.24	1.28	1.25	1.28	1.29	1.23	1.31	1.27	1.26	1.23 Å

The thickness of the polish layer on gold has been investigated by Hopkins<sup>5</sup> who showed that the pattern of two haloes persisted as the gold was spluttered off from the specimen to a depth of about 10 Å. When more material was removed further diffuse rings of larger diameter appeared which were

<sup>1</sup> Raether, *l.c.*

<sup>2</sup> Cf. Dobinski, *Phil. Mag.* 23, p. 397 (1937).

<sup>3</sup> Miwa, *Sc. Rep. Tohoku Imp. Univ.* 24, p. 222 (1935).

<sup>4</sup> Darbyshire and Dixit, *l.c.*

<sup>5</sup> Hopkins, *Trans. Farad. Soc.* 31, p. 1095 (1935).

finally resolved into the sharp ring pattern. Hopkins came to the conclusion that the polish layer is about  $20 \text{ \AA}$  thick, although the crystallites are considerably broken up and disturbed beyond this depth; the normal grain size and random orientation is not attained until a depth of  $500 \text{ \AA}$ . Lees<sup>1</sup> obtained very similar results with copper.

Although all the writers mentioned above have deduced some kind of 'amorphous' structure for the polish layer on metals, there is, nevertheless, another interpretation of the halo pattern which demands consideration. After the preliminary

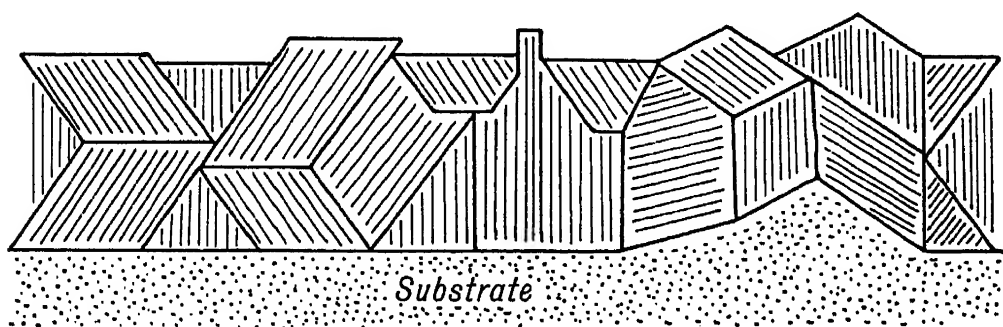


FIG. 60.

account of French's results had appeared, Kirchner<sup>2</sup> suggested that polishing might simply cause the surface to be levelled and that the electrons therefore pass through extremely small projections only a few atoms high. Since the number of scattering centres in such projections is small, the effect is the same as if one were dealing with very small crystallites and the rings of the normal pattern are broadened, resulting in haloes. In support of his view, he was able to produce experimental evidence that halo patterns could, in fact, arise from non-amorphous metal.<sup>3</sup> This Kirchner effect was obtained by evaporating gold on to a thin celluloid base so as to form a film about  $100 \text{ \AA}$  thick. When this was examined by 'reflected' electrons at almost grazing incidence it yielded a pattern of two diffuse rings similar to the 'polish' pattern. When transmitted electrons were used a sharp ring pattern was found, characteristic of polycrystalline metal of normal grain size. Clearly this was an instance where the projections on the

<sup>1</sup> Lees, *Trans. Farad. Soc.* 31, p. 1102.

<sup>2</sup> Kirchner, *Nature*, 129, p. 545 (1932).

<sup>3</sup> Kirchner, *Ergebnisse d. ex. Naturwiss.* 11, p. 112 (1932).

surface must have been extremely minute, as illustrated in Fig. 60, causing broadening of the rings in the reflection case. For, in transmission, the size of the projections has no effect, and the sharpness of the rings showed that the metal had the ordinary grain structure. Further results of this kind have been given by Papsdorf.<sup>1</sup>

An attempt has been made by one of the authors<sup>2</sup> to decide between French's and Kirchner's views as to the nature of the polish on metals. Gold and chromium were used. A thin layer of the metal was deposited on to a nickel base and polished. Dilute nitric acid (which does not attack gold and chromium) was employed to free the polished metallic film from the nickel. This procedure was most successful in the case of gold, and a transmission pattern was obtained from the film, showing three diffuse rings, the two inner ones being the usual polish haloes (Plate VIII *b*).<sup>3</sup> It is evident therefore that the film was made up of very small crystal grains. The fact that three diffuse rings were found agrees with Hopkins' results, for the film was approximately 200–300 Å thick and Hopkins showed that, beyond 20 Å thickness, further diffuse rings appear.

After the polished gold film had been stripped from its base for about 15 hours the pattern had completely changed, and showed sharp rings indicating normal grain size. Evidently crystal growth had taken place, possibly aided by some straining in the film owing to the manner of mounting. When an ordinary polished specimen was left for several days at room temperature, no change appeared in the diffraction pattern. However, Bruce<sup>4</sup> has shown that when a polished gold block is heated for 1 hour at 280° C. crystal growth occurs in the polish layer and the polish pattern disappears. At lower temperatures no change occurred.

The transmission method of investigation also shows that the polish pattern cannot be produced by a blurring of the sharp rings, caused by refraction. This possibility had been suggested by Germer,<sup>5</sup> but in transmission experiments no such effect can arise.

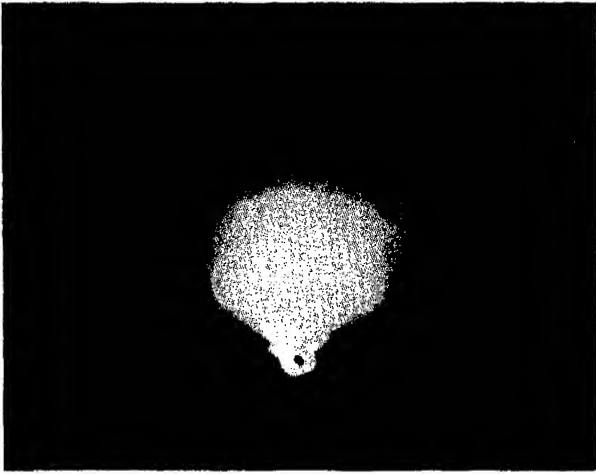
<sup>1</sup> Papsdorf, *Ann. d. Phys.* 28, p. 555 (1937).

<sup>2</sup> Cochrane, *Proc. Roy. Soc.* 166, p. 228 (1938); cf. also Plessing, *Phys. Zeit.* 39, p. 618 (1938).

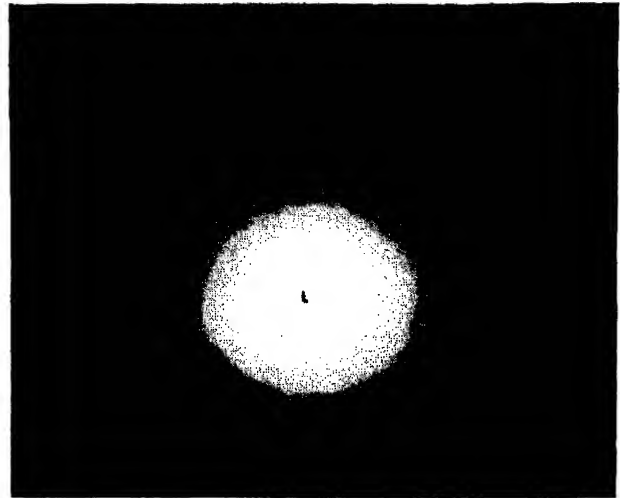
<sup>3</sup> From chromium the rings were not quite so diffuse.

<sup>4</sup> Bruce, unpublished observation. <sup>5</sup> Germer, *Phys. Rev.* 43, p. 724 (1933).

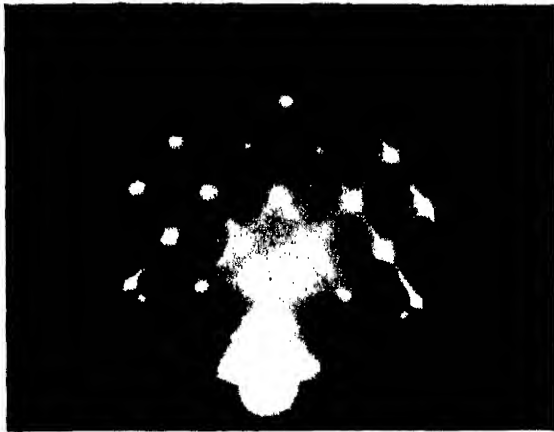
PLATE VIII



(a) Polished gold, reflection



(b) Polished gold, transmission



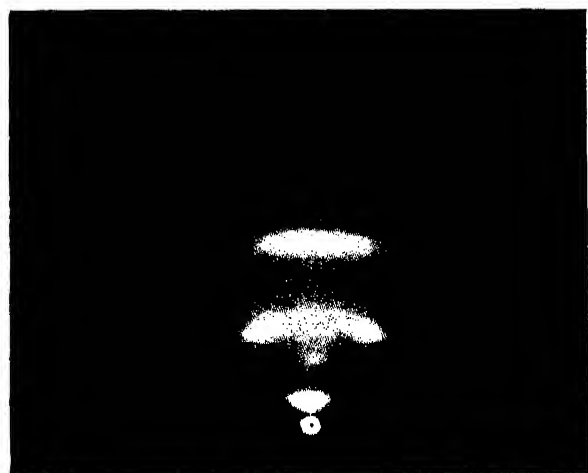
(c) Nickel deposit on copper crystal,  
(110) face, beam parallel to cube-face  
diagonal



(d) Lard. (*Murison*)



(e) Vaseline. (*Murison*)



(f) Stearic acid. (*Murison*)



To summarise, it may be said that a 'reflection' electron diffraction pattern taken from a polished metal surface shows two diffuse circular rings or haloes. The transmission experiments which have been made indicate that these haloes do in fact arise from the atomic arrangement in the polish layer. The polished surface is not perfectly flat and there are at least a few projections on the surface, through which the electrons pass in a 'reflection' experiment. It is deduced that the atoms in the polish layer occupy the positions which they would have, at any instant, in the liquid state. The polish layer extends, in the case of gold and copper, to a depth of about 20 Å. Beyond this larger and larger crystallites are found, until, at a depth of a few hundred Ångstroms, normal grain size is reached.

In addition to the investigations which we have described, other methods have been used to study the polish layer on metals. These cannot be discussed in any detail here. Mention must be made, however, of the work of Finch, Quarrell and Roebuck,<sup>1</sup> who found, using electron diffraction, that zinc atoms dissolved in the polish layer on copper but not on an etched copper surface so that the layer possesses one of the properties of a liquid. Bowden showed that melting may occur locally during polishing<sup>2</sup> and that the polishing material must have a higher melting point than the object to be polished;<sup>3</sup> Recently Moore<sup>4</sup> has examined, by electron diffraction, the surface of copper which had undergone the so-called 'anodic polishing' treatment. His results showed that such a surface was, in fact, covered with polycrystalline cuprous oxide.

### Polish on Non-Metals

There are not many polycrystalline non-metallic substances which can be polished. Raether<sup>5</sup> obtained the usual halo pattern from polycrystalline haematite ( $\text{Fe}_2\text{O}_3$ ) and Darbyshire and Dixit<sup>6</sup> found a similar result with silicon and selenium.

Much more interest attaches to the polishing of single

<sup>1</sup> Finch, Quarrell and Roebuck, *Proc. Roy. Soc.* 145, p. 676 (1934).

<sup>2</sup> Bowden and Ridler, *Proc. Roy. Soc.* 154, p. 640 (1936).

<sup>3</sup> Bowden and Hughes, *Nature*, 139, p. 152 (1937).

<sup>4</sup> Moore, *Ann. d. Phys.* 33, p. 133 (1938).

<sup>5</sup> Raether, *l.c.*

<sup>6</sup> Darbyshire and Dixit, *l.c.*

crystals such as calcite, etc. The first electron diffraction experiments on such surfaces were performed by Raether.<sup>1</sup> He began with a cleavage face of rock-salt which was ground with emery. This gave a pattern of fairly sharp rings characteristic of polycrystalline material, the grinding having the effect of breaking up the surface into small crystals. On polishing and again examining in the electron camera, he found that the rings were replaced by arcs, indicating that the crystallites had been oriented, so as to have a 'fibre-structure'. No halo patterns were obtained. With a calcite cleavage face, Raether obtained quite a different polish pattern, consisting of an array of rather large spots, somewhat similar to the 'cross-grating' pattern from an etched single crystal (p. 141). The spots were not, however, regularly arranged as in a cross-grating but showed displacements due to the effect of inner potential causing refraction. It was thus deduced that the polished surface was made up of blocks of crystal arranged nearly in conformity with the underlying crystal, but slightly tilted to angles of a few degrees from the exact position of alignment with the main crystal. Unlike the case of the etched crystal, the electrons in this case enter and leave through the same plane surface and the Bragg condition is more or less satisfied as in reflection from cleavage planes (p. 146). Owing to the varying tilts, however, an extended array of spots is found. The same author also tried polished fluorspar. Some parts of the surface gave the fibre-pattern as obtained with rock-salt; other parts yielded the spot pattern like calcite.

It is suggested by Raether that the initial grinding causes the formation of a rather loosely-bound dust of small crystals on the surface of the crystal. The polishing action has the effect of dragging these crystallites about until, in the case of calcite, they orient themselves so as to continue the main crystal structure. In rock-salt, however, this stage is never reached and only a fibre-structure is found. Fluorspar forms an intermediate case.

Later Darbyshire and Dixit<sup>2</sup> studied galena and iron pyrites cleavage faces. When galena was ground with emery it gave a pattern of fairly sharp rings which became diffuse when the surface was polished. On continuing the polishing

<sup>1</sup> Raether, *l.c.*

<sup>2</sup> Darbyshire and Dixit, *Phil. Mag.* 18, p. 133 (1933).

the rings sharpened up again and the cycle repeated itself. With pyrites, even after prolonged polishing, the single crystal pattern of spots still persisted along with diffuse rings.<sup>1</sup> The authors do not state whether these spots showed any effect of refractive index. They are of the opinion that in these cases the main effect of polishing is the detachment of small pieces of crystal which are subsequently rubbed away.

Further work on calcite cleavage faces has been done by Hopkins.<sup>2</sup> He confirmed Raether's results and proceeded to find the thickness of the distorted layer on the polished surface. After etching away the material to a depth of 200 Å, Kikuchi lines appeared, so that this may be taken as the thickness of the layer. But even at 6000 Å the polishing action must have had some effect, for the patterns at this depth showed spots due to twinned lattices. There is an apparent decrease in inner potential as the material is removed, but Hopkins shows that this arises from the way in which the etching action proceeds, and does not refer to any real change in the lattice.

Finch<sup>3</sup> has also studied the polish on calcite. As well as taking electron diffraction patterns from the polished cleavage faces with the same results as Raether, he examined faces which had been cut at different angles to the cleavage. A polished face which makes large angles with the cleavage planes shows a halo pattern and one making a smaller angle with a cleavage gives a pattern of haloes superimposed on a spot pattern. After heating for two hours at 500°, all the polished faces showed spot patterns. It is well known that sodium nitrate crystals deposited from a solution on a calcite cleavage face, orient themselves in a regular array. Finch and Whitmore<sup>4</sup> have shown that they also do this on a polished calcite cleavage face, but not on other polished faces. The crystalline and non-crystalline nature of these types of surfaces as revealed by electron diffraction is thus confirmed in a striking way.

In addition to calcite, Finch and Wilman<sup>5</sup> have taken

<sup>1</sup> Raether (*l.c.*) could not obtain any pattern from finely ground pyrites.

<sup>2</sup> Hopkins, *Phil. Mag.* 21, p. 820 (1936).

<sup>3</sup> Finch, *Trans. Farad. Soc.* 33, p. 425 (1937).

<sup>4</sup> Finch and Whitmore, *Trans. Farad. Soc.* 34, p. 640 (1938).

<sup>5</sup> Finch and Wilman, *Nature*, 138, p. 1010 (1936); also *Science Progress*, 31, p. 609 (1937), where an application of these results to aeroplane engines is suggested.

electron diffraction patterns from polished faces of many single crystals, the faces having been cut in arbitrary directions. Three main types of pattern arise : quartz, diamond, sapphires, garnets, topaz, chrysoberyl, epidote, olivine, sphene and andalusite give spot patterns ; white beryl, zircon, tourmaline and cassiterite give halo patterns ; and brown beryl, moonstone, orthoclase and cordierite give a composite pattern of both spots and haloes.

In contrast to Raether's view, Finch suggests that the polishing action results in the actual flow of the material over the surface in a liquid-like form. Usually, owing to the strong orienting effect of the underlying lattice, crystallisation takes place and a spot pattern is found when the surface is examined in the electron camera. But in some cases, as, for example, the steeply cut calcite surface, the orienting forces are not so strong and the polish layer is amorphous. The theory that polishing causes small crystallites to be dragged over the surface also requires the postulation of orienting forces to explain the re-formation of the surface. The fact that these forces are strongest on the *cleavage* plane of calcite is extremely interesting.

Germer<sup>1</sup> obtained a reflection pattern of diffuse rings from an unpolished face of a silicon carbide crystal. He put forward the view that this result threw doubt on the usual interpretation of the halo pattern, and considered that probably the pattern arose from an adsorbed gas layer on the surface. Finch and Wilman,<sup>2</sup> however, showed that silicon carbide crystals are actually covered with an amorphous skin of silica, produced by oxidation, and that, on removing this skin, the usual single crystal pattern of spots and lines is found.

To sum up, no simple statement can be made as to the crystal structure of the polish layer on single crystals of non-metals. In some cases the layer is liquid-like, in others polycrystalline with fibre structure and in others the layer is a single crystal (or a distorted single crystal) which continues the lattice of the underlayer. The latter type of structure appears to be the most common. The thickness of the layer on a polished calcite cleavage face is about 200 Å.

<sup>1</sup> Germer, *Phys. Rev.* 49, p. 163 (1936).

<sup>2</sup> Finch and Wilman, *Trans. Farad. Soc.* 33, p. 337 (1937).

### Structure of a Liquid Mercury Surface

Although liquid mercury has been examined by X-rays, it is interesting to find what kind of pattern is yielded from a mercury surface when electrons are incident on it at a small angle. The matter is appropriate to this chapter since it would be expected that a 'polish pattern' of diffuse haloes would be found. However, Raether,<sup>1</sup> Trillat<sup>2</sup> and Papsdorf<sup>3</sup> did not obtain any pattern at all but only diffuse background. On the other hand, Wierl<sup>4</sup> obtained sharp rings indicating a polycrystalline structure and crystalline patterns have also been found by Kakesita<sup>5</sup> and by Berdennikov and others.<sup>6</sup> In his *London University Thesis*, Jenkins gives a short account of some experiments on electron diffraction by mercury in which he obtained two diffuse haloes. The mercury was contained in a shallow glass dish 3.5 cm. in diameter, the bottom of which communicated with a barometer tube. A fresh surface was formed by overflowing the mercury. Often the patterns also showed a faint streak normal to the shadow edge and through the central spot, in addition to the haloes. Jenkins considered the possibility of refraction in interpreting these results. On varying the angle of incidence of the incident beam he found no change in the radii of the haloes, so that refraction was not taking place and the mercury surface was not electron-optically flat. The spacings deduced from the haloes (2.47 and 1.33 Å) were slightly lower than the X-ray values of Debye and Menke<sup>7</sup> which was attributed to the fact that the atoms are more closely packed near the surface as a result of the atomic forces on them being asymmetrical. Recently Bailey and others<sup>8</sup> have obtained an electron diffraction pattern from a mercury surface showing two diffuse rings with a streak, such as Jenkins sometimes found. It

<sup>1</sup> Raether, *Zeit. für Phys.* 86, p. 82 (1933).

<sup>2</sup> Trillat, *Trans. Farad. Soc.* 29, p. 995 (1933).

<sup>3</sup> Papsdorf, *Ann. d. Phys.* 28, p. 555 (1937).

<sup>4</sup> Wierl, *Verh. Deut. Phys. Ges.* 11, p. 29 (1930).

<sup>5</sup> Kakesita, *Mem. Coll. Sci. Kyoto*, 17, p. 241 (1934).

<sup>6</sup> Berdennikov, Bresler, Zelmanov and Strauff, *Jour. Phys. Chem. U.S.S.R.* 5, p. 584 (1934).

<sup>7</sup> Debye and Menke, *Phys. Zeit.* 31, p. 797 (1930); and 33, p. 593 (1932).

<sup>8</sup> Bailey, Fordham and Tyson, *Proc. Phys. Soc.* 50, p. 63 (1938).

should be mentioned that Raether<sup>1</sup> and Papsdorf<sup>2</sup> have also observed this streak which might be due to a surface reflection as explained on p. 146.

The sharp ring patterns which have been obtained by electron diffraction do not agree with one another as regards the radii of the rings and it is natural to suppose that they are due to surface films of foreign substances which readily form on mercury. Although the diffuse rings found by Jenkins and by Bailey and others agree roughly with the X-ray results, it is rather puzzling to find that there is no displacement due to refractive index, for one would expect that the surface would be very smooth. Jenkins also points out that the haloes observed are practically identical with those obtained from a thin layer of oil. The results which gave only diffuse blackening of the plate are easiest to understand, since any curvature at the edge of the surface would have a varying effect on the diameters of the rings and would cause a general blurring. This should not arise, however, with reasonably large surfaces. In view of these facts, we consider that the electron diffraction patterns which have been found by reflection from mercury surfaces are not of such a nature as to allow any very definite conclusions to be drawn.

<sup>1</sup> Raether, *l.c.*

<sup>2</sup> Papsdorf, *l.c.*

## CHAPTER XIV

### OILS, GREASES, ETC.; LUBRICATION

*General.*—The study of thin films of oils, greases and similar substances by electron diffraction is of interest because the results may be used to estimate roughly the efficiency of these films in lubrication. In addition, the work has the usual physical and chemical importance.

As regards lubrication, we are concerned here only with 'boundary' lubrication in which the metal bearing surfaces are pressed closely together, being separated by an extremely thin layer of oil. For this layer to be retained under the pressure, strong adhesive forces must exist between the ends of the oil molecules and the bearing surfaces. When the lubricant is spread thinly on a metal surface, such adhesion manifests itself as an orienting influence so that the molecules tend to stand up on end. These ideas are originally due to Hardy, Langmuir and others and reference may be made to Adam's book *The Physics and Chemistry of Surfaces* for a fuller discussion. Any orientation can, of course, be detected in the electron diffraction patterns.

To begin with, consider the nature of the lubricants usually employed in practice. The mineral oils obtained in various parts of the world are mixtures of hydrocarbons such as  $C_nH_{2n+2}$  (paraffins);  $C_nH_{2n}$ ; etc. These are long-chain compounds made up of the unit  $(CH_2)$ . Animal and vegetable oils are mixtures of the glycerol esters of fatty acids, *i.e.* of compounds such as tristearin, the glyceride of stearic acid. The latter acid has the formula  $CH_3[CH_2]_{16}COOH$ . Again we encounter the long chain of  $(CH_2)$  units with, of course, various groups at the ends of the chains. The greases used in engineering are mixtures of soaps with mineral oils, but rubber greases are often employed in the laboratory; in both cases, there are long chains of recurring  $(CH_2)$  groups.

Now Müller<sup>1</sup> has shown that this type of long chain has

<sup>1</sup> Müller, *Proc. Roy. Soc. A*120, p. 437 (1928).

a zig-zag structure PQRS . . . with all the carbon atoms in one plane. The distance between consecutive  $\text{CH}_2$  groups is  $1.90 \text{ \AA}$  and between alternate ones  $2.54 \text{ \AA}$  as illustrated (Fig. 61).<sup>1</sup>

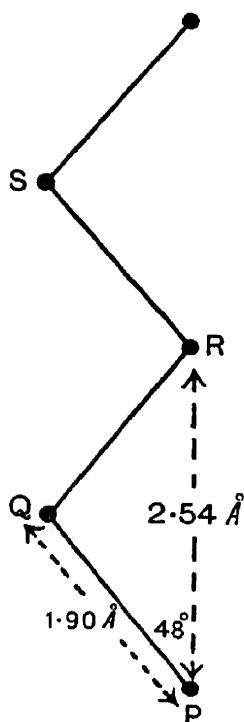


FIG. 61

### Early Transmission Experiments

Lebedeff<sup>2</sup> examined films of paraffins by electron diffraction and obtained sharp-ring patterns showing that the films were crystalline. A detailed study was made by Trillat and Hirsch<sup>3</sup> using both paraffin and stearic acid. The substances were dissolved in ether and a drop of the solution evaporated on water. In this way single crystals could be obtained giving sharp spot patterns. X-ray<sup>4</sup> work shows that the cell of a paraffin is orthorhombic, the height of the  $c$  axis depending on the length of the chain. Saturated fatty acids form a monoclinic cell (Fig. 62), of three different possible forms. The electron diffraction patterns confirmed these facts,

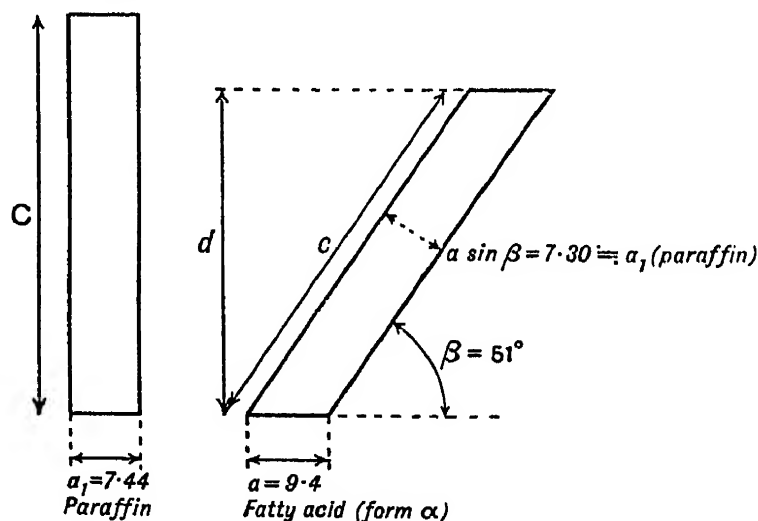


FIG. 62

the basal plane (001) being always parallel to the surface of the

<sup>1</sup> Müller considers the whole  $\text{CH}_2$  group to be replaced by a point scattering centre. Some authors, however, neglect the hydrogen atoms and consider only the carbon atoms. In this case the distance PQ (Fig. 61) becomes  $1.5 \text{ \AA}$ , but PR is unaltered.

<sup>2</sup> Lebedeff, *Nature*, 128, p. 491 (1931).

<sup>3</sup> Trillat and Hirsch, *J. de Phys. et le radium*, 4, p. 38 (1933).

<sup>4</sup> Cf. Trillat and Hirsch, *l.c.*

film. The results could not therefore give information regarding the length of the  $c$  axes of the crystals, but the lengths deduced for the other two axes agreed fairly well with the X-ray values. Garrido and Hengstenberg<sup>1</sup> had previously obtained similar results by electron diffraction from thin films of paraffin ( $C_{21}H_{44}$ ). They used the Kirchner method of forming the films on thin collodion sheets. The patterns found consisted of spots corresponding to indices ( $hko$ ) although in some cases the pattern apparently arose from a crystal structure with hexagonal symmetry. It was shown, however, that this was due to twinning occurring on the usual orthorhombic lattice. Prolonged exposure to the electron beam caused the film to melt and the patterns then showed six broad rings such as would arise from a liquid or gas.

### Murison's Reflection Experiments

The first experiments on long-chain organic compounds, using the 'reflection' of fast electrons, were made by Murison.<sup>2</sup> He formed thin films of oils, greases, waxes, etc., on metal blocks — spreading the oil or grease over the surface with a glass rod or tissue paper. Solid substances were prepared by heating the metal until the substance melted and then smoothing it, while still liquid, with a glass rod. His films varied in thickness from about 60 Å to 0.1 mm. From a consideration of the penetrating power of electrons it is clear that the patterns only gave information regarding the structure near the surface of the layer. However, by using a somewhat rough backing surface and smoothing out the substance well, one can be fairly sure that, in some parts at least, the film will only be a few molecules thick. Hence if any orientation due to the backing occurs, it will be present in the thin parts of the film and appear in the pattern, even although the orientation does not extend to the surface in the thicker parts of the film. If a thick film exhibits orientation, this may exist right through the film or else it may arise near the vacuum-oil interface. In

<sup>1</sup> Garrido and Hengstenberg, *Zeit. für Krist.* 82, p. 477 (1932).

<sup>2</sup> Murison, *Phil. Mag.* (7) 17, p. 201 (1934); Thomson and Murison, *Nature*, 131, p. 237 (1933).

the latter case one can safely assume that orientation will also be present at the metal-oil interface. We now discuss the different types of pattern found by Murison.

**TYPE I. SHARP RINGS.**—This pattern was only given by  $\alpha$ -bromostearic acid. It indicates that the substance was made up of crystal grains arranged at random. Apparently the orienting forces were weak compared with the forces of crystal-

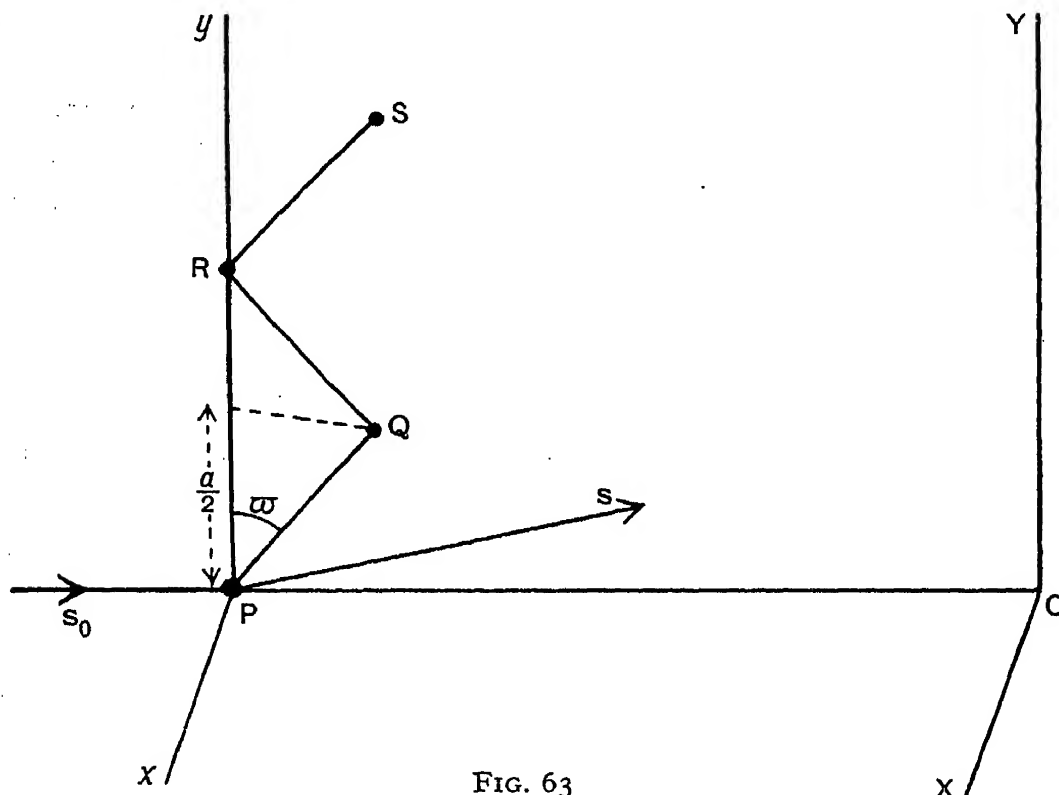


FIG. 63

lisation. It is indeed a rule that pure substances, which naturally tend to crystallise, are usually poor lubricants.

**TYPE II. TWO DIFFUSE RINGS.**—This two-halo pattern arose from light oils which had not been smoothed over the block with a glass rod or tissue paper and also, in a few cases, even when smoothed. The Bragg spacings corresponding to the diffuse rings were 2.55 and 1.39 Å and did not depend on the particular oil used. This pattern seemed to indicate a random distribution of molecules. Assuming a chain with eight  $\text{CH}_2$  groups, Murison therefore applied the Wierl formula for vapours (p. 250) to calculate theoretically what the pattern should be from such a random distribution. He finds that the agreement with the experimental result is good, so that

there is little doubt that the rings are formed in the way suggested.

TYPE III. STRAIGHT LINE PATTERN, given by tallow, lard, cetyl alcohol, and tripalmitin (Plate VIII *d*). To explain the origin of this pattern it must be supposed that the long-chain molecules are oriented normal to the backing surface, and it is readily seen that the lines (which are parallel to the shadow edge or specimen surface) arise from the periodic spacing of the carbon atoms along the normal to the surface.

Consider the scattering of a plane electronic wave of wavelength  $\lambda$  by a single zigzag molecule of scattering centres PQR . . . (Fig. 63) which may be considered to be carbon atoms.

Take PR as the  $y$  axis of rectangular coordinates and let  $Px$ ,  $Pz$  lie in the plane of the specimen surface, with  $Pz$  in the direction of the incident beam  $s_0$ , which we assume parallel to the specimen surface. Let the diffracted beam considered be  $s$  with direction cosines  $\alpha$ ,  $\beta$ ,  $\gamma$ .  $s_0$  and  $s$  are unit vectors. Let  $\angle QPR = \omega$ ,  $PR = a$  and the angle between the planes PQR,  $xPy$  be  $\phi$ . The path difference between the waves scattered by P and Q in the direction  $s$  is given by

$$(\mathbf{PQ}, \mathbf{s}) - (\mathbf{PQ}, \mathbf{s}_0).$$

Writing down the coordinates of Q and expanding the scalar products this gives

$$\frac{a}{2} \tan \omega \cdot \cos \phi \cdot \alpha + \frac{a}{2} \cdot \beta + \frac{a}{2} \tan \omega \cdot \sin \phi \cdot \gamma - \frac{a}{2} \tan \omega \cdot \sin \phi \cdot \gamma \\ \equiv U \text{ (say).}$$

Similarly, the path difference between waves scattered from P and R is

$$(\mathbf{PR}, \mathbf{s}) - (\mathbf{PR}, \mathbf{s}_0) = a\beta \\ \equiv V \text{ (say).}$$

Now, the wave scattered by each carbon atom depends on the direction  $s$ , because of the atomic scattering factor (p. 86). This is the same for all the atoms and is left out of account at present. To find the resultant amplitude in the direction  $s$  we sum the scattered waves from P, Q, R . . . allowing for

phase differences. If

$$K = \frac{2\pi}{\lambda}$$

we get

$$\begin{aligned} & I + e^{iKU} + e^{iKV} + e^{i(KV+U)} + e^{iK(2V)} + e^{iK(2V+U)} + \dots \\ & \equiv (I + e^{iKV} + e^{iK \cdot 2V} + \dots + e^{iKNV})(I + e^{iKU}) \end{aligned}$$

if there are  $2N+2$  atoms. We have supposed as usual that the screen where the effect is recorded is very far off. The resultant intensity  $I$  is found by taking the modulus and squaring :

$$I \propto \frac{\sin^2 \frac{NKV}{2}}{\sin^2 \frac{KV}{2}} (I + \cos KU). \quad (1)$$

The first factor in this expression gives the effect of the grating of spacing  $a$  formed by the alternate atoms P, R, . . . . If the screen is at O where  $PO=L$  and if OX, OY are parallel to  $Ox, Oy$  then the coordinates (X, Y) on the screen are given by

$$X = aL, Y = \beta L.$$

The first factor in (1) becomes

$$\frac{\sin^2 N\pi \frac{aY}{L\lambda}}{\sin^2 \pi \frac{aY}{L\lambda}},$$

and is a maximum where

$$\frac{aY}{L\lambda} = 0, 1, 2 \dots \text{etc.},$$

indicating lines of intensity on the screen parallel to the shadow edge. The second factor in (1) is a kind of 'structure factor' and modulates the intensity of the lines.

In order to illustrate the effect of this factor we consider two cases.

(a) Suppose  $\phi = 0$ , i.e. the plane of the chain is normal to the incident beam. Then

$$U = \frac{a \tan \omega}{2L} \cdot X + \frac{a}{2L} \cdot Y.$$

Along a line of intensity,

$$\frac{aY}{L\lambda} = n; \quad n = 0, 1, 2 \dots \text{etc.}$$

Hence

$$\begin{aligned} 1 + \cos KU &= 1 + \cos \left( n\pi + \frac{\pi a \tan \omega \cdot X}{L\lambda} \right) \\ &= 1 \pm \cos \frac{\pi a \tan \omega \cdot X}{L\lambda}, \end{aligned}$$

according as  $n$  is even or odd. Thus when  $X = 0$ , the intensity is zero on the odd order lines but, as  $|X|$  increases, the odd order lines begin to appear and the even order lines become weaker. There are, in fact, alternations in intensity along the lines.

(b) Suppose next that  $\phi = \pi/2$ , i.e. the plane of the chain is parallel to the plane of incidence. Then

$$U = \frac{a}{2}\beta + \frac{a}{2} \tan \omega (\gamma - 1).$$

But

$$\begin{aligned} \gamma &= \sqrt{1 - (\alpha^2 + \beta^2)} \\ &= 1 - \frac{1}{2}(\alpha^2 + \beta^2); \end{aligned}$$

$\alpha, \beta$  being small. Therefore  $\gamma - 1$  is small compared with  $\beta$  and we have

$$\begin{aligned} U &= \frac{a\beta}{2} \quad (\text{to the first order}) \\ &= \frac{aY}{2L}. \end{aligned}$$

In practice,  $\alpha$  and  $\beta$  will be  $\sim 1/10$  at the most, so that the error involved when we neglect  $\gamma - 1$  is less than 1 per cent. Thus

$$1 + \cos KU = 1 + \cos \frac{\pi a Y}{L\lambda},$$

and, along a line of intensity, this becomes  $1 \pm 1$  according as  $n$  is even or odd. The odd lines disappear entirely and the effect is equivalent to a linear chain of atoms spaced  $a/2$  apart.

In the general case, the molecules are considered to be arranged all parallel to one another and otherwise at random.

Thus all values of  $\phi$  appear and the total effect, obtained by adding up, is intermediate between the two cases (a) and (b) discussed above. The odd order lines are practically zero at  $X=0$  but become appreciably strong as  $|X|$  increases. The even order lines are strong at  $X=0$  and get less intense as  $|X|$  increases. The appropriate expression is found by integrating (1) from  $\phi=0$  to  $\phi=\pi$  and the complete result has been given by Murison<sup>1</sup> and also by Germer and Storks.<sup>2</sup> The latter give the general solution in a form involving a Bessel function thus:

$$\frac{\sin^2 N\pi \frac{aY}{L\lambda}}{\sin^2 \pi \frac{aY}{L\lambda}} \left\{ 1 + J_0 \left( \pi \frac{aX}{L\lambda} \tan \omega \right) \cdot \cos \pi \frac{aY}{L\lambda} \right\}.$$

Along a line, the intensity varies as

$$1 \pm J_0 \left( \pi \frac{aX}{L\lambda} \tan \omega \right),$$

according as  $n$  is even or odd. In these expressions  $\gamma-1$  is assumed negligibly small. Finally, the atomic scattering factor, which was neglected, will superimpose a general fall-off in intensity as we go out from the origin.

Murison found that the lines were of the form given by theory but not equally spaced. This was due to the effect of refractive index (cf. p. 106). By postulating an inner potential  $\Phi$  and calculating the values of  $a$  and  $\Phi$  in the usual way (p. 156), Murison obtains  $a=2.65 \text{ \AA}$  — in good agreement with Müller. The value of  $\Phi$ , he finds, depends on the substance and ranges from 3.1 to 6.5 volts.

TYPE IV. STRAIGHT-LINE PATTERN WITH SPOTS ON THE LINES.—This was given by tap grease, vaseline, paraffin wax, picein and a heavy oil. It is generally referred to as the grease-pattern, although this name is sometimes extended to include the straight-line pattern (Type III). The straight lines have the same origin and characteristics as explained under Type III above. However, the superposition of the spots on the lines indicates that the packing of the chains is no longer quite

<sup>1</sup> Murison, *l.c.* (There appear to be errors in Murison's calculations of the intensities.)

<sup>2</sup> Germer and Storks, *J. Chem. Phys.* 6, p. 280 (1938).

random. It is known from the X-ray results on paraffin single crystals<sup>1</sup> that the chains tend to pack with their bases on a centred rectangular network (Fig. 64). It was therefore supposed that some of the molecules are packed together into small groups with this type of structure. Further periodicities now appear and new factors arise in the intensity formula. Consequently the continuity of the line pattern is interrupted, spots are superposed on the lines and the lines themselves become fainter. The most intense spot is that on the second order line in the position  $X=0$ . On either side of this are

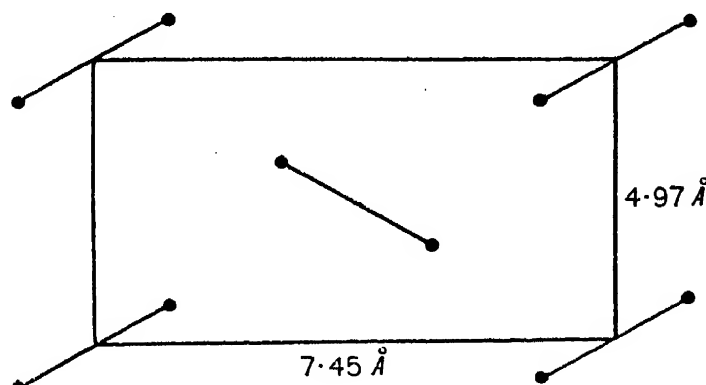


FIG. 64

fairly strong spots and, when these are measured up as 'side-spacings', they give spacings which agree well with the value ( $4.13 \text{ \AA}$ ) for the  $(110)$  plane of the structure illustrated above (Fig. 64). Such spots therefore arise from planes of the type  $(11l)$ . Other fainter spots are seen further out and on the other lines. Their 'side-spacings' again agree with the X-ray crystal structure except for the fact that, in three cases, a side-spacing corresponding to  $(010)$  appears, which is clearly forbidden.

If the orientation were complete the substance would form a single crystal and give a pattern of regularly arranged spots. Actually this never occurs, indicating that the best orientation which is achieved is a collection of crystals with their long axes all parallel but otherwise arranged at random. Sometimes, however, the line and spot pattern is referred to as indicating 'complete orientation' since it is the best that is ever found with oils and greases (see Plates VIII *e* and X *b*).

TYPE V. TWO DIFFUSE RINGS WITH A SPOT JUST INSIDE

<sup>1</sup> Müller, *l.c.*

THE SECOND RING AND, SOMETIMES, OTHER FAINT SPOTS NEAR THE SECOND RING.—Such a pattern was found from light oils which had been smoothed out with tissue paper, although all light oils did not give the effect. We can regard this as a superposition of Types II and IV (diffuse ring pattern and spot pattern). As explained earlier, if the backing surface is irregular in contour and the film is rubbed over it with paper, in some places the film will only be a few molecules thick and may show orientation due to the backing (Type IV). But in other places the film is thicker, the orientation does not persist to the surface, there is no orienting effect at the vacuum-oil interface, and a random pattern (Type II) is found. Accordingly we may say that the orientation indicated by Type V pattern is not so strong as that of Types III and IV (‘grease’ patterns).

TYPE VI. CURVED LINES AND SHORT ARCS OF CIRCLES.—This is rather a complicated pattern which arises from many alcohols and fatty acids (pure substances). The first two rings of the pattern appear as arcs. The outer rings are continuous and appear as slightly curved lines, rather than as parts of circles. The whole pattern is rather diffuse (Plate VIII *f*). The arcs seem to indicate that some crystallites have been formed, and that these have been oriented with one definite crystal plane parallel to the surface.

The curved lines have quite a different origin from the arcs; they represent a slight modification of the straight-line pattern (Type III) which was explained to be due to the single molecules standing normal to the surface). Now, imagine these molecules tilted through a small angle from the normal and in different directions. Then the straight-line pattern will be rotated through small angles about the direction of the incident beam. It has to be remembered, however, that the intensity always depends on the atomic scattering factor and falls off with distance from the central spot. Taking this into consideration, it may easily be shown that a pattern of diffuse curved lines is obtained by superposition of the original straight lines. If these explanations are accepted, then the complete pattern of curved lines and arcs shows that part of the substance is constituted of oriented crystallites, and the remaining molecules are oriented at small angles to the normal. Murison considers that possibly the units which are thus tilted from the

normal may be small crystals and not single molecules. It will be recalled that the fatty acids form a monoclinic type of cell (cf. p. 198 and Fig. 62), so that this seems reasonable.

### Investigation of Lubricating Oils

Following on Murison's work, Andrews<sup>1</sup> examined some fifteen samples of commercial lubricating oils with a view to verifying the suggested correlation between the diffraction patterns and the lubricating properties. He spread the oils thinly over a smooth copper block with tissue paper. The electron diffraction patterns were either diffuse rings, diffuse rings with spots, or grease patterns. These indicate an increasing degree of orientation in the order given, and the oils were classified in this way, according to their pattern. It was actually found that this classification gave in most cases the efficiency of lubrication as determined in practice. Thus good lubricants can be picked out from an examination of electron diffraction patterns, although the method is only qualitative and does not distinguish between specimens of about the same efficiency. Further points (such as the corrosion of the backing and the oxidation of the oils) were investigated in the same way. The influence of the backing metal was also studied using one particular oil and it was shown that steel and iron were the most 'unctuous' metals.

### Further Experiments

Similar results to Murison were obtained by Nelson,<sup>2</sup> who used thin films of greases and paraffins deposited on metal in various ways. Germer and Storks<sup>3</sup> found that stearic acid films on metal gave a reflection pattern of diffuse lines inclined to the shadow edge, the inclination varying from sample to sample. They suppose that large crystals are present with the *c* axes inclined at angles of 33° to the normal, but with the inclination to the plane of incidence different in different specimens. Methyl stearate and lard yielded the same type of pattern, but tristearin gave bands parallel to the shadow edge.

<sup>1</sup> Andrews, *Trans. Farad. Soc.* 32, p. 607 (1936).

<sup>2</sup> Nelson, *Phys. Rev.* 44, p. 717 (1933).

<sup>3</sup> Germer and Storks, *J. Chem. Phys.* 5, p. 131 (1937).

In a recent paper, Germer and Storks<sup>1</sup> have obtained electron diffraction patterns from barium stearate and stearic acid when these are formed as films one, two, or more molecules thick. To prepare such films of definite thicknesses, the Langmuir-Blodgett<sup>2</sup> technique is employed. Both transmission and reflection specimens were used, the former being supported on a film of amorphous material referred to as 'Resoglaz'.<sup>3</sup> A single layer of barium stearate molecules gives a reflection pattern of diffuse lines (Type III above) and thicker layers give a 'grease' pattern (Type IV above). The transmission experiments yield spot patterns or sharp rings depending on the details of preparation, and the spot patterns are like those from paraffin, described on p. 199. A single layer of stearic acid gives, by reflection, a somewhat similar pattern to a single layer of the stearate. Thicker layers yield grease patterns with strong spots and with the whole pattern usually inclined to the shadow edge. This inclination is related to the direction of dipping of the metal into the trough during the preparation of the films. The pattern is not inclined when the electron beam is *parallel* to the direction of dipping; on the other hand the inclination is a maximum with the beam *normal* to the direction of dipping. The transmission patterns confirm the assumption of monoclinic crystals. The single layer reflection pattern is not inclined or only slightly so. Germer and Storks suppose that the molecules of the first layer of acid combine with the metal to form the stearate so that one would expect a non-inclined pattern. Further layers, however, do not react in this way.

Maxwell<sup>4</sup> has been able to obtain liquid films of phytol, 'Nujol' and pump oil, the films being across a small wire loop and about  $10^{-4}$  cm. thick. The electron diffraction patterns from these specimens showed 3 diffuse rings, the spacings being the same as those obtained from liquid pentadecane ( $C_{15}H_{32}$ ) and tetradecane ( $C_{14}H_{30}$ ) using X-rays.

Thiessen and Schoon<sup>5</sup> have taken reflection patterns from single crystals of paraffins, stearic acid and cetyl palmitate.

<sup>1</sup> Germer and Storks, *ibid.* 6, p. 280 (1938).

<sup>2</sup> Blodgett, *J. Am. Chem. Soc.* 57, p. 1007 (1935).

<sup>3</sup> Cf. Germer, *J. App. Phys.* 9, p. 143 (1938).

<sup>4</sup> Maxwell, *Phys. Rev.* 44, p. 73 (1933).

<sup>5</sup> Thiessen and Schoon, *Zeit. für Phys. Chem.* (B) 36, p. 216 (1937).

The photographs are very clear and form a useful adjunct to the X-ray results in determining the structures. The inner potentials come out to be about 6.5 volts which is of the same order as Murison found.

Attention has been drawn by Finch and Wilman<sup>1</sup> to an effect observed by them in transmission patterns from single crystals of certain aromatic compounds such as anthracene, etc. Superimposed on the usual array of spots are broad bands or areas of diffuse blackening (Plate IX *a*). They state that the positions of these areas correspond to the spacing of the carbon atoms in the molecule, and it thus seems as if some of the molecules do not form part of the single crystal arrangement, though they are perhaps partially under the influence of the atomic forces of the crystal.

### Lubrication with Graphite

Besides oils and greases, graphite is also used as a lubricant, either alone or mixed with oil. The electron diffraction experiments of Jenkins<sup>2</sup> indicate the mechanism of graphite lubrication. He prepared a thin layer of powdered graphite on a ground glass plate. This gave a 'reflection' pattern of sharp rings. On rubbing with cotton-wool and again examining in the electron camera, the rings were found to have disappeared and were replaced by a row of strong diffuse spots along the normal to the shadow edge through the central spot, accompanied by fainter diffuse side spots (Plate IX *b*). The spacings of the diffuse central line spots corresponded with the cleavage plane spacing of the graphite crystal, showing that the crystal grains had been reduced in size and also oriented with their cleavage planes all parallel to the surface. Experiments were also made with oil containing colloidal graphite ('Oildag'). A piece of Swedish iron was ground and polished. It was then rubbed over a smooth iron table continuously for three hours. The surfaces were kept lubricated with Oildag all the time. On removing the Swedish iron, washing and examining it in the camera, a pattern of uniform rings was found due to both graphite and iron. After giving the surface a vigorous

<sup>1</sup> Finch and Wilman, *Ergebnisse d. exakt. Naturwiss.* 16, p. 353 (1937).

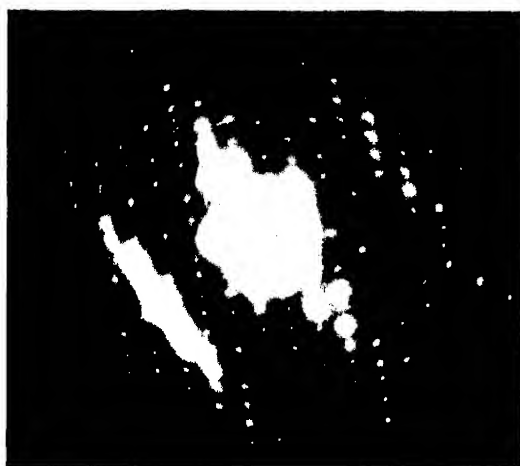
<sup>2</sup> Jenkins, *Phil. Mag.* (7), 17, p. 457 (1934).

rubbing with cotton-wool in an attempt to reproduce the more intense pressures met with in practice, the diffraction pattern was nearly the same as the polished graphite pattern. Hence both in the case of dry graphite and 'Oildag', a film of very small carbon grains is formed on each of the bearing surfaces. These grains are oriented with their cleavage planes parallel to the surfaces. Slip will thus take place along the cleavage planes of the graphite between which the atomic forces are weak, and the comparatively rough metal surfaces do not touch. This idea can also be used to explain the 'self-lubricating' properties of cast-iron (which contains a fairly large amount of carbon).<sup>1</sup> Finch<sup>2</sup> considers that, when both oil and graphite are used for lubrication, the oil is for the most part the principal agent in reducing friction. But the oil film is ruptured from time to time, and during these short periods when the oil is ineffective the graphite functions as a lubricant and 'seizure' is avoided.

<sup>1</sup> Finch, Quarrell and Wilman, *Trans. Farad. Soc.* 31, p. 1050 (1935).

<sup>2</sup> Finch, *La diffraction des électrons et la structure des surfaces*, p. 45. Liège: Maison Desoer.

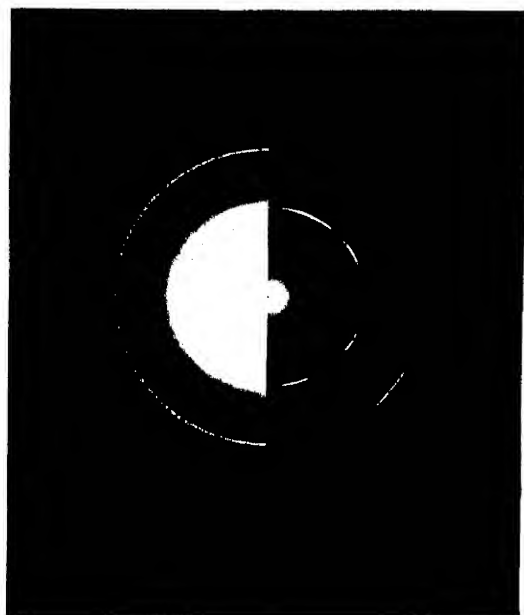
# PLATE IX



(a) Anthracene. (*Finch*)



(b) Polished graphite. (*Jenkins*)



(c) Comparison photograph, graphite (left) and gold. (*Finch*)



(d) Spinel fracture. (*Finch*)



## CHAPTER XV

### MISCELLANEOUS APPLICATIONS

THE descriptions given in this chapter are intended to indicate the kind of problems which have been successfully studied by means of electron diffraction, and the nature of the information which the method can yield. They do not attempt to give a discussion of the problems themselves, or to describe the work which has been done by other methods. It is hoped that these short accounts may be of service to anyone who is considering applying electron diffraction to these or similar problems.

#### Structure of Rubber

The structure of stretched and unstretched rubber has been examined by electron diffraction by several workers.<sup>1</sup> Using films thin enough to transmit the electrons, most experimenters find that the stretched rubber gives point patterns, at least at first, implying a well-defined structure, while the unstretched rubber usually gives diffuse rings, implying an almost random arrangement of molecules. Patterns of points and sharp rings observed by some workers even in unstretched rubber may perhaps be due to local strains. The results confirm in general those obtained with X-rays. Krylow has also examined several artificial rubbers, some of which give point patterns.

#### Cellulose

Natta and Baccaredda <sup>2</sup> have succeeded in getting diffraction from cellulose deposited from cuprammoniacal solution, great care being taken to avoid the complication due to layers of foreign substances referred to on p. 151. The rings were rather

<sup>1</sup> Bresler Strauff and Zelmanoff, *Phys. Zeit. Sowjet.* 4, p. 885 (1933); Bruni and Natta, *Acad. Lincei*, 19, p. 536 (1934); Trillat and Motz, *Compt. rend.* 198, p. 2147 (1934); Krylow, *Phys. Zeit. Sowjet.* 8, p. 136 (1935).

<sup>2</sup> Natta and Baccaredda, *Acad. Lincei*, 23, p. 444 (1936).

diffuse, but agreed well with the structure of cellulose as determined by X-rays.

### Minerals

Aminoff and Broomé<sup>1</sup> have developed a method for examining minerals by transmitted electrons, including some that cannot be split into thin sheets. They have applied it to the study of talc which has not been analysed by X-rays. Some work has also been done on the clays.<sup>2</sup> The technique in this case is to deposit fine particles from a suspension on to a cellulose backing, and examine them in transmission. Shishacow finds that many of these substances show the same set of rings, which he attributes to a two dimensional lattice of  $\text{Si}_2\text{O}_3$ .

### Platinised Asbestos

When asbestos is platinised by immersion in platinic chloride and reduction in hydrogen, no trace can be found of the platinum when the asbestos is examined by electron diffraction,<sup>3</sup> even when the substance has become almost black. Richards<sup>4</sup> has shown that this is because the platinum is deposited in cracks in the asbestos, and that when the process is repeated till the asbestos has been split into such small fibres that it gives a diffuse ring pattern, the platinum begins to appear. This occurs when the weight of platinum is about 1.8 that of the asbestos.

### Position of Hydrogen Atoms

It is well known that it is almost impossible to determine the position of hydrogen atoms in a crystal by means of X-rays, for the only electron is displaced by acting as a chemical bond. In electron diffraction the nucleus produces an appreciable effect, and Laschkarew and Usyskin<sup>5</sup> have shown that it is possible to determine the distance between the hydrogen and

<sup>1</sup> Aminoff and Broomé, *Zeit. für Krist.* 89, p. 80 (1934), 91, p. 77 (1935); *Arch. f. Kemi. Min. Geo. (Stockholm)* 11B, No. 10, No. 25 (1933).

<sup>2</sup> Hendricks, *Zeit. für Krist.* 95, p. 247 (1936); Shishacow, *Phil. Mag.* 24, p. 687 (1937).

<sup>3</sup> Thomson, *Proc. Roy. Soc.* 128, p. 653 (1930).

<sup>4</sup> Richards, *Phil. Mag.* 16, p. 778 (1933).

<sup>5</sup> Laschkarew and Usyskin, *Zeit. für Phys.* 85, p. 818 (1933).

nitrogen nuclei in ammonium chloride from measurements of the intensities of rings.

### Catalysis

The catalysis of hydrogen and oxygen mixtures by platinum has been studied<sup>1</sup> by the reflection method. It was found among other results that certain surfaces which had been supposed to be metallic platinum were really platinum dioxide.

### Accommodation Coefficient

In a rather similar way Mann<sup>2</sup> has been able to explain some anomalous measurements of the accommodation coefficient for the energy interchange of helium atoms with a platinum surface. On examination by electron diffraction it was found that in some cases a thin protective film of an unidentified compound covered the surface of the platinum. This film had the effect of reducing the change in the accommodation coefficient due to chance contamination.

### Diffusion of Metals

Eisenhaut and Kaupp<sup>3</sup> have examined the interdiffusion of films of copper and gold each about  $10^{-6}$  cm. thick. They find that a uniform alloy is formed at a rate which increases exponentially with the temperature, the time taken being of the order of a few minutes at  $200^{\circ}$  C. At high temperatures the alloy assumes a new crystal structure.

### Structure of Polonium

Owing to the small quantities of polonium obtainable its crystal structure cannot be determined by X-ray methods. Using about  $10^{-7}$  gm. of polonium, volatilised on to a thin collodion film, Rollier, Hendricks and Maxwell<sup>4</sup> were able to

<sup>1</sup> Finch, Murison, Stuart and Thomson, *Proc. Roy. Soc.* 141, p. 414 (1933).

<sup>2</sup> Mann, *Proc. Roy. Soc.* 161, p. 236 (1937).

<sup>3</sup> Eisenhut and Kaupp, *Zeit. für Elektrochem.* 37, p. 466 (1931).

<sup>4</sup> Rollier, Hendricks and Maxwell, *J. Chem. Phys.* 4, p. 648 (1936).

show that the structure closely resembles that of tellurium, and to assign a probable lattice and atomic arrangement.

### Thermionic Emission

Gaertner and Darbyshire<sup>1</sup> have examined the surfaces of oxide-coated filaments and followed the changes which occur in the diffraction patterns during formation and poisoning. When the surface is emitting well it consists mostly of strontium oxide.

### Photographic Action

Trillat and his co-workers<sup>2</sup> have used the process of electron diffraction to study the changes which take place in photographic materials under the action of the electrons themselves. The effect on silver bromide, deposited on a thin film of cellulose acetate, is to promote the crystallisation. By a remarkable feat of technique, Trillat and Merigoux have been able to prepare films of photographic emulsion thin enough to give electron diffraction patterns by transmission. At first the only pattern is due to the gelatine, after a few seconds rings due to silver appear in most cases, but occasionally those due to crystalline silver bromide appear instead, the two patterns seeming to be mutually exclusive. Films which have previously been exposed to light and developed give rings due to silver at once.

### Semi-permeable Membranes

Fordham and Tyson<sup>3</sup> have obtained transmission patterns from a number of the best known semi-permeable membranes, namely the ferrocyanides, hydroxides, silicates and tannates, of copper, lead and ferric iron. The ferrocyanides and hydroxides were found to be crystalline with a crystal size of at least 100 Å, but the tannates were amorphous, giving diffuse rings. The silicate membranes consisted in general of mixtures gels of crystalline metal hydroxides and amorphous silicic acid.

<sup>1</sup> Gaertner, *Phil. Mag.* 19, p. 82 (1935); Darbyshire, *Proc. Phys. Soc.* 50, p. 635.

<sup>2</sup> Trillat and Motz, *Jour. de Phys.* 7, p. 89 (1936); Trillat and Merigoux *ibid.* p. 497 (1936).

<sup>3</sup> Fordham and Tyson, *J. Chem. Soc.* p. 483 (1937).

**Distortion due to Cold Working**

A series of experiments on galena, the surface of which had been ground and filed, have been carried out by Germer.<sup>1</sup> He has been able to show that a type of distortion occurs to the scratched areas, which corresponds to a partial rotation of blocks of the crystal about an axis in the surface normal to the direction of filing.

<sup>1</sup> Germer, *Phys. Rev.* 50, p. 659 (1936).

## CHAPTER XVI

### TECHNIQUE

#### Introduction

THE mean free path of an electron in air at atmospheric pressure is  $\sim 10^{-5}$  cm. Electron diffraction experiments must therefore be performed in apparatus which has been evacuated to a low pressure, and part of the electron diffraction technique is, in fact, ordinary vacuum practice. However, no difficulty is generally encountered in attaining the requisite vacuum conditions, for the apparatus is almost invariably continuously pumped during the progress of an experiment, using high-speed diffusion pumps.

Because of the large number of results which have been obtained by diffraction of *fast* electrons, and on account of the applicability of this method to such a variety of problems, it will be discussed at some length in the present chapter. The diffraction of *slow* electrons is more limited in its scope, and the apparatus for this purpose is described on pp. 263, 278.

Confining our remarks, therefore, to fast electrons, we are at once confronted by the diversity of the types of electron diffraction cameras which have been evolved by experimenters. Evidently all such cameras must have certain common features, and it will be sufficient to describe one camera in detail and to indicate some of the alterations which may be introduced.

#### Modified Thomson-Fraser Camera <sup>1</sup>

A brief description of the Thomson-Fraser design has been given on p. 49. For some years several cameras of a slightly modified Thomson-Fraser type have been used in the Imperial College of Science and Technology. These cameras are intended primarily for the examination of solid specimens by transmission or reflection. There are five main parts (Fig. 65) :

<sup>1</sup> Thomson and Fraser, *Proc. Roy. Soc.* A128, p. 641 (1930).

the plate chamber, the main tube C, the specimen chamber B, the collimating tube and the discharge tube A. Usually the camera rests on a wooden stand in such a position that the electron beam is approximately along the direction of the

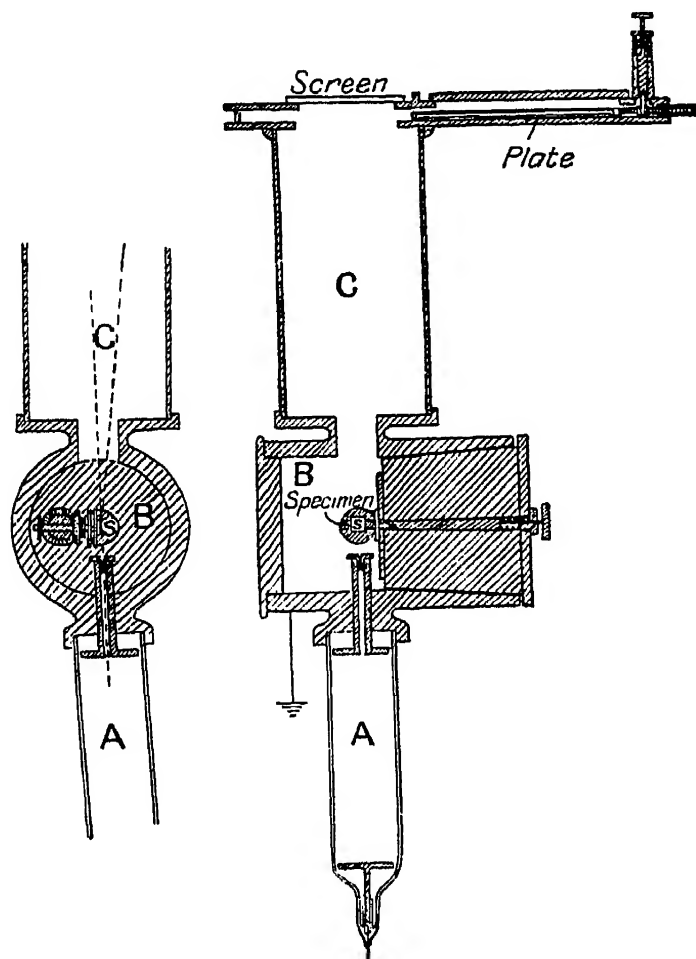


FIG. 65<sup>1</sup>

earth's magnetic field; the plate chamber is uppermost and the discharge tube is lowest.<sup>2</sup>

**THE PLATE CHAMBER.**—This is a built-up brass box and contains the photographic plate in its carrier *a* (Fig. 66). The latter is attached to a rack *b* which can move in the glass tube *c*. A pinion, controlled by the handle *d*, is in mesh with the rack, the shaft of the pinion passing through the brass box by way of a conical ground joint *e*. By rotating the handle *d* the plate may be moved down into the position for recording a pattern and withdrawn again when required. The position of the plate may be gauged from the height of the rack in the

<sup>1</sup> The connections to the pumps are omitted from Fig. 65 for simplicity.

<sup>2</sup> Taken from R. Beeching, *Electron Diffraction* (Methuen).

glass tube *c*. A large circular opening *f* is cut in the plate chamber to fit on to the main tube *g*. Immediately opposite there is a square opening over which is placed the fluorescent screen *h*. On the same side of the chamber there is a door in

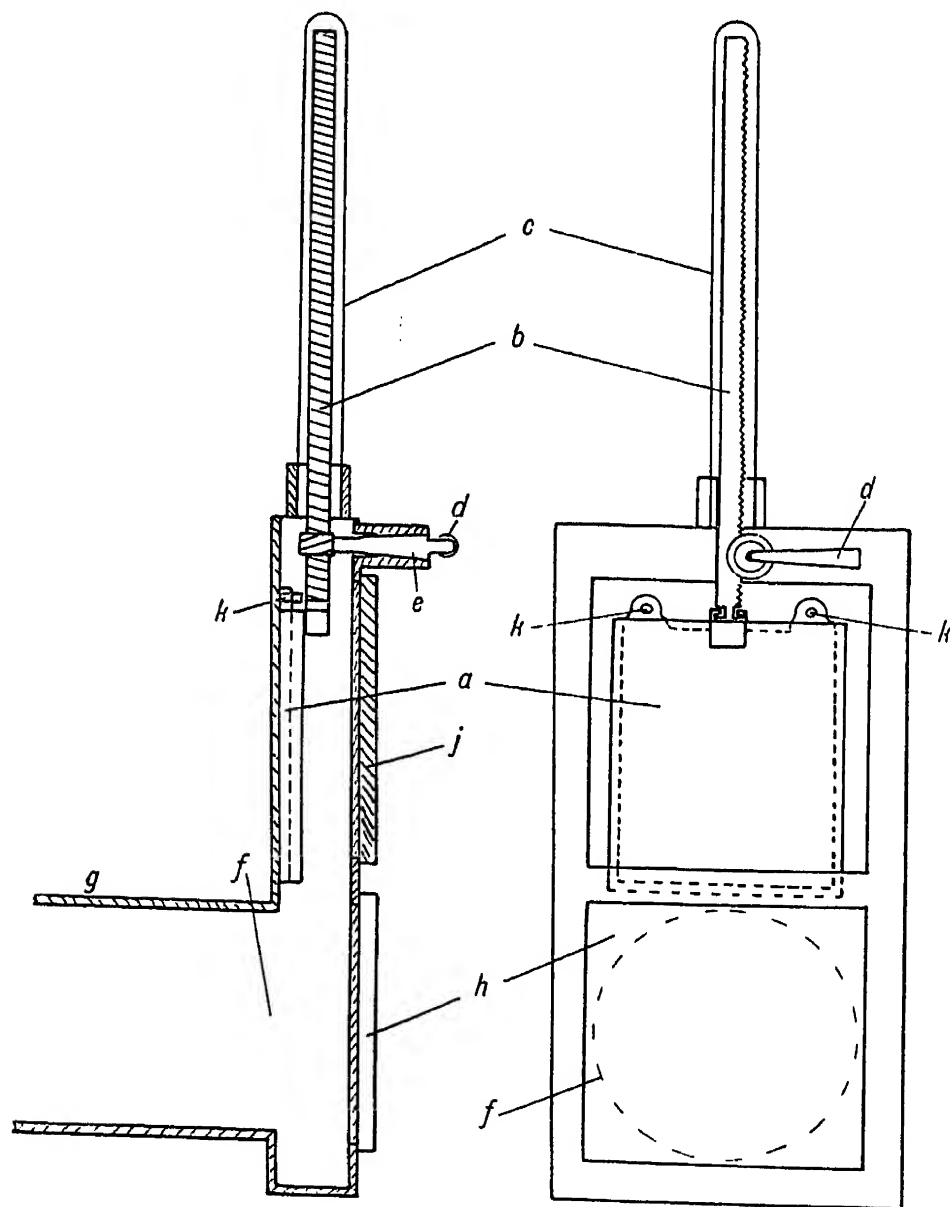


FIG. 66

the form of a brass plate *j*, which allows the plate carrier *a* to be taken out and replaced. The fluorescent screen and the brass door are fixed on to the plate chamber with Everett's wax or 'Q-compound' ('plasticene'). The chamber itself, being constructed of separate pieces of brass, must be sealed up with picein or other sealing compound.

The plate-carrier is in two parts, one containing the plate

and the other forming a light-tight cover (as used in ordinary photographic work). When in position in the plate chamber the cover cannot move, being held by two pins, *k*, *k*, which pass through holes in it. The plate-containing part is attached to the rack *b* by a simple interlock, and, when the handle *d* is turned, the plate container moves down into position in front of the fluorescent screen *h*, leaving the cover behind. By using this type of carrier the camera may be loaded in daylight, the carrier itself being opened and refilled in the dark room.

The fluorescent screen consists of a piece of plate-glass with fine willemite powder on one side. The willemite is mixed with water-glass and a very thin layer is spread over the glass plate and allowed to dry. Canada balsam in xylol may be used as an adhesive in place of water-glass; and other fluorescing materials, such as calcium tungstate, may be substituted for willemite.

THE MAIN TUBE.—This is a cylindrical brass tube 11 cm. in diameter and of such a length as to give a suitable distance (30 to 40 cm.) between the specimen and the screen. It is joined to the plate chamber and to the specimen chamber by screwed joints which are made vacuum-tight in the usual way.

THE SPECIMEN CHAMBER.—In the original design the specimen chamber was a built-up brass box, but this is now replaced by a bronze casting. The main feature is a large solid frustum of a cone (also a casting) which fits into the specimen chamber. It is usually referred to simply as a 'cone'. This large 'cone' *a* (Fig. 67) has two smaller 'cones' (*b*, *c*) passing through it. All these are cut to a 1-in-10 taper and are ground into their seatings so that, with a thin film of tap-grease between the contacting surfaces, the cones may be rotated while the apparatus is evacuated. Such rotations are necessary to enable a reflection specimen to be correctly placed with regard to the electron beam so as to give a pattern, as explained on p. 50. The three movements of the specimen are generally referred to as (1) 'motion in and out of the beam', (2) 'change of angle of incidence', and (3) 'rotation in azimuth'. Movement (1) results from rotation of the cone *c*. The rotational motion has to be changed into a to-and-fro motion at right angles to the axis of the cone of the specimen holder *i*. This

is accomplished by attaching a disk *e* to the end of the cone and by having a short pin *f* projecting from the edge of the disk. The pin engages loosely in a circumferential slot in the disc *g* attached to the rod *h* which carries the specimen holder. A linear motion of the specimen is thus produced. Movement (2) is obtained by rotating the large cone *a*, and handles *j*, *j* are attached for this purpose. Finally, movement (3) results from the cone *b*. The rotation of this cone has to be changed

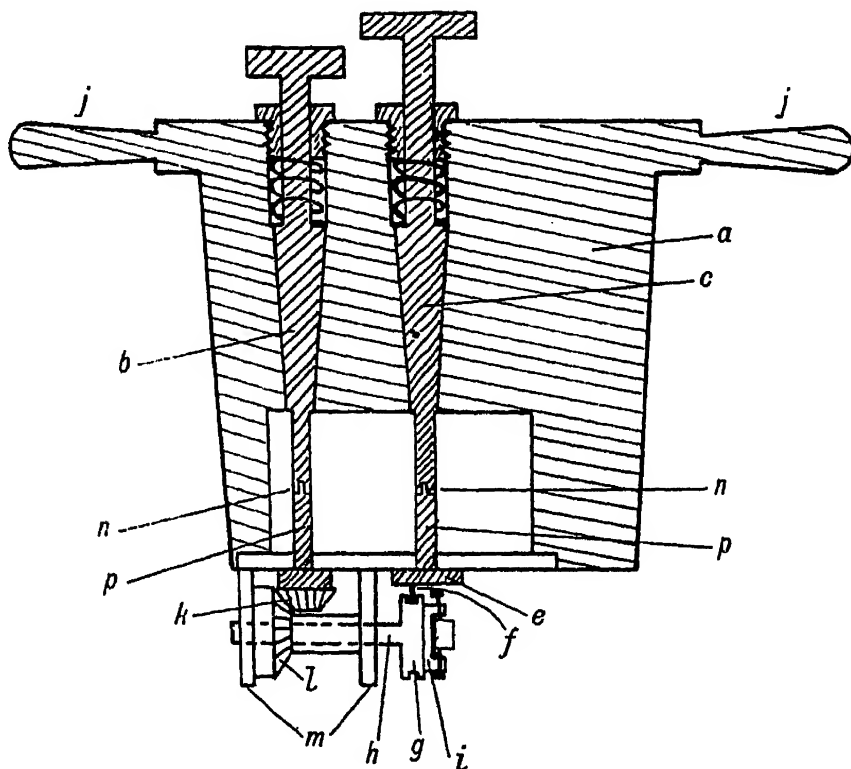


FIG. 67

into a rotation about an axis at right angles to the axis of the cone. This is effected by the use of mitre wheels *k*, *l*. The rod *h* must, of course be keyed to the wheel *l* and, at the same time, be free to slide through it. Fixed pillars *m*, *m* attached to the large cone, serve to carry the rod *h* while allowing it to rotate and slide to and fro as necessary. It is found that the cones require to be removed about every week for re-greasing since the grease is slowly squeezed out — especially in warm weather. The small cones therefore terminate at *n*, *n* and are slotted so that they connect up with the spindles *p*, *p*.

Fig. 68 is a diagram of the specimen chamber as viewed along the axis of the large cone. It shows the main tube *a*

joining on to the specimen chamber at *b*. The side pipe *c* connects to the pumps and is used for evacuating the air from the camera with the exception of the discharge tube, the latter being pumped out through a separate pipe *d*. A mechanical shutter is provided by the rod *l* attached to the ground joint *m*. It is omitted from Fig. 65 for simplicity.

**THE COLLIMATING TUBE.**—This is also seen in Fig. 68 at *f*. It is made of aluminium and one end projects a little into the specimen chamber. It carries, at its other end, the alu-

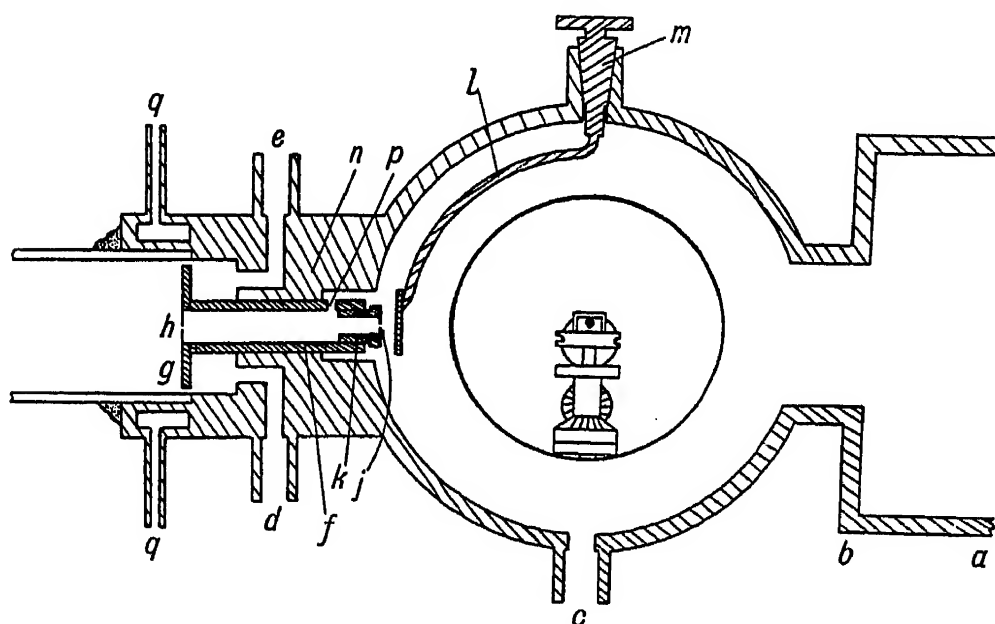


FIG. 68

minium disk *g* which acts as the anode of the discharge tube. At the ends of the collimating tube are inserted molybdenum disks *j*, *h*, 0.25 mm. thick and each containing a circular aperture 0.1 mm. in diameter. These apertures serve to collimate the electron beam and, for convenience in cleaning them, the disk *j* is actually mounted in an aluminium plug *k* which fits snugly into the collimating tube and may be removed when necessary. The distance from *h* to *j* is 9 cm. The collimating tube is made to fit tightly into the part *n* of the specimen chamber casting, specially prepared to receive it. It is evacuated through one or more openings such as *p*. The internal diameter of the collimating tube is 6 mm.

**THE DISCHARGE TUBE.**—The discharge tube is cylindrical in shape, and is made of pyrex glass. It is sealed into the specimen chamber casting, as shown (Figs. 65, 68), with a picein

joint. Water-cooling is provided through the pipes  $q, q$ . The cathode is an aluminium disk carried at the end of a stiff wire which is sealed through the discharge tube. Both the anode and cathode are machined and, if necessary, polished.

THE PUMPING SYSTEM.—This calls for little comment. A small mercury diffusion pump, backed by a 'Hyvac', is commonly employed, with an arrangement for by-passing the diffusion pump.

HIGH-TENSION SUPPLY.—An induction coil is used for the high-tension electrical supply. The primary of the coil is connected through a mercury jet interrupter (with condenser

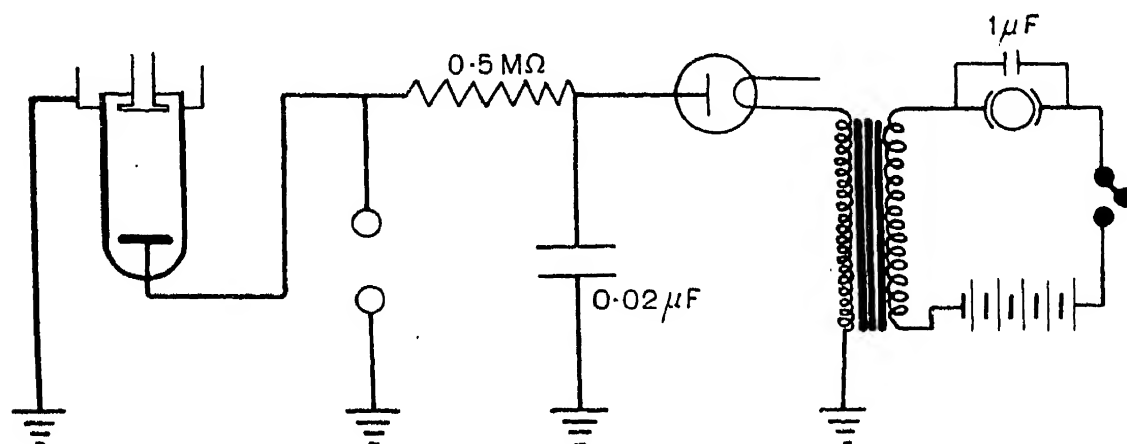


FIG. 69

in parallel) to a battery of storage cells giving 20-40 volts. The mean primary current is about 1 amp. The potential pulses from an induction coil are very much larger in one direction than in the other, and, effectively, we may speak of the ends of the secondary as being positive and negative respectively. These having been determined with an old X-ray or Crookes tube, the positive pole is earthed and the pulses from the negative pole are completely rectified by a diode valve (for example : Marconi-Osram E.H.T.). Smoothing is obtained by utilising a  $0.02 \mu\text{F}$  high-tension condenser and a half-megohm water resistance as shown in the circuit diagram (Fig. 69). All connections are made with thick rubber-covered cable to prevent brushing. The circuit through the discharge tube is completed by earthing the body of the camera — usually at several points — and the voltage across the tube is measured by connecting, in parallel, an adjustable spark-gap of aluminium spheres 5 cm. in diameter.

LEAK SYSTEM.—In order to keep the discharge running steadily and also to control the voltage across the discharge tube, a continuous leak of dry air is allowed to flow into the tube by way of the pipe *e* (Fig. 68) and is pumped out through *d*. The leak comes through an adjustable needle valve from a partially evacuated bottle of about 2.5 litres capacity. A specially designed valve has also been employed which allows the leak to come direct from air at atmospheric pressure and thus enables one to dispense with the bottle or reservoir.

THE PHOTOGRAPHIC PLATE.—A 'Paget' process plate or a 'photomechanical' plate is used; but many plates intended for ordinary photographic work are suitable for recording fast electrons. The speed of a plate for light is not, in general, any indication of the speed for electrons and, a fine-grained negative being desirable, slow plates are usually employed. Exposure times are very short — of the order of a few seconds or less. With slow electrons photographic recording is more difficult, and the use is then made of Schumann plates or ordinary plates coated with oil.<sup>1</sup>

It may be remarked that, although photographic plates are normally used, the intensity of the patterns from fast electrons is sufficient to be recorded on paper. Trillat<sup>2</sup> recommends 'Velox' for this purpose. Roll film has also been employed by various experimenters.

OPERATING CONDITIONS.—The pressure in the discharge tube is adjusted by means of the needle valve so that the potential across the tube is about 30-35 kV. The discharge then takes the form of a thin pencil of reddish glow extending from the centre of the cathode disk up the axis of the tube. This 'focusing' effect of the gas discharge gives rise to a very strong electron beam. The current in the tube generally lies between 0.1 and 1 mA., and the pressure is somewhere in the region of 0.005 mm. of mercury. The electron beam appears as a bright spot on the fluorescent screen but it is usually necessary to move a small bar magnet about near the anode until the best position is found in order that the beam may pass through the second collimating aperture. Failure to find

<sup>1</sup> Cf. Rupp, *Ann. d. Phys.* 85, p. 981 (1928); or MacFarlane, *Phil. Mag.* 22, p. 801 (1936); or Thomson, *Proc. Roy. Soc. A* 125, p. 352 (1929).

<sup>2</sup> Trillat, *Kolloid Zeit.* 69, p. 378 (1934).

a beam can usually be attributed to bad 'aiming' or alignment. The cathode and anode surfaces should be normal to the axis of the discharge tube and this axis should also pass through the collimating apertures. Sometimes, however, the 'geometrically' correct position is not 'electrically' correct owing to various unknown factors. The collimating apertures should be perfectly clean when examined under a microscope. The spot on the screen is seen surrounded by one or more peculiar rings of fluorescence ('spurious rings'). These do not appear on the photographs, and have been explained by Hughes<sup>1</sup> as due to total reflection of light from the spot at the glass surface. After a time one gets into the way of ignoring the presence of the spurious ring. The spot may be deflected by a bar magnet in order to test the homogeneity of the rays. If no 'tail' appears it may be considered satisfactory.

Louw<sup>2</sup> has investigated the inhomogeneity of the electron beam in an apparatus such as we have described. He examined the magnetically deflected spot using a stroboscopic method. As might have been expected, the results showed that the main influences were the value of the smoothing condenser and the frequency of the break. With a  $0.01 \mu\text{F}$  condenser and a discharge tube current of  $0.8 \text{ mA.}$ , the voltage varied from  $29.8$  to  $28.2 \text{ kv.}$  in an interrupter cycle ( $0.03 \text{ sec.}$ ) — a variation of  $5\frac{1}{2}$  per cent. The wave-length change will only be half of this since  $\lambda \propto P^{-\frac{1}{2}}$ . Smaller condensers gave a bigger variation. We have obtained similar results to Louw, using a cathode ray oscillograph. Louw also found that the measured variation in voltage was rather less than that calculated from a simple theory of the circuit.

Jenkins<sup>3</sup> has determined the electrical current carried by the collimated electron beam in a camera of the type we are describing. It varied from  $6 \times 10^{-9}$  to  $3 \times 10^{-9}$  amps. as the voltage ranged from  $20$  to  $32 \text{ kv.}$  The corresponding currents in the discharge tube were  $1$  to  $0.3 \text{ mA.}$  The apertures used for collimating were  $0.15 \text{ mm.}$  in diameter.

The adjustment of the specimen into the electron beam is

<sup>1</sup> Hughes, *Proc. Phys. Soc.* 45, p. 434 (1933).

<sup>2</sup> Louw, Thesis: Imperial College (1934).

<sup>3</sup> Jenkins, unpublished observation.

a comparatively simple matter. With reflection specimens, one concentrates first on obtaining a shadow edge on the screen — a positive angle of incidence being, of course, required. Azimuthal adjustments can then follow. It is a common practice, at the end of the exposure of a reflection pattern, to pull the specimen out of the beam and then rack the plate up. This leaves a trace of the undeviated beam on the plate, which is useful when measurements are being made afterwards. A spark-gap measurement of the voltage is taken before and after the exposure.

The complete operations — placing a specimen in position, pumping out the camera, photographing and developing — take from twenty to forty-five minutes, depending largely on the pumping speed. By using very fast pumps, many experimenters have reduced this time to about 10 minutes.

### Alternative Arrangements

*General.*—There is a tendency to eliminate the extensive use of wax joints in electron diffraction cameras on the ground

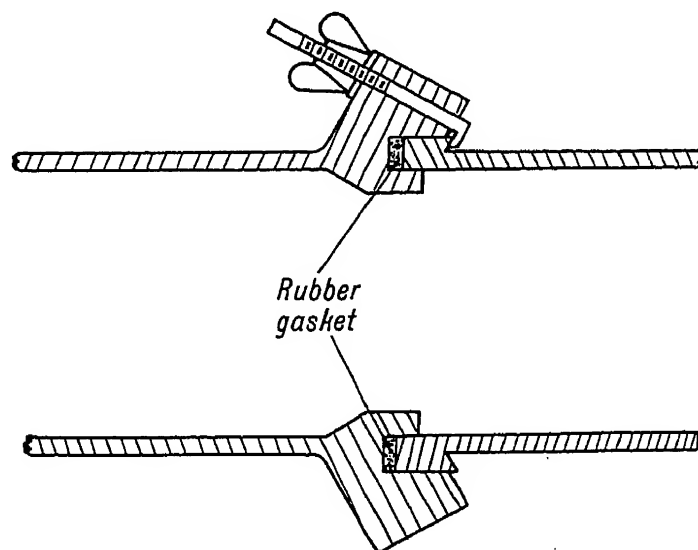


FIG. 70

that these joints are difficult to make, and that they are inconvenient when it is wished to disassemble the apparatus. Instead, there have been introduced rubber gaskets (cf. Fig. 70)<sup>1</sup> and flat metal-to-metal joints spread with tap grease.

<sup>1</sup> Taken from Burgers and Basart, *Physica*, 1, p. 543 (1934).

In place of metal cones many cameras have flat metal-to-metal ground joints ; others have glass ground joints. Practi-

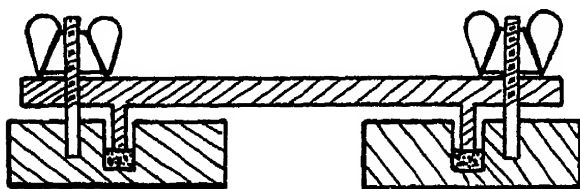


FIG. 71

cally all the recently described cameras have a rubber gasket at the plate-chamber end of the apparatus. Fig. 71 illustrates how the door of the plate-chamber may be fitted on

in this way. Many additional points are illustrated in Finch's camera which will be briefly described.

FINCH'S CAMERA.<sup>1</sup>—This is illustrated in Fig. 72. The source of electrons is a gaseous discharge and only one aperture in the anode tube is necessary owing to the magnetic focusing method which has been adopted. This idea is due to Lebedeff.<sup>2</sup> The focusing coil is indicated in the diagram. The current through it is adjusted until the electron image of the anode pin-hole is formed on the fluorescent screen. The theory of such focusing is due to Busch.<sup>3</sup> From a simple treatment, it appears that the focal length of such a magnetic ' lens ' is

$$f = \frac{8P}{i^2 \eta \int_{-\infty}^{+\infty} (H_z)_0^2 dz},$$

where  $i$  is the current in the coil,  $(H_z)_0$  is the value of the magnetic field  $H_z$  on the axis of the coil when unit current flows,  $\eta = e/m$  and  $P$  is the accelerating (voltage e.m.u.). The  $z$ -axis is taken along the axis of the coil with origin at the centre. The value of the integral has to be evaluated numerically from the dimensions of the coil. Tillman<sup>4</sup> found that, with a coil of 490 turns of 22 gauge insulated copper wire in 10 layers, of length 5.25 cm. and radius 2.87 to 3.70 cm.  $f$  is given by

$$f = 0.001515 \frac{P}{i^2} \text{ cm.},$$

<sup>1</sup> Finch and Quarrell, *Proc. Roy. Soc. A* 141, p. 399 (1933) ; Finch, Quarrell and Wilman, *Trans. Farad. Soc.* 31, p. 1051 (1935) ; Finch and Wilman, *Ergebn. exak. Naturwiss.* 16, p. 353 (1937).

<sup>2</sup> Lebedeff, *Nature*, 128, p. 491 (1931).

<sup>3</sup> Busch, *Ann. d. Phys.* p. 974 (1926) ; and *Arch. für Elektrotechnik*, p. 583 (1927).

<sup>4</sup> Tillman, *Phil. Mag.* 8, p. 656 (1934).

where  $P$  is in volts and  $i$  in amperes. Usually, coils are made with more turns than this and are rather shorter. The ordinary lens formula  $1/u + 1/v = 1/f$  applies, where  $u$  is the distance from anode aperture to coil and  $v$  is the distance from coil to screen.

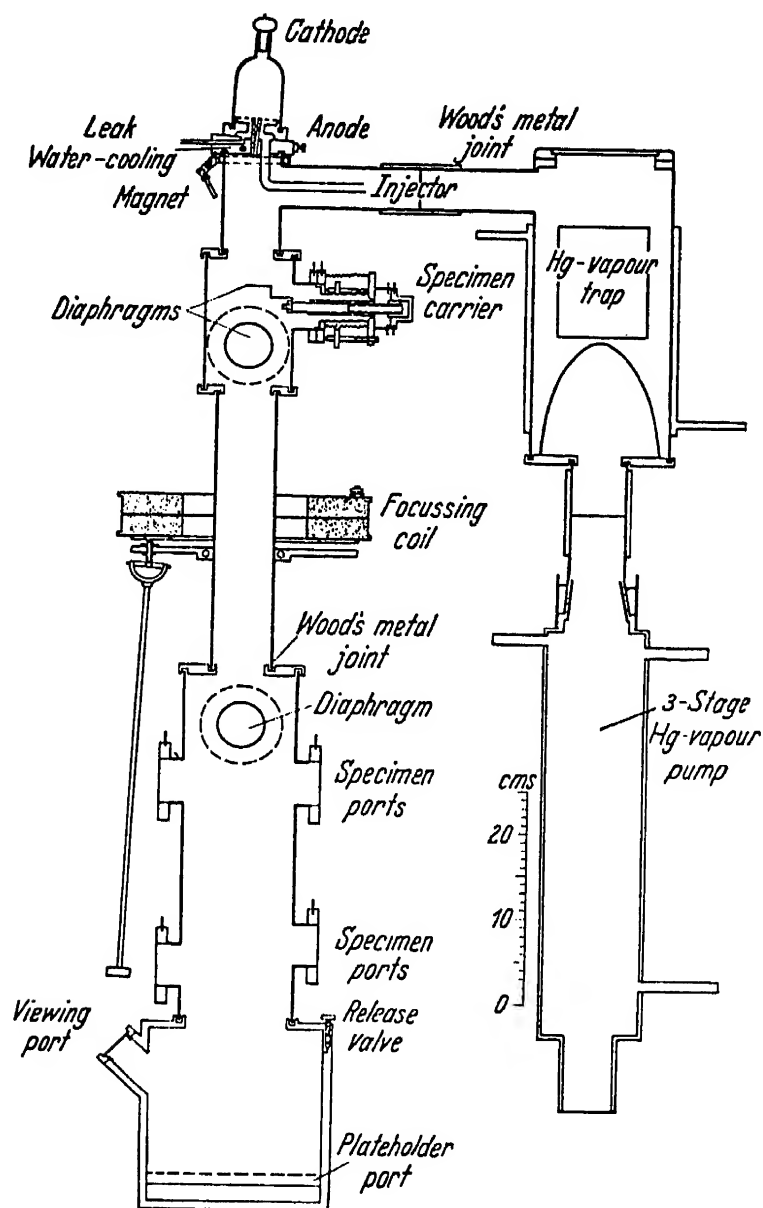


FIG. 72

It may be noted that rays initially lying in one axial plane also lie in one axial plane after passing through the lens, but the plane is turned through an angle  $\phi$  about the axis where

$$\phi = \frac{i}{2} \sqrt{\frac{\eta}{2P}} \cdot \int_{-\infty}^{+\infty} (H_z)_0 dz.$$

In practice, however, no use is made of this fact.

The discharge tube in the Finch camera is seen to be tilted so that the electron beam does not go along the axis of the coil. This results in the beam being deflected as well as focused. By altering the tilt of the coil, different parts of a large specimen

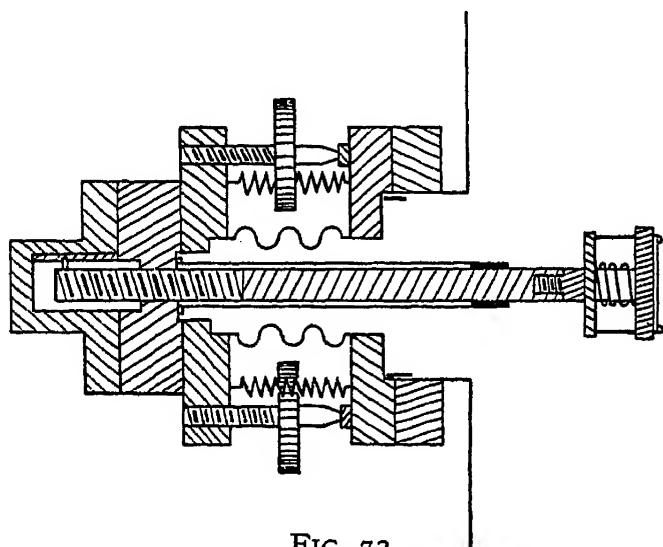


FIG. 73

may be examined. In addition, deflecting the beam eliminates any heavy negative ions which may be present along with the electrons and which might, by their impact, damage the specimen. The heavy ions are not deflected to any great extent by the tilted focusing coil and are trapped by the dia-

phragm, containing a small aperture, placed a little above the specimen and set so that the electrons pass through. Since the electron beam is not along the axis of the magnetic lens, defects of the image arise, and we have found, on using this arrangement ourselves, that the spot has a curved tail when the diaphragm is not in position. The tail is eliminated, however, on bringing the diaphragm into place. When two or more holes are used to collimate the beam, as in the Thomson-Fraser camera, the heavy ions do not appear, since a small magnetic field is almost always required to

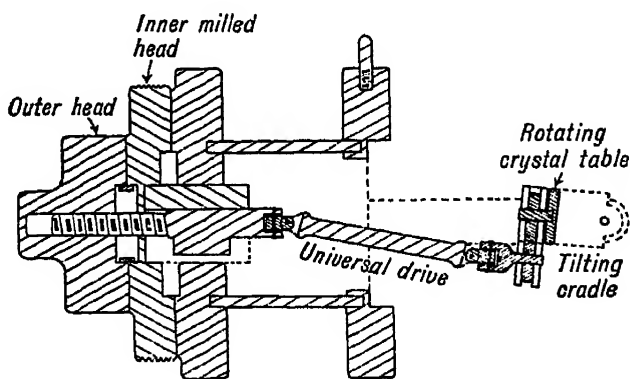


FIG. 74

guide the electrons through, and any heavy ions are consequently trapped. In Lebedeff's arrangement, as also in the apparatus used by Mongan,<sup>1</sup> there is no tilting of the focusing coil and no second aperture in front of the specimen. These workers were primarily concerned with transmission specimens and the area

<sup>1</sup> Mongan, *Helv. Phys. Acta*, 5, p. 341 (1932).

struck by the beam was rather larger than if a second aperture had been introduced. Thus, in Mongan's case, the pattern represented the average structure over an area of about 10 mm<sup>2</sup>. of specimen. Sometimes this may prove useful.

Two types of specimen-holder have been adopted by Finch and are shown in Figs. 73 and 74. The first of these, it may be noted, uses flexible bellows. This is a common procedure and is used, in one form or another, by Germer<sup>1</sup> and Morgan and Smith.<sup>2</sup>

The plate-carrier in Finch's camera is another interesting feature (Fig. 75). The fluorescent screen is formed on an aluminium plate which is hinged and lies above the two shutter flaps, so that, when either shutter is raised, the fluorescent screen is lifted also, and half of the photographic plate is exposed. The double-shutter arrangement enables 'comparison' photographs to be taken from transmission specimens.

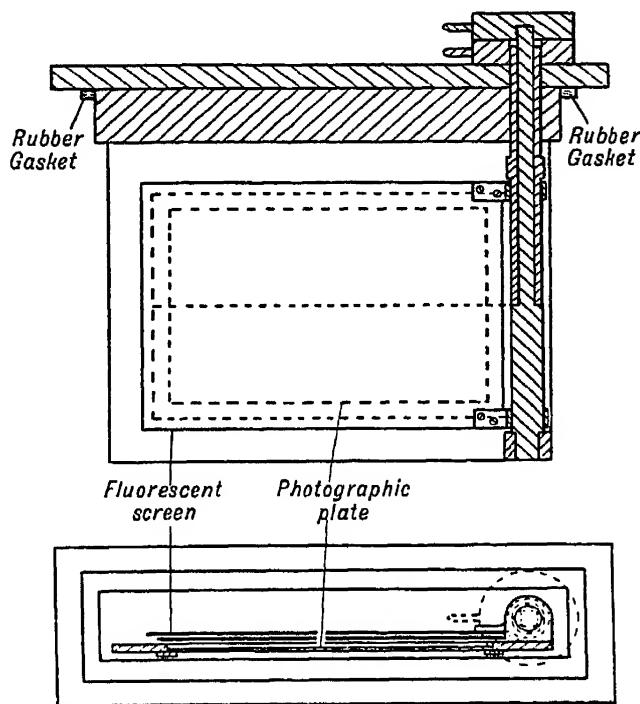


FIG. 75

When it is desired to adopt this procedure, the two specimens to be compared are mounted side by side. One of these may be, for example, a gold foil whose lattice constants are accurately known. The specimens are moved into the beam in turn and, by exposing first with one flap and then with the other, the patterns are obtained side by side. It is arranged that the central spot falls on the dividing line. An example of such a photograph is shown in Plate IX c.

'Comparison' photographs may be taken, of course, with other types of camera, but they are not then obtained with the two patterns placed in juxtaposition in the striking way which results from Finch's procedure. The moving of the appropriate

<sup>1</sup> Germer, *Rev. Sci. Instr.* 6, p. 138 (1935).

<sup>2</sup> Morgan and Smith, *ibid.* 6, p. 316 (1935).

ground joints is performed fairly quickly so as to minimise the risk of a change in the accelerating voltage, which would spoil the accuracy of the comparison. The fluorescent screen is observed through a window in the side of the camera, so that direct measurements cannot be made on the screen as is possible when it is formed on a glass window. A very simple method of obtaining comparison photographs is due to Riedmiller.<sup>1</sup> The electron beam is allowed to diverge from the first anode aperture and is then split into two fine pencils. One of these pencils yields a pattern from a gold film or standard substance

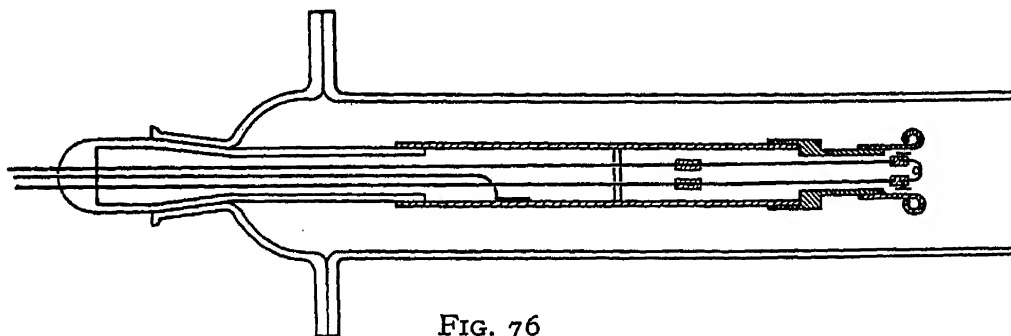


FIG. 76

and the other gives a pattern from the specimen under examination. The patterns are seen a little apart on the screen and are photographed simultaneously.

**HOT CATHODE TUBES.**—While the cold cathode discharge is simple to operate, it sometimes becomes unsteady and will refuse to pass at all at very high voltages. Consequently, many experimenters prefer the hot cathode.<sup>2</sup> Fig. 76 illustrates such a tube used by Tillman. The cathode is a spiral of tungsten wire or an oxide-coated nickel strip. The anode is placed about 2.5 cm. from the cathode and, in order to obtain a strong beam, adjustments are provided by ground joints. Usually a small bias is applied to the control sheath which surrounds the filament. A detailed description of a hot-cathode tube is given by Brockway.<sup>3</sup> Kirchner,<sup>4</sup> who uses pin-hole collimating, introduces a third, slightly larger, aperture between the other two, so that light from the hot filament is cut down.

**HIGH-TENSION SUPPLY.**—Although the induction coil is con-

<sup>1</sup> Riedmiller, *Zeit. für Phys.* 102, p. 408 (1936). Cf. also Thiessen and Schoon, *Zeit. für Phys. Chem. B*, 36, p. 195 (1937).

<sup>2</sup> Cf. Kirchner, *Ann. d. Phys.* 11, p. 741 (1931).

<sup>3</sup> Brockway, *Rev. Mod. Phys.* 8, p. 231 (1936).

<sup>4</sup> Kirchner, *l.c.*

venient, it should be stated that few experimenters use it, transformers being preferred. A typical smoothing circuit is

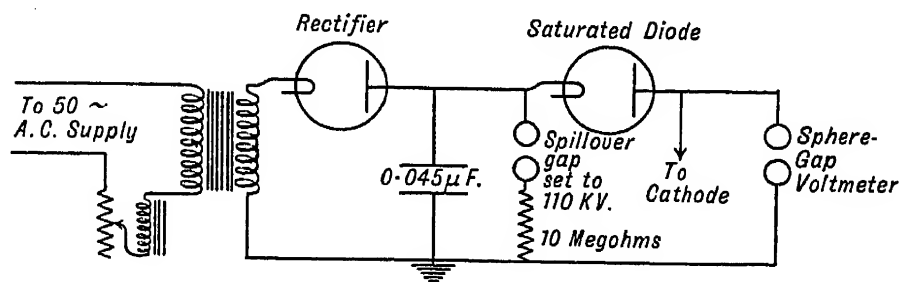


FIG. 77

given by Finch, Quarrell and Wilman<sup>1</sup> (Fig. 77). It is intended for a cold cathode discharge and employs a saturated diode which keeps the *current* in the discharge tube constant. If the gas pressure does not alter, this means that the *voltage* is steady across the discharge tube. In the Thomson-Fraser circuit previously described (p. 222 and Fig. 69) the aim is to keep the voltage across the condenser constant by using a large capacity and a fast interrupter.

**DOUBLE ACCELERATION CAMERA.**—Because of the unsteadiness of the gas discharge above 45 kv. one of the authors<sup>2</sup> has designed a 'double acceleration' apparatus which is illustrated in Fig. 78. The lower part of the camera calls for no comment, being the normal Thomson-Fraser design. The connections to the upper part are shown in Fig. 79. Referring to the diagrams, an insulated induction coil supplies the current rectified by a valve, for the discharge tube A, which is fitted on to the copper base B by a ground joint with a plasticene seal. Copper

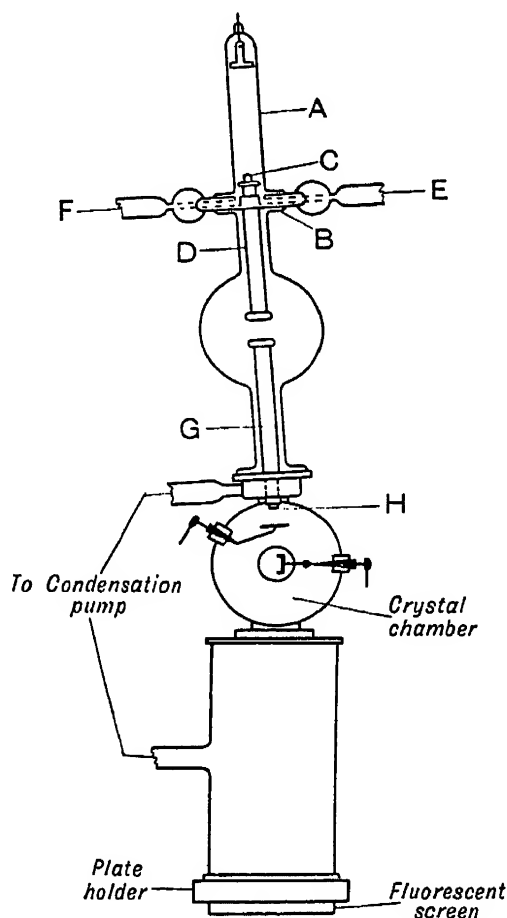


FIG. 78

<sup>1</sup> Finch, Quarrell and Wilman, *Trans. Farad. Soc.* 31, p. 1051 (1935).

<sup>2</sup> G. P. Thomson, *Trans. Farad. Soc.* 31, p. 1049 (1935).

fans and a small fan help to keep the joint cool. A leak of air enters the tube A through E and is pumped out through F by an insulated Hyvac pump with a long leather belt drive. The electrons generated in the discharge tube pass through a small hole (0.2 mm. diameter) in the anode C, which is formed by the top of the copper tube D. The electrons are accelerated again in the field between the copper tubes D and G and finally pass through a second 0.2 mm. aperture at H into the specimen chamber. The high voltage is applied between A and earth and is supplied by a Cockroft doubling-circuit set which happens

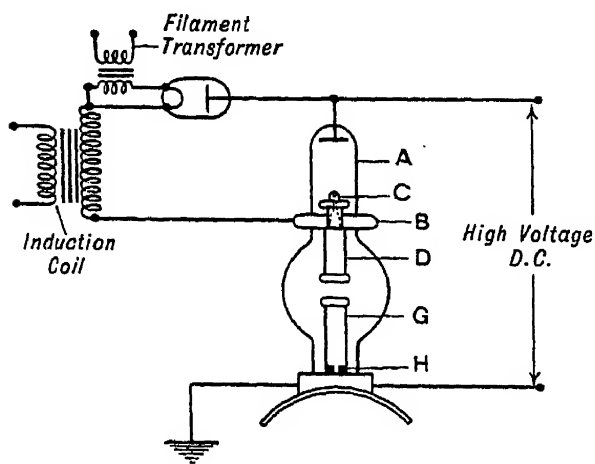


FIG. 79

to be available. Since the current carried by the electron beam between D and G is very small, a steady voltage can be obtained without elaborate smoothing. Owing to the 'electrostatic lens' formed by the field between D and G, the aperture H may be dispensed with and an extremely strong spot can be obtained by adjusting the fields.

With faint patterns this is very useful, but owing to the fact that the focusing depends on the constancy of both discharge potentials it is considered necessary, in normal circumstances, to have the aperture H in position. This apparatus has been worked at 100 kv.

**VOLTAGE OR WAVE-LENGTH MEASUREMENT.**—The spark-gap method of measurement is usually considered<sup>1</sup> to be liable to an error of about 2 per cent in voltage, but it is doubtful whether other methods of measuring high voltages are any more accurate. Kikuchi,<sup>2</sup> in his early experiments on mica used the device shown in Fig. 80. The cathode rays from the discharge tube A were deflected by a magnetic field into two collimating slits  $S_1$ ,  $S_2$  (this also helped to make the rays monochromatic). He determined the wave-length of the rays

<sup>1</sup> Cf. Kaye and Laby, *Physical and Chemical Constants*.

<sup>2</sup> Kikuchi, *Proc. Imp. Jap. Acad.* 4, pp. 271, 275, 354 and 417 (1928); *Japanese Journ. of Physics*, 5, p. 83 (1928).

from the current in the coils producing the field. This was calibrated by taking patterns from a thin aluminium film, and observing the sizes of the diffraction rings for various currents in the coils. The lattice constants of aluminium were assumed to be known. Reid's procedure is described on p. 38.

Germer,<sup>1</sup> and also Aminoff and Broomé,<sup>2</sup> use a standard film of known structure and calibrate the wave-length of the rays in terms of the *primary* volts on the high-tension transformer. They use, of course, a hot filament as source of electrons. De Laszlo,<sup>3</sup> as well as Brockway,<sup>4</sup> employs a high resistance of about 50 megohms across the discharge tube.

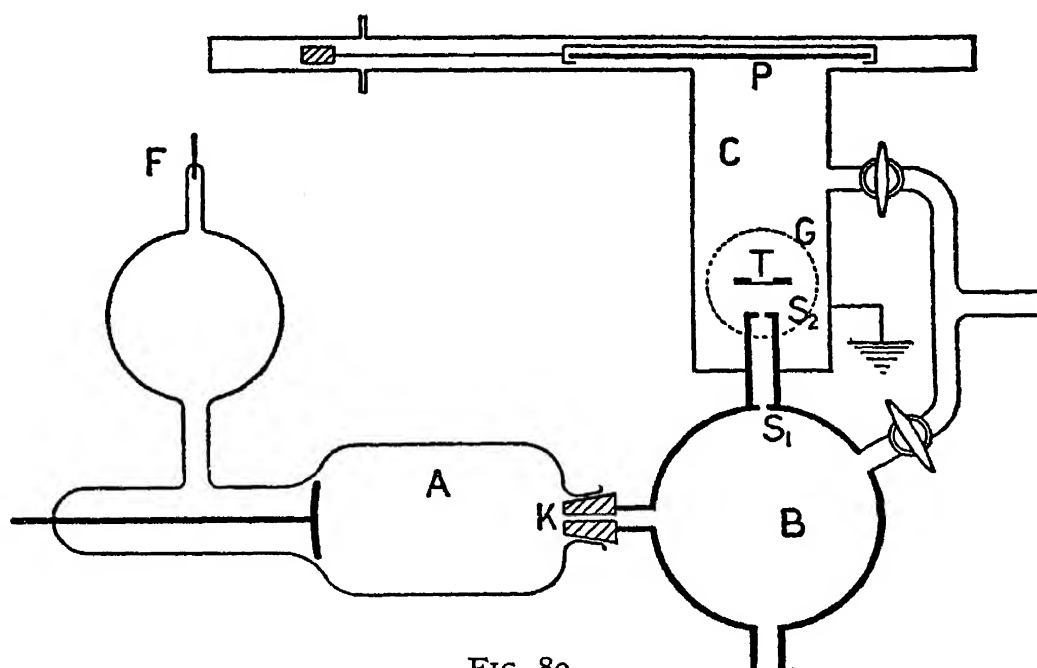


FIG. 80

De Laszlo states that the resistance is mounted in a glass tube round which oil circulates to keep the temperature constant. The current in the resistance is a measure of the voltage and may be calibrated with a standard film such as gold. It is probably better to measure the voltage across a fraction of the resistance rather than measure the current. Unless care is taken in designing the resistance, the results are not usually very accurate.

<sup>1</sup> Germer, *Rev. Sci. Inst.* 6, p. 138 (1935).

<sup>2</sup> Aminoff and Broomé, *Zeit. für Krist.* A91, p. 77 (1935).

<sup>3</sup> De Laszlo, *Proc. Roy. Soc. A*146, p. 672 (1934).

<sup>4</sup> Brockway, *Rev. Mod. Phys.* 8, p. 231 (1936).

Mongan,<sup>1</sup> using a fixed focusing coil, calculated the wavelength  $\lambda$  from the current in the coil when the spot was in focus. Since the focal length is given, it follows from the formula (p. 226) that  $P/i^2$  is a constant. Now  $\lambda \propto P^{-\frac{1}{2}}$  and therefore  $\lambda \propto \text{const.}/i$  if the relativity correction is neglected. The constant was determined by calibrating with a magnesium oxide transmission specimen. A somewhat similar method was used by Tillman.<sup>2</sup>

Finally it may be mentioned that a few investigators employ electrostatic voltmeters.<sup>3</sup>

SHUTTER ARRANGEMENTS.—In place of the shutters already described, many workers use an electromagnet placed near the discharge tube. When the magnet is switched on, the beam is diverted and does not pass down the anode tube. Yearian and Howe<sup>4</sup> use a thyatron circuit with a telephonic stepping relay which operates the electromagnet and gives definite exposures over the range 1/10 sec. to 1 min. Wierl<sup>5</sup> also worked with a relay.

PLATE-HOLDERS.—Although many workers use simply designed plate chambers, not differing essentially from the Thomson-Fraser type, others have introduced more elaborate arrangements. Darbyshire and Cooper<sup>6</sup> have allowed for the accommodation of six plates with separate winches for lowering each plate in turn in front of the fluorescent screen.

Hendricks, Maxwell, Mosley and Jefferson<sup>7</sup> mount five plates in the sectors of a disk which can be rotated with a ground joint. One of the sectors is not occupied by a plate but holds the fluorescent screen, which is observed through a window behind the disk. Eight plates can be mounted in the magazine used by Yearian and Howe,<sup>8</sup> which is of fairly elaborate design.

Trendelenburg and Wieland<sup>9</sup> employ an octagonal drum

<sup>1</sup> Mongan, *Helv. Phys. Acta*, 5, p. 341 (1932).

<sup>2</sup> Tillman, *Phil. Mag.* 8, p. 656 (1934).

<sup>3</sup> Cf. for example Dornte, *J. Chem. Phys.* 1, p. 566 (1933).

<sup>4</sup> Yearian and Howe, *Rev. Sci. Instr.* 7, p. 26 (1936).

<sup>5</sup> Wierl, *Ann. d. Phys.* 8, p. 521 (1931).

<sup>6</sup> Darbyshire and Cooper, *J. Sci. Instr.* 12, p. 10 (1935).

<sup>7</sup> Hendricks, Maxwell, Mosley and Jefferson, *J. Chem. Phys.* 1, p. 549 (1933).

<sup>8</sup> Yearian and Howe, *Rev. Sci. Instr.* 7, p. 26 (1936).

<sup>9</sup> Trendelenburg and Wieland, *Wiss. Veröff. Siemens-Konz.* 13, p. 41 (1934).

containing six plates  $P_1$ ,  $P_2$ , etc. The fluorescent screen  $L$  (Fig. 81) is opposite an opening  $O$ , which allows the screen to be observed through the window  $Gl$ . The slits  $B_1$ ,  $B_2$  and cathode  $K$  present no new features. In de Laszlo's camera<sup>1</sup> a drum is also used; the fluorescent screen is on a hinged metal flap which has to be raised before a photograph is taken. The pattern is observed through a window as in Finch's design. Aminoff's camera<sup>2</sup> has an octagonal drum and, as in de Laszlo's, the drum is surrounded by another cylinder so that the plate-holder assembly may be removed from the camera in daylight. Other arrangements for the accommodation of several plates have been described by Rudiger<sup>3</sup> and by

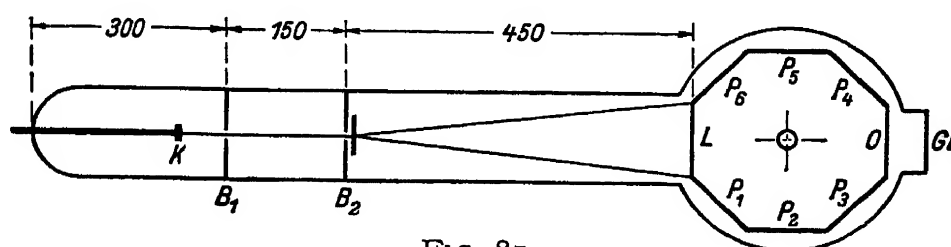


FIG. 81

Richards,<sup>4</sup> the plates being moved along, in turn, from a side chamber into the position for recording patterns by means of ground joints or windlasses.

We have recently set up a camera with the Finch type of plate-holder and, in addition, have provided a 'gate' in the form of a large brass plate which may be moved across so as to cut off the plate-chamber from the rest of the camera. The 'gate' normally rests in a side chamber and is moved by a ground joint. As it goes over into the 'cut-off' position, it rises slightly on ramps and presses against the bottom of the camera tube. A rubber ring is inset into the upper surface of the gate so that a tight fitting is obtained. Thus air can be let in, the plate changed and the plate chamber pumped out again, while a high vacuum is kept in the main part of the camera. This may be useful when it is desired to work with specimens which are prepared in the camera and which must not be allowed to come into contact with the atmosphere.<sup>5</sup>

<sup>1</sup> De Laszlo, *Proc. Roy. Soc. A* 146, p. 672 (1934).

<sup>2</sup> Aminoff, *Intern. Assoc. for Testing Materials, Lond. Congr. Group A* (2), p. 80 (1937).

<sup>3</sup> Rüdiger, *Ann. d. Phys.* 30, p. 505 (1937).

<sup>4</sup> Richards and Bound, *J. Sci. Instr.* 14, p. 402 (1937).

<sup>5</sup> Cf. also Thiessen and Schoon, *Zeit. für Phys. Chem. (B)* 36, p. 195 (1937).

SPECIMEN CHAMBERS.—Either ground joints or flexible bellows have to be used to move the specimen inside the apparatus and sufficient has already been said to indicate how this is done. Usually, only three motions are required, but one of our modified Thomson-Fraser cameras has now been fitted with another small cone which gives a fourth motion, parallel to the surface of the specimen. Scales can also be provided at the tops of the cones so that the positions of the specimen can be quantitatively related to one another.

Aminoff and Broomé,<sup>1</sup> in their earlier camera, placed both the specimen-holder and plate-holder in a large rectangular box. The arrangement inside the box is something like an optical bench, and very precise adjustments of specimen and plate can be made.

Heating coils and evaporating assemblies are often introduced near the specimen, and generally mounted on ground joints so as to be movable. A simple heating device has been described by one of the authors;<sup>2</sup> a nickel capsule with an internal heating coil is used as a base on which the specimen is deposited. Yearian and Howe<sup>3</sup> describe a specimen holder which enables the specimen to be heated up to 600° C. and also to be cooled down to liquid air temperatures.

For the diffraction of electrons by gas molecules, the arrangement required is different from what is used in dealing with solids. Details are given in Chapter XVII (p. 246).

When it is wished to take diffraction patterns by reflection from liquid surfaces, a horizontal camera will generally be desirable. Patterns are readily obtained from a small drop of oil on a metal block. Otherwise, the liquid may be held in a not too small cup filled to the brim, an arrangement being provided for raising and lowering the cup.<sup>4</sup> Clearly, liquids with a large vapour pressure will be difficult to deal with.

ELECTRICAL MEASUREMENTS OF ELECTRONIC PATTERNS.—Kirchner<sup>5</sup> has described the use of a Faraday cylinder (with a small opening) to detect parts of the diffraction pattern. He deflected the pattern, as required, with a magnetic field

<sup>1</sup> Aminoff and Broomé, *Zeit. für Krist.* A91, p. 77 (1935).

<sup>2</sup> Thomson, *Proc. Roy. Soc.* A128, p. 641 (1930).

<sup>3</sup> Yearian and Howe, *Rev. Sci. Instr.* 7, p. 26 (1936).

<sup>4</sup> Jenkins, *Proc. Phys. Soc.* 47, 109 (1935).

<sup>5</sup> Kirchner, *Ann. d. Phys.* 11, p. 741 (1931).

and measured the charge entering the cylinder in a given time, using a string electrometer. One of us<sup>1</sup> has employed a Faraday cylinder the small opening of which can be moved about by means of ground joints. Beeching<sup>2</sup> moved the Faraday cylinder into different positions by means of a ground joint and measured the current with a Lindeman electrometer shunted with a  $10^{11}$  ohm resistance. The electronic currents to be measured are so small ( $\sim 10^{-12}$  amps. or less) that a galvanometer can scarcely be used.

### Preparation of Specimens

*General.*—The sensitivity and peculiarities of the electron diffraction method of investigation necessitate some care in the choice and preparation of specimens. Thus materials which have been touched with the fingers, or exposed for an appreciable time to the atmosphere of a laboratory or workshop, are almost certain to be covered with a thin film of grease or other contamination, and this may be sufficient to prevent the formation of a pattern characteristic of the material itself. In many cases immersion in ether, benzene or some other solvent may serve to remove such impurities and leave the specimen clean. A more serious difficulty arises from the fact that the material presented to the experimenter may not be in the most suitable form for obtaining distinct patterns. Reflection specimens should preferably have a plane surface and not be too rough, but it is quite often possible to obtain patterns from curved specimens, and even from comparatively rough surfaces. Thus it may be said that most specimens will give a reflection pattern if a good camera is used, and it is always worth while to try. The investigator is, moreover, usually in the position of being able to begin by choosing his material in a convenient form for examination in the electron diffraction camera during any stage of a given physical or chemical treatment. One can thus be sure of obtaining distinct patterns and, in this way, a large number of surface structure problems have been attacked — oxidation, corrosion, passive layers, polish, crystal growth and orientation, etc., as described

<sup>1</sup> Cochrane, *Phil. Mag.* 18, p. 956 (1934).

<sup>2</sup> Beeching, *Phil. Mag.* 20, p. 84 (1935).

in Chapters XII-XV. In what follows a brief résumé is given of various ways in which specimens may be prepared in a form suitable for electron diffraction.

**REFLECTION SPECIMENS.**—Normally the reflection specimen is a rectangular block measuring  $1 \times 1 \times 0.5$  cm. and one of the square faces is used as the surface to be investigated. In preparing a metal specimen, the surface is ground on various grades of emery paper using benzene as a lubricant. It is then gently etched either by total immersion in the etching liquid or by applying the reagent with a camel-hair brush; subsequently the specimen is washed—usually in water (distilled), then absolute alcohol and finally in benzene. The aim is to obtain a clean and slightly matt surface of the material.<sup>1</sup> Typical etching solutions are: for copper, 10 per cent ammonium persulphate in water; for iron, 5 per cent nitric acid in absolute alcohol followed by 5 per cent picric acid in absolute alcohol; for chromium, concentrated hydrochloric acid; for gold, *aqua regia*; and so on. In many cases, however, where the metal is to be oxidised or chemically treated, etching is dispensed with and the surface is simply ground as flat as possible or even polished. When, for example, an oxide layer is then formed, it is almost invariably sufficiently matt in texture to give excellent patterns. Reflection specimens of metals may also be obtained by evaporating (*in vacuo*) from a tungsten filament or some kind of oven, or by spluttering, on to glass or quartz; or by electrodeposition on to another metal surface. For many purposes it is desirable to use the metal in the form of a single crystal. The production of such metal crystals entails a somewhat elaborate technique and is not described here.<sup>2</sup> A single-crystal rod of metal having been obtained, the crystallographic axes have to be determined in order that a specimen may be cut out with a simple face such as (100). These axes may be found by an X-ray examination or by the use of Bridgman's 'sphere method'.<sup>3</sup> It is usually found difficult to cut the crystal exactly to a given plane. Examination in the electron diffraction camera will indicate how much the actual surface deviates from the desired crystallo-

<sup>1</sup> Cf. French, *Proc. Roy. Soc. A*140, p. 637 (1933).

<sup>2</sup> Cf. Desch, *Metallography* (4th ed.), p. 187 (Longmans, Green & Co.).

<sup>3</sup> Bridgman, *Proc. Am. Acad. Arts Sci.* 60, p. 313 (1925).

graphic plane, and the specimen may be corrected by grinding. We have found that a small metal crystal can often be made by simply allowing a molten bead to cool very slowly. Sometimes single crystals may be cut out of large pieces of cast metal. Metal crystals must be etched after grinding, since such treatment renders the surface polycrystalline.

The same general principles apply to the preparation of non-metallic reflection specimens as in the case of metals. The method of depositing the material as a thin layer on a block of glass or metal is often used. In addition, a very large number of single crystals (such as calcite, rock-salt, zinc blende, etc.) may be cleaved, and the diffraction patterns from such cleavage faces are of great interest since they yield information regarding the inner potential of the crystal (cf. p. 155). In some cases (for example, diamond) the natural face may also be examined directly without treatment. A difficulty sometimes occurs with reflection specimens, in that they 'charge up' and repel the electron beam. The result is that only a flickering smudge is seen on the fluorescent screen. With metals this charge is immediately balanced through the earth connection. But insulators may retain the charge for a time. The difficulty is generally surmounted by careful adjustment of the angle of incidence and position with regard to the beam, neutralisation being brought about by the emission of secondary electrons. It is sometimes helpful to coat the side of the specimen with a conducting layer where contact is made with the screws of the specimen holder.

TRANSMISSION SPECIMENS.—Many metals are obtainable in the form of foil or leaf, in some cases thin enough to allow electrons to pass through and give a pattern. Generally, however, it will be necessary to thin the foil by floating it on the surface of some etching bath. When the foil is just on the point of disintegrating it is removed on a glass spoon and transferred to other baths to wash it. Finally, it is lifted out on a small aluminium or brass disk pierced with a hole 1-3 mm. in diameter and allowed to dry. Finch, Quarrell and Wilman<sup>1</sup> recommend the use of fine nickel gauze as a support. Thinning may also be done by the electrolytic method.

Commercial foils sometimes contain impurities and, in addi-

<sup>1</sup> Finch, Quarrell and Wilman, *Trans. Farad. Soc.* 31, p. 1050 (1935).

tion, owing to rolling and beating, the crystal grains are often large. Consequently it is common practice to make metallic films by spluttering or evaporation of the metal on to a cellulose acetate base. A solution of pure cellulose acetate in acetone is clarified by filtering. Some of the solution is poured on to a clean glass plate, allowed to solidify and stripped off; this is done in order to remove specks or dust particles from the plate. When the plate has warmed up again to room temperature enough solution is poured on to form a film rather too thick to show interference colours but of that order. Round the edges of this film more solution, is applied with a paint brush as the first lot dries. In this way a kind of frame is built up round the thin centre portion which can be lifted off by means of the frame. Spluttering is done by producing a direct current discharge in a bell jar with a current of 1-3 mA. and a Crookes dark space of 1 cm. The cellulose acetate base is placed 3 cm. below the cathode, which is made of the metal to be spluttered. Evaporation may also be done in a bell jar from a bead of metal on an electrically heated tungsten loop or strip on to the cellulose acetate base, which is placed 3-4 cm. away. In the case of evaporation, a 'black' vacuum is desirable in the bell jar. After spluttering or evaporation, the composite film is removed from the bell jar and the cellulose acetate dissolved off in a bath of acetone. Subsequently, the metal film is washed in several separate dishes of acetone before being mounted in the usual way. In order to obtain films free from holes, it is necessary to make the cellulose acetate films and transfer them to the bell jar in a carefully sealed fume cupboard through which a stream of filtered air is drawn. Otherwise, minute dust particles settle on the surface of the cellulose acetate and interrupt the continuity of the metal film. A variant of this method is to substitute a piece of polished rock-salt for the cellulose acetate, the rock-salt being removed from the metal film by solution in brine. Films prepared by spluttering often give rather broad rings, indicating small grain size. The size and orientation of the crystal grains depend on the temperature of the base and on the discharge conditions. A warm base helps the formation of oriented crystallites and fast deposition favours small grain size.<sup>1</sup> Evaporated films

<sup>1</sup> Finch, Murison, Stuart and Thomson, *Proc. Roy. Soc. A*141, p. 414 (1933).

usually have a tendency to show preferred orientation of the crystallites, this effect being controlled by the temperature of the base <sup>1</sup> and the geometry of the arrangement <sup>2</sup> (cf. p. 168).

Another 'stripping' method is due to Finch and Sun.<sup>3</sup> A thick film of copper or other basis metal is plated on to a stainless steel surface. On top of this a suitable thickness of the required metal is plated, using the customary electroplating baths. The copper is freed from the steel with a knife and the composite film floated on an etching reagent (such as KCN solution) which dissolves the copper or basis metal and leaves a film of the required metal. Washing follows as before.

Transmission photographs of many substances may be obtained by Kirchner's method, which utilises a thin celluloid, collodion or cellulose acetate film as a support.<sup>4</sup> In this case the pattern from the supporting film is also obtained. Usually, however, this pattern consists of very diffuse rings and does not cause any confusion. These films are made by dissolving cellulose acetate or celluloid in amyl acetate (or alcohol ether),<sup>5</sup> flowing a drop of the solution over the surface of a dish of water and allowing the solvent to evaporate. A piece of the film can then be picked up on a diaphragm or on gauze. It is desirable that the supporting films should be as thin as possible. The substance to be examined has now to be deposited on the celluloid film. This may be done by crystallisation from solution or by colloid precipitation,<sup>3</sup> or by vaporisation.

Mongan <sup>5</sup> has obtained specimens of 'soots' by allowing the substance to collect on a fine-meshed copper-wire gauze. The wire was 0.04 mm. in diameter and there were 64 meshes/mm.<sup>2</sup>. Muto and Yamaguti <sup>6</sup> as well as Trendelenburg and Wieland <sup>7</sup> have used a spider's web in a similar way to gauze, allowing a 'dust' to settle on it.

Otty, working at Aberdeen, found that good transmission specimens of zinc oxide could be made by dipping a loop of wire, covered with a little chloride as flux, under the surface

<sup>1</sup> Dixit, *Phil. Mag.* 16, p. 1046 (1933).

<sup>2</sup> Beeching, *Phil. Mag.* 22, p. 938 (1936).

<sup>3</sup> Cf. Finch, Quarrell and Wilman, *Trans. Farad. Soc.* 31, p. 1057 (1935).

<sup>4</sup> Kirchner, *Phys. Zeit.* 31, p. 772 (1930).

<sup>5</sup> Mongan, *Helv. Phys. Acta*, 5, p. 341 (1932).

<sup>6</sup> Muto and Yamaguti, *Proc. Imp. Jap. Acad.* 5, p. 122 (1929).

<sup>7</sup> Trendelenburg and Wieland, *Wiss. Veröff. Siemens-Konz.* 13, p. 14 (1934).

of molten zinc and slowly withdrawing the wire. This may be done with other metals (see, for example, Plate I), and a wire gauze may be used in place of a loop.<sup>1</sup> It will be recalled that in Kikuchi's early experiments, cleavage slips of mica  $\sim 10^{-5}$  cm. thick were examined by transmission. Aminoff and Broomé have prepared specimens of other crystals which split into flakes like mica — these were brucite, talc, graphite, auripigmentum (orpiment), molybdenite and waluewite. When 'spot' patterns are desired they state that the mica should be of such a thickness that Newton's colours of the first order are seen by reflection from the surface. The same applies to brucite and talc. Some of the others are difficult to split. Aminoff and Broomé recommend that a piece of the crystal should be pressed on to some wax and then torn, so that a sufficiently thin piece is left on the wax. The molybdenite flake should appear yellow when held in front of a strong light, and graphite a bright grey, according to these authors. They have also been able to obtain transmission patterns from other crystals which do not cleave into flakes. This was done simply by finding a piece in the form of a wedge-shape, the faces of the wedge being cleavages. Usually there are various cleavage planes so that a piece of this shape is possible. The crystal was mounted so that the beam struck just at the sharp edge of the wedge.

Thin films of paraffin, stearic acid and similar compounds have been made by Trillat and Hirsch.<sup>2</sup> A solution of the substance was prepared using ether or other solvent and a drop of solution was allowed to flow over the surface of water. After evaporation of the solvent, the films were picked up with disks in the usual way.

Maxwell<sup>3</sup> obtained transmission specimens of liquids by holding a film of the liquid in a small wire loop.

### Measuring Patterns

Although it is possible to tell much merely by looking at a pattern, it is always advisable to measure up the distances of the rings or spots from the central spot and calculate out the

<sup>1</sup> Finch, Quarrell, and Wilman, *l.c.*

<sup>2</sup> Trillat and Hirsch, *J. de Phys. et le radium*, 4, p. 38 (1933).

<sup>3</sup> Maxwell, *Phys. Rev.* 44, p. 73 (1933).

Bragg spacings,  $d$ , from the formula  $d = L\lambda/r$ , where  $L$  represents the camera length (from specimen to screen),  $\lambda$  is the wave-length and  $r$  the distance measured on the plate.<sup>1</sup> In addition any other features such as side-spacings and angular width of arcs, etc., should be quantitatively determined. The plate may be held up to the northern sky and measured with dividers. Otherwise a piece of opal glass with a lamp behind it serves as a source of illumination. Sometimes a frame with two needles sliding in two directions at right angles, along graduated scales, is used in place of dividers. For plates with

TABLE XVI

SPARKING POTENTIALS AND ELECTRONIC WAVE-LENGTHS  
For 5 cm. diameter spheres and 760 mm. pressure at 20° C. ;  
one sphere earthed

Gap (cm.)	Kilovolts	$\lambda$ (Å)
0.50	17.5	0.0915
0.60	20.4	0.0846
0.70	23.2	0.0792
0.80	26.1	0.0745
0.90	28.9	0.0708
1.00	31.8	0.0674
1.10	34.5	0.0646
1.20	37.1	0.0622
1.30	39.9	0.0599
1.40	42.5	0.0579
1.50	45.0	0.0567

$$\text{Note. — } \lambda_{\text{Å}} = \frac{12.21}{\sqrt{P_{\text{volts}}}} \times \frac{1}{\sqrt{1 + 9.82 \times 10^{-7} P_{\text{volts}}}}$$

diffuse rings such as arise in work with gases some experimenters<sup>2</sup> recommend a 100-watt 'Pearl' light rather than a *uniform* source of illumination. A rheostat is also used to adjust the brightness. When working with a spark-gap we use a graph which gives  $\lambda$  directly as a function of gap-width under normal atmospheric conditions. The relativity correction has to be included in calculating  $\lambda$  for fast electrons.

<sup>1</sup> In cases where  $r$  is large, allowance may be made for the fact that the tan of the angle of deviation is not the same as the angle itself.

<sup>2</sup> Gregg, Hampson, Jenkins, Jones and Sutton, *Trans. Farad. Soc.* 33, p. 852 (1937).

Table XVI gives  $\lambda$  in Ångströms against spark width in cm. and will enable a graph to be drawn.

### Intensity Measurements

For some purposes, as, for example, the determination of 'E' curves, intensity measurements of the electron diffraction patterns are required. A Faraday cylinder may be introduced for this purpose but the intensities may also be found from the photographic plate using a microphotometer.<sup>1</sup> In the latter case, however, it cannot be assumed that the blackening is simply proportional to the electronic intensity. Ellis has shown that for electrons the blackening or density,  $D$ , is a function of  $It$ , the product of intensity and time. The procedure to be adopted is therefore as follows. Two exposures of the pattern are made side by side on the same plate, which is developed in a Dobson tank to ensure equal development all over. The times of the two exposures are in a known ratio; for example, 2:1. The patterns are then microphotometered, and densities of pairs of corresponding points on the two exposures are tabulated. Each pair of densities is plotted with density as ordinate and a difference of abscissa equal to  $\log 2$  (the logarithm of the exposure ratio). Each pair of points is shifted parallel to the axis of abscissae until the whole lie on a smooth curve, which gives  $D$  as a function of  $\log (It)$ . From this a second curve is drawn giving density against  $It$ .

### Reproduction of Diffraction Patterns

Patterns from single crystals are usually fairly strong and relatively free from background so that no difficulty is encountered in making prints from the plates. Ring patterns, however, and especially those with diffuse rings, are always very intense near the central spot. If a soft printing paper is used, such patterns do not show up very well, while if a contrasty paper is used it is difficult to get the whole of the pattern clearly reproduced. Trendelenburg<sup>2</sup> has suggested a method of overcoming this difficulty. The printing is done on a rotating

<sup>1</sup> Cf. Thomson, *Proc. Roy. Soc.* 125, p. 352 (1929).

<sup>2</sup> Trendelenburg and Franz, *Wiss. Veröff. Siemens-Konz.* 13, p. 48 (1934).

gramophone table, the centre of the pattern being at the centre of the table. Light falls on the plate through a radial slot in a cover held over the table. The central part of the pattern therefore receives more light than the parts further out. A further refinement of the method is possible by altering the shape of the slot to suit any particular plate.

## CHAPTER XVII

### DIFFRACTION BY GAS MOLECULES

*General.*—The diffraction of fast electrons by gas molecules has now become of considerable importance in the study of molecular structure and, where comparison is possible, the results usually agree well with those obtained by other methods (X-rays, infra-red and Raman spectra, dipole moments). The first detailed results were published by Wierl<sup>1</sup> in 1931 following on the preliminary announcement of the experiments in 1930.<sup>2</sup> Other workers have since entered the field. A notably large number of investigations have been made in the United States, and have been published in such periodicals as the *Journal of the American Chemical Society* and the *Journal of Chemical Physics*.

Experiments on the diffraction of *slow* electrons by gas molecules are quite distinct from those mentioned above. They may be said to have begun with the work of Ramsauer (1921), and only monatomic or simple polyatomic gases have been used. The interest of such experiments lies mainly in such matters as the determination of the angular distribution of scattered electrons over large angles and in the comparison of the results with precise wave-mechanical collision theory. Since accounts of this work have been given by Arnot<sup>3</sup> and Mott and Massey,<sup>4</sup> it will not be discussed here.

#### Apparatus

Except for having a special device for obtaining a jet of gas, the apparatus used in the diffraction of electrons by gas molecules does not differ essentially from the ordinary electron camera. Wierl<sup>1</sup> used a gas discharge tube, collimating the beam

<sup>1</sup> Wierl, *Ann. d. Phys.* 8, p. 521 (1931), and 13, p. 453 (1932).

<sup>2</sup> Mark and Wierl, *Naturwiss.* 18, p. 205 (1930).

<sup>3</sup> Arnot, *Collision Processes in Gases*. Methuen.

<sup>4</sup> Mott and Massey, *Atomic Collisions*. Oxford.

with the usual two pin-holes 10 cm. apart and 0.16 mm. (or less) in diameter. Since the patterns consist of a series of diffuse rings, it is desirable to keep down any random scattering in the apparatus as much as possible, since such scattering will make it difficult to distinguish the rings in the pattern. There is no doubt that a certain amount of scattering takes place at the edge of the last col-

limating aperture. Hence Wierl mounted the last aperture behind a small disk which contained a slightly larger opening in the form of a cylinder 0.18 mm. in diameter and 1 mm. long. This kept back these scattered electrons and improved the photographs. The gas nozzle (see Fig. 82) was cone-shaped, terminating in an opening of 0.1 mm. diameter, and the adjustment of the end of the nozzle close to and in line with the last collimating aperture, was very important. The substance under examination was contained in the glass bulb shown, which was connected through a tap

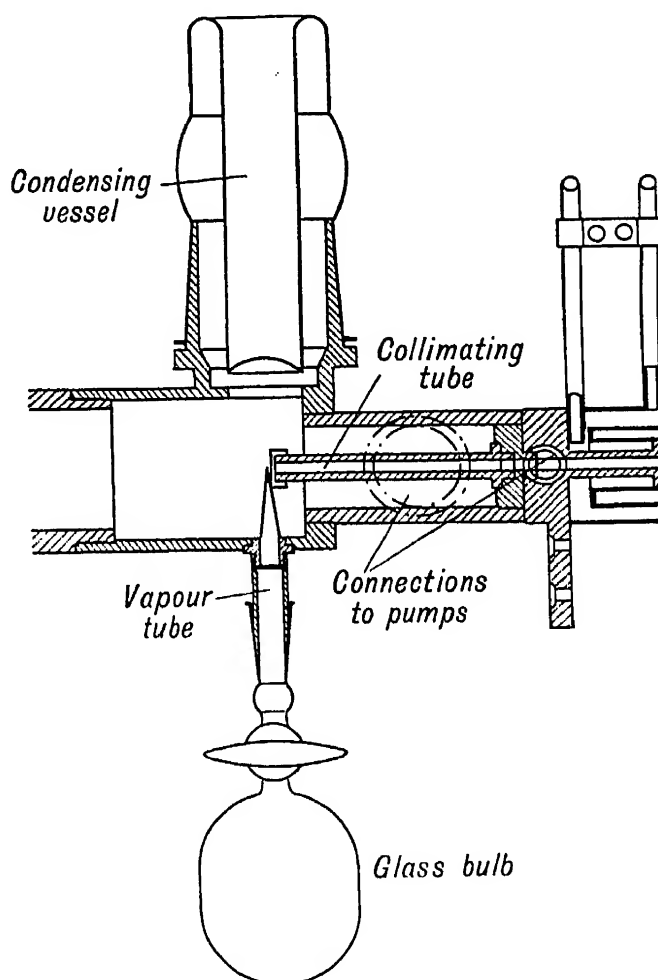


FIG. 82

to the nozzle, a ground joint allowing the bulb to be removed easily when necessary. The flow of vapour out of the nozzle had to be controlled to some extent. If the substance did not give sufficient vapour at room temperature, a bath of hot water was placed round the bulb; if the vaporisation was too rapid, an ice bath was used. In the case of gases, a suitable pressure in the bulb had to be found by experience. The emerging gas or vapour, after crossing the electron beam, was condensed on a metal surface cooled by liquid air, so that a good vacuum

was maintained in the camera. Substances which were difficult to vaporise were carried in a small tungsten boat which could be electrically heated. The tungsten was placed behind the

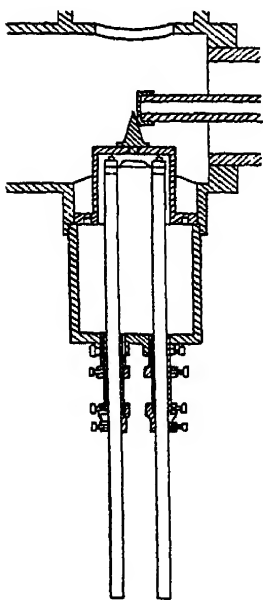


FIG. 83

nozzle and mounted in a small side chamber (see Fig. 83, taken, with 82, from Wierl, *l.c.*).

An electromagnet, near the discharge tube, was used to deflect the beam and thus act as a shutter. A relay was arranged to 'open' the shutter for, say,  $\frac{1}{10}$ th sec. during the period when the tap on the bulb was opened and closed, the electron beam passing during the time that vapour was emerging. Often several exposures under identical conditions were made on the same plate or film in order to get a stronger pattern. Obvious modifications in the procedure were adopted when the substance had to be heated on tungsten.

Another design of camera for 'gas diffraction' is due to de Laszlo.<sup>1</sup> In this camera Wierl's type of nozzle is replaced by the one shown (Fig. 84). On leaving the narrow exit-tube the vapour does not pass immediately to the cooled surface, but is made to flow along a short tube 2 mm. in diameter, down which the electron beam travels. In this way a strong concentration of the vapour is attained over an appreciable volume. By means of a ground joint the nozzle can be moved slightly in order to get good alignment.

Brockway<sup>2</sup> has given an account of another camera which is being used extensively in the United States. The gas jet is a small hole 0.3 mm. diameter in the top of a cylindrical tube which fits into the side of the camera (Fig. 85). A ground joint is also provided, so that the jet may be adjusted exactly under the electron beam, which passes 2 mm. above it. No condensing surface is used but, instead, a tube fits quite closely right over the nozzle. This tube is connected to a fast pump and most of the vapour is removed immediately. Two small apertures

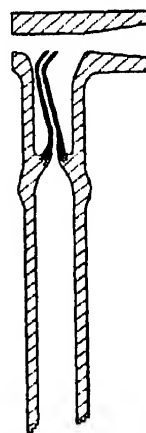


FIG. 84

<sup>1</sup> De Laszlo, *Proc. Roy. Soc. A*146, p. 672 (1934).

<sup>2</sup> Brockway, *Reviews of Modern Physics*, 8, p. 231 (1936).

have to be made in the pumping-off tube to allow the electron beam to pass through the vapour. In Fig. 85 the electron beam follows the path of the horizontal dotted line, moving from the collimating apertures on the left towards the right. In order to get a good jet of molecules the vapour pressure in the side bulb, containing the substance under investigation, must be from 100 to 200 mm. of mercury.

Maxwell,<sup>1</sup> Hendricks, Mosley and Jefferson describe a camera with a nozzle 0.3 mm. diameter and 5 mm. long. The pressure in the side chamber or boiler has to be about 10 mm. of mercury. In a later apparatus<sup>2</sup> they have the last collimating aperture fixed to the jet. Dornte<sup>3</sup> uses a nozzle 0.1 mm. in diameter with a pressure of 150 mm. of mercury in the side chamber.

Other cameras for diffraction by gases have been described by Cosslett<sup>4</sup> and Grether.<sup>5</sup>

### Theory

We consider first a single molecule consisting of various atoms in fixed positions. Take one of the atoms as origin and let  $\mathbf{r}_i$  be the vector to a representative atom  $i$ . When an electron wave, of wave-length  $\lambda$ , falls on the molecule each atom will scatter a wavelet. The path difference between the waves scattered in a direction  $\mathbf{s}$  by the atom at the origin and the  $i$ th atom is  $(\mathbf{r}_i, \mathbf{s} - \mathbf{s}_0)$ , where  $\mathbf{s}_0$  is the direction of the incident wave;  $\mathbf{s}$  and  $\mathbf{s}_0$  being unit vectors. Hence, if we take the phase of the wave scattered at the origin as zero, we obtain for the amplitude of the wave scattered by the molecule in the direction  $\mathbf{s}$ :

$$\sum E_i e^{-iK(\mathbf{r}_i, \mathbf{s} - \mathbf{s}_0)},$$

where  $E_i$  is the atomic scattering factor for the  $i$ th atom and is

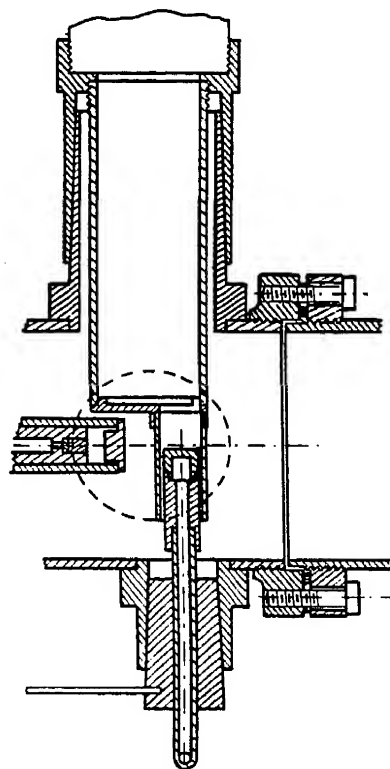


FIG. 85

<sup>1</sup> Maxwell, etc., *J. Chem. Phys.* 1, p. 549 (1933).

<sup>2</sup> Maxwell, etc., *ibid.* 3, p. 699 (1935). <sup>3</sup> Dornte, *ibid.* 1, p. 566 (1933).

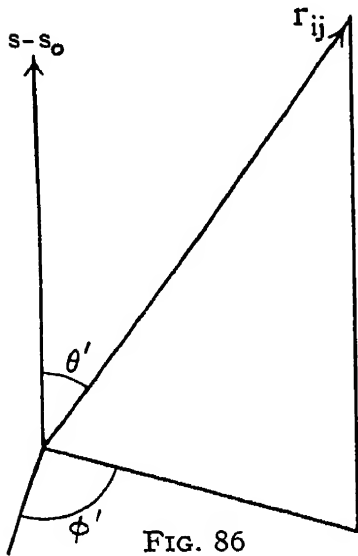
<sup>4</sup> Cosslett, *Trans. Farad. Soc.* 30, p. 981 (1934).

<sup>5</sup> Grether, *Ann. d. Phys.* 26, p. 1 (1936).

a function of  $\mathbf{s}$  and  $\mathbf{s}_0$ ;  $K = 2\pi/\lambda$ . We neglect certain unessential factors which are the same for all atoms, the screen being very far off. To get the intensity of the wave (which gives the probability of an electron being scattered in the direction  $\mathbf{s}$ ) we multiply by the complex conjugate.<sup>1</sup> The result is

$$\sum_i \sum_j E_i E_j e^{iK(\mathbf{r}_{ij}, \mathbf{s} - \mathbf{s}_0)}, \quad . \quad . \quad . \quad (1)$$

where  $\mathbf{r}_{ij} = \mathbf{r}_i - \mathbf{r}_j$  and is the vector from the  $i$ th to the  $j$ th atom.



Now, suppose that there is a large number,  $N$ , of molecules in all possible orientations and randomly distributed. The intensity of the scattered wave for all the molecules is obtained by summing expression (1) over all possible orientations. We may simply fix on one direction  $\mathbf{r}_{ij}$  in the molecule and allow it to be varied continuously. To perform the necessary integration choose  $\mathbf{s} - \mathbf{s}_0$  as polar axis of spherical polar coordinates  $\theta'$ ,  $\phi'$  (Fig. 86). The number of molecules with  $\mathbf{r}_{ij}$  lying between the directions  $\theta'$  and

$\theta' + d\theta'$ ,  $\phi'$  and  $\phi' + d\phi'$  is

$$\frac{N}{4\pi} \sin \theta' \cdot d\theta' d\phi'.$$

Also  $(\mathbf{r}_{ij}, \mathbf{s} - \mathbf{s}_0) = |\mathbf{r}_{ij}| \cdot |\mathbf{s} - \mathbf{s}_0| \cdot \cos \theta'$

and  $|\mathbf{s} - \mathbf{s}_0| = 2 \sin \frac{\phi}{2},$

where  $\phi$  is the angle between  $\mathbf{s}$  and  $\mathbf{s}_0$ . Hence if

$$x_{ij} \equiv \frac{4\pi}{\lambda} \sin \frac{\phi}{2} \cdot r_{ij}$$

we find for the number of electrons scattered through an angle  $\phi$

$$\begin{aligned} I(\phi) &\propto \int_0^\pi \int_0^{2\pi} \sum_i \sum_j E_i E_j e^{ix_{ij} \cos \theta'} \sin \theta' d\theta' d\phi' \\ &\propto \sum_i \sum_j E_i E_j \frac{\sin x_{ij}}{x_{ij}}. \end{aligned}$$

<sup>1</sup> The intensity is the modulus squared. If the wave is  $a + ib$ , the intensity is  $a^2 + b^2$ , which is  $(a + ib)(a - ib)$ .

This is sometimes referred to as Wierl's formula.<sup>1</sup> A similar expression was given by Debye<sup>2</sup> and Ehrenfest<sup>3</sup> for X-rays.

If 
$$\mu \equiv \frac{4\pi}{\lambda} \sin \frac{\phi}{2}$$

we can write

$$I = \sum_i \sum_j E_i E_j \frac{\sin \mu r_{ij}}{\mu r_{ij}}. \quad (2)$$

It is seen that terms where  $i = j$  reduce to  $E_i^2$ , they represent the scattering by single atoms. Also it will be noticed that each *pair* of atoms enters *twice* into the summation, but in practice each pair will only be considered once. An expression for  $E_i$ , the atomic scattering factor, has already been given on p. 93. Omitting constants, it may be written,

$$E_i = \frac{Z_i - f_i}{\mu^2},$$

where  $Z_i$  = the atomic number and  $f_i$  = the X-ray atomic form-factor, which is a function of  $\phi$ . The function  $E_i$  does not show any maxima or minima and so the terms in (2) for which  $i = j$  do not give rise to any distinctive pattern. Strictly, one must also add a term to (2) to represent the incoherently scattered electrons. If we consider each atom to scatter separately, we can utilise the expression for the incoherent intensity given by Morse (see p. 104). For the  $i$ th atom it is of the form

$$\frac{S_i(v_i)}{\mu^4},$$

where  $v_i = \mu \times 0.176 \times Z_i^{-\frac{1}{3}}$  and  $S_i(v_i)/Z_i$  has been tabulated as a function of  $v_i$  by Bewilogua.<sup>5</sup>  $S_i/\mu^4$  shows no maxima or minima, and tends to zero rapidly as  $\phi$  increases. The final value for  $I$  now becomes

$$I(\phi) = \frac{1}{\mu^4} \sum_i \sum_j (Z_i - f_i)(Z_j - f_j) \frac{\sin \mu r_{ij}}{\mu r_{ij}} + \frac{1}{\mu^4} \sum_i S_i(v_i). \quad (3)$$

It is clear from this rather complicated expression that the

<sup>1</sup> For an alternative proof cf. Thomson, *Conduction of Electricity through Gases*, vol. ii. p. 62.

<sup>2</sup> Debye, *Ann. d. Phys.* 46, p. 809 (1915).

<sup>3</sup> Ehrenfest, *Amsterdam Acad.* 23, p. 1132 (1915).

<sup>4</sup> This is now usually denoted by  $s$  in experimental papers.

<sup>5</sup> Bewilogua, *Phys. Zeit.* 32, p. 740 (1931).

interpretation of electron diffraction patterns from gas molecules is not so straightforward as in the case of crystalline solids. Generally speaking, a trial and error method must be adopted; a molecular model of definite dimensions has to be found such that  $I(\phi)$  calculated from (3) agrees with the experimental results. The patterns obtained are all of the same form — a central spot surrounded by a number of concentric diffuse rings (Plate X *d*). However, when microphotometer records are made from the plates they do not, as a rule, show any definite maxima at all, but only a general fall-off in intensity with points of inflexion corresponding to the rings which are seen by the eye. Apparently the eye discounts the steady decrease in the background and interprets any change in the rate of decrease as a maximum or a minimum. Also the eye detects many rings far out from the central spot which do not show up in the microphotometer records.

In interpreting the photographs the 'visual method' is therefore commonly used. The incoherent scattering and the coherent atomic scattering, which do not give maxima and minima, are neglected. The factor  $(Z_i - f_i)$  is replaced by  $Z_i$  and the factor  $\mu^{-4}$  is omitted. This leaves the expression

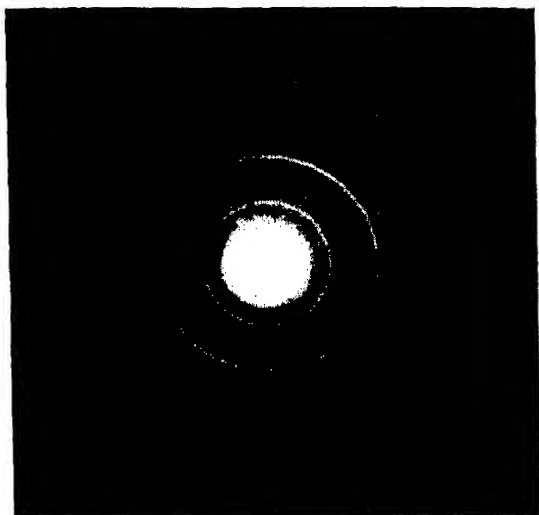
$$I_v(\phi) = \sum_i \sum_j' Z_i Z_j \frac{\sin \mu r_{ij}}{\mu r_{ij}} \quad . \quad . \quad . \quad (4)$$

where the dash indicates that terms with  $i=j$  are not to be included. Introducing a notation due to Wierl we may write  $[r_{ij}]$  for  $\sin \mu r_{ij} / \mu r_{ij}$  and find

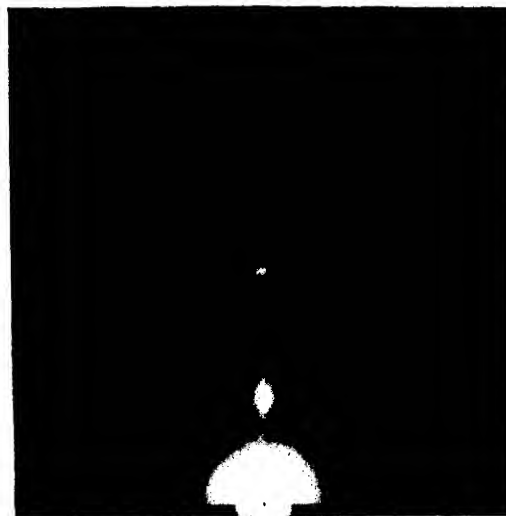
$$I_v = \sum_i \sum_j' Z_i Z_j [r_{ij}] \quad . \quad . \quad . \quad (4A)$$

The molecular model has then to be chosen so that the maxima (and minima) of  $I_v(\phi)$  have the same positions and approximately the same intensity as visually observed on the plate or film. The neglect of the  $f_i$ 's and  $S_i$ 's is most serious in regard to the positions of the first maximum and first two minima, so that more weight must be given to the rings further out. It is clear that increasing the scale or 'size' of a molecular model does not change any of the angles and increases all interatomic distances in the same ratio. Thus, if  $I_{\text{expt.}}$  is plotted against  $\mu$  on one graph and  $I_{\text{theor.}}$  against  $\mu$  on another and if the

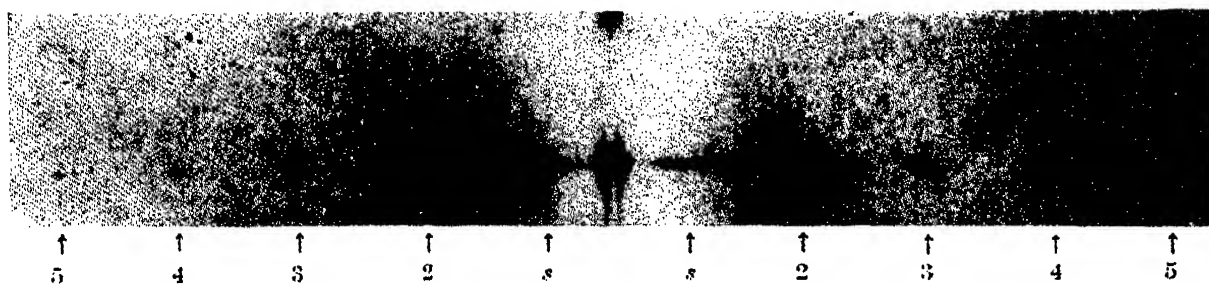
PLATE X  
(*c* and *d* are 'negatives')



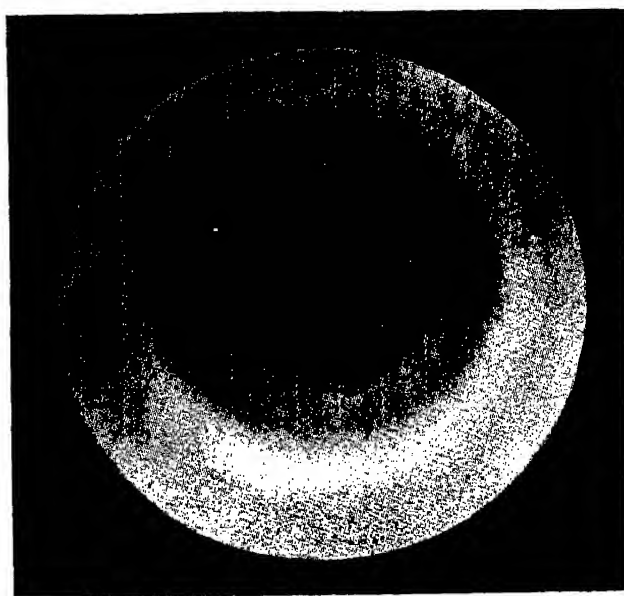
(*a*) Mica powder. (*Finch*)



(*b*) Paraffin,  $C_{32}H_{66}$ . (*Finch*)



(*c*) Rotation photograph from zinc blende cleavage face; *s* denotes surface reflection, 2, 3, 4, . . . denote orders of reflection. (*Miyake*.) Taken from *Sci. Pap. Inst. Phys. Chem. Res.* 26, Pl. I, (1935).



(*d*)  $CCl_4$  vapour. (*Wierl*)  
Taken from *Ann. d. Phys.* 8, p. 546 (1931)



correct *type* of model has been chosen, then the two graphs can be superimposed merely by stretching one of the  $\mu$  scales; for  $r_{ij}$  enters into the formula as the product  $\mu r_{ij}$ . This change in the scale gives the factor by which the size of the model has to be altered in order to obtain the true description of the molecule.

Pauling and Brockway<sup>1</sup> have evolved a direct method — referred to as the 'radial distribution method' — of deducing interatomic distances from the diffraction photographs. Instead of considering the molecule in terms of discrete atoms they imagine it to be a general distribution of scattering matter. Then the Wierl expression for the coherent scattering is replaced by

$$I(\mu) = k \int_0^{\infty} \frac{r^2 D(r)}{\mu^4} \cdot \frac{\sin \mu r}{\mu r} \cdot dr.$$

The quantity

$$\frac{r^2 D(r)}{\mu^4} dr$$

represents the sum of the products of the scattering powers of all elements of volume distant  $r$  apart and  $k$  is some constant. Rewriting this,

$$\mu^5 I(\mu) = k \int_0^{\infty} r D(r) \sin \mu r \cdot dr,$$

and inverting the integral, one finds

$$r D(r) = k \int_0^{\infty} \mu^5 I(\mu) \sin \mu r \cdot d\mu,$$

or,

$$D(r) = k \int_0^{\infty} \mu^6 I(\mu) \frac{\sin \mu r}{\mu r} d\mu. \quad (5)$$

From the experimental results,  $I(\mu)$  is known, so that  $D(r)$  can be determined as a function of  $r$ . As the nuclear scattering of fast electrons is very large, a maximum of  $D(r)$  will indicate an internuclear distance equal to the corresponding value of  $r$ . In this way it is possible to determine the principal interatomic distances. In practice the factor  $\mu^6$  is dropped since visual investigation is adopted, and Pauling and Brockway, replacing the integral by a summation, write

$$D(r) = \sum_{p=1}^n I_p \frac{\sin \mu_p r}{\mu_p r} \quad (6)$$

<sup>1</sup> Pauling and Brockway, *J. Am. Chem. Soc.* 57, p. 2684 (Dec. 1935).

In (6),  $I_p$  represents the visually estimated integrated intensity of the  $p$ th ring and  $\mu_p$  is the value of  $\mu$  for that ring. In a recent modification of this method, due to Schomaker,<sup>1</sup> weighted intensities  $C_p$  are used. These are calculated from the formula

$$C_p = I_p \mu_p^2 e^{-a \mu_p^2},$$

where  $a$  is so chosen that  $C_n = C_1/n$ , for a photograph with  $n$  rings. The reasons for the use of this formula have not yet been made clear.

### Example of the Method

BENZENE,  $C_6H_6$ .—In order to illustrate the methods involved in the interpretation of diffraction patterns from gas molecules, we consider the results from benzene. This

TABLE XVII  
 $\mu_{\text{obs}}$  (IN  $\text{\AA}^{-1}$ ) FOR  $C_6H_6$

	Wierl *	Pauling and Brockway (with $I_p$ in brackets)	Jones
1st Min. . .	..	..	..
1st Max. . .	2.86	3.35 (50)	4.50
2nd Min. . .	..	4.39	..
2nd Max. . .	5.30	5.80 (160)	5.70
3rd Min. . .	..	7.56	7.55
3rd Max. . .	max.	9.55 (20)	9.75
4th Min. . .	at	..	10.6
4th Max. . .	10.2	11.5 (5)	11.2
5th Min. . .	..	12.6	12.5
5th Max. . .	13.6	13.8 (15)	13.8
6th Min. . .	..	..	..
6th Max. . .	..	16.2 (3)	..
7th Min. . .	..	..	..
7th Max. . .	..	18.7 (8)	..

\* It is possible that Wierl used photometer records in measuring his inner rings. For this reason it is not proposed to use his results to illustrate the 'visual method'.

has been investigated by Wierl,<sup>2</sup> Pauling and Brockway,<sup>3</sup> and Jones.<sup>4</sup> The observed values of  $\mu_p$  at maxima and minima are collected in the above table (Table XVII).

<sup>1</sup> Used by Springall and Brockway, *J. Am. Chem. Soc.* 60, p. 996 (May 1938), and by others. It is understood that Schomaker's paper will appear in the same *Journal* shortly.

<sup>2</sup> Wierl, *Ann. d. Phys.* 8, p. 521 (1931).

<sup>3</sup> Pauling and Brockway, *J. Chem. Phys.* 2, p. 867 (1934).

<sup>4</sup> Jones, *Trans. Farad. Soc.* 31, p. 1036 (1935).

It will be seen that there is quite good agreement between the results except for the first ring or maximum. As we have already noticed, this ring is usually left out of account, along with the second minimum. Wierl does not distinguish between the 3rd and 4th maxima, which in fact form a shelf with a very faint minimum in between.

In choosing a model for the molecule of benzene  $C_6H_6$ , one knows from its chemical properties that a ring of carbon atoms is to be considered. One therefore postulates six carbon atoms at the corners of a plane hexagon. Pauling and Brockway state that the inclusion of hydrogen atoms makes very little difference to the theoretical scattering curve. Taking the side of the hexagon as unity, it is seen (Fig. 87) that there are three C-C 'periods', viz. 1 (occurring 6 times),  $\sqrt{3}$  (6 times) and 2 (3 times). Thus from (4A) we obtain

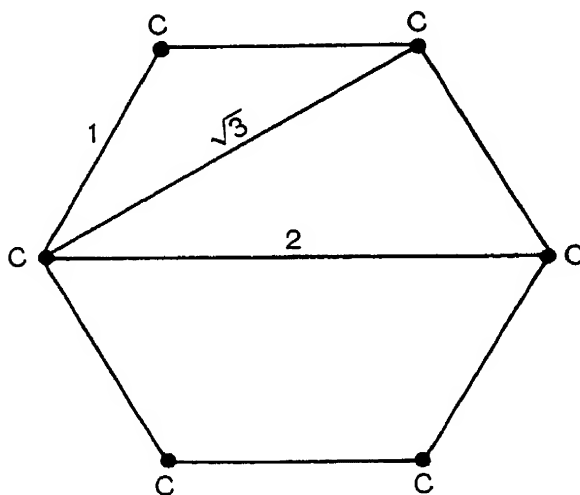


FIG. 87

$$I \doteq 6 \cdot 6 \cdot 6[I] + 6 \cdot 6 \cdot 6[\sqrt{3}] + 3 \cdot 6 \cdot 6[2].$$

The expression to be calculated is therefore

$$2[I] + 2[\sqrt{3}] + [2]. \quad (7)$$

For this purpose tables of  $\sin x/x$  are available.<sup>1</sup> A graph of (7) is then plotted and the positions of the maxima and minima

TABLE XVIII

$\bar{\mu}_{\text{theor.}}$  AT MAXIMA AND MINIMA FOR A PLANE HEXAGON

	$\bar{\mu}_{\text{theor.}}$		$\bar{\mu}_{\text{theor.}}$
1st Max . . .	4.1	4th Min. . . .	14.7
2nd Min. . . .	5.8	4th Max. . . .	15.5
2nd Max. . . .	8.1	5th Min. . . .	17.5
3rd Min. . . .	10.6	5th Max. . . .	19.2
3rd Max. . . .	13.7	6th Min. . . .	21.2
		6th Max. . . .	22.5

<sup>1</sup> Sherman, *Zeit. für Krist.* 85, p. 404 (1933).

recorded. We have averaged the values thus obtained by Jones, Wierl, and Pauling and Brockway, and evolved the preceding table (Table XVIII) of values of  $\bar{\mu}$  (theoretical) for the hexagonal model.

From the tables of  $\mu_{\text{obs.}}$  and  $\bar{\mu}_{\text{theor.}}$  we can draw up a list of values of  $\bar{\mu}_{\text{theor.}}/\mu_{\text{obs.}}$  as in Table XIX.

TABLE XIX  
 $\bar{\mu}_{\text{theor.}}/\mu_{\text{obs.}}$  (IN Å)

	Pauling and Brockway	Jones
1st Max. . .	1.23	0.915
2nd Min. . .	1.32	..
2nd Max. . .	1.395	1.42
3rd Min. . .	1.405	1.405
3rd Max. . .	1.43	1.405
4th Min. . .	..	1.385
4th Max. . .	1.35	1.385
5th Min. . .	1.39	1.40
5th Max. . .	1.39	1.39
6th Max. . .	1.39	..

The constancy of the values of  $\mu_{\text{theor.}}/\mu_{\text{obs.}}$  is a criterion of the validity of the model chosen. The first maximum and second minimum must, of course, be ignored. A little trouble seems to arise in regard to the 3rd and 4th maxima. But this 'shelf' is difficult to measure up and indeed the actual existence of the shelf in both the experimental data and the theoretical curve is an important point in deciding whether the model is correct. Thus Pauling and Brockway have made the calculations for other models in which the carbon atoms do not lie in one plane, but are staggered above and below the original plane. If the staggering is such that the C-C bond angle is  $112^\circ$ , then the shelf disappears. Even for a very slight staggering, corresponding to a bond angle of  $118^\circ$ , the agreement with experiment is not quite so good as for the plane model (bond angle  $120^\circ$ ). Wierl also shows that the plane model is most likely. Having decided that the model is correct, the value of  $\mu_{\text{theor.}}/\mu_{\text{obs.}}$  gives the factor by which all interatomic distances are to be increased. Since the C-C<sub>arom</sub>

distance<sup>1</sup> was taken to be unity, this factor is the true value of C-C<sub>arom.</sub> Pauling and Brockway give their result as  $1.390 \pm 0.005$  Å, Jones gives  $1.40 \pm 0.01$  Å, and Wierl gives  $1.39 \pm 0.03$  Å. The first-named authors thus claim an accuracy of better than  $\frac{1}{2}$  per cent. Since the graphs, as printed in the literature, are rather small, we have only attempted an accuracy of about one per cent in compiling the tables, which are intended primarily to illustrate the method and to show the agreement between the data of the different experimenters.

We have already given in Table XVII the data necessary for the application of the 'radial distribution' method of investigation. Substituting the values of  $I_p$  and  $\mu_p$  into formula (6), Pauling and Brockway<sup>2</sup> obtain the radial distribution curve shown (Fig. 88). Maxima are found at  $r = 1.381$  Å and  $2.390$  Å and a fainter maximum further out as indicated.

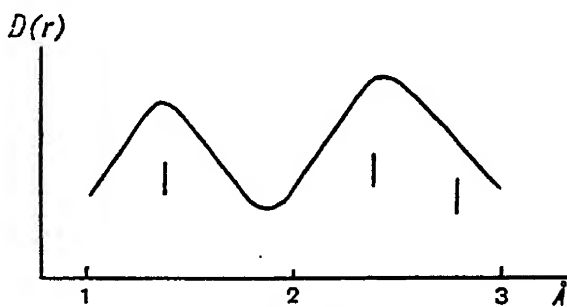


FIG. 88

The first of these corresponds to the six 'ortho' C-C distances and the second to the six 'meta' C-C distances. The ratio of the two is  $1.731 = \sqrt{3}$ , which again indicates the validity of the plane hexagonal configuration. The C-H distances do not appear on the curve. It is stated that the values of interatomic distances given by this method are not usually so accurate as those obtained from the 'visual method'. In general, Pauling and Brockway recommend that the radial distribution function  $D(r)$  should be first calculated. The knowledge obtained from  $D(r)$  will often be of value in deciding on a molecular model, which can then be tested by the visual method and altered if necessary.

## Results

In his first *Annalen* paper Wierl gives the structures of twenty different molecules as determined by electron diffraction.

<sup>1</sup> C-C<sub>arom</sub> denotes the distance between neighbouring carbon atoms in benzene and other aromatic compounds.

<sup>2</sup> Pauling and Brockway, *J. Am. Chem. Soc.* 57, p. 2684 (1935).

tion. The positions of the theoretical maxima were calculated, using the complete coherent scattering formula with  $f$ -values derived from the Thomas-Fermi atomic model. Bromine ( $\text{Br}_2$ ) gave a Br-Br separation of  $2.28 \pm 0.04 \text{ \AA}$  which compares well with the result ( $2.26$ ) found from band spectra. Linear structures were found for  $\text{CO}_2$  and  $\text{CS}_2$ . The tetrachlorides of carbon, silica, germanium, titanium and tin had all a tetrahedral structure with the chlorine atoms at the corners of the tetrahedron, the Cl-Cl distance increasing from  $2.98 \text{ \AA}$  in  $\text{CCl}_4$  to  $3.81$  in  $\text{SnCl}_4$ . Benzene, cyclopentane and cyclohexane were studied, assuming in each case a ring of carbon atoms, not necessarily to be considered plane. The results indicated that the first two molecules were plane and the third puckered. Pentane and hexane (both long-chain carbon compounds) gave identical patterns of two rings. When measured up these rings were found to correspond to the 'Bragg' spacings  $1.5 \text{ \AA}$  and  $2.5 \text{ \AA}$ . These are respectively the distances between the neighbouring and alternate carbon atoms in the carbon chain. The angle between the carbon bonds thus turns out to be  $110^\circ$ , which is the 'tetrahedral' angle and, along with the data for  $\text{CCl}_4$ , confirms the fact that the four carbon valencies are directed to the corners of a regular tetrahedron. The C-C bond in pentane and hexane is single and the C-C distance of  $1.5 \text{ \AA}$  agrees well with the value  $1.52$  found in cyclohexane and cyclopentane, which have also single C-C bonds.

In his second *Annalen* paper Wierl shows that it is unnecessary to introduce the atomic form-factors and the  $\mu^{-4}$

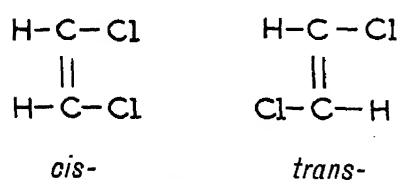


FIG. 89

factor in the calculations if the rings are measured visually. He finds the C-C distance for a double bond as in ethylene to be  $1.3 \pm 0.1 \text{ \AA}$  and the triple bond in acetylene gives C-C as  $1.22 \pm 0.1 \text{ \AA}$ . A successful attempt is made to distinguish between the *cis*- and *trans*-forms of dichloroethylene (Fig. 89). The Cl-Cl distance in the compound with a boiling-point of  $48^\circ \text{ C}$ . is  $4.3 \text{ \AA}$  and in the one with boiling-point  $60^\circ$  it is  $3.3 \text{ \AA}$ . The former is evidently the *trans*-form. In this paper Wierl also studies the question of free rotation in a molecule round a single C-C bond. The substances investigated are 1, 2-dichloroethane and 1, 2-dibromo-

ethane. He finds that the patterns do not agree with the intensity curves calculated allowing for free rotation.

The above brief account of Wierl's two *Annalen* papers indicates the diversity of problems which can be attacked by electron diffraction in gases. In addition, we may mention that the interatomic distances in different cases are of value to chemists as they are a characteristic of the bond between the atoms. It is possible to consider an atom as having a particular radius for each type of covalent bond and, when two atoms are linked together by such a bond, their interatomic distance is the sum of the appropriate radii (Pauling-Sidgwick rule). In some instances the observed interatomic distance is intermediate between the values for two types of bond, and it is then deduced that there is 'resonance' between these two kinds of binding. Thus for benzene there are the two Kekulé formulae shown in Fig. 90, and it may be said that the C-C bond 'resonates' about equally between a single bond and a double bond. In agreement with this the C-C<sub>arom</sub> distance of 1.39 Å is intermediate between the C-C single bond value of 1.5 Å and the double bond value of 1.3 Å.<sup>1</sup> The fact that C-C<sub>arom</sub> is nearer to the double-bond distance has been shown to be reasonable.<sup>2</sup> Many cases of such resonances have been proposed on the basis of the electron diffraction results for interatomic distances. A critical account of some of this work is given by Glasstone in the 1936 *Annual Report of the Chemical Society*.

Some results of importance to physicists have been provided by Maxwell, Hendricks and Mosley,<sup>3</sup> who, using a furnace at 1200°C., were able to investigate the vapours of alkali halides

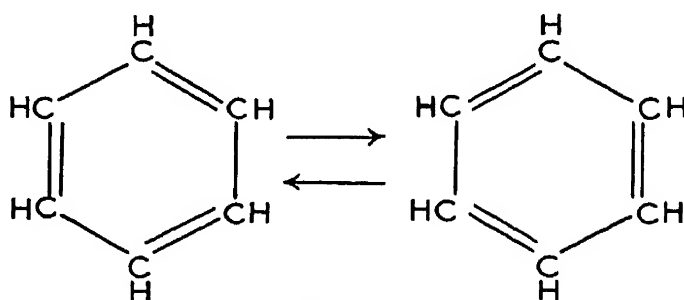


FIG. 90

— the chlorides, bromides and iodides of sodium, potassium, rubidium and caesium. The spacing between the alkali atom and the halogen atom in the free molecule was always about

<sup>1</sup> A better value is probably 1.38 Å.

<sup>2</sup> Pauling, Brockway and Beach, *J. Am. Chem. Soc.* 57, p. 2705 (1935).

<sup>3</sup> Maxwell, etc., *Phys. Rev.* 52, p. 968 (1937).

12 per cent smaller than in the solid state. The actual figures are given, accurate to 1 per cent, and will be of interest to those concerned with the theory of the binding between such atoms.

The number of types of molecules that have been investigated by the methods described in this chapter is now very large. Brockway<sup>1</sup> has compiled a table showing all the results up to the year 1936. We have reproduced the essentials of his table and also included some recent data which have appeared since Brockway's article was published. (See Table XX.) Inorganic compounds have been arranged according to the periodic classification and organic compounds according to the number of carbon atoms. Certain data which Brockway considers less reliable are enclosed in parentheses.

TABLE XX

Compound	Configuration and Bond Distance (Å)	Compound	Configuration and Bond Distance (Å)
NaCl	2.51±0.03	N <sub>2</sub> O	Linear 2.38±0.05
NaBr	2.64±0.01		between end atoms
NaI	2.90±0.02	NO <sub>2</sub>	Bent ?
KCl	2.79±0.02	NOCl	Cl-O=2.65±0.01
KBr	2.94±0.03		Cl-N=1.95±0.01
KI	3.23±0.04		N-O=1.14±0.02
RbCl	2.89±0.01		∠ClNO=116°±2°
RbBr	3.06±0.02	NOBr	Br-O=2.85±0.02
RbI	3.26±0.03		Br-N=2.14±0.02
CsCl	3.06±0.03		N-O=1.15±0.04
CsBr	3.14±0.03		∠BrNO=117°±3°
CsI	3.41±0.03		P-O=1.67±0.03
ZnI <sub>2</sub>	Linear Zn-I=2.42±0.02	P <sub>4</sub> O <sub>6</sub>	∠POP=128.5°±1.5°
CdI <sub>2</sub>	Linear Cd-I=2.60±0.02	P <sub>4</sub>	Tetrahedral 2.21±0.02
HgCl <sub>2</sub>	Linear Hg-Cl=2.34±0.01	PF <sub>3</sub>	Pyramidal 1.52±0.04 104°±4°
HgBr <sub>2</sub>	Linear Hg-Br=2.44±0.01	PF <sub>5</sub>	1.57±0.03
HgI <sub>2</sub>	Linear Hg-I=2.61±0.01	PFCl <sub>2</sub>	P-Cl=2.00±0.03
B <sub>2</sub> H <sub>6</sub>	Tetrahedral B-B=1.86±0.04	PCl <sub>3</sub>	Pyramidal 2.00±0.02 101°±2°
	angle B-H=1.27±0.03	PBr <sub>3</sub>	2.23±0.01
B <sub>4</sub> H <sub>10</sub>	Free B-B=1.84±0.04		100°±2°
	rotation B-H=1.28±0.04	PI <sub>3</sub>	2.52±0.01
	Like B-B=1.81±0.03		98°±4°
B <sub>5</sub> H <sub>11</sub>	pentane B-H=1.26±0.03	PSCl <sub>3</sub>	P-Cl=2.01±0.02
	(long chain)		P-S=1.94±0.03
B <sub>5</sub> H <sub>9</sub>	Planar B-B=1.76±0.02		∠Cl.P.Cl=107°±3°
	B-H=1.17±0.04	As <sub>4</sub>	Tetrahedral 2.44±0.03
B <sub>2</sub> N <sub>2</sub> H <sub>6</sub>	B-N=1.47±0.07	As <sub>4</sub> O <sub>6</sub>	As-As=3.2±0.05
BF <sub>3</sub>	B-F=1.30±0.02	AsF <sub>3</sub>	Pyramidal 1.72±0.02
BCl <sub>3</sub>	Planar 1.73±0.02	AsCl <sub>3</sub>	Pyramidal 2.16±0.03 103°±3°
BBr <sub>3</sub>	Planar 1.87±0.02	AsBr <sub>3</sub>	2.36±0.02
TiCl <sub>4</sub>	2.55±0.03		100°±2°
TiBr <sub>4</sub>	2.68±0.03	AsI <sub>3</sub>	2.58±0.01
TiI <sub>4</sub>	2.87±0.03		100°±2°
SiF <sub>4</sub>	Tetrahedral 1.54±0.02	SbCl <sub>3</sub>	2.37±0.02
SiHCl <sub>3</sub>	2.00±0.03 110°±3°		104°±2°
SiHBr <sub>3</sub>	Tetrahedral 2.19±0.05 110°±3°	SbBr <sub>3</sub>	2.52±0.02
SiCl <sub>4</sub>	Tetrahedral 2.00±0.02		96°±2°
TiCl <sub>4</sub>	Tetrahedral 2.21±0.05	SbI <sub>3</sub>	2.75±0.02
GeCl <sub>4</sub>	Tetrahedral 2.08±0.03		98°±2°
SnCl <sub>4</sub>	Tetrahedral 2.30±0.03	OF <sub>2</sub>	Bent 1.41±0.05 100°±3°

<sup>1</sup> Brockway, *Reviews of Modern Physics*, 8, p. 231 (1936).

TABLE XX—continued

Compound	Configuration and Bond Distance (Å)		Compound	Configuration and Bond Distance (Å)	
				C—C (Å)	C—Z (Å)
Cl <sub>2</sub> O	Bent	1.68±0.03 115°±4°	C <sub>2</sub> H <sub>4</sub> Cl <sub>2</sub> (1, 1—)		Cl—Cl=2.9±0.3
S <sub>2</sub> (>800° C.)		1.92±0.03	C <sub>2</sub> H <sub>5</sub> Br	(2.02±0.07)	
S <sub>2</sub> +n(<800° C.)		2.1	C <sub>2</sub> H <sub>4</sub> Br <sub>2</sub> (1, 1)		Br—Br=3.56±0.15
		∠S.S.S.=100°	C <sub>2</sub> H <sub>4</sub> Br <sub>2</sub> (1, 2)		Br—Br=4.75±0.15
SO <sub>2</sub>	Bent	1.45±0.02 124°±15°	C <sub>2</sub> H <sub>5</sub> I	(2.32±0.05)	
SF <sub>6</sub>	Octahedral	1.57±0.03	CH <sub>3</sub> CHO	1.51±0.05	C—O=1.20±0.05
S <sub>2</sub> Cl <sub>2</sub>		{S—Cl=1.98±0.05			∠CCO=122°
		{S—S=2.04±0.05	CH <sub>3</sub> COCl	1.54	(C—O=1.14±0.05)
SeF <sub>6</sub>	Octahedral	1.68±0.03			(C—Cl=1.82±0.10)
TeF <sub>6</sub>	Octahedral	1.83±0.03	CH <sub>3</sub> COBr	1.54	(C—O=1.13±0.05)
TeCl <sub>2</sub>	Linear (?)	2.36±0.03 >150°			(C—Br=2.06±0.10)
TeBr <sub>2</sub>	Linear (?)	2.49±0.03 >150°	C <sub>2</sub> H <sub>4</sub> O (ethylene oxide)	1.49±0.1	C—O=1.49±0.1
Cl <sub>2</sub>		2.01±0.03	C <sub>2</sub> H <sub>4</sub>	1.3±0.1	
ClO <sub>2</sub>	Bent	1.53±0.02 137°±15°			∠CCX
Br <sub>2</sub>		2.28±0.02	C <sub>2</sub> H <sub>3</sub> Cl	1.38	1.69±0.02 122°±2°
BrCCl <sub>3</sub>		C—Br=2.01	C <sub>2</sub> H <sub>2</sub> Cl <sub>2</sub> (1, 1)	1.38	1.69±0.02 122°±1°
		Br—Cl=3.00	C <sub>2</sub> H <sub>2</sub> Cl <sub>2</sub> (cis)	1.38	1.67±0.03 123.5±1°
		C—Cl=1.76	C <sub>2</sub> H <sub>2</sub> Cl <sub>2</sub> (trans)	1.38	1.69±0.02 122.5±1°
		Cl—Cl=2.95	C <sub>2</sub> HCl <sub>3</sub>	1.38	1.71±0.03 123°±2°
I <sub>2</sub>		2.65±0.10	C <sub>2</sub> Cl <sub>4</sub>	1.38	1.73±0.02 123.75±1°
ICl		2.30±0.03	C <sub>2</sub> H <sub>3</sub> Br	(1.32±0.08)	(2.05±0.08)
OsO <sub>4</sub>		1.66±0.05	C <sub>2</sub> H <sub>2</sub> Br <sub>2</sub> (cis)	(1.32±0.08)	(2.05±0.08)
OsF <sub>6</sub>	Archimedes antiprism (?)	2.52±0.10	C <sub>2</sub> H <sub>2</sub> Br <sub>2</sub> (trans)	(1.32±0.08)	1.91 (±0.05)
CH <sub>3</sub> F		1.42±0.02	C <sub>2</sub> HBr <sub>3</sub>	(1.32±0.08)	(2.05±0.08)
CF <sub>4</sub>	Tetrahedral	1.36±0.02	C <sub>2</sub> Br <sub>4</sub>		1.91 (±0.05)
CH <sub>2</sub> Cl <sub>2</sub>		C—F=1.36±0.02	C <sub>2</sub> H <sub>2</sub> I <sub>2</sub> (trans)		2.10 (±0.05)
		C—Cl=1.74±0.03	C <sub>2</sub> I <sub>4</sub>		2.10 (±0.05)
CF <sub>2</sub> Cl <sub>2</sub>		C—F=1.36±0.02	C <sub>2</sub> H <sub>2</sub>	1.22±0.1	
		C—Cl=1.75±0.03	C <sub>2</sub> Br <sub>2</sub>	1.20±0.03	1.80±0.03
CH <sub>3</sub> Cl		1.77±0.02	C <sub>2</sub> I <sub>2</sub>	1.18	2.03 (±0.05)
CH <sub>2</sub> Cl <sub>2</sub>		1.77±0.02 112°±2°	(CH <sub>3</sub> ) <sub>2</sub> O		C—O=1.42±0.03
CHCl <sub>3</sub>		1.77±0.02 112°±2°	(HCOOH) <sub>2</sub>	Planar	∠COC=111°±4°
CCl <sub>4</sub>	Tetrahedral	1.755±0.005			C—O=1.29±0.02
CH <sub>3</sub> Br		(2.06±0.05)	CH <sub>3</sub> NNCH <sub>3</sub>	Planar	O—O=2.67±0.04
CH <sub>2</sub> Br <sub>2</sub>		1.91±0.03			∠OCO=125°±5°
CHBr <sub>3</sub>		∠BrCBr=112°±2°	(CH <sub>3</sub> ) <sub>2</sub> NH		C—N=1.47±0.06
		19.1±0.03			N—N=1.24±0.05
		∠BrCBr=111°±2°	(CH <sub>3</sub> ) <sub>2</sub> NH		∠CNN=110°±10°
CBr <sub>4</sub>	Tetrahedral	1.91±0.03			C—N=1.46±0.03
CH <sub>3</sub> I		(2.28±0.05)	(CN) <sub>2</sub>	Linear	C—H=1.08±0.03
CH <sub>2</sub> I <sub>2</sub>		(2.28±0.05)			∠CNC=108°±4°
CHI <sub>3</sub>		2.12(±0.03)	CH <sub>3</sub> CN	Linear	C—C=1.43±0.03
COCI <sub>2</sub>	Planar	C—O=1.28±0.02			C—N=1.16±0.02
		∠CICCl=117°±2°	CH <sub>3</sub> CN	Linear	C—C=1.55±0.02
		C—Cl=1.68±0.02	CH <sub>3</sub> NC	Linear	C—N=1.16±0.02
COBr <sub>2</sub>	Planar	(C—O=1.13,			H <sub>3</sub> C—N=1.48±0.03
		C—Br=2.05±0.04)	S(CH <sub>3</sub> ) <sub>2</sub>	Bent	N—C=1.17±0.02
CSCl <sub>2</sub>	Planar	C—S=1.63,	Hg(CH <sub>3</sub> ) <sub>2</sub>		C—S=1.82±0.03
		∠CICCl=116°	CH <sub>3</sub> CO		Hg—C=2.20±0.10
		C—Cl=1.70±0.02			C—C=1.35±0.02
CH <sub>2</sub> O	Planar	(C—O=1.15±0.05)	C <sub>3</sub> H <sub>6</sub>		C—O=1.17±0.02
CO <sub>2</sub>	Linear	1.13±0.04	C <sub>3</sub> H <sub>4</sub> (cyclopropane)		C—C=1.52±0.05
CH <sub>3</sub> ONH <sub>2</sub>	Bent	C—O=1.44±0.02,	C <sub>3</sub> H <sub>4</sub> (allene)		1.53±0.02
		111°±3°	(CH <sub>3</sub> ) <sub>2</sub> CO	Linear	C—C=1.31±0.05
		N—O=1.37±0.02			C—C=1.57±0.04
CH <sub>3</sub> NO <sub>2</sub>	Planar	C—N=1.46±0.02,	C <sub>3</sub> O <sub>2</sub>		C—C=1.29±0.03
		∠ONO=127°±3°			C—O=1.20±0.02
		N—O=1.21±0.02	N(CH <sub>3</sub> ) <sub>3</sub>	Planar	C—N=1.47±0.02
COS	Linear	C—O=1.16±0.03,	B(CH <sub>3</sub> ) <sub>3</sub>		B—C=1.56±0.02
		C—S=1.56±0.04	C <sub>4</sub> H <sub>10</sub> (isobutane)		C—C=1.54±0.02
CH <sub>3</sub> N <sub>2</sub>	Linear	C—N=1.34±0.05,			∠C.C.C.=113°30'±2°
		N—N=1.13±0.04	C <sub>4</sub> H <sub>8</sub>		{C—C (single)=1.56±0.04
CH <sub>3</sub> N <sub>3</sub>		C—N <sub>1</sub> =1.47±0.02,	(trans 2-butene)		{C—C (double)=1.40±0.04
		N <sub>1</sub> —N <sub>2</sub> =1.26±0.02	C <sub>4</sub> H <sub>6</sub>		{C—C (single)=1.54±0.03
		N <sub>2</sub> —N <sub>3</sub> =1.10±0.02,	(cis 2-butene)		{C—C (double)=1.38±0.03
		∠CN <sub>1</sub> N <sub>3</sub> =120°±5°	C <sub>4</sub> H <sub>6</sub> (butadiene)		C—C (single bond)
CS <sub>2</sub>	Linear	1.54±0.03			=1.52±0.08
	C—C (Å)	C—Z (Å)	C <sub>4</sub> H <sub>2</sub> (diacetylene)	Linear	C—C (centre)=1.43±0.03
					C—C (end)=1.21±0.02
C <sub>2</sub> H <sub>6</sub>	1.52±0.1	1.81±0.1	C <sub>4</sub> H <sub>8</sub> O (trans butene oxide)		C—C=1.54±0.02
C <sub>2</sub> H <sub>5</sub> Cl					C—O=1.43±0.02

TABLE XX—continued

Compound	Configuration and Bond Distance (Å)	Compound	Configuration and Bond Distance (Å)
$C_4H_8O$ (cis butene oxide)	$C-C=1.53 \pm 0.02$ $C-O=1.42 \pm 0.02$	$(CH_3-CHO)_3$	Staggered $C-O=1.43 \pm 0.02$ hexagon $C-C=1.54 \pm 0.02$ $C-C$ (Å)
$(C_2H_5)_2O$	$(C-O=1.33 \pm 0.08)$	$C_6H_6$	$1.390 \pm 0.005$ Planar
$(C_2H_5O)_2$ (1, 4)	$C-C=1.54 \pm 0.04$ $C-O=1.46 \pm 0.04$ $\angle COC=110^\circ \pm 5^\circ$	$C_6Cl_6$	$1.41 (\pm 0.02)$
$C_4H_8Cl$ (tert.)	$C-Cl=1.78 \pm 0.03$ $\angle C-C-C=111^\circ 30' \pm 2^\circ$	$C_6H_2Cl_4$ (1, 2, 4, 5)	$1.40$
$C_4H_8Br$ (tert.)	$C-Br=1.92 \pm 0.03$ $\angle C.C.C=111^\circ 30' \pm 2^\circ$	$C_6H_2Cl_3$ (1, 3, 5)	$1.41$
$Ni(CO)_4$	Tetrahedral $Ni-C=1.82 \pm 0.03$ $C-O=1.15 \pm 0.02$	$m-C_6H_4Cl_2$	$1.40$
$Si(CH_3)_4$	Tetrahedral $Si-C=1.93 \pm 0.03$	$p-C_6H_4Cl_2$	$1.40$
$Ge(CH_3)_4$	Tetrahedral $Ge-C=1.98 \pm 0.03$	$o-C_6H_4Cl_2$	$1.40$
$Sn(CH_3)_4$	Tetrahedral $Sn-C=2.18 \pm 0.03$	$C_6H_5Cl$	$1.39$
$Pb(CH_3)_4$	Tetrahedral $Pb-C=2.30 \pm 0.05$	$C_6H_4Br_3$ (1, 4)	$1.41$
$C_5H_{12}$	$C-C=1.53 \pm 0.05$	$C_6H_3Br_3$ (1, 3, 5)	$1.41$
$C_5H_{10}$ (cyclo)	$C-C=1.52 \pm 0.03$	$C_6Br_6$	$1.41$
$C(CH_3)_4$	$C-C=1.55 \pm 0.02$	$C_6H_4I_2$ (1, 2)	$1.42$
$C_6H_{14}$	$C-C=1.54 \pm 0.05$	$C_6H_4I_3$ (1, 3)	$1.42$
$C_6H_{12}$ (cyclo)	$C-C=1.51 \pm 0.05$	$C_6H_4I_4$ (1, 4)	$1.42$
		$C_6H_3I_3$ (1, 3, 5)	$1.41$
		$C_6H_4(CH_3)_2$ (1, 4)	$1.40 \pm 0.01$
		$C_6H_3(CH_3)_3$ (1, 3, 5)	$1.40 \pm 0.01$
		$C_6(CH_3)_6$	$1.40 \pm 0.01$
		$(IC_6H_4)_2O$ (4, 4')	$1.42$
			$C-I=2.00, C-O=1.42,$ $\angle C-O-C=118^\circ \pm 3^\circ$

## CHAPTER XVIII

### SLOW ELECTRONS

*General.*—Experiments on the diffraction of slow electrons (up to a few hundred volts energy) fall into a class by themselves. The classical work of Davisson and Germer on the diffraction of slow electrons by a nickel single crystal forms a part of the original experimental evidence for the existence of electron waves and has already been briefly described in Chapter IV. Further work has generally been along the same lines, but in addition a different type of experiment has been performed, using polycrystalline films or powders, by Tartakowsky, Rupp, Bühl and others. With slow electrons the refractive index  $\mu = \sqrt{1 + \Phi/P}$  (cf. p. 107) is larger than it is for fast electrons; also the slow electrons are affected quite appreciably by the gas molecules which normally form an adsorbed layer on the surface of the specimen; there are, besides, certain anomalous effects which cannot be explained on the simple theory. For these reasons the diffraction of slow electrons by crystals is a complicated matter which even yet is not completely understood.

DAVISSON AND GERMER.—In their first experiments, Davisson and Germer allowed the electrons to fall normally on the (111) face of a nickel crystal, and diffracted beams were detected by a Faraday cylinder. Of the three quantities involved,  $P$ , the accelerating voltage,  $\phi$ , the colatitude angle, and  $\theta$ , the azimuth angle, two may be kept fixed and the other varied, while the current to the cylinder is measured. By combining the results, a complete investigation of the diffraction effects in the case of normal incidence is obtained.

The apparatus is illustrated in Fig. 91. A tungsten filament,  $F$ , serves as the source of electrons, which are accelerated through the 'electron gun'  $G$ . The outer walls of  $G$ , the target  $T$ , the outer box of the collector  $C$ , and the box enclosing these parts are maintained always at the same potential. Electrons leaving the target with energy less than 90 per cent

of that of the initial beam are excluded from the collector by a retarding potential between the inner and outer boxes of the latter. The two parts of the collector are insulated from each other by quartz; the openings in the inner and outer boxes are circular, their diameters being 1 mm. and 2 mm. respectively. The collector is suspended by arms from bearings outside the enclosing box and is free to rotate about a horizontal axis normal to the plane of Fig. 91, passing through the bombarded area. Its position is adjusted by rotating the whole apparatus, which is sealed from the pump, about this axis. The position

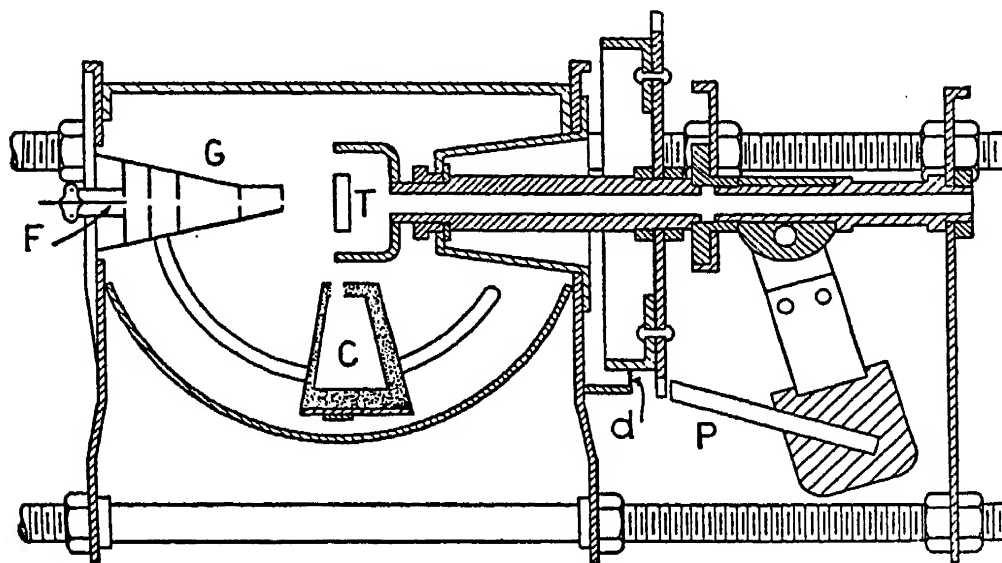


FIG. 91

can be read from a pointer outside the box (not shown in Fig. 91). The distance from the opening of the gun to the bombarded area is 7 mm. and from this to the opening in the outer box is 11 mm.

The target can be rotated about an axis perpendicular to its face by means of the mechanism shown on the right side of Fig. 91. If the tube is rotated counter-clockwise about the collector axis, so as to bring the collector into position to catch the electrons, the molybdenum plunger *P*, attached to a heavy pendulum, passes through an opening in a toothed wheel locked to the target and engages with the milled edge of a strip of molybdenum attached to the frame. The target is then locked. If, however, the apparatus is rotated clockwise through a small angle with the horizontal, the plunger disengages from the milled edge *d* but remains in the opening of

the toothed wheel. The pendulum, with the engaged wheel and the target, is then free to rotate about a fixed hollow shaft normal to the target face. The range of this rotation is only  $20^\circ$  to  $30^\circ$ , but by tilting the apparatus further in a clockwise direction the plunger can be withdrawn from the slot in the toothed wheel, and the pendulum is then disconnected from the target and its shaft. By a rotation about the axis of this shaft, the plunger can be brought back into another slot in the toothed wheel and the rotation of the latter can be repeated. Thus by a step-by-step process any desired rotation can be given to the target.

The target was a block of nickel  $8 \times 5 \times 3$  mm. cut from a bar in which crystal growth had been induced by straining and annealing. Crystal facets were developed by etching, which, in nickel, usually gives a (111) face. The faces so formed were examined by optical reflection and the crystal was cut approximately parallel to one of them. The surface so exposed was polished, etched, examined and corrected. A photomicrograph was taken of the surface, and the best area selected for bombardment. A small tungsten filament (not shown) was mounted behind the target and supplied electrons for heating the latter by bombardment.

Great care was taken with the vacuum conditions. The metal parts of the apparatus were preheated to  $1000^\circ$  and were then assembled and sealed into the bulb with the least possible delay. The bulb was of pyrex and had sealed to it two auxiliary tubes, one containing coconut charcoal, and the other a mischmetall vaporiser. During the pumping, which lasted several days, the tube itself and the tubing connecting it with the pumps were baked for hours at a time at  $500^\circ$ . This baking was alternated by the heating by bombardment of such of the metal parts as could be reached from the filaments. The target in particular was heated several times to a temperature at which it vaporised freely. The tube was sealed from the pumps while the target was at a high temperature and the charcoal at  $400^\circ$  to  $500^\circ$  (it had previously had a prolonged heating at  $550^\circ$ ). The pressure at the time was 2 or  $3 \times 10^{-6}$  mm. The mischmetall was vaporised when the pumping was nearly completed; it improves the vacuum by forming solid compounds with the residual gas. As soon as

the tube with the charcoal had cooled sufficiently it was immersed in liquid air. No means were available for measuring the final pressure, but from previous experience it was estimated at  $10^{-8}$  mm. or less. In making the measurements the current from the filament to an (insulated) diaphragm of the gun was kept constant. The ratio of collector to bombarding current in these experiments was of the order  $10^{-4}$ , the latter being of the order  $10^{-6}$  ampère, and the collector currents were measured with a sensitive galvanometer. The total integrated current of full-speed scattered electrons was  $1/10$  to  $1/20$  of the incident beam. The proportion of full-speed electrons in a diffracted beam was much larger than in the diffusely scattered background. The beams appeared to contain, in addition to full-speed electrons, others which had lost energy up to a quarter of the original amount. Owing to the variation with angle of the background scattering, the beams are, as it were, added on to a sloping curve; the apparent maximum is therefore probably not the true one. An allowance for this was made by sketching in an assumed background and subtracting it from the observed curve to give the part due to the beam itself. The relative intensity of the beams to the background was greatly increased by heating the target shortly before an observation. In these conditions 'the ratio of full-speed electrons scattered into any one of the most intense sets of beams to the total number scattered in all directions is about two-tenths'.<sup>1</sup> The 'spurs' or maxima in the colatitude curves are rather wide,  $\sim 25^\circ$ , and indeed twice the width which one would expect from the dimensions of the slits, etc., but this point is not further considered as there are several unknown factors.

The results, when the surface was thoroughly outgassed, indicated that there are two kinds of diffracted beams from the nickel crystal when the incidence is normal. The first set are Laue beams arising from several lattice planes and the second are 'plane-grating' beams resulting from scattering in a single lattice plane. The latter occur at large scattering angles and are particularly affected by the presence of gas. As stated on p. 33 the Laue beams do not in general satisfy the Laue interference condition for phase agreement

<sup>1</sup> Davisson and Germer, *Phys. Rev.* 30, pp. 722-740 (1927).

between the wavelets scattered in successive lattice planes. They do, however, satisfy the surface interference condition approximately.

In their next experiments <sup>1</sup> Davisson and Germer directed the electron beam at various angles on to the surface of the nickel crystal and observed the diffracted beams in the plane of incidence for different accelerating voltages. In this case one expects to find Bragg reflection from the (111) nickel planes, but again, as in the case of Laue diffraction, the interference condition is not exactly satisfied (cf. Fig. 14, p. 36). As in normal incidence, 'plane grating' beams were also seen.

According to the suggestion of Bethe <sup>2</sup> and Eckart,<sup>3</sup> the inner potential of the nickel lattice must be introduced in considering the Laue and Bragg beams. If  $\mu$  is the corresponding 'refractive index' of the nickel, then the Bragg condition,  $n\lambda = 2d \cdot \cos i$ , becomes (cf. p. 107)

$$n\lambda = 2d\sqrt{\mu^2 - \sin^2 i}$$

or 
$$\mu = \sqrt{\frac{150n^2}{4Pd^2} + \sin^2 i},$$

where 
$$\mu = \sqrt{1 + \frac{\Phi}{P}}.$$

A little difficulty occurs in deciding on the 'orders' of the maxima, and at first the results were interpreted as giving a value of  $\mu$  less than unity. In the case of the Bragg beams, Davisson and Germer, by taking  $\mu > 1$  obtained values of  $\Phi$ , many of which did not deviate much from 18 volts. It will be noticed that in Fig. 14 (p. 36) there are indications of beams at the 3rd and 4th orders for which the simple Bragg relation is satisfied, or  $\mu = 1$ . Davisson considers that these may represent the constructive interference of waves from the top layers of adjacent portions of crystal at different levels, so that the path difference occurs *in vacuo*.

<sup>1</sup> Davisson and Germer, *Proc. Nat. Acad. Sci.* 14, p. 317 (1928).

<sup>2</sup> Bethe, *Naturwiss.* 15, p. 787 (1937), 16, p. 333 (1928).

<sup>3</sup> Eckart, *Proc. Nat. Acad. Sci.* 13, p. 460 (1927).

Returning to the consideration of the index of refraction we note that

$$\mu = \sqrt{1 + \frac{\Phi \lambda^2}{150}},$$

so that if  $\mu$  is plotted against  $1/\lambda$  as abscissa we should expect a smooth monotonic curve. Fig. 92 shows such a curve together with the experimental data furnished from the second experiments. For values of  $\lambda$  greater than  $1 \text{ \AA}$  there is no agreement at all between theory and experiment, and there is

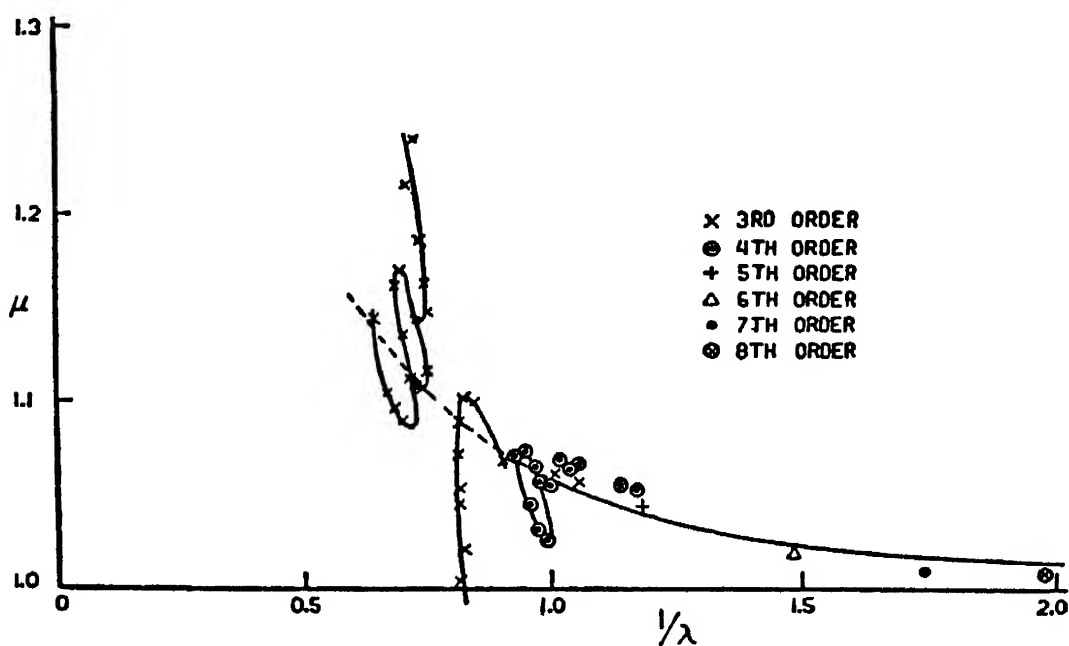


FIG. 92

a definite gap in the experimental results near  $1/\lambda = 0.8 \text{ \AA}^{-1}$ . Davisson and Germer suggested tentatively that this may be an effect analogous to the anomalous dispersion of light involving some resonance phenomenon. This point has been further discussed by Davisson and Germer,<sup>1</sup> who examined again the Laue beams. One of these occurs near the anomalous region ( $\lambda = 1.3 \text{ \AA}$ ). It first comes in at  $\lambda = 1.37 \text{ \AA}$  and reaches a maximum at  $\lambda = 1.33 \text{ \AA}$ . From this point it decreases and is scarcely apparent through the anomalous range. It then becomes strong again to a maximum at  $\lambda = 1.19 \text{ \AA}$  and finally decreases, vanishing at  $\lambda = 1.07 \text{ \AA}$ . The wave-length in the crystal is  $\lambda' = \lambda/\mu$  and Davisson and Germer conclude: 'It looks

<sup>1</sup> Davisson and Germer, *Phys. Rev.* 33, p. 292 (1933).

as if with  $\mu$  changing rapidly with  $\lambda$  that there are two values of  $\lambda$  ( $1.19 \text{ \AA}$  and  $1.33 \text{ \AA}$ ) for which the relation (interference condition) is satisfied and the beam really occurs twice'.

Besides the diffraction beams mentioned above, Davisson and Germer found others when the surface of the crystal was covered with gas. When the crystal was heated the first effect was a *reduction* in intensity of all the beams. This reduction lasted only while the crystal was hot and is presumably analogous to the corresponding reduction of intensity of X-ray diffraction by heating, which is due to the disturbance of the regularity of the crystalline arrangement by the heat motion of the atoms. When the crystal had cooled, most of

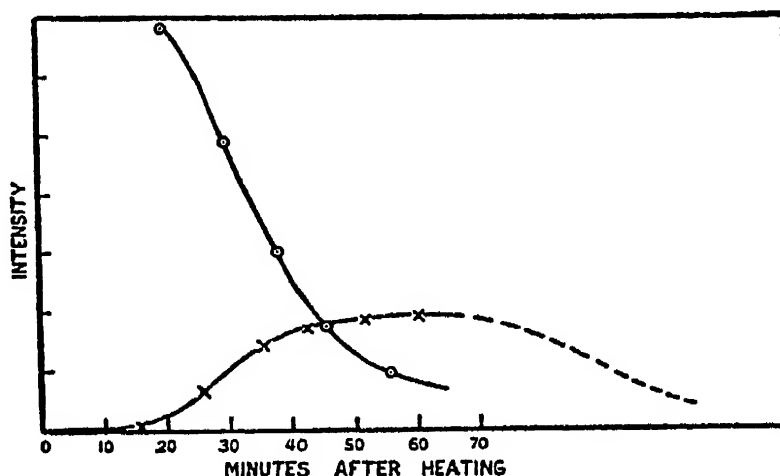


FIG. 93

the beams were increased in intensity and the plane-grating beams at grazing emergence (p. 35) made their appearance for the first time. These beams are extremely sensitive to gas and slowly disappear as the gas gradually re-forms on the crystal. This effect is shown in Fig. 93 (points indicated by circles). The time involved depends greatly on the vacuum conditions; under the most favourable circumstances the changes went more than twenty times as slowly as shown in the figure, under the worst conditions they were so rapid that the plane-grating beams could not be observed. Davisson and Germer attribute these beams to the action of the top layer of atoms, and consider that they become quite weak with only a monomolecular layer of gas on the surface. The temperature required to clean the surface is only about  $900^\circ$ , which is a

good deal less than would be expected from the results of thermionic experiments. It is understood from a conversation that, in some further experiments with a different nickel crystal, the plane-grating beams failed to appear even after prolonged heating under the best vacuum conditions. The reason is not known.

There is one set of beams in each of the principal azimuths which is permanently destroyed by heating, though it can be restored by releasing a quantity of gas from the charcoal. The beams all attain their maximum intensity at an angle close to  $58^\circ$  from the normal at an energy of 110 volts. They are presumed to be due to a considerable layer of gas and have the character of 'space' beams, but it has not been possible to assign a definite structure to the layer.

Another group of beams is more amenable. These show an increase to a maximum after heating, followed by a decrease (Fig. 93, points indicated by crosses), and it is natural to ascribe them to a monomolecular layer of gas which would gradually form and then in turn get covered by more gas. At the same time the space-grating beams gradually weaken, but the change is slight even when the new beams have entirely disappeared, and it may take weeks for the space-grating beams to diminish to their original intensity. Under poorer vacuum conditions the whole change may occur in a few minutes. The new beams vary in position over a considerable range as the wave-length changes, without very great change in intensity. They thus possess the character of plane- rather than space-grating beams. Measurement shows, however, that the plane-grating spacing to which they correspond is in each case exactly twice that of the nickel atoms in the azimuth in question. The assumed distribution of the gas atoms (or molecules) is shown in Fig. 94. It clearly fulfils the condition that the spacing of the lines of gas atoms perpendicular to any azimuth is twice that of the nickel ones. Though mainly a surface effect, the fact that these beams do show weak maxima for certain wave-lengths shows that another layer must come into action to some extent. Davisson and Germer point out that the presence of the gas atoms divides the nickel atoms of the top layer into two classes which are differently shielded from the electrons by the gas. There is, thus, a possibility of

their combining with the gas atoms to give an effect corresponding to the double-spacing. From the voltages at which the beams are strongest, Germer estimates the distance of the gas layer from the nickel at 3 Å, but this is necessarily subject to considerable probable error.

An interesting peculiarity of these beams is that they disappear at a temperature of 150°, though this does not

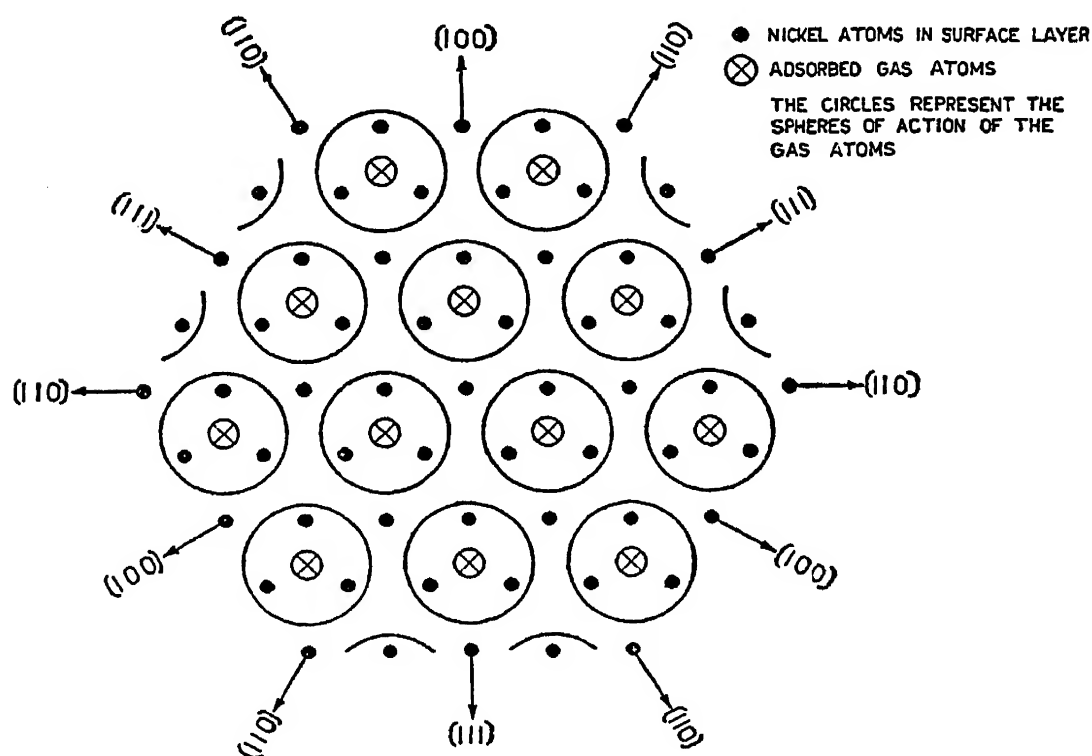


FIG. 94

appreciably affect the appearance of the plane-grating beams from nickel. Germer suggests that at this temperature the two-dimensional gas crystal has 'melted' and lost its regular arrangement.

### Discussion

So far we have examined the results only from the point of view of simple kinematic theory. Morse<sup>1</sup> considers the crystal as a periodic field represented by the sum of three cosine alternations in three different directions. From Schrödinger's equation he finds the directions and wave-lengths of possible electron waves in the crystal. An incident wave is then introduced and, by means of boundary conditions, the wave

<sup>1</sup> Morse, *Phys. Rev.* 35, p. 1310 (1930).

emerging from the crystal in the plane of incidence is found. The result indicates that the reflected beams are almost exactly in the directions and with the wave-lengths given by the simple theory of the Bragg case (assuming refractive index), except near certain critical values of  $\lambda$  over which reflection does not take place. If we plot  $\lambda$  against  $\cos \theta_n$  for a given reflection, where

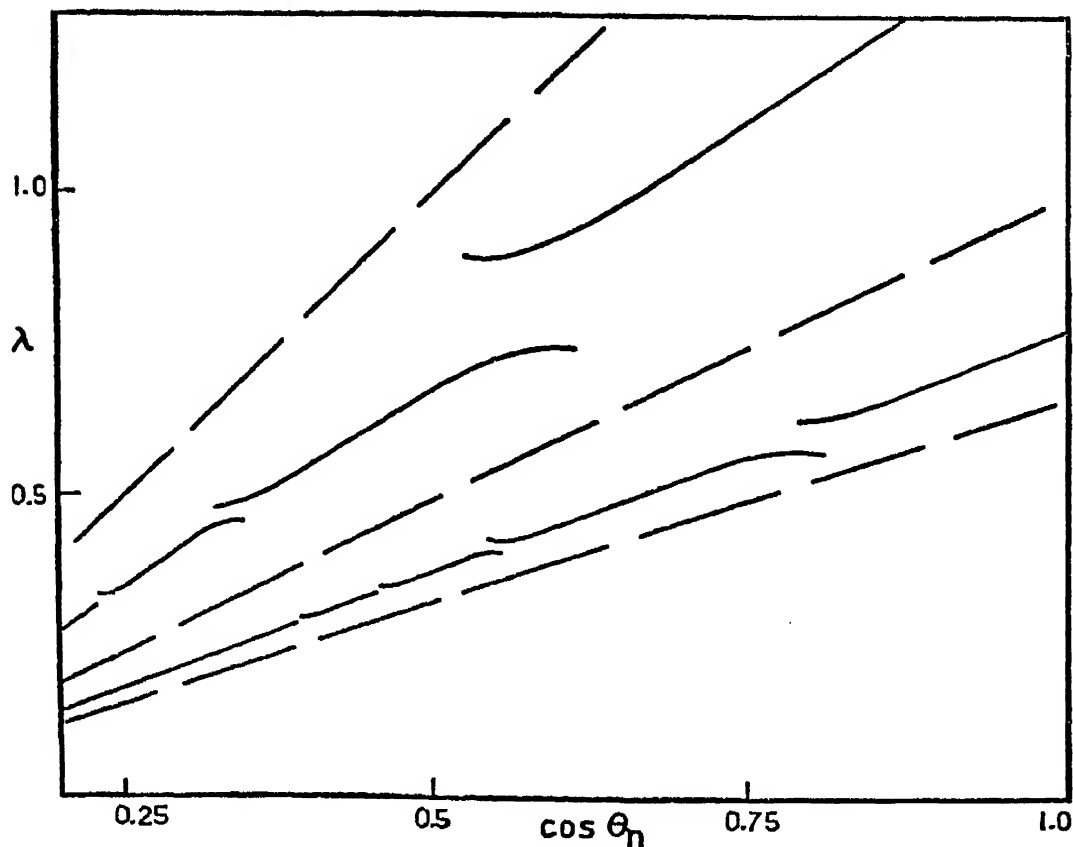


FIG. 95

$\theta_n$  is the angle with the normal, we therefore obtain a graph of the type shown in Fig. 95. The forbidden ranges occur near the values given by  $m\lambda \doteq 2b \sin \theta_n$ , where  $b$  is the spacing of planes normal to the plane of incidence and also normal to the crystal surface;  $m$  is an integer. Physically this means that Bragg reflection takes place from this new set of planes and energy is abstracted from the beam which was being considered. The special form of potential chosen by Morse is not in fact necessary and the theory is worked out quite generally in Fröhlich's book,<sup>1</sup> where the connection with the theory of metals is seen. Fig. 96 shows the experimental results of

<sup>1</sup> Fröhlich, *Elektronen Theorie der Metalle*, p. 95.

Davisson and Germer, which have the same appearance as Morse's curves in Fig. 95. The anomalous dispersion probably occurs at other places besides the point  $\lambda = 1.3 \text{ \AA}$  mentioned above. Other dynamical treatments have been given by Bethe and Shinohara and are dealt with in Chapter XIX. It

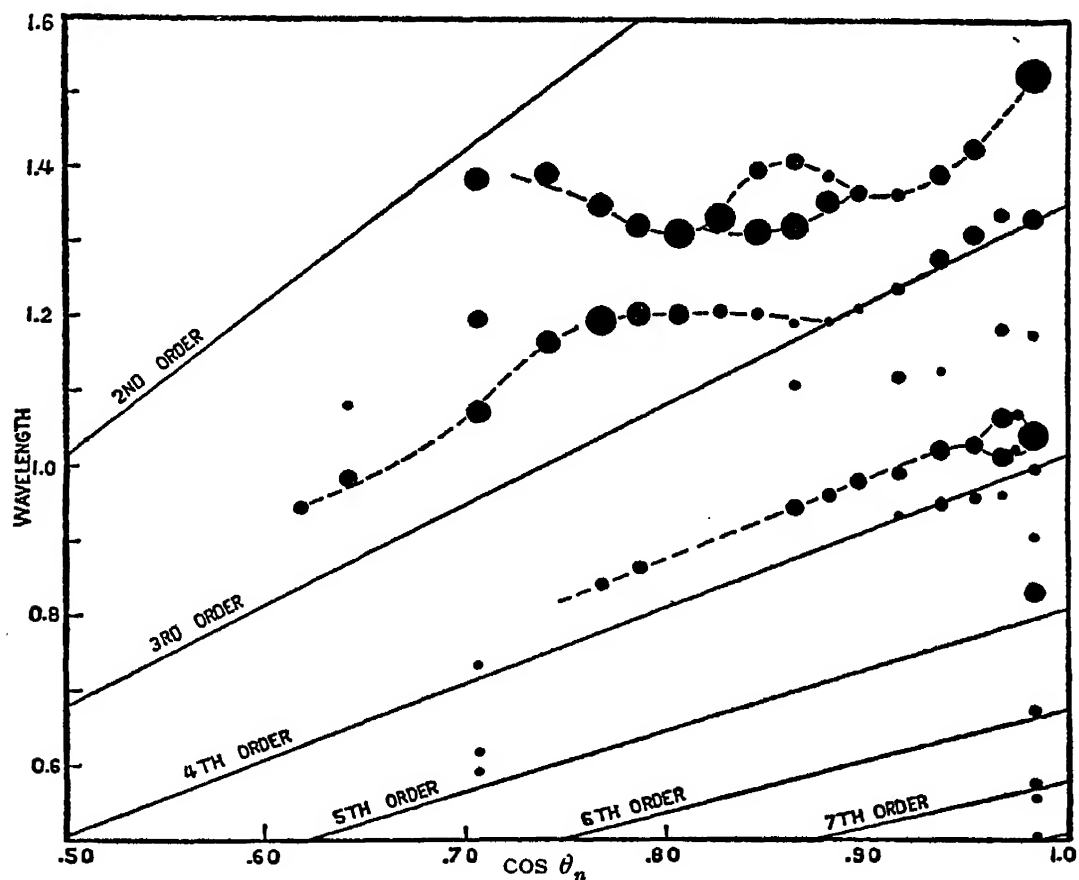


FIG. 96

should be noted that Bethe only considers the case of one diffracted beam, although it is dealt with very fully.

FARNSWORTH.<sup>1</sup>—Single crystals of copper, silver and gold were used in Farnsworth's experiments. The apparatus was similar to that of Davisson and Germer and, in addition, a side tube was provided into which the crystal could be withdrawn for the purpose of strong heating. Consequently the main tube did not become covered with evaporated metal.

The first results from the copper crystal ((100) face) were obtained with normal incidence, both azimuthal and co-

<sup>1</sup> Farnsworth, *Phys. Rev.* 34, p. 679 (1929); *ibid.* 35, p. 1131 (1930); *ibid.* 40, p. 684 (1932); *ibid.* 43, p. 900 (1933); *ibid.* 49, p. 598 (1936); *ibid.* 49, p. 605 (1936).

latitude curves being investigated. In addition to the "Laue" beams with a refractive index greater than unity, Farnsworth found many other Laue beams requiring a spacing twice that of copper (or a wave-length  $\lambda/2$ ). In spite of the fact that these beams occurred even under the best vacuum conditions it was concluded that they arise from gas forming a double-spaced face-centred structure and which was apparently difficult to remove from the copper. When the out-gassing was not so complete, Farnsworth deduced from his results that the gas atoms form a simple cubic lattice.

Further results were obtained with another copper crystal, again using the (100) face and normal incidence. The feature of these results was the occurrence of numerous double peaks and subsidiary peaks (satellites) in the diffracted beams. These were found, for example, when the voltage was varied in small steps and the collecting cylinder adjusted for maximum current at each voltage; then a plot was made of the current to the collecting cylinder against the voltage of the electrons. The appearance of these satellites was found to depend on the precise angle of incidence. A deviation of a few degrees from the normal caused a considerable alteration in the character of the satellites. Some results were also obtained with oblique incidence, the collector being fixed to record the specularly reflected beam (Bragg case). On varying the voltage and plotting collector current against voltage, the curve found (Fig. 97) was similar to Fig. 14 (p. 36), but had, in addition, many subsidiary peaks.

When a silver crystal was substituted for the copper one, the gas beams were scarcely found at all, but again the subsidiary peaks were noted. The number of subsidiary components for each beam was generally greater for silver than for copper and the intensities in the two cases were different, as far as could be judged.

Farnsworth also investigated the diffracted beams from a gold crystal, using normal incidence. No resemblance could be found with silver either as regards intensity or fine structure in corresponding beams. No gas beams were found with gold even when the experimental conditions indicated that gas was present. It was deduced that gas does not form a lattice on gold as it does in other cases.

Even if refraction occurs, one should expect the diffracted beams to satisfy roughly the surface grating interference condition. Thus, in the case of normal incidence, if  $\lambda$  is plotted against  $\sin \phi$ , as in Fig. 13 (p. 34), a straight line through the origin should be found for each order. Farnsworth's results on silver and gold show that this is by no means always the case. When experiments were performed with a silver crystal cut to a (110) plane, it was noticed that (111) and (100) facets were developed during heating of the crystal. It is natural to suppose that these new planes are the surface gratings which are to be considered in this connection. Examination of the diffraction results from this point of view showed agreement with the new surface grating conditions, and it was deduced that after evaporation of silver the (110) planes did not occur at all. Farnsworth<sup>1</sup> and one of the authors<sup>2</sup> had indeed previously suggested that other facets must be introduced to explain some of Sproull's results (cf. p. 277).

Farnsworth found that a thin layer of silver deposited by evaporation on a gold crystal gave the same beams as a large silver crystal, so that the layer must have been oriented like a single crystal. On the other hand, silver on copper did not form a single crystal. This may be compared with our own results using fast electrons and electrodeposition (p. 171). In the case of silver on gold, Farnsworth, knowing the rate of silver deposition, could calculate the thickness of the silver crystal formed. From the diffraction results he estimated that 50 per cent of the diffracted beam arises from the first atomic layer and 90 per cent from the first two layers, for voltages up to 300 V.

Farnsworth gives figures for the inner potential of copper, silver and gold, obtained from the results at normal incidence. In this case there is no bending of the rays on entering the crystal. If the beam under consideration arises from reflection at a particular set of Bragg planes of spacing  $d$  then we have  $n\lambda' = 2d \sin \theta$ , where  $\lambda'$  is the wave-length in the crystal, and  $\theta$  is the angle of incidence on the planes. From the geometry of the crystal we can determine  $\theta$  and  $d$  so that  $\lambda'$  may be calculated, and may be re-expressed in terms of volts,  $P'$ . The

<sup>1</sup> Farnsworth, *Phys. Rev.* 44, p. 417 (1933).

<sup>2</sup> Thomson, *ibid.*

measured voltage being  $P$ , we find in the usual notation

$$\mu^2 = \frac{\lambda^2}{\lambda'^2} = \frac{P'}{P} = 1 + \frac{\Phi}{P}$$

and hence

$$\Phi = P' - P.$$

Thus the inner potential is found by subtracting the experimental voltage from the calculated voltage, as is indeed evident *a priori*. This method is adopted by Farnsworth. The results found for any particular metal are by no means constant for different beams, and the variations do not show any definite trend.

Laschkarew<sup>1</sup> has examined some of Farnsworth's observations for the copper (100) face. He shows that the fine structure of the diffraction maxima can be accounted for by supposing that other planes reflect, and the intensity of the particular maximum under consideration is thus reduced as in Morse's theory. The symmetrical reflection curve may therefore be expected to have depressions on it at those voltages for which other planes reflect strongly. One result of this is to affect the apparent positions of the main maxima (cf. Fig. 97). The three graphs A, B, C represent results at the three different angles of incidence and the calculated positions of the maxima, neglecting refraction, are shown by arrows on the axes of abscissae. The dotted line indicates, on each of the graphs A, B, C, what the shape of the main maxima would be if the other reflections had not occurred. When the new positions, marked 3-10, are used to calculate the inner potential of copper, a smooth curve is obtained asymptotic for large orders to 25 volts. The incidence not being normal, Farnsworth's method of calculating inner potential cannot, of course, be used.

The subsidiary peaks are thus adequately explained in this particular instance and it is natural to suppose that some similar considerations apply to the case of normal incidence. However, in the absence of detailed calculations, a very large number of the observations must be regarded as remaining unexplained.

SPROULL.—In Sproull's experiments<sup>2</sup> both the (112) and

<sup>1</sup> Laschkarew, *Trans. Farad. Soc.* 31, p. 1081 (1935).

<sup>2</sup> Sproull, *Phys. Rev.* 43, p. 516 (1933); and *Rev. Sci. Instr.* 4, p. 1933.

(100) faces of tungsten single crystals were used and the apparatus allowed azimuthal and co-latitude observations to be made, as in Davisson and Germer's work. The electrons were incident normal to the crystal surface and it was possible to measure the beam scattered back in the direction of incidence ( $\phi = 0$ ). The maxima observed in each principal azimuth were plotted as usual on graphs of  $\sin \phi$  against  $\lambda$  and, in order to compare with simple theory, curves were drawn showing the

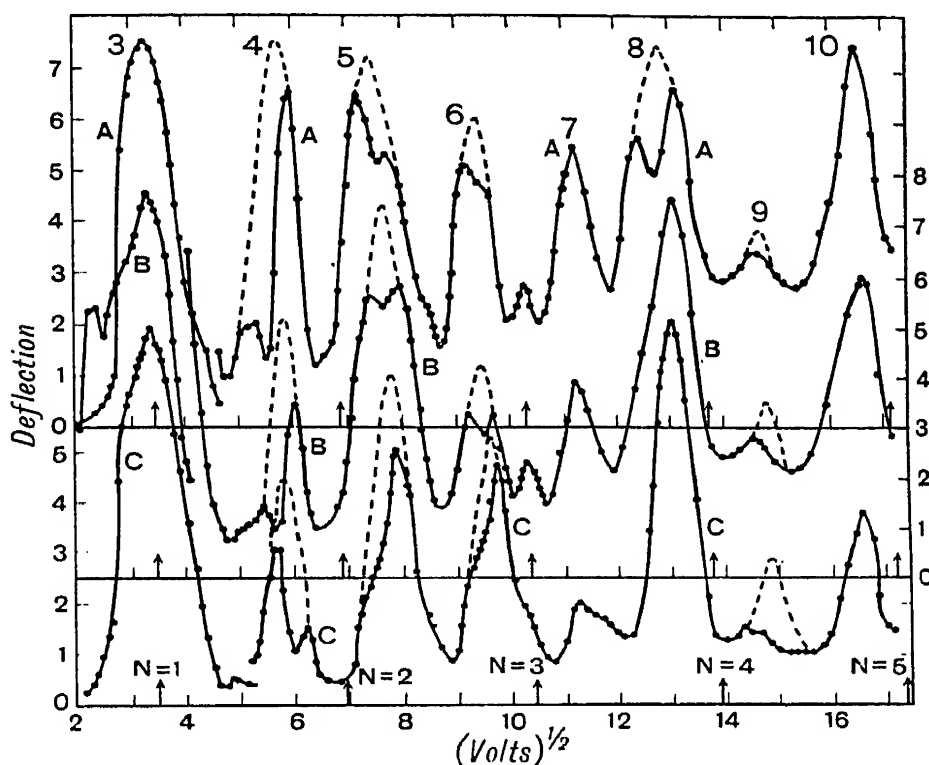


FIG. 97

relations appropriate to surface and depth interference for each azimuth (ignoring refraction). The main feature of Sproull's results is the fact that the maxima lie near to the theoretical depth interference curves but do not, as a rule, seem to be connected in any way with the surface interference curves. Sproull calculated the inner potential  $\Phi$ , using the depth interference condition and assuming bending of the rays at emergence from the crystal face but not at incidence. The values of  $\Phi$  which he found were fairly constant, with a mean of 5.7 volts.

We have already indicated, in describing Farnsworth's experiments, that when results in the diffraction of slow

electrons fail to conform with the surface interference condition it is due to the development of several different facets on the crystal surface during the preliminary out-gassing process. This being so, it is difficult to see how the inner potential can be calculated, since for such a calculation it is essential that the exact conditions of incidence should be known.

EHRENBERG.—Ehrenberg<sup>1</sup> used a visual method of detecting the diffracted beams of slow electrons. In order to get good fluorescence on the screen, the electrons were accelerated by a potential of about 10,000 volts after diffraction, and the accelerating grids and the screen were curved in such a way that the electrons were not deviated by this auxiliary apparatus. Arrangements were made for rotating the crystal, which was of copper with a (111) face.

Generally speaking, the diffraction maxima observed with different angles of incidence and different voltages, when plotted in the usual way, lay near the theoretical curves derived from the interference conditions of simple theory. Certain groups of results could not, however, be explained theoretically. The inner potential values which were deduced were irregular but showed a tendency to increase with voltage. In contrast to Farnsworth's observations on the (100) copper face, Ehrenberg found no gas beams from the (111) face.

In view of the fact that this apparatus has not been further used, it is difficult to assess its importance or say whether it is an improvement on the more usual Faraday cylinder method. The fluorescent screen does not seem to show up the variation in intensity as well as a series of Faraday cylinder current readings, and thus faint maxima and subsidiary peaks may be missed.

LASCHKAREW.—Laschkarew, Barengarten and Kuzmin<sup>2</sup> studied the diffraction of slow electrons by a plate of Ceylon graphite. They used a constant angle of incidence and measured the specularly reflected beam for different voltages. The apparatus is illustrated in Fig. 98, showing the electron gun C, specimen P, Faraday cylinders A, and subsidiary apparatus for out-gassing and temperature measurement.. When the surface was covered with gas very little current was obtained, and no

<sup>1</sup> Ehrenberg, *Phil. Mag.* 18, p. 878 (1934).

<sup>2</sup> Laschkarew, Barengarten and Kuzmin, *Zeit. für Phys.* 85, p. 631 (1933).

maxima. But after out-gassing at red heat and keeping the specimen always at  $200^{\circ}\text{C}$ ., strong diffracted beams were found. These results are indicated in Fig. 99 *e*, *b*, *c* and *a* representing different stages of the out-gassing process. In addition to the expected Bragg reflections, which gave an inner potential of about 20 volts, the odd order maxima forbidden by structure factor considerations also occurred.<sup>1</sup> It is interesting to note that they tried a polycrystalline specimen and no maxima were found. But a *worked* polycrystalline specimen of copper, showing preferential orientation of the crystal grains, did give a strong diffracted ray.

Although the elaborate experimental technique of Davisson and Germer, and of Farnsworth, is necessary for a complete examination of the diffracted

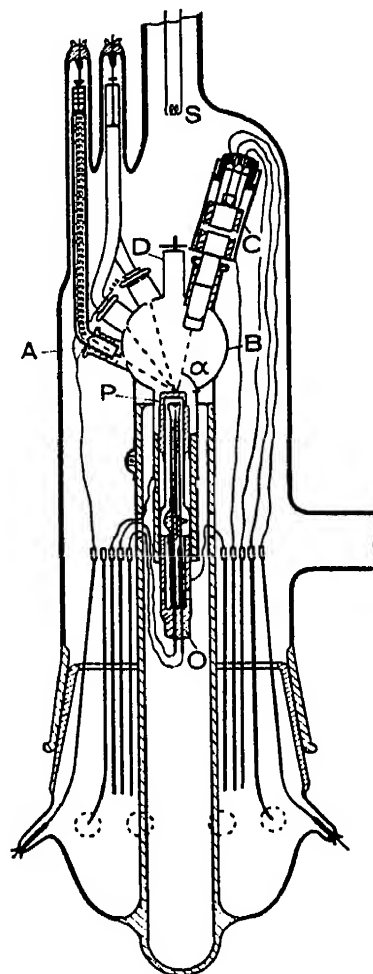


FIG. 98

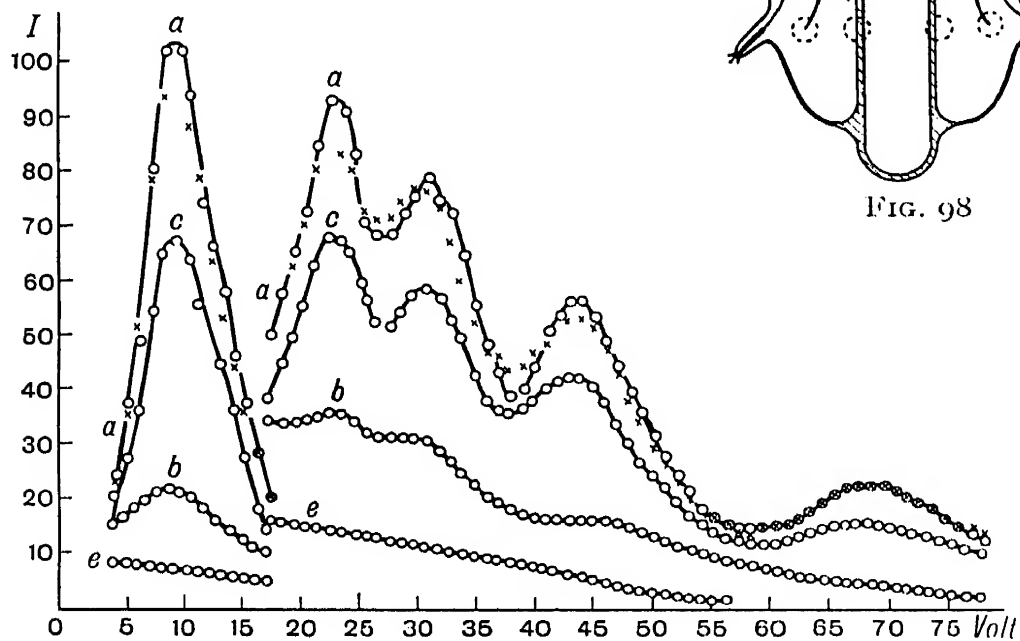


FIG. 99

beams of slow electrons from single crystals, it appears that much can be learned from experiments, such as Laschkarew's,

<sup>1</sup> These may, however, be explained, as on p. 296, by means of dynamic interaction.

in which the specularly reflected beam is examined for different voltages and for one or two angles of incidence. It is not yet clear whether all types of crystals can be studied successfully,<sup>1</sup> but it is seen that non-metallic crystals may be used and may have, indeed, the advantage of not evaporating during the out-gassing process.

In a further paper Laschkarew and Kusmin<sup>2</sup> studied the relation between the intensity of the diffracted beams and the temperature of the graphite. The results were represented by an equation of the form

$$I_T = I_0 \exp \left\{ -\frac{a \sin^2 \theta}{150} \left( P + \frac{\Phi}{\sin^2 \theta} \right) (T - T_0) \right\},$$

where  $I$  represents intensity,  $\theta$  the angle of incidence,  $P$  the voltage,  $\Phi$  the inner potential and  $T$  the temperature. The analogous X-ray equation, valid for high temperature, is

$$I_T = I_0 \exp \left\{ -\frac{a \sin^2 \theta}{\lambda^2} (T - T_0) \right\}.$$

Good agreement is found between the X-ray value of the constant  $a$  ( $0.0038 \text{ \AA}^2 \text{ deg.}^{-1}$ ) for graphite and the value for electrons ( $a = 0.0036 \text{ \AA}^2 \text{ deg.}^{-1}$ ).

### Further Experiments

Kassatotschkin<sup>3</sup>, using a fixed angle of scattering, examined the diffraction of slow electrons from sublimed tungsten. He obtained maxima which gave an inner potential of 10.5 volts and, in addition, some maxima for which the simple Bragg relation was satisfied. The latter were explained in the usual way by supposing that the surface was 'stepped' and the path difference was occurring *in vacuo*.

Kalaschnikow and Jakowlew<sup>4</sup> also employed the constant angle of deflection, but with normal incidence, to investigate

<sup>1</sup> Cf. Dames, *Ann. d. Phys.* 12, p. 185 (1932) (calcite and aragonite); also Suhrman and Haiduck, *Zeit. für Phys.* 96, p. 726 (1935) (galena, pyrites and stibnite). Also Moon and Harkins, *J. Phys. Chem.* 40, p. 941 (1936) (rock-salt and galena).

<sup>2</sup> Laschkarew and Kusmin, *Phys. Zeit. d. Sowjetunion*, 9, p. 211 (1934).

<sup>3</sup> Kassatotschkin, *Acta Physicochimica*, 2, p. 317 (1935).

<sup>4</sup> Kalaschnikow and Jakowlew, *Phys. Zeit. d. Sowjetunion*, 9, p. 13 (1936).

diffraction from zinc crystals. They found that the inner potential increased asymptotically to about 27 volts as the order of reflection increased. The effect of temperature on the intensities was also studied and compared with Debye's theory for X-rays.

### Transmission Experiments

Rupp<sup>1</sup> performed 'transmission' experiments using thin metallic films and detecting the electrons either by a photographic plate coated with oil or by a Faraday cylinder. Some 'forbidden' rings were found. The other rings gave fair agreement with simple theory. Their use to calculate a value for the refractive index was due to an erroneous argument.<sup>2</sup>

It should be understood that the normal experience of workers in the field of fast electrons tends to show that the thinnest obtainable metal films will not transmit electrons with energy much less than about 10,000 volts. Possibly, however, films may occur with extremely thin 'windows' in them such as Andrade<sup>3</sup> observed. These films might then transmit low-energy electrons.

Buhl<sup>4</sup> carried out an experiment with 220-volt electrons in which the specimen was polycrystalline silver deposited by evaporation round the edge of a pin-hole through which the electrons passed. Maxima were observed corresponding to the usual rings obtained with X-rays or high-speed electrons and no forbidden maxima occurred.

### Conclusions

The most interesting feature of the diffraction of slow electrons is the sensitivity to adsorbed gas, which may either manifest itself by a series of diffraction maxima due to a gas lattice or, in other cases, by a general reduction in the intensity of the electrons diffracted from the crystal. It is in this point that slow electrons have an advantage over fast electrons.

The introduction of a refractive index or inner potential

<sup>1</sup> Rupp, *Ann. d. Phys.* 85, p. 981 (1928); 1, p. 773 (1929); cf. also Tartakowsky, *Zeit. für Phys.* 56, p. 416 (1929).

<sup>2</sup> Thomson, *Phil. Mag.* 6, p. 939 (1928).

<sup>3</sup> Andrade and Martindale, *Phil. Trans.* 234, p. 69 (1935).

<sup>4</sup> Buhl, *Phys. Zeit.* 32, p. 842 (1932).

is a matter which evidently requires further discussion and investigation. In some cases constant values of inner potential are found for different maxima, in other cases the values increase asymptotically, and in others the values are scattered over a wide range. Bethe has indeed given reasons for supposing that  $\Phi$  should increase with voltage — the fast electrons spending more of their time in the regions of high potential in the lattice than the slow electrons. It is probable, however, that one of the difficulties lies in the fact that the first layer of atoms scatters a large fraction of the incident electrons and the effect of this layer is so important that the usual conceptions of inner potential do not always apply. Von Laue,<sup>1</sup> with the dynamical theory in mind, has discussed whether it is legitimate to consider the potential as stopping abruptly at the surface, when in fact the field dies away asymptotically at the surface. He concludes that for electrons above about 200 volts energy the approximation is justified, but not for lower voltages. This, of course, is just in the region of voltages normally used. Further theoretical work is necessary, but it is evident from what has been done that the meaning of inner potential for slow electrons is by no means simple.

<sup>1</sup> Von Laue, *Phys. Rev.* 37, p. 53 (1931).

## CHAPTER XIX

### DYNAMICAL THEORY

WE have assumed so far that the action of a crystal on electronic waves can be adequately represented by finding the amplitude of the wave scattered by each small element of volume and combining these amplitudes, with phases depending on the situation of the element, to form a resultant scattered wave. To this approximation, we have seen that the scattered amplitude is proportional to the potential of the elementary volume above its surroundings. The mean potential of the crystal as a whole has been taken to act in a way analogous to the refractive index of an optical medium. The first assumption involves neglecting the interaction of the scattered wave with the crystal. But the resultant scattered intensity of even a few atom planes is comparable with that of the original beam, so that it is not clear *a priori* that the assumption is even approximately justified. Again, in treating the inner potential as a refractive index, the surface of the crystal is taken as a mathematical discontinuity which is not in accordance with the facts. In this chapter we will describe a more thoroughgoing dynamical treatment, and discuss the extent to which it has removed these approximations in the theory and the modifications which it involves in the predicted diffractions.

Schrödinger's equation has been applied to the study of electron diffraction by a number of authors, among whom we may mention Sir J. J. Thomson,<sup>1</sup> P. M. Morse,<sup>2</sup> S. Kikuchi<sup>3</sup> and Bethe.<sup>4</sup> The general character of the results obtained by these different authors is the same, but as Bethe's theory is more detailed than the others, and in certain respects more general, we select it for description.

Bethe treats the problem in the same general way in which Ewald has dealt with the allied case of the diffraction of

<sup>1</sup> Thomson, *Phil. Mag.* (7) 8, p. 1073 (1929).

<sup>2</sup> Morse, *Phys. Rev.* 35, p. 1310 (1930).

<sup>3</sup> Kikuchi, *Sci. Pap. Inst. Phys. Chem. Res.* 26, p. 225 (1935).

<sup>4</sup> Bethe, *Ann. d. Phys.* 85 (1928).

X-rays by a crystal. The crystal is treated as a triply periodic field of potential the expression for which is substituted in Schrödinger's equation. When we try to solve this equation the first point which appears is that there is no solution representing a single-plane wave. Any such wave must therefore generate others, and only an assemblage of waves can represent the steady state with which Schrödinger's equation, which does not involve the time, necessarily deals.

Starting from Schrödinger's equation

$$\nabla^2\psi + \frac{8\pi^2me}{h^2}(E + V)\psi = 0,$$

Bethe writes 
$$\frac{8\pi^2me}{h^2}E \equiv K^2,$$

so that  $K/2\pi$  is the wave number for the electron outside the crystal where  $V=0$ . Inside the crystal he writes

$$\frac{8\pi^2me}{h^2}V \equiv U \equiv \sum_{\mathbf{g}} v_{\mathbf{g}} e^{2\pi i(\mathbf{g}\mathbf{r})},$$

where  $\mathbf{g}$  is a vector to a point of the reciprocal lattice, and  $\mathbf{r}$  is the current vector, both taken from the origin. This is a three dimensional Fourier Series, for any multiple of a  $\mathbf{g}$  is itself a  $\mathbf{g}$ . Further, it is periodic in the period of the crystal, for if  $\mathbf{r}$  changes by a step which is a multiple of a step in the crystal lattice,  $(\mathbf{g}\mathbf{r})$  changes by an integer owing to the properties of the reciprocal lattice. If there is a centre of symmetry,  $v_{\mathbf{g}} = v_{-\mathbf{g}}$  and the sum reduces to a series of cosines and the quantities  $v_{\mathbf{g}}$  are real. To show that one plane wave cannot exist by itself, try

$$\psi = c_0 e^{i(\mathbf{k}_0\mathbf{r})},$$

then <sup>1</sup>

$$\nabla^2\psi = k_0^2\psi$$

and

$$(K^2 - k_0^2)c_0 e^{i(\mathbf{k}_0\mathbf{r})} + \sum_{\mathbf{g}} c_0 v_{\mathbf{g}} e^{i(\mathbf{k}_0\mathbf{r}) + 2\pi i(\mathbf{g}\mathbf{r})} = 0,$$

which cannot hold for *all*  $\mathbf{r}$ . Try  $\psi$  as the set of waves represented by

$$\psi = \sum \psi_{\mathbf{h}} e^{i(\mathbf{k}_{\mathbf{h}}\mathbf{r})}$$

where

$$\mathbf{k}_{\mathbf{h}} = \mathbf{k}_0 + 2\pi\mathbf{h}.$$

<sup>1</sup> We write  $k_0$  for  $|\mathbf{k}_0|$ ; similarly we shall put  $k_{\mathbf{h}} = |\mathbf{k}_{\mathbf{h}}|$ .

These waves have, as wave numbers, vectors AH (Fig. 100), which are the vector sums of a primitive wave number  $\mathbf{k}_0/2\pi$ , and vectors  $\mathbf{h}$  to all points of the reciprocal lattice. Substituting in Schrödinger's equation we get

$$\sum_h \psi_h (K^2 - k_h^2) e^{i(\mathbf{k}_h \mathbf{r})} + \sum_h \psi_h e^{i(\mathbf{k}_0 + 2\pi \mathbf{h} \cdot \mathbf{r})} \sum_g v_g e^{2\pi i(\mathbf{g} \mathbf{r})} = 0.$$

Equating to zero the coefficients of individual exponentials gives the set of equations

$$\psi_h (K^2 - k_h^2) + \sum_g v_g \psi_{h-g} = 0,$$

or taking the term  $v_0$  out from the sum,

$$\psi_h (K^2 + v_0 - k_h^2) + \sum'_g v_g \psi_{h-g} = 0, \quad (A)$$

where in  $\sum'_g$  the term  $g=0$  is omitted.

Equations (A) form a triply infinite set of relations between the amplitudes of the set of waves.

So far  $k_0$  is arbitrary, and unconnected with  $K/2\pi$  the wave number in free space. A connection is supplied by the boundary conditions. Suppose  $z=0$  is a plane such that  $V=0$  for  $z<0$ .

In the vacuum there will be one or more waves of wave number  $K/2\pi$  and we write

$$\psi = \sum_m \psi_m e^{i(\mathbf{K}_m \mathbf{r})},$$

where

$$|\mathbf{K}_m| = K.$$

As usual in problems in wave mechanics, we take  $\psi$  and its normal derivative as continuous on the two sides of the boundary. Hence

$$\sum_m \psi_m e^{i(\mathbf{K}_m \mathbf{r}')} = \sum_g \psi_g e^{i(\mathbf{k}_g \mathbf{r}')},$$

where  $\mathbf{r}'$  is a vector in the surface, and

$$\sum_m \psi_m (\mathbf{K}_m \mathbf{n}) e^{i(\mathbf{K}_m \mathbf{r}')} = \sum_g \psi_g (\mathbf{k}_g \mathbf{n}) e^{i(\mathbf{k}_g \mathbf{r}')},$$

where  $\mathbf{n}$  is the unit vector normal to the surface. Since this holds for all  $\mathbf{r}'$  the exponents are equal, and the tangential components of  $\mathbf{K}_m$  and  $\mathbf{k}_g$  are equal. Now for the given wave

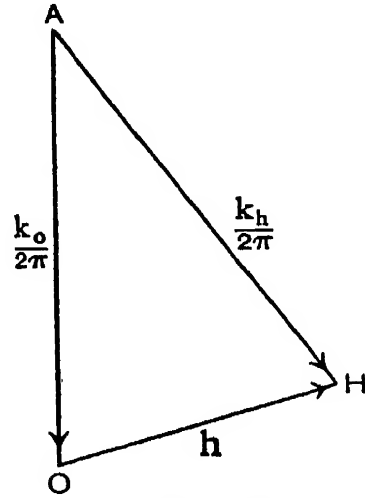


FIG. 100

number  $K/2\pi$  there are two waves outside the crystal with the same tangential component and equal and opposite normal components. Thus

$$\mathbf{K}_m = \mathbf{T} \pm \Gamma_m \mathbf{n},$$

$$\mathbf{k}_g = \mathbf{T} + \gamma_g \mathbf{n},$$

where the two terms in each case represent respectively the tangential and normal components, but since  $|\mathbf{k}_g|$  is not yet fixed there will be many vectors satisfying the second equation. The conditions of amplitude give

$$\left. \begin{aligned} \Psi_m + \Psi_m' &= \sum \psi_g \\ \Psi_m - \Psi_m' &= \sum \frac{\gamma_g}{\Gamma_m} \psi_g \end{aligned} \right\} \quad (B)$$

where  $\Psi_m, \Psi_m'$  refer to the two vacuum waves  $\mathbf{K}_m$ , and the summation refers to the amplitudes  $\psi_g$  of waves which satisfy the condition  $\mathbf{k}_g = \mathbf{T} + \gamma_g \mathbf{n}$ .

Corresponding to a vacuum wave with tangential component  $\mathbf{T}$ , the possible waves in the crystal are  $\mathbf{k}_0 = \mathbf{T} + \gamma_0 \mathbf{n}$  and  $\mathbf{k}_g = \mathbf{k}_0 + 2\pi \mathbf{g}$ . These can coexist with other vacuum waves for which  $\mathbf{T}' = \mathbf{T} + 2\pi \mathbf{g}_{\text{tang}}$ , provided the normal component is chosen so as to make the total wave number equal to  $K/2\pi$ . It can be seen that the tangential components of  $\mathbf{g}$  are determined only by the atoms in the surface layer, since two axes of the lattice can be chosen to lie in the surface.<sup>1</sup> Hence the directions, but not the intensity, of the vacuum waves can be found from a knowledge of the surface atoms alone.

The system of equations (A) cannot in general be solved. If, however, it is assumed that the value of the summation in (A) is of the same order of magnitude for all  $h$ , the important waves will be those for which  $K^2 + v_0 - k_h^2$  is small. The value of  $K$  is supposed given but  $k_0$  is arbitrary so far, apart from the boundary conditions. We assume that there is a primary wave for which  $K^2 + v_0 - k_0^2$  is small. It cannot be zero, which

<sup>1</sup> If  $\alpha_1, \alpha_2$  are the axes in the surface then we have, in the notation of Chapter VI,  $\beta_1 = [\alpha_2 \alpha_3] / (\alpha_1 [\alpha_2 \alpha_3])$ . The component of  $\beta_1$  along  $\alpha_2$  is  $\beta_1 \alpha_2 / |\alpha_2| = 0$  and the component along  $\alpha_1$  is  $(\beta_1 \alpha_1) / |\alpha_1| = 1 / |\alpha_1|$ . Similarly the component of  $\beta_2$  along the surface is  $1 / |\alpha_2|$  and the component of  $\beta_3$  is zero. Thus the tangential component of  $\mathbf{g}$  is determined wholly by  $\alpha_1$  and  $\alpha_2$ . The proof assumes that  $\alpha_1, \alpha_2$  have been chosen at right angles to one another. The extension to the general case is simple.

would give the ordinary change of wave-length by refraction, because then  $\psi_0$  would be infinite compared with the other waves, which could therefore be neglected, giving a single wave solution which we have seen to be impossible. The interesting case is when the Laue conditions are nearly satisfied. If they were exactly fulfilled, Fig. 101 would represent the condition with

$$2\pi LO = \mathbf{k}_0 = 2\pi LH = \mathbf{k}_h = \sqrt{\mathbf{K}^2 + v_0};$$

thus

$$\mathbf{K}^2 + v_0 - k_0^2 \quad \text{and} \quad \mathbf{K}^2 + v_0 - k_h^2$$

would vanish simultaneously. Actually, for a reason similar to that given above, they do not vanish exactly and other

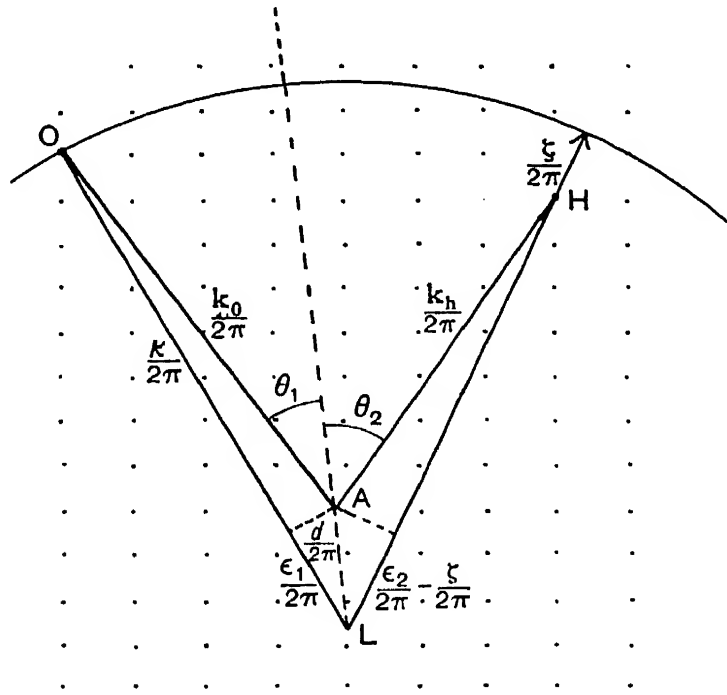


FIG. 101

waves exist, though small compared with the main ones. Write  $\mathbf{K}^2 + v_0 = \kappa^2$  so that  $\kappa$  is the value of  $k_0$  in the crystal on the simple theory. Then  $\epsilon_1 = \kappa - k_0$  and  $\epsilon_2 = \kappa - k_h$  are called 'resonance errors'. We know that the component of  $\mathbf{k}_0$  tangential to the free surface is the same, *i.e.*  $\mathbf{T}$ , as that of  $\mathbf{K}_m$ , which is supposed given. Let the dotted line represent the normal to the free surface (Fig. 101), drawn through the point of the surface whose vector distance from O is  $\mathbf{T}/2\pi$ . Then if A is any point<sup>1</sup> on this line, AO is a possible position for

<sup>1</sup> The normal is not necessarily in the plane of OAH, hence L, also, will not in general be in this plane.

$\mathbf{k}_0/2\pi$ . The 'Laue point' is defined by making  $LO = \kappa/2\pi$ . With L as centre and radius LO we describe a sphere, the Ewald sphere. If H is the point of the reciprocal lattice which nearly satisfies the Laue conditions the sphere will pass near H and if the intercept on LH is  $\zeta/2\pi$ ,  $\zeta$  is called the 'excitation error'. If  $\kappa_0$  is the value of  $\kappa$  which at the particular incidence would exactly satisfy the Laue conditions, it can be shown that  $\zeta = (\kappa - \kappa_0)(1 - \cos \phi)$ , where  $\phi$  is the angle between the chief rays in the crystal. The quantity  $AL = d/2\pi$ , called by Bethe the '*anpassung*', plays an important part in the theory. The excitation error is a geometrical quantity determined by the crystal lattice and the direction of the incident ray, while ' $d$ ' depends on the dynamics of the problem, and is to be found. We find it, and at the same time determine the amplitudes  $c_1, c_2$ , of the principal waves, from equations (A). First find the small amplitudes  $\psi_g$  in terms of  $c_1, c_2$ , neglecting the other waves in  $\sum'_g v_g \psi_{h-g} = 0$ .

Then

$$\psi_0(\kappa^2 - k_0^2) = 2c_1\kappa\epsilon_1 = -\sum \psi_g v_{-g},$$

$$\psi_h(\kappa^2 - k_h^2) = 2c_2\kappa\epsilon_2 = -\sum \psi_g v_{h-g},$$

and substituting for  $\psi_g$  we get

$$c_1(2\kappa\epsilon_1 - V_{11}) - c_2V_{12} = 0,$$

$$c_2(2\kappa\epsilon_2 - V_{22}) - c_1V_{21} = 0,$$

where (in the case of a crystal with a centre of symmetry)

$$V_{11} = \sum'_g \frac{v_g^2}{\kappa^2 - k_g^2},$$

$$V_{12} = V_{21} = \sum'_g \frac{v_g v_{g-h}}{\kappa^2 - k_g^2} - v_h,$$

$$V_{22} = \sum'_g \frac{v_g^2 - v_h^2}{\kappa^2 - k_g^2},$$

the suffices 0 and  $h$  being omitted,

In these equations the values of  $k_g^2$ , etc., are taken from the first approximation, *i.e.*  $\mathbf{k}_g = \mathbf{K} + 2\pi\mathbf{g}$ . To find  $d$  we have that

$$\epsilon_1 = d \cdot \cos \theta_1,$$

$$\epsilon_2 = \kappa - k_h = LH + \zeta - AH = d \cdot \cos \theta_2 + \zeta,$$

where  $\theta_1, \theta_2$  are the angles which the two principal wave normals make with the normal to the surface. Hence

$$\left. \begin{aligned} c_1(2\kappa d \cos \theta_1 - V_{11}) - c_2 V_{12} &= 0 \\ c_2(2\kappa \cdot \overline{d \cos \theta_2 + \zeta} - V_{22}) - c_1 V_{12} &= 0 \end{aligned} \right\}, \quad (C)$$

and on eliminating  $c_1/c_2$  we get a quadratic for  $d$ .

Two cases present themselves. In case 1 (Laue case)  $\cos \theta_1$  and  $\cos \theta_2$  are positive, and the values of  $d$  are always real; the reflected ray does not emerge from the face on which the electrons are incident. In case 2 (Bragg case)  $\cos \theta_2$  is negative, the reflected ray emerges from the face of incidence, and for certain values of  $\zeta$  the values of  $d$  become complex. As we shall see, this corresponds to a region of selective (total) reflection.

To treat this case in greater detail we neglect the variation in  $\kappa^2 - k_g^2$  in the small range of  $\zeta$  with which we are concerned and we can therefore take the  $V$ 's as constants. It can then be shown by simple algebra that the region of complex  $d$  extends over a range of  $\zeta$  given by  $\zeta_0 \pm w$ , where

$$\zeta_0 = \frac{V_{22}}{2\kappa} + \frac{V_{11}}{2\kappa} \cdot \frac{-\cos \theta_2}{\cos \theta_1} \quad \text{and} \quad w = \frac{|V_{12}|}{\kappa} \sqrt{\frac{-\cos \theta_2}{\cos \theta_1}}.$$

Finally

$$d = \frac{V_{11}}{2\kappa \cos \theta_1} - \frac{w}{2 \cos \theta_2} (W \pm \sqrt{W^2 - 1}), \quad \text{where} \quad W = \frac{\zeta_0 - \zeta}{w}$$

and ranges from  $-1$  to  $+1$  over the region of selective reflection. For each value of  $d$  we have one value of  $\mathbf{k}_0$ , and one of  $\mathbf{k}_h$ , so that the solution involves in all four waves of considerable magnitude. Since  $d$  affects only the components of the wave vector normal to the surface, the four waves can be written  $\mathbf{k}_0' \pm \omega \mathbf{n}$ ,  $\mathbf{k}_h' \pm \omega \mathbf{n}$ , where  $2\omega$  is the difference in the  $d$ 's. Here  $\mathbf{k}_0'$  differs from  $2\pi \mathbf{OL}$  by the mean of the two  $d$ 's, and  $\mathbf{k}_h' = \mathbf{k}_0' + 2\pi \mathbf{h}$ . For large values of  $W$  the quantity  $2\omega$  is proportional to  $\zeta_0 - \zeta$ , and is equal to it if  $\theta_2 = 0$ . The ratio of the amplitudes of the waves  $\psi_0, \psi_h$  for each of the two values of  $d$  is determined by equations (C).

It remains to calculate the intensity in terms of that of the

incident wave by means of the boundary conditions (B). To do so we neglect the weak waves, and in forming the summation on the right-hand side of (B) it must be remembered that only those crystal waves are to be included which have the same tangential components of wave number as the vacuum wave. It can be seen from (B) that of the two vacuum waves  $\Psi_m, \Psi_m'$  corresponding to any principal crystal wave only one is important. For since the principal crystal waves differ only slightly in total wave number from the vacuum waves, and since the tangential components are equal, the normal components must be nearly equal also, *i.e.*  $\gamma_g \approx \pm \Gamma_m$ . Hence either  $\Psi_m$  or  $\Psi_m'$  is small. In other words there is no appreciable reflection of a wave from the surface of the crystal as such. Bethe treats the Bragg case, in which the known amplitude of the vacuum wave at the entrance surface gives a relation with the amplitudes of the two crystal waves  $\psi_0$ . Another relation is given at the back of the crystal, assumed parallel sided. Here there is no vacuum wave corresponding to the  $\psi_n$  waves, and this gives a relation between their two amplitudes. The two relations given by equations (C) complete the equations required to solve for the four amplitudes.<sup>1</sup>

In consequence of the existence of two nearly parallel waves of nearly the same wave-length in each of the two principal directions, systems of beat waves are set up on the crystal, and  $\psi$  involves terms in the sine and cosine of  $\omega z$ . From an experimental point of view, the important quantities are the currents of electrons entering and leaving the crystal.

Outside the range of selective reflection,  $W$  is greater than 1 and  $\omega$  real. For the reflected beam

$$S_2 = S_0 \frac{\sin^2 \omega H}{W^2 - \cos^2 \omega H}$$

and for the transmitted beam

$$S_1 = S_0 \frac{W^2 - 1}{W^2 - \cos^2 \omega H},$$

<sup>1</sup> It might be thought that difficulty might arise when the Bragg plane is parallel to the surface, since then the tangential components of  $\mathbf{k}_0, \mathbf{k}_g$  are equal, but further analysis shows that no exception occurs.

where  $S_0$  is the intensity of the incident beam and  $H$  the thickness of the crystal. These thus fluctuate with the thickness of the plate, like the light reflected from a thin film. In practice it would be very difficult to get electrons of sufficiently constant wave-length, on which  $\omega$  depends, to detect the effect even if the crystal had accurately parallel sides. The best chance of observing it would be with slow electrons, but even here there might be difficulty owing to inelastic collisions. Taking an average over a range of  $\omega$  or  $H$  we get

$$S_2 = S_0 \left( 1 - \frac{\sqrt{W^2 - 1}}{W} \right), \quad S_1 = S_0 \frac{\sqrt{W^2 - 1}}{W}.$$

In the region of selective reflection the transmitted wave rapidly diminishes as the thickness of the crystal increases. For crystals more than about 100 atoms thick

$$S_1 \approx S_0 4(1 - W^2)e^{-2|\omega|H}.$$

The maximum value of  $|\omega|$  occurs when  $W = 0$ , *i.e.*  $\zeta = \zeta_0$ , which is not usually exactly zero, so that the wave-length is not that calculated by the simple theory. To get an idea of the magnitude of the extinction, consider a reflection for which  $\kappa = 10^2 \text{ \AA}^{-1}$ , corresponding to electrons of 36,500 volts,  $V_{12} \sim 1 \text{ \AA}^{-2}$ , which corresponds to a reflection of moderate strength, and let  $\cos \theta_2 = -\cos \theta_1 = 0.02$ , corresponding to a Bragg angle of about a degree. Then  $w = 10^{-2}$ , and the maximum value of  $|\omega| = 1/4$ , which gives an extinction to  $1/e$  in  $2 \text{ \AA}$ . The extinction is thus very rapid, in agreement with the rough calculation on p. 99. If, however, the crystal is thick enough, total reflection occurs over the whole range for which  $\omega$  is imaginary or  $1 > W > -1$ . For a wide range of incident wave-length it is found that  $2/\pi$  of the total reflection occurs in this region, so the 'half-breadth' of a reflected line can be taken without much error as the region in which  $W$  changes from 0 to  $\pm 1$ .<sup>1</sup> Bethe also considers a 'third approximation' in which account is taken of the variation of the denominators in the expressions  $V_{11}$ ,  $V_{12}$ , etc., with change in the wave-length. The general character of the conclusions is not greatly altered.

<sup>1</sup> A more accurate calculation shows that it is greater in the ratio  $\sqrt{\frac{4}{3}}$ .

## Laue Case

We are indebted to Dr. M. Blackman for the following comparison between the formulae for the Laue with those for the Bragg case, which are the only ones quoted by Bethe :

<i>Laue Case</i>	<i>Bragg Case</i>
$\theta_1 \approx \theta_2 \approx 0^\circ,$	$\theta_1 \approx \theta_2 \approx 90^\circ; \cos \theta_2 \text{ is } -ve,$
$w = \frac{ V_{12} }{\kappa} \sqrt{\frac{\cos \theta_2}{\cos \theta_1}},$	$w = \frac{ V_{12} }{\kappa} \sqrt{-\frac{\cos \theta_2}{\cos \theta_1}},$
$W = \left\{ \frac{1}{2\kappa} \left( V_{11} \frac{\cos \theta_2}{\cos \theta_1} - V_{22} \right) + \zeta \right\} / w,$	$W = \left\{ \frac{1}{2\kappa} \left( V_{22} - V_{11} \frac{\cos \theta_2}{\cos \theta_1} \right) - \zeta \right\} / w,$
$\omega = \frac{w}{2 \cos \theta_2} \sqrt{W^2 + 1},$	$\omega = \frac{w}{2 \cos \theta_2} \sqrt{W^2 - 1},$
$d = A \pm \frac{w}{2 \cos \theta_2} \sqrt{W^2 + 1},$	$d = A \pm \frac{w}{2 \cos \theta_2} \sqrt{W^2 - 1},$
where	$A = \frac{V_{11}}{2\kappa \cos \theta_1} - \frac{wW}{2 \cos \theta_2} \text{ in both cases.}$

$S_1 \text{ at } z = H \text{ is } S_0 \frac{W^2 + 1 - \sin^2 \omega H}{W^2 + 1},$	$S_1 \text{ at } z = H \text{ is } S_0 \frac{W^2 - 1}{W^2 - \cos^2 \omega H},$
$S_2 \text{ at } z = H \text{ is } S_0 \frac{\sin^2 \omega H}{W^2 + 1},$	$S_2 \text{ at } z = H \text{ is } S_0 \frac{\sin^2 \omega H}{W^2 - \cos^2 \omega H}$
Averaged $S_1 = S_0 \frac{2W^2 + 1}{2(W^2 + 1)},$	(outside the range of total reflection), Averaged $S_1 = S_0 \sqrt{W^2 - 1} / W,$
Averaged $S_2 = S_0 \frac{1}{2(W^2 + 1)}.$	Averaged $S_2 = S_0 \left( 1 - \frac{\sqrt{W^2 - 1}}{W} \right).$
<p><i>Note.</i>—<math>\omega</math> being very small, the averaging is not permissible for very thin films.</p>	

Relation between  $\zeta$  and Direction of the Rays

The quantity  $\zeta$  is fundamental in Bethe's theory as measuring the departure of the conditions from those corresponding to the exact relations of the simple theory. When the wavelength is small compared with the lattice constants, the geometrical relations take a simple form. The vector LO (Fig. 102) represents the direction which the incident ray would take in the crystal after undergoing the amount of refraction given by the elementary theory. If the sphere cuts LH at H' then

$$|LO| = \kappa / 2\pi \quad \text{and} \quad LH - LO = HH' = \zeta / 2\pi.$$

If the incidence is varied and the wave-length kept constant,  $L$  moves on a circle with  $O$  as centre. To find  $\zeta$  we have that

$$HH' = \zeta/2\pi = OH \cdot \Delta\theta = \kappa/2\pi \cdot O\hat{L}H \cdot \Delta\theta,$$

where  $\Delta\theta$  is the corresponding variation in the glancing angle from the value given by Bragg's law, or

$$\zeta = 2\kappa\theta \cdot \Delta\theta.$$

Now the range of  $\zeta$  is that which corresponds to the range  $1 > W > -1$ , for within this region lies most of the intensity

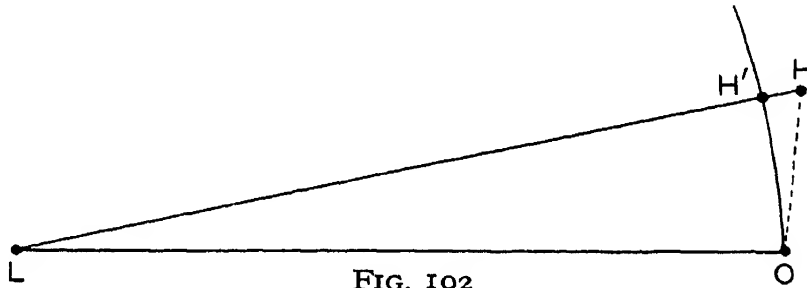


FIG. 102

of reflection both for the Bragg and Laue cases. For fast electrons, the terms involving  $V_{11}$  and  $V_{22}$  are unimportant, and the range in question is from  $\zeta = w$  to  $\zeta = -w$ , where  $w \sim |V_{12}|/\kappa$ . If the angle is kept fixed at that given by Bragg's law, and the wave-length varied, the value of  $\zeta$  is given by  $\zeta = (\kappa - \kappa_0)(1 - \cos \phi)$ . See p. 288.

### Deviation of the Electrons

It is possible to give a geometrical construction for the deviation of the rays, even when the Bragg condition is not satisfied, without solving the general dynamical problem or knowing the quantities  $V_{12}$ , etc. Consider first Fig. 103a. Here,  $O$ ,  $H$ ,  $L$  and  $A$  have the same meanings as in Fig. 101 and the dotted line  $z$  is the normal to the crystal surfaces supposed parallel. Since, by the boundary conditions, the tangential component of the wave vector is the same on both sides of the surface,  $LO$ , whose magnitude is  $\kappa/2\pi$ , gives the direction of the ray in the crystal which would be formed by refraction of the incident ray if the elementary theory of refraction held. To find the direction which corresponds in

the same way to the emergent ray, we have to find an imaginary wave vector having the magnitude  $\kappa/2\pi$  and the same tan-

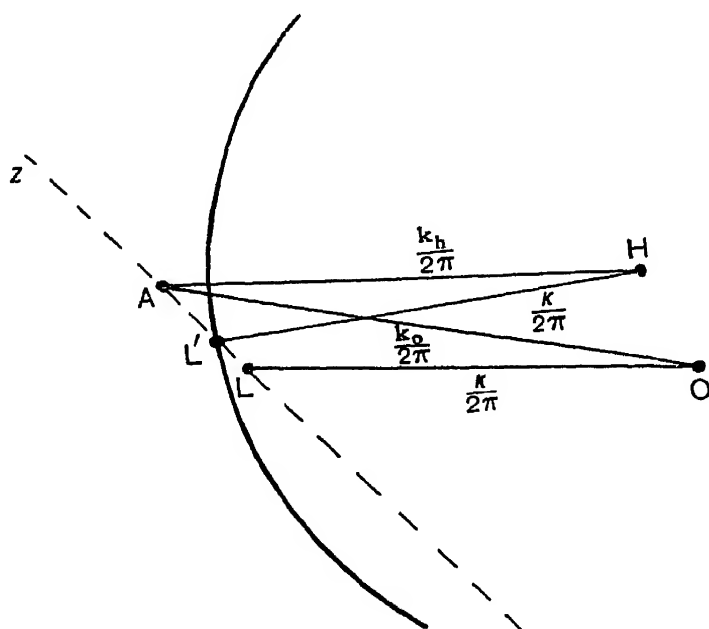


FIG. 103a

gential component as  $k_h/2\pi$ ; for the actual external ray has this tangential component in virtue of the boundary con-

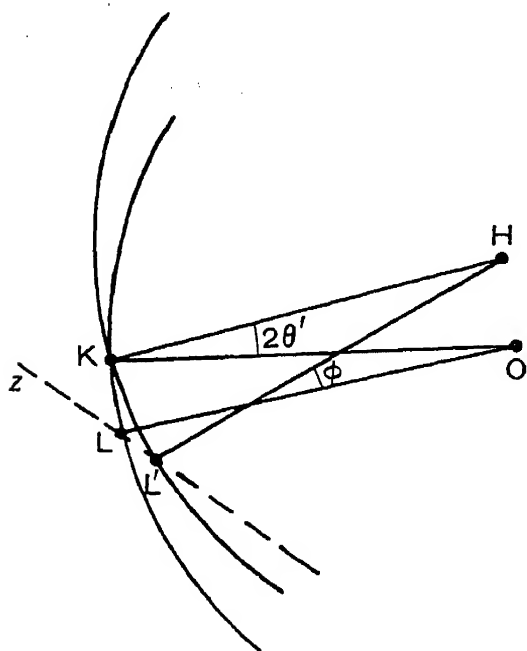


FIG. 103b

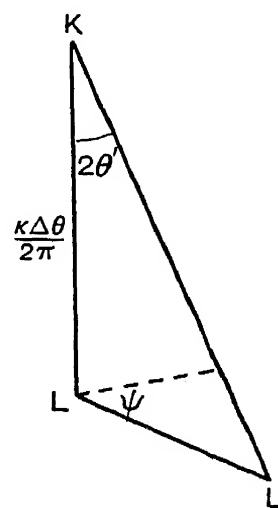


FIG. 103c

ditions, and our imaginary wave vector will be related to the external ray by Snell's law if the above condition applies. To construct this vector  $L'H$  we have merely to draw a sphere

with H as centre and radius  $\kappa/2\pi$  and join H to that point L' of intersection of the sphere with  $z$  which makes L'H correspond to a ray emerging from the crystal. The sphere will always cut  $z$  since  $\kappa > K$  and a similar sphere with radius  $K/2\pi$  must cut  $z$  to make the boundary conditions for  $k_k$  possible of fulfilment.

The construction for the deviation is shown free from unessentials in Figs. 103*b*, 103*c*. With O and H as centres, equal spheres of radius  $\kappa/2\pi$  are drawn. To a primary direction LO in the crystal corresponds a secondary direction L'H, where LL' lies along  $z$ . The angle  $\phi$  between them is the deviation if refraction can be neglected. If not, its effect must be calculated by treating LO, L'H as rays in the crystal and applying Snell's law.

For fast electrons, except in one special case, the variation in the deviation is much less than the range  $\pm\Delta\theta'$  of glancing angle within which appreciable reflection occurs. When  $z$  lies in the plane LOH this can easily be proved. If the spheres intersect at K the angle  $OKH = 2\theta'$ , where  $\theta'$  is the Bragg angle for electrons inside the crystal. Now

$$\phi - 2\theta' = \Delta\phi = \angle KHL' - \angle KOL = (KL' - KL)2\pi/\kappa.$$

Since KLL' is approximately a triangle with small vertical angle  $2\theta'$ ,  $KL' - KL = KL \cdot 2\theta' \cdot \tan \psi$ , where  $\psi$  is the angle between  $z$  and LO, *i.e.* approximately the angle between the surface of the crystal and the normal to the reflecting plane. Also  $KOL = \Delta\theta'$ . Hence  $\Delta\phi = 2\theta' \cdot \tan \psi \cdot \Delta\theta'$  and is small compared with  $\Delta\theta'$ , unless  $\psi$  is nearly  $\pi/2$ . This last is the case of reflection from a plane parallel to the surface of the crystal. In this case also refraction is important, and  $\Delta\phi$  no longer gives the observed deviation as measured outside the crystal.

In the more general case in which  $z$  is oblique to KOH the same formula for  $\Delta\phi$  can be shown to hold, but  $\psi$  is now the angle between the projection of  $z$  on the plane OLH, and OL.

The importance of the above result comes from the fact that in most cases the deviation of the ray is what is actually observed.

### Widths and Intensities of Reflections

If the beam is not exactly monochromatic, or if the crystal is not exactly perfect, or if the incident rays are inclined over

a wide range of angle, the effective intensity in the Bragg case will be proportional to the width within which reflection is perfect. In the Laue case the region within which  $|W| < 1$  measures the width, and plays a similar rôle. In either case width and intensity go together.

The importance of a reflection depends on the magnitude of  $V_{12}$ . In general the largest term in  $V_{12}$  is  $-v_h$ , so that the intensity of a reflection depends on the corresponding coefficient in the Fourier expansion of the potential, as it does in the simple theory.<sup>1</sup>  $V_{12}$ , however, also contains the summation

$$\sum \frac{v_g v_{g-h}}{\kappa^2 - k_g^2},$$

which may be finite even if  $v_h$  vanishes. Thus forbidden reflections may occur, though weakly, but this is only possible in certain cases. Thus for face-centred cubic structure if  $v_h = 0$  either  $v_g$  or  $v_{g-h}$  will be zero. In the case, however, of diamond, for which the 222 reflection is forbidden but 111 and 333 allowed, these terms would be finite, though they would be small for fast electrons because the large quantity  $\kappa^2$  occurs in the denominator. This reflection is actually observed for diamond, and is surprisingly strong.<sup>2</sup> It is probable, however, that this case is to be explained by the fact that the reflection is only forbidden if the carbon atoms show spherical symmetry. Actually the reflection occurs weakly for X-rays, where it is explained as due to the unsymmetrical character of the carbon atom. It is possible that this might give a greater effect in the case of electrons.

For fast electrons  $\zeta_0$  is small compared with  $w$ , and the region of selective reflection is approximately symmetrically disposed about the theoretical Bragg angle or wave-length. The width in angle of the region of selective reflection is the range  $\pm \Delta\theta$  for which  $\zeta < w$  and is  $V_{12}/2\kappa^2\theta$ . Shinohara<sup>3</sup> has calculated this quantity for rock-salt, using values of  $v_h$  derived from  $f$  values obtained by Havighurst<sup>4</sup> from the inten-

<sup>1</sup> Note, however, that the range of reflection is proportional to  $v_h$ , while in the elementary theory the intensity is proportional to the square of the corresponding quantity. A similar difference occurs for X-rays, the first power law holding for the 'ideal' crystal.

<sup>2</sup> Beeching, *Phil. Mag.* 20, p. 841 (1935).

<sup>3</sup> Shinohara, *Sci. Pap. Inst. Phys. Chem.* 18, p. 223 (1932).

<sup>4</sup> Havighurst, *Phys. Rev.* 29, p. 1 (1927).

sity of X-ray reflections, and the results are reproduced in Table XXI.

TABLE XXI

SHINOHARA'S CALCULATED VALUES OF THE WIDTHS OF REFLECTIONS FROM ROCK-SALT FOR 36,500 VOLT ELECTRONS

$(h \cdot k \cdot l)$	$v_{hkl}$ in $\text{\AA}^{-2}$	$ V_{12} $ in $\text{\AA}^{-2}$	Effective Spacing in $\text{\AA}$	$\theta$	Complete Width at Half Maximum
(200)	1.57	1.88	2.81	38'	57'
(220)	1.31	1.35	1.99	54'	30'
(400)	0.87	0.88	1.41	1° 17'	13'
(420)	0.76	0.77	1.26	1° 26'	11'
(440)	0.56	0.56	1.00	1° 49'	6'
(620)	0.47	0.47	0.89	2° 1'	5'
(640)	0.39	0.39	0.78	2° 18'	3'
(800)	0.27	0.27	0.70	2° 23'	3'

Unfortunately these and similar calculations do not agree well with experiment. Thus Kikuchi found that for zinc blende the reflections extended over angles of the order of 20 times that calculated, and did not vary with the order of the reflection as much as was to be expected. Beeching found a similar result for diamonds. The curves are also unsymmetrical in contradiction to the theory. Kikuchi suggested that this was due to the atoms being in two sets of parallel planes. The structure factor due to this is unsymmetrical on the two sides of the Bragg angle, but Beeching has shown that this will not explain the results with diamond. Some of his results are shown in Fig. 104, in which intensities of reflection, measured with a Faraday cylinder, are plotted against the angle of incidence for the (111) face of diamond. The width of reflection for the 3rd order was found to be 28', against about 2' calculated. Harding<sup>1</sup> has investigated this discrepancy very carefully. Absorption has the effect of producing a dissymmetry, but actually narrows the width of reflection. Harding has, however, shown that if there are two top layers of atoms whose spacing differs from the rest, as might happen if the diamond were covered with a layer of gas, and if suitable absorption is assumed, Beeching's results can be accounted for. In any case it is probable that the spacing of the top layer of atoms differs

<sup>1</sup> Harding, *Phil. Mag.* 23, p. 271 (1937).

from that in the rest of the crystal, but Harding shows that this effect is not likely to be large enough to account by itself for the observed spread.

The width of a reflection in the Laue case is not very different from that in the Bragg case, though the distribution of intensity is altered as the reflection is never total. At first sight Table XXI would seem incompatible with the narrow rings observed in transmission.<sup>1</sup> Thus the more intense reflections correspond to widths of the order of  $1^\circ$ , while it is

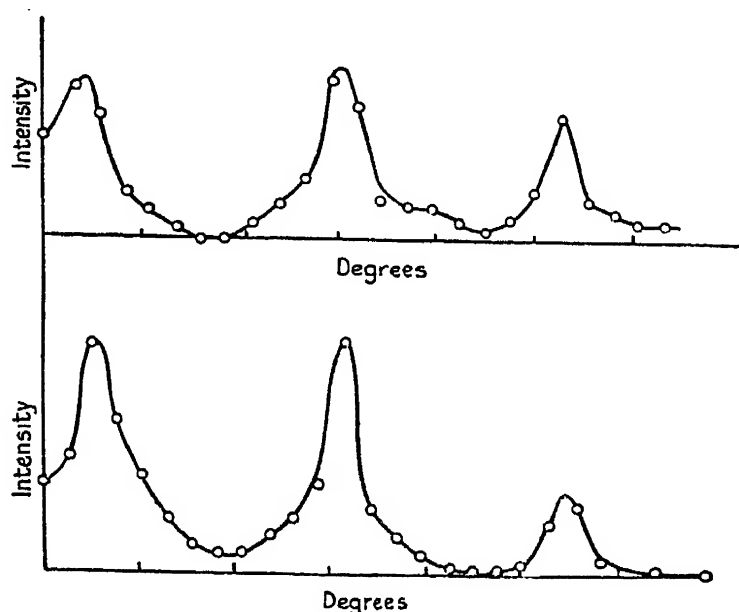


FIG. 104

easy to get patterns in which the rings corresponding to these reflections are ten times finer than this. The reason is that in a ring pattern we are concerned with deviations, and the range of incidence over which the reflection occurs merely affects the intensity. Now we have seen that the deviation is very nearly constant, the variation being  $\pm 2\theta' \tan \psi \Delta\theta'$ . For a strong reflection, for which  $\Delta\theta' \sim 1^\circ$ , and taking the mean value of  $\tan \psi$  as of the order unity, the range in deviation is thus about  $1/30$  of the deviation itself, which is of course equal to  $2\theta$ . Only the inner rings will have a value of  $\Delta\theta$  as large as this, and the width is about that actually observed.

The principle of constancy of deviation may also explain spots observed, in the Bragg case, by Kikuchi and Nakagawa<sup>2</sup>

<sup>1</sup> Hautot and Trillat, *Jour. de Phys.* 9, p. 133 (1938).

<sup>2</sup> Kikuchi and Nakagawa, *Sci. Pap. Inst. Phys. Chem. Res.* 21, p. 80 (1933).

for zinc blende, and by one of us for diamond.<sup>1</sup> These spots represent reflections by the surface plane with deviations equal to those corresponding to Bragg reflections, but occur at angles of incidence widely differing from the Bragg angle. They must not be confused with the specular reflections from the surface layers which often occur at the same time. When the incidence is about midway between the values corresponding to two Bragg orders, two of these new spots may appear with deviations corresponding to the two orders. A straightforward calculation shows that the  $n_{th}$  and  $n + 1_{th}$  reflections can occur simultaneously if

$$V_{12} > \frac{\pi^2 2n + 1}{4d^2},$$

where  $d$  is the spacing and  $V_{12}$  the Bethe coefficient assumed to be the same for both orders. The values of  $V_{12}$  are admittedly uncertain, but it does not seem impossible for this inequality to be satisfied for  $n = 1$  or  $2$  when the reflection is from the cleavage planes of a typical ionic crystal. Kikuchi and Nakagawa explain their spots by supposing that small parts of the crystal surface make appreciable angles with the main body. For our explanation it would be necessary to suppose that the surface had ridges, through which the electrons pass, since the principle of constant deviation does not hold for reflection from a plane parallel to the surface of the crystal.

### Case of several Principal Rays

Another possible source of error in Bethe's theory is its limitation to two principal waves. Shinohara<sup>2</sup> has examined the case in which two strong reflected waves are present. Morse,<sup>3</sup> in an early paper, showed that the peculiarities associated with this case explained some of the abnormalities found by Davisson and Germer, but he only considered in detail the case of two dimensions. The appearance of several beams is connected with the permissible range of  $\zeta$ . For small angles, the tolerance represented by the possibility of  $\zeta$  having a finite value has very nearly the same effect as an extension of

<sup>1</sup> Thomson, *Phil. Mag.* 18, p. 640 (1934).

<sup>2</sup> Shinohara, *Sci. Pap. Inst. Phys. Chem. Res.* 20, p. 39 (1932).

<sup>3</sup> Morse, *Phys. Rev.* 35, p. 1310 (1930).

the spots of the reciprocal lattice in the direction of the incident electrons, such as would be caused by a limitation of the crystal in this direction. The extension is

$$\zeta/2\pi = \frac{V_{12}}{2\pi\kappa}.$$

For  $V_{12} \sim 1$ , and  $\kappa = 100$  the extension is equivalent to that produced by a limitation of the crystal, in the direction of the rays, to about 600 Å. For the stronger reflections the extensions are of the order of a few parts in a thousand of the distance between lattice points. This may seem small, but the Ewald sphere is so little curved that it may allow reflections to occur which would otherwise be impossible. Suppose that the electrons are incident along a principal direction, *i.e.* normal to a plane through a set of points of the reciprocal lattice. Then a simple calculation shows that, for the Ewald sphere to pass within the effective distances of a point in the plane,  $V_{12} > 2\pi^2/d^2$ , where  $d$  is the spacing corresponding to the point. This inequality may not often be satisfied, but, if the direction of the incident rays is somewhat inclined, the sphere will cut the plane in a circle representing the Laue zone of zero order. Several points of the reciprocal lattice may lie near the circle, and the values of  $V_{12}$  corresponding to them will not have to be large for reflections to take place. This may be the explanation of the group of spots seen near the central spot in diffraction by a single crystal, though, as can readily be seen, it is difficult to distinguish between the dynamical effect and an extension of the spots of the lattice in the direction of the beam, due to a limitation of the coherent regions of the crystal in this direction. At any rate it would seem that the case in which more than two principal rays appear is not very unusual, and then Bethe's theory in its ordinary form is not strictly applicable.

### Further Limitations and Results

Von Laue<sup>1</sup> has pointed out that Bethe's boundary conditions are not entirely satisfactory. The potential of the crystal cannot suddenly become zero on one side of the plane

<sup>1</sup> Von Laue, *Phys. Rev.* 37, p. 53 (1931).

$z=0$  without violating Poisson's equation, and the assumption of a mathematical surface of discontinuity of this kind is inadmissible. It appears, however, from von Laue's analysis that the error is likely to be small in the case of fast electrons.<sup>1</sup>

It must be remembered that Bethe's theory applies to a crystal unbounded except in one direction, and so takes no account of the influence of size and shape.

Finally, Bethe's theory entirely neglects the absorption of the electrons by inelastic collisions, as a result of which the wave-length is changed and the waves become incapable of interference with the original beam. Now the free path for an inelastic collision in an average solid is only a small multiple of  $10^{-6}$  cm. for electrons of the voltage commonly used ( $\sim 30,000$  volts), and if an electron is incident on the free surface of a crystal at a glancing angle of the order of  $1^\circ$ , it will in general only penetrate a very few atoms layers before making an inelastic collision. The damping of the waves due to this type of absorption is therefore a serious matter, and its neglect must affect the accuracy of Bethe's conclusions.

Using a one-dimensional model, Miyake<sup>2</sup> has shown that the dynamical theory leads to the same conclusions, as to the apparent variation of inner potential with angle of incidence, as does the kinematical theory of Laschkarew (see p. 157).

### Kikuchi Lines

The simple theory originally put forward by Kikuchi himself predicts correctly the position of the lines, and in most cases also their character, *i.e.* whether they represent an excess or defect of electrons. It does not, however, explain the character of the first scattering which it postulates, nor does it cover certain exceptional cases. Thus it has long been known (p. 113) that lines occur corresponding to planes parallel to the direction of the original rays. According to the original theory, the scattering should be symmetrical with respect to these planes and no effect be observed. Shinohara<sup>3</sup> has examined

<sup>1</sup> Von Laue actually considers a crystal in which the surface layer contains only a single unit of positive and negative charge in each lattice cell. Even with the larger charges which occur in most crystals the result is still valid.

<sup>2</sup> Miyake, *Sci. Pap. Inst. Phys. Chem. Res.* 27, p. 286 (1935).

<sup>3</sup> Shinohara, *Sci. Pap. Inst. Phys. and Chem. Res.* 18, p. 223 (1932).

this case in some detail. He finds that the effect only occurs for planes of considerable effective spacing, which are usually strong planes. When such a plane is in the symmetrical position the pair of black and white lines is replaced by a band of which the middle contains an excess, and the edges a defect of electrons.

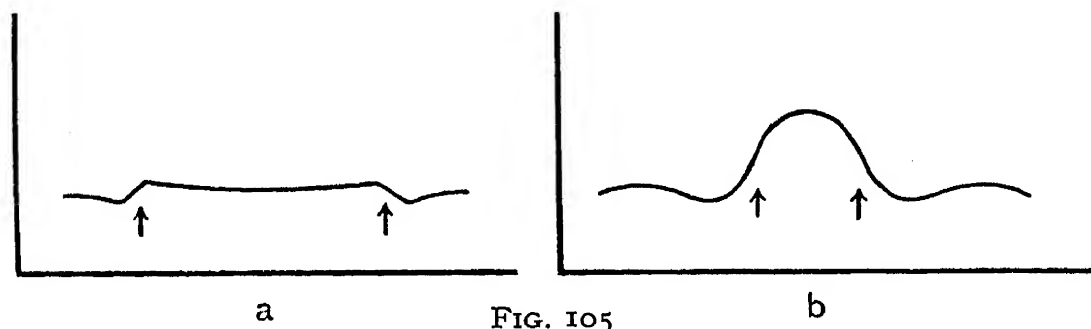


Fig. 105 shows this, the ordinates representing the density of the negative, 'a' being due to the (420) plane of rock-salt and 'b' to the (200) plane of the same substance.

In some cases of transmission patterns the character of the band varies along its length, the portion near the central spot being the reverse of that described above, *i.e.* it receives

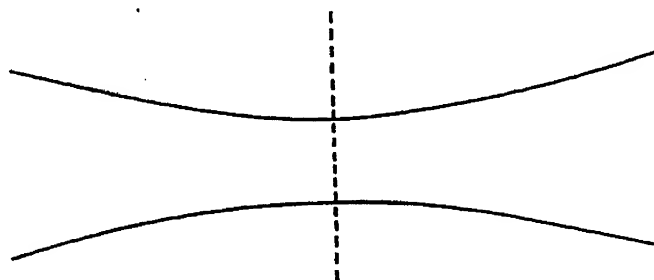


FIG. 106

an excess of electrons at the edges and a defect in the middle.<sup>1</sup> In such cases there is an intermediate region in which the band is invisible.

### Interference of Kikuchi Lines

We have seen that (p. 115) when two Kikuchi lines intersect, especially if they do so at a small angle, they often appear to influence one another, taking up the form shown in Fig. 106. The point of intersection corresponds to a very special

<sup>1</sup> Shinohara and Matukawa, *Sci. Pap. Inst. Phys. Chem. Res.* 21, p. 21 (1933).

direction in the crystal. The electrons proceeding towards it are at an angle to be simultaneously reflected by two crystal planes. In such a case it is necessary to consider three waves in Bethe's theory. Shinohara<sup>1</sup> investigates the way in which the intensity of reflection would vary with angles of incidence, under conditions which represent (roughly) a variation of the direction of the reflected beam along the dotted line in Fig. 106, and shows that a double maximum of intensity occurs. His analysis shows that  $v_h$ ,  $v_{j-h}$ ,  $v_j$  are important, where  $h$  and  $j$  are the reflecting planes. Now,  $v_{j-h}$  will be large when  $j-h$  is small, *i.e.* when the points **j**, **h** of the reciprocal lattice are near together, but when this is the case the corresponding planes, and therefore the corresponding Kikuchi lines, intersect at a small angle.

### Width of Kikuchi Lines

One would expect the angular width of a Kikuchi line to be the same as the range in glancing angle over which appreciable reflection occurs from the corresponding plane. In fact, Beeching<sup>2</sup> found that the width of the line is less than the range in glancing angle, as Table XXII shows in the case

TABLE XXII

	2nd Order	3rd Order	4th Order
Range of glancing angle for half intensity of reflection	35'	28'	22'
Width of Kikuchi line . . .	17.2'	9.7'	6.1'

of the orders of the (111) plane in diamond. The widths are given in minutes of arc, and should all be reduced by about 1.5' to allow for the finite width of the beam of electrons used.

The Kikuchi lines corresponding to planes of small spacing are considerably narrower than these, if the crystal is a perfect one. Though less than the range in glancing angle, the widths of Kikuchi lines are much more than would be predicted on Bethe's theory, if they were regarded as caused by the reflection of diffused electrons coming from a distant part of the crystal.

<sup>1</sup> Shinohara, *Sci. Pap. Ins. Phys. Chem. Res.* 20, p. 40 (1932).

<sup>2</sup> Beeching, *l.c.*

It is difficult to say what effect layers of gas, or other irregularities of the top layers of the crystal, would have on the width.

### Symmetrical Bands

To explain the occurrence of a band when a plane in the crystal is parallel to the direction of the incident electrons

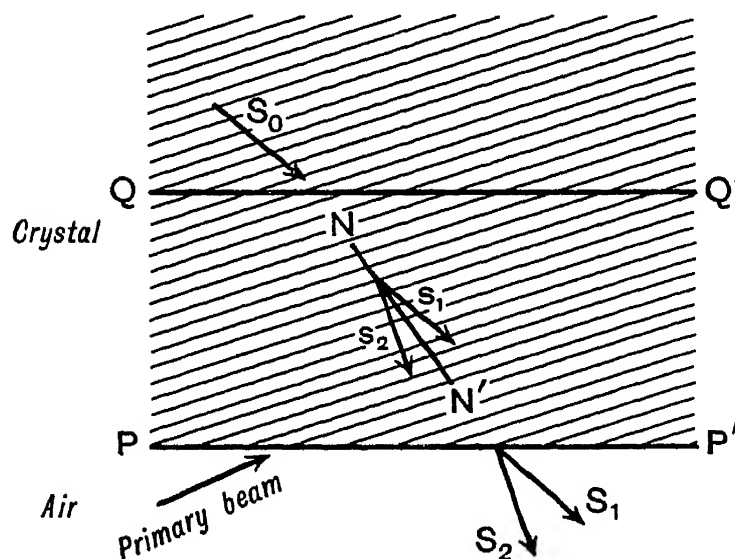


FIG. 107

Shinohara<sup>1</sup> argues as follows: Regard the crystal as divided into two parts by the plane QQ' (Fig. 107) and suppose that electrons are diffused by the upper part, which is regarded as an isotropic medium. A beam of intensity  $S_0$  entering the lower

region may be treated as an incident beam for the purposes of Bethe's theory, and will give rise to transmitted and reflected beams  $S_1$  and  $S_2$  if it makes an angle near to the Bragg angle, with the plane NN'

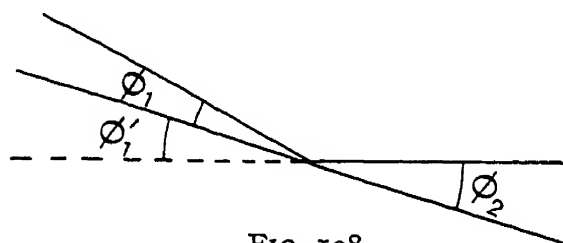


FIG. 108

under consideration. Following Kikuchi's original idea, we need to consider the balance between the intensity lost by a transmitted beam and that gained from a reflected one. Consider the electrons leaving at an angle  $\phi_2$  (Fig. 108) to the plane. They will be due to reflection of a beam originally

<sup>1</sup> Shinohara, *Sci. Pap. Ins. Phys. and Chem. Rec.* 18, p. 223 (1932).

incident at  $\phi_1$ , nearly but not necessarily exactly equal to  $\phi_2$ , and transmission of a beam incident at an angle  $\phi_1'$  exactly equal to  $\phi_2$ . The fractions reflected and transmitted depend on the values of  $\zeta$  for these beams. Now

$$\phi_1 = \theta + \frac{\zeta}{2\kappa\theta}, \quad \phi_2 = \theta - \frac{\zeta}{2\kappa\theta} \quad (\text{see p. 293})$$

for a plane normal to the surface. If  $\zeta'$  is the value for the transmitted beam

$$\phi_1' = \theta + \frac{\zeta'}{2\kappa\theta},$$

and since  $\phi_1' = \phi_2$ ,  $\zeta' = -\zeta$ . The transmitted and reflected intensities for a beam  $S_0$  are

$$\frac{2W^2 + 1}{2(W^2 + 1)} S_0 \quad \text{and} \quad \frac{1}{2(W^2 + 1)} S_0.$$

In this case  $\cos \theta_2 = \cos \theta_1$  and both are positive (Laue case). Here

$$W = \frac{\zeta_0 - \zeta}{w} = \frac{V_{22} - V_{11} - 2\kappa\zeta}{2|V_{12}|},$$

the appropriate values of  $\zeta$  being taken.

Shinohara modifies the expressions for the intensities, and for  $W$ , by proceeding to Bethe's third approximation, and shows that the sum of the two intensities differs from  $S_0$  by a quantity which is a function of  $\zeta$ . The resulting intensity in the neighbourhood of the Bragg angle varies in the same way as the observed blackening in the Kikuchi band, but the amplitude of the variation from the mean value is less than is observed.

We think that an alternative explanation might be given as follows. Since  $\phi_1 \neq \phi_1'$ , the beams  $S_0$ ,  $S_0'$  diffused in these directions by the primary scattering will not be equal, and the total intensity is

$$\frac{S_0}{2(W^2 + 1)} + \frac{S_0'(2W'^2 + 1)}{2(W'^2 + 1)},$$

where  $W = \frac{\zeta_0 - \zeta}{w}$ ,  $W' = \frac{\zeta_0 - \zeta'}{w} = \frac{\zeta_0 + \zeta}{w}$ .

Now  $\zeta_0$  is small, and as Shinohara points out, will vary from point to point along the line, suggesting a variation not usually

observed, though perhaps connected with the changes found by him and Matukawa. Neglecting  $\zeta_0$ , we get for the intensity

$$S'_0 + \frac{\Delta S}{2(W^2 + 1)}, \text{ where } \Delta S = S_0 - S'_0.$$

The fractional divergence from the mean value is

$$\frac{1}{S_0} \frac{\Delta S}{2(W^2 + 1)} = \frac{\Delta S}{2S_0} \frac{w^2}{\zeta^2 + w^2} = \frac{1}{2S_0} \frac{dS}{d\phi} \frac{\zeta w^2}{(\zeta^2 + w^2)\kappa\theta}.$$

This vanishes at  $\zeta = 0$  and when  $\zeta$  is large, it has maxima when  $\zeta = \pm w$  and is then

$$\pm \frac{1}{4S_0} \frac{dS_0}{d\phi} \frac{w}{\kappa\theta}.$$

For the 200 reflection of rock-salt, the fraction is

$$\pm \frac{.0043}{S_0} \frac{dS_0}{d\phi};$$

we shall not be overestimating

$$\frac{1}{S_0} \frac{dS_0}{d\phi}$$

if we take it as 10, corresponding to an increase of  $S_0$  by a factor of  $e$  in about  $6^\circ$ . The sign of the effect gives an excess of electrons inside the band and a defect on the edges. Shinohara estimates for this band that the difference in intensity between maxima and minima is about 1/10th of the background, so the method gives at least the right order of magnitude.

### Von Laue's Theory of the Kikuchi Lines

Some recent experiments by Kossel have provided the X-ray analogy to the Kikuchi lines. Using a single crystal of copper as anticathode, he obtains on a photographic plate held near it a series of lines, some darker and some fainter than the background. From their positions, these represent the intersections with the plate of cones with the normals to the various crystal planes as axes, and semi-vertical angles equal to the complement of the Bragg angle for the characteristic K radia-

tion of copper. Clearly these lines are caused by fluorescent radiation from individual copper atoms, and their close analogy with the Kikuchi lines suggest that these latter also arise from energy changes in individual atoms of the crystal, *i.e.* inelastic collisions.

The calculation of the effect of a wave spreading from an atom in a crystal, which would otherwise present great difficulties, is greatly helped by the principle of reciprocity introduced for this purpose by von Laue.<sup>1</sup> It states that the effect at a point B of a source at A is the same as the effect at A of an equal source at B. In the electron case von Laue proves it as follows. Consider an extended Schrödinger equation of the form

$$-\frac{h^2}{8\pi^2m}\nabla^2\psi + (V - E)\psi = \rho,$$

where  $\rho$  measures the volume density of an electron source.

By Green's theorem

$$\begin{aligned} & \frac{h^2}{8\pi^2m} \int \left( \psi_1 \frac{\partial \psi_2}{\partial n} - \psi_2 \frac{\partial \psi_1}{\partial n} \right) dS \\ &= \int (\psi_1 \rho_2 - \psi_2 \rho_1) dv, \end{aligned}$$

where  $\psi_1$ ,  $\psi_2$  correspond to volume distributions  $\rho_1$ ,  $\rho_2$ . The surface integral vanishes for the sphere at infinity, and also over all surfaces of discontinuity because of the boundary conditions for  $\psi$ . If we suppose  $\rho_1$  restricted to a region near A, and  $\rho_2$  to one near B, the result follows in the form  $\psi_{1(B)} = \psi_{2(A)}$ . In order, then, to determine the effect in a given direction of an electron inelastically scattered at A, we have only to determine the intensity at A of waves coming from the given direction. Von Laue shows that, if the direction is at the Bragg angle to a crystal plane, the waves coming from this direction interfere with the reflected waves to form a set of standing waves nearly parallel to the plane in question. As the angle passes through the Bragg angle the maxima and minima interchange places. The intensity of the interference effect is greatest near the Bragg angle, and if the atom with which the inelastic collisions occur lies near a maximum or minimum, the intensity of the radiation from it will differ

<sup>1</sup> Von Laue, *Ann. d. Phys.* 23, p. 705 (1935).

greatly from the background. The positions of these maxima depend on the depth of the atoms below the surface, which complicates the calculations, but it appears that cones of enhanced and diminished intensity appear in pairs on the two sides of the plane.

Certain details of the Kossel phenomenon, for example changes from light to dark lines <sup>1</sup> which recall the effect found by Shinohara and Matukawa, have not been fully explained, and the application of the theory to the Kikuchi lines needs to be carried further. It does, however, explain, in a qualitative fashion, why abnormalities should occur at the edge of the bands associated with planes parallel to the incident electrons. In the further working out of the theory, von Laue considers that more account will have to be taken of the surface layers, and this must apply with especial force to the case of electrons where the depth of penetration is slight.

Perhaps the most important feature of the theory is that it implies that the electrons concerned have suffered an inelastic collision. The loss of energy must be slight, since no change in wave-length has been detected, but energy losses of a few volts, which are the most probable, would be negligible for the fast electrons with which the effect is observed. The important point is that the inelastic collision makes the electronic waves incoherent with the original beam, and incapable of interfering with it. Even electrons which have made inelastic collisions with the same energy loss are incapable of mutual interference.<sup>2</sup>

Such electrons thus lie outside the Bethe theorem as applied to the original beam. The question arises whether collisions with the conductivity electrons of a metal are incoherent scattering in this sense. In an analysis of this question von Laue<sup>2</sup> shows that they are not. The conductivity electrons have wave functions extending over the whole crystal, collision with them is more like a collision with the crystal as a whole, and would give rise to diffracted beams which, though not coinciding with those ordinarily observed, agree with them in depending for their direction on that of the incident beam, unlike the Kikuchi lines.

<sup>1</sup> Von Laue, *Ann. d. Phys.* 28, p. 528 (1937).

<sup>2</sup> Von Laue, *ibid.* 25, p. 569 (1936).

Hayashi<sup>1</sup> has attacked the problem of the Kikuchi lines, and the allied one of the distribution of the electrons produced photoelectrically in a crystal by X-rays. His method differs from those used by Laue and by Shinohara. Instead of using the Bethe theory, he considers the scattering, by the atoms of the crystal, of a primary wave produced at a point in the crystal. Further interaction is not considered. Hayashi finds that there will be cones of strong and weak radiation in the positions given by the simple Kikuchi theory. He also predicts the occurrence of bands in symmetrical cases with an intensity distribution similar to that observed. The results depend essentially on the primary wave being stronger in some directions than in others. In Kossel's experiments with X-rays, the secondary radiation from each atom corresponds to a symmetrical wave with intensity the same in all directions, yet lines and bands appear. From the close similarity of the effects with electrons and X-rays one would not expect the electron phenomenon to depend essentially on asymmetry of scattering, though this hypothesis gives, as we have seen, an explanation of the first order, and even some second order effects. It would seem that von Laue's method of approach is the more fundamental, though no doubt the non-uniform distribution of the electrons scattered inelastically by an atom, which he neglects, must affect the result.

### Kikuchi Envelopes

In many cases, as Von Laue<sup>2</sup> has pointed out, a Kikuchi envelope is the locus of rays which, if reversed, would give rise to diffracted rays lying along the surface of the crystal; but this is not universally the case. Lamla<sup>3</sup> has applied the dynamical theory to the case of Kikuchi envelopes by considering in detail cases when more than two of the beams in the crystal have large amplitudes, and applying von Laue's principle of reciprocity. It is necessary to consider a group of waves corresponding to a family of planes. Actually two sets are considered, one of which corresponds to planes parallel to the surface. It appears

<sup>1</sup> Hayashi, *Sci. Rep. Tohoku. Imp. Univ.* 23, p. 490 (1934).

<sup>2</sup> Von Laue, *Phys. Zeit.* 37, p. 544 (1936).

<sup>3</sup> Lamla, *Ann. d. Phys.* 32, p. 178, p. 225 (1938).

that excitation of the atoms in the surface is primarily responsible for an 'envelope', slightly displaced in position from that calculated on the simple theory. The Kikuchi lines nearly touch this envelope but not quite, where they would come nearest to it they are weakened, while the envelope is strongest at these points. The envelope is sharp on the side nearest the lines and diffuse on the other. All these points are in agreement with observations (see p. 117). As regards the envelopes which do not correspond to the surface layer, Lamla considers that they may be due to faults in the crystal. It seems, however, possible that they might be explained by taking, as the second set of planes, one parallel to another important crystal plane, but in view of the special influence of the surface on the boundary conditions, which play an important part in the theory, this cannot be decided without a further investigation.

## CHAPTER XX

### POLARISATION

TOWARDS the end of the history of the orbit theory of spectra it became apparent that a simple point electron was inadequate to explain the observed facts. To take only one difficulty, it was found that four quantum numbers had to be assigned to each electron. Now each quantum number may be regarded as fixing one degree of freedom, and a point has only three of these. This and other difficulties were overcome by Goudsmit and Uhlenbeck,<sup>1</sup> who suggested that the electron was to be regarded as a spinning body whose axis of spin could vary. Actually it was only necessary to suppose two possible directions for the axis, or rather one direction associated with a spin of either sense. One could think of the axis, for example, as always perpendicular to the orbit and the electron as spinning with or against its orbital motion. Such an electron would be expected to behave like a small magnet and it was found in fact that agreement with experiment resulted if the moment was taken as  $eh/4\pi mc$ . This value fits with the results of the Stern-Gerlach experiments.

Nothing in the preceding theory at all corresponds with this conception of the electron as a magnet to whose axis a definite direction in space is to be assigned, and it is not surprising, therefore, that the theory in this form should fail to account for those facts which made the hypothesis of the spinning electron necessary on the older theory. The necessary extension of the equations to cover this aspect of the electron has been made by Dirac, using the methods of non-commutative algebra; his results have been expressed in more ordinary form and considerably extended by Darwin, whose method we shall follow.<sup>2</sup>

The process is essentially a rather tentative one of finding

<sup>1</sup> Uhlenbeck and Goudsmit, *Nature*, 117, p. 264 (Feb. 20, 1926).

<sup>2</sup> C. G. Darwin, *Proc. Roy. Soc. London*, A118, p. 654 (1928); *ibid.* A120, p. 621 (1928).

a scheme which shall approximate to that of de Broglie and Schrödinger in the absence of a magnetic field, conform to the relativity principle, and be capable of explaining those results which led to the invention of the spinning electron. It is possible that the scheme suggested may not be final. It is found necessary to substitute for the single wave function  $\psi$  of an electron a set of four functions  $\psi_1, \psi_2, \psi_3, \psi_4$ . These satisfy the group of simultaneous equations :

$$\begin{aligned}(p_0 + mc)\psi_1 + (p_1 - ip_2)\psi_4 + p_3\psi_3 &= 0, \\(p_0 + mc)\psi_2 + (p_1 + ip_2)\psi_3 - p_3\psi_4 &= 0, \\(p_0 - mc)\psi_3 + (p_1 - ip_2)\psi_2 + p_3\psi_1 &= 0, \\(p_0 - mc)\psi_4 + (p_1 + ip_2)\psi_1 - p_3\psi_2 &= 0,\end{aligned}$$

where  $c$  is the velocity of light,

$$p_0 = -\frac{h}{2\pi i} \frac{1}{c} \frac{\partial}{\partial t} + \frac{e}{c} V, \quad p_1 = \frac{h}{2\pi i} \frac{\partial}{\partial x} + \frac{e}{c} A_1,$$

$V$  being the scalar potential and  $A_1, A_2, A_3$  being the three components of the magnetic vector potential. [This last quantity obeys the equation

$$\alpha = \frac{\partial A_3}{\partial y} - \frac{\partial A_2}{\partial z}, \quad \beta = \frac{\partial A_1}{\partial z} - \frac{\partial A_3}{\partial x}, \quad \gamma = \frac{\partial A_2}{\partial x} - \frac{\partial A_1}{\partial y},$$

where  $\alpha, \beta, \gamma$  is the magnetic force.]

The first principle in dealing with these equations is that  $\psi_1$  and  $\psi_2$  are small compared with  $\psi_3$  and  $\psi_4$ . In fact the first approximation leads, as follows, to the old  $\psi$  equation in  $\psi_3$  and  $\psi_4$  if there is no magnetic field. In this case

$$p_1 = \frac{h}{2\pi i} \frac{\partial}{\partial x}, \text{ etc.}$$

If  $\psi_1, \psi_2$  are neglected in the last two equations we find <sup>1</sup>

$$(eV - mc^2)\psi_3 = \frac{h}{2\pi i} \frac{\partial \psi_3}{\partial t},$$

thus  $\psi_3$  and  $\psi_4$  vary as

$$\exp\left\{-\frac{i2\pi}{h}(mc^2 - eV)t\right\}.$$

<sup>1</sup> The charge on the electron is taken as  $-e$ , so that  $-eV$  is the potential energy. In this chapter  $m$  is written for  $m_0$  throughout.

Hence  $\psi_1$  and  $\psi_2$  will vary as the same exponential and

$$(p_0 + mc)\psi_1 = \left(mc - \frac{eV}{c} + \frac{eV}{c} + mc\right)\psi_1 = 2mc\psi_1.$$

Hence we can take

$$\psi_1 = -\frac{h}{2\pi i} \frac{1}{2mc} \left[ \left( \frac{\partial}{\partial x} - \frac{i\partial}{\partial y} \right) \psi_4 + \frac{\partial}{\partial z} \psi_3 \right]$$

and

$$\psi_2 = -\frac{h}{2\pi i} \frac{1}{2mc} \left[ \left( \frac{\partial}{\partial x} + \frac{i\partial}{\partial y} \right) \psi_3 - \frac{\partial}{\partial z} \psi_4 \right].$$

Substituting in the third equation we get

$$\left( -mc^2 + eV - \frac{h}{2\pi i} \frac{\partial}{\partial t} \right) \psi_3 = \left( \frac{h}{2\pi i} \right)^2 \frac{1}{2m} \nabla^2 \psi_3,$$

and the same for  $\psi_4$ . This is Equation (6) on p. 17 with the addition of the term  $mc^2$ , which is merely a rather crude way of taking the internal energy of the electron into account, and is the same approximation to the correct relativity equation that the expression  $mc^2 + \frac{1}{2}mv^2$  for the energy is to the exact expression

$$\frac{mc^2}{\sqrt{1 - v^2/c^2}}.$$

The equations thus fulfil the condition of reducing to the old form as an approximation. Darwin has shown that they also satisfy the requirements of relativity.

Darwin also shows that they are related to the electrodynamic potentials by the equations

$$\frac{1}{4\pi} \square V = e \sum_n \psi_n^* \psi_n,$$

$$\frac{1}{4\pi} \square A_1 = -c \{ \psi_1^* \psi_4 + \psi_2^* \psi_3 + \psi_3^* \psi_2 + \psi_4^* \psi_1 \},$$

and so on, where

$$\square \text{ signifies } \frac{\partial^2}{\partial x^2} + \frac{\partial^2}{\partial y^2} + \frac{\partial^2}{\partial z^2} - \frac{1}{c^2} \frac{\partial^2}{\partial t^2}$$

and  $\psi^*$  is the complex quantity conjugate to  $\psi$ .

On analogy with classical electrodynamics we take the

electron as equivalent to a density  $\rho$  and current density  $j_1, j_2, j_3$ , where

$$\begin{aligned}\rho &= -e(\psi_1^* \psi_1 + \psi_2^* \psi_2 + \psi_3^* \psi_3 + \psi_4^* \psi_4), \\ j_1 &= ce(\psi_1^* \psi_4 + \psi_2^* \psi_3 + \psi_3^* \psi_2 + \psi_4^* \psi_1), \\ j_2 &= ce(-i\psi_1^* \psi_4 + i\psi_2^* \psi_3 - i\psi_3^* \psi_2 + i\psi_4^* \psi_1), \\ j_3 &= ce(\psi_1^* \psi_3 - \psi_2^* \psi_4 + \psi_3^* \psi_1 - \psi_4^* \psi_2).\end{aligned}$$

The quantities  $\rho$  and  $j$  satisfy the equation of continuity  $\partial\rho/\partial t + \text{div } j = 0$ , as may be verified by the use of the original equations. We thus have a current density expressible entirely in terms of the  $\psi$ 's and have avoided the difficulty mentioned at the end of Chapter V that, on the old equations, the motion of the electron was in a direction determined to some extent by the magnetic field and not wholly by the waves. We are not, however, entitled to take  $j/\rho$  as the electron velocity, for part of  $j$  will be due to the magnetic moment of the electron and only part to its velocity.

For the case of the free motion of the electron  $V$  and  $A$  disappear. Assume as a solution

$$\psi_n = a_n e^{\frac{i2\pi}{h}(px + qy + rz - Wt)},$$

so that the wave normal is in the direction  $p, q, r$  and the wave-length is

$$\frac{h}{\sqrt{p^2 + q^2 + r^2}},$$

on substituting we have a determinant which reduces to

$$\frac{W^2}{c^2} - m^2 c^2 - p^2 - q^2 - r^2 = 0.$$

This may be regarded as fixing the wave-length for a given frequency  $W/h$ . We have, in fact,

$$\lambda = \frac{h}{\left[ \frac{W^2}{c^2} - m^2 c^2 \right]^{\frac{1}{2}}}.$$

If  $W$  is taken as the total energy,

$$W = \frac{mc^2}{(1 - u^2/c^2)^{\frac{1}{2}}},$$

and thus 
$$\lambda = \frac{h}{\left[ \frac{m^2 c^2}{1 - u^2/c^2} - m^2 c^2 \right]^{\frac{1}{2}}} = \frac{h}{mu/(1 - u^2/c^2)^{\frac{1}{2}}},$$

which is de Broglie's formula.

The four quantities  $a_n$  are not all arbitrary. If we choose  $a_3$  and  $a_4$  as the arbitrary complex quantities A and B, we find from the original equations that

$$a_1 = -\frac{Ar + B(p - iq)}{mc + W/c}, \quad a_2 = -\frac{A(p + iq) - Br}{mc + W/c}.$$

If these are substituted in the expressions for  $\rho$  and  $j$  we find that both are proportional to  $|A|^2 + |B|^2$  and that  $j$  is along  $p, q, r$ , the wave normal.

It is noteworthy that *four* quantities are needed to fix the simplest electron wave, two for each of the complex quantities A and B. One of these variables may be taken as the intensity  $|A|^2 + |B|^2$ , the other three are needed to fix the 'polarisation'. Now, for a light wave of the most general steady type we have elliptical polarisation which is defined by two quantities, *e.g.* the direction of the major axis and the eccentricity. The difference is an expression of the fact that the 'magnetic moment' of the electron is not necessarily in the wave front as are the vectors of a light wave. Consequently it takes two angles to fix its direction, as against one in the case of light.

To separate the part of the 'current' which should be attributed to the magnetic moment from that which is caused by the convection of electricity, Darwin starts from the classical electromagnetic equations. As long as there are no magnetic poles these can be written in the simple form

$$\begin{aligned} \frac{1}{c} \frac{\partial \mathbf{E}}{\partial t} + 4\pi \mathbf{j}/c &= \text{curl } \mathbf{H}, \quad \text{div } \mathbf{E} = 4\pi \rho, \\ -\frac{1}{c} \frac{\partial \mathbf{H}}{\partial t} &= \text{curl } \mathbf{E}, \quad \text{div } \mathbf{H} = 0, \end{aligned}$$

where  $\rho$  and  $j = \rho v$  are the density and the convection current. The effect of introducing magnetic moments is to change H into  $\mathbf{B} = \mathbf{H} + 4\pi\mu$  in the last two equations only. Eliminating H from the first equation we have

$$\frac{1}{c} \frac{\partial \mathbf{E}}{\partial t} + 4\pi \left( \rho \frac{\mathbf{v}}{c} + \text{curl } \mu \right) = \text{curl } \mathbf{B}.$$

At the distant point of observation we need not distinguish between  $H$  and  $B$ , and so can attribute the effects to a current  $j = \rho v + c \text{ curl } \mu$ . Thus if part of the current can be attributed to the electron's velocity and part is the curl of a certain vector, the latter can be taken as the magnetic moment of the electron.

By considering the behaviour of a 'wave packet', like that considered on p. 64, Darwin is able to do this approximately for the case of a slowly moving electron; he finds for the components of  $\mu$ :

$$\begin{aligned}\mu_1 &= -\psi_3^* \psi_4 - \psi_3 \psi_4^*, \\ \mu_2 &= i\psi_3^* \psi_4 - i\psi_3 \psi_4^*, \\ \mu_3 &= -\psi_3 \psi_3^* + \psi_4 \psi_4^*,\end{aligned}$$

the total moment being  $eh/4\pi mc$ , as it should be if the amplitude of the wave is chosen to make  $\rho$  correspond to the charge on a single electron. In the more general case terms in  $\psi_1$  and  $\psi_2$  have to be added to the above expression, and there is also a vector corresponding to an electric moment. The direction of the magnetic moment is given by the complex ratio of  $A : B$ . In fact, if  $A$  and  $B$  are respectively proportional to  $(1 - n)$  and  $(-l - im)$  the magnetic moment will be along the direction with direction cosines  $l, m, n$ . If a unit sphere is drawn round the origin and we project stereographically from the point where the positive  $z$ -axis cuts the sphere, the ratio  $-B : A$  is a complex quantity whose components are the coordinates of the projection of the point in which the magnetic axis cuts the sphere. The plane  $z = -1$  is taken as plane of projection.

The above expressions for the magnetic moments are accurate for a system of co-ordinates moving with the electron. An 'unpolarised' beam of electrons would be one in which the magnetic axes were distributed at random in this system of coordinates. For other systems Darwin shows that the moments will tend towards the equatorial plane of the moving electrons, in a manner recalling the distribution of the lines of force round a classical electron moving at high speeds. The electric moment is found to be always transverse to the motion.

The detection of any effect due to magnetic moment or

polarisation in free electrons is not an easy matter. Bohr<sup>1</sup> has shown that any experiment of the Stern-Gerlach type, or one involving magnetometers, is bound to fail because of the uncertainty principle. Darwin has considered the effect of a plane grating, composed of a periodically variable electric or magnetic potential, on a beam of electrons. He finds that no polarisation would occur for either a purely electric or a purely magnetic grating. In some cases where both periodic electric and magnetic fields are present Darwin finds that some polarisation should occur, but it seems improbable that natural crystal gratings could produce sufficiently strong magnetic fields to make this a practical experiment.<sup>2</sup> Frenkel<sup>3</sup> has investigated the reflection of Dirac waves at a surface of discontinuity and finds no polarisation effect, while Alexandrov<sup>4</sup> and Förster<sup>5</sup> have confirmed this for any form of potential barrier.

On the other hand, Mott finds that nuclear scattering ought to produce an appreciable asymmetry of the scattered beam if certain conditions are fulfilled. This asymmetry can be shown by a second scattering under similar conditions, which would yield different numbers of electrons according to whether the second scattering is in the same or the opposite direction to the first. The asymmetry is thus one of  $180^\circ$  round the axis of the beam, and not of  $90^\circ$  as it is for light or X-rays. Mott's conditions are :

- (1) The scattering must be through large angles, comparable with  $90^\circ$ .
- (2) The scattering nucleus must be of large atomic number.
- (3) The speed of the electrons must be comparable with that of light.

In the particular case of two right-angled scatterings by gold nuclei, Mott finds that the ratio of electrons scattered

<sup>1</sup> Published in an appendix to a paper by Mott, *Proc. Roy. Soc.* 124, p. 425 (1929).

<sup>2</sup> Halpern, *Zeit. für Phys.* 67, p. 320 (1931), finds that a plane grating gives polarisation effects if the calculations are carried to the second order. He does not attempt a numerical estimate of the effect.

<sup>3</sup> Frenkel, *Comp. rend.* 188, p. 153 (1929).

<sup>4</sup> Alexandrov, *Zeit. für Phys.* 60, p. 387 (1930).

<sup>5</sup> Förster, *Zeit. für Phys.* 85, p. 514 (1933).

twice the same way to those scattered first one way and then back again is  $(1 + \frac{1}{2}d)/(1 - \frac{1}{2}d)$ , where  $d$  is given in the table.

Energy in kilovolts	10.5	25	45	79	127	204
Per cent polarisation (100d)	0.5	0.2	3.0	11.5	15.5	14

The maximum  $d$ , 15.5 per cent occurs at 137 kv., but the variation is slow and at 100 kv.  $d$  is 14.2 per cent.

Mott's conclusions have been quantitatively confirmed by Sauter,<sup>1</sup> who finds in addition that the effect of the K electrons would be small under those conditions for which the theory predicts considerable polarisation.

Hellmann<sup>2</sup> has studied the polarisation of Dirac waves by a crystal, extending Bethe's theory to meet this case. He finds that no polarisation should be produced by an infinite crystal with a centre of symmetry in the case in which only two principal waves need be considered. The calculation, however, involves certain approximations. A finite crystal should give an effect, as should one with no centre of symmetry, but the effect in the latter case would probably be small.

Weisskopf<sup>3</sup> has suggested that considerable polarisation might occur in crystals as a result of a double reflection from Bragg planes, but David<sup>4</sup> finds that in all practical cases it would be immeasurably small.<sup>5</sup>

### Experiments to test Mott's Theory

A large number of experiments have been made to try to detect polarisation; in most cases the results have been negative and in those cases in which a positive result has been found it has not been confirmed by later work. The most interesting experiments are those in which an attempt was made to satisfy Mott's conditions. Experiments on these lines have been made by Dymond,<sup>6</sup> by one of the authors,<sup>7</sup> and by Richter,<sup>8</sup> In their general features all three sets of experi-

<sup>1</sup> Sauter, *Ann. d. Phys.* 18, p. 61 (1933).

<sup>2</sup> Hellmann, *Zeit. für Phys.* 69, p. 495 (1931); 96, p. 247 (1935).

<sup>3</sup> Weisskopf, *Zeit. für Phys.* 193, p. 561 (1935).

<sup>4</sup> David, *ibid.* 105, p. 747 (1937).

<sup>5</sup> It is understood that papers by Winter (*Compt. rend.* 202, pp. 1265, 1416 (1936)) will be withdrawn.

<sup>6</sup> Dymond, *Proc. Roy. Soc.* 136, p. 638 (1932); 145, p. 657 (1934).

<sup>7</sup> Thomson, *Phil. Mag.* (7) 17, p. 1058 (1934).

<sup>8</sup> Richter, *Ann. d. Phys.* 28, p. 533 (1937).

ments show a close resemblance except that the first two workers used Faraday cylinders to detect the twice scattered electrons, and the third observed them photographically. In principle the apparatus is shown in Fig. 109; a beam AB of electrons, collimated by fine holes, strikes a thin gold foil B, and the scattered electrons pass through other holes to the second foil C which can be rotated about BC, scattering the electrons to E or F, where the intensities are measured. Dymond in his first experiments found asymmetries which changed with the energy of the rays in the direction required by Mott's theory, though not to the required extent. Later work convinced him that the effect was due to inaccurate centring of the first film, and he reached the conclusion that there was no evidence of a polarisation greater than 1 per cent for electrons of energies up to 160 kv. He also showed that the variation with voltage of the fraction of the beam which suffered the double scattering was approximately that predicted by Mott's theory, which as far as this feature is concerned does not give results

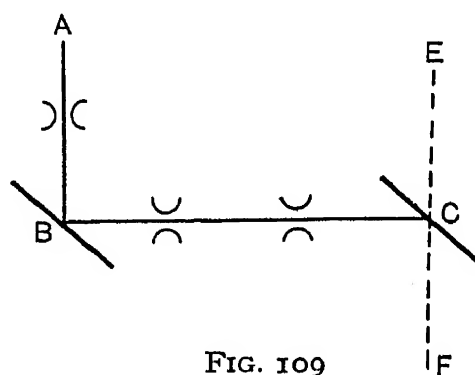


FIG. 109

in the range in question very different from the simple inverse square law. This is important, for the theory has to be used to calculate the permissible thickness of film which will give single scattering, and if it is badly wrong the conditions may not be fulfilled. The author's experiments were made with gold films at 30 kv., 100 kv., and 120 kv. In no case did they show a polarisation greater than the probable error, which in the case of the 100 kv. experiment certainly did not exceed 1 per cent. In view of Richter's results it is probable that the scattering in the case of the 30 kv. experiment was mostly multiple, but the low voltage experiments were mainly important as a test of the symmetry of the apparatus.

Richter took great care to avoid possible disturbing effects due to X-rays, stray electrons, etc., and by measuring the variation of scattering with angles was able to show that the scattering of his films was mostly single. He found no detect-

able polarisation and considers that he would have detected  $1/30$  of that predicted by Mott.<sup>1</sup> He worked with aluminium and gold scatterers over the range 20 to 120 kv.

### Discussion

These results definitely prove that Mott's theory is not correct as applied to the scattering of electrons by thin films of gold. If Sauter is right this cannot be explained by the presence of the electrons round the gold nucleus. A possible line of explanation, to which some of the recent theoretical work gives support, is to suppose that there is a fundamental difference between scattering by single atoms and by a crystal. While such a difference may well exist when the crystal is of infinite extent, it is very doubtful how far the idea of an infinite crystal is applicable to the actual experiments. Electrons of 150,000 volts will be reflected<sup>2</sup> through  $90^\circ$  by a plane of spacing  $0.23 \times 10^{-9}$ . The density of gold atoms in such a plane is  $1.36 \times 10^{13}$ . Now the average dimensions of the crystals in the spluttered foils used was probably about  $10^{-6}$ , so that there would only be of the order of ten atoms in the reflecting plane. This is very far from the infinite plane required by the theory, and if there is an important difference between single atoms and infinite crystals one would expect the results of the experiments to refer more nearly to single atoms. Hellmann (*l.c.*), however, considers that the conditions for polarisation by crystals are, even at the best, less favourable than for single atoms. If a theoretical estimate could be made of the influence of the size of the crystals, it might prove worth repeating the experiments with films composed of crystals containing only a few atoms each. Halpern and Schwinger<sup>3</sup> report in a letter that the polarisation by a bare nucleus can be made to vanish by assuming a field of force departing from the inverse square, without involving contradiction with other

<sup>1</sup> It is not clear from Richter's paper if allowance was made for the non-linear relation between the readings of a photometer and the density of the electrons causing the blackening (cf. p. 244).

<sup>2</sup> It can readily be seen that high order reflections by planes of large spacing are relatively unlikely.

<sup>3</sup> Halpern and Schwinger, *Phys. Rev.* 48, p. 109 (1935).

known nuclear effects. The calculations are not given. In view of the importance of Dirac's equations it is very desirable that these theoretical points should be cleared up.

### Other Experiments

The remaining experiments may be briefly noticed, the absence of an effect might be taken as a kind of negative confirmation of the theory, but it could have been predicted in most cases on general grounds. Thus it is unlikely that a detectable effect would be found for slow electrons, since the magnetic forces only become comparable with the electrostatic near the velocity of light. Also, scattering through small angles is not likely to lead to a large effect, from analogy with the corresponding cases of light and X-rays. Multiple scattering is likely to diminish the effect, since it is equivalent to a number of small angle scatterings.

Davisson and Germer,<sup>1</sup> using slow electrons, tried double reflections through  $90^\circ$  from nickel crystals. No effect was found within the probable error, which was of the order of 1 per cent.

Joffe and Arsenieva<sup>2</sup> found no effect with a double reflection apparatus at glancing angles of  $10^\circ$  and  $30^\circ$ . The 'mirrors' were of steel, brass and glass and the electron energies from 80 to 6400 volts.

Wolf<sup>3</sup> showed that a transverse magnetic field produced in a beam of electrons no dissymmetry detectable by their reflection from various targets.

Myers and Cox<sup>4</sup> passed a beam of  $\beta$  rays normally through two sheets of iron foil 0.0025 cm. thick. The foils were magnetised in their own planes, but the orientation of the magnetic axes did not affect the fraction transmitted.

Rupp<sup>5</sup> repeated Davisson and Germer's experiment, but with copper crystals, and a magnetic field between the two reflections. Again there was no effect.

<sup>1</sup> Davisson and Germer, *Phys. Rev.* 23, p. 760 (1929).

<sup>2</sup> Joffe and Arsenieva, *Compt. rend.* 188, p. 152 (1929).

<sup>3</sup> Wolf, *Zeit. Phys.* 52, p. 314 (1928).

<sup>4</sup> Myers and Cox, *Phys. Rev.* 34, p. 106 (1929).

<sup>5</sup> Rupp, *Zeit. für Phys.* 53, p. 548 (1929).

Experiments on the double right-angled scattering of  $\beta$  rays by solid targets made by Cox, McIlwraith and Kurrelmeyer,<sup>1</sup> and continued by Chase,<sup>2</sup> led to no very definite conclusions except that the effect, if any, was not large.

Langstroth<sup>3</sup> examined the double right-angled scattering by thick tungsten targets with 10 kv. and found no effect.

As a result of a positive effect at small glancing angles announced by Rupp, but for which he afterwards suggested an instrumental explanation, one of the authors<sup>4</sup> examined the rings formed when a beam of cathode rays, scattered or diffracted by one gold film, is diffracted by a second. These rings were uniform as far as could be detected photographically for electron energies up to 70 kv. Kirchner<sup>5</sup> has found a similar result, as have Thibaud, Trillat and Hirsch<sup>6</sup> for energies up to 110 kv. Myers, Byrne and Cox<sup>7</sup> have worked up to 225 kv. and find an effect certainly less than 10 per cent and probably less than 5 per cent.

Rupp and Szilard<sup>8</sup> found a positive effect when electrons were first scattered through  $90^\circ$  by a thick gold target, and then diffracted by a thin gold foil. The outer rings showed an appreciable asymmetry with a period of  $180^\circ$  increasing with the voltage from 150 to 240 kv. This asymmetry was affected by a magnetic field in the manner to be expected of a polarisation. One of the authors<sup>9</sup> repeated these experiments but was unable to find any effect at 150 kv. Breit, in an appendix to the paper of Myers, Byrne and Cox, has shown that the action of a magnetic field gives no proof that an asymmetry is due to polarisation, and suggests a geometrical explanation of Rupp and Szilard's results.

Mention should perhaps be made of some papers by Rupp<sup>10</sup>

<sup>1</sup> Cox, McIlwraith and Kurrelmeyer, *Proc. Nat. Acad. Sci.* 14, p. 544 (1928).

<sup>2</sup> Chase, *Phys. Rev.* 34, p. 1069; 36, p. 1060 (1930).

<sup>3</sup> Langstroth, *Proc. Roy. Soc.* 136, p. 558 (1932).

<sup>4</sup> Thomson, *Nature*, 126, p. 842 (1930).

<sup>5</sup> Kirchner, *Phys. Zeit.* 31, p. 772 (1930).

<sup>6</sup> Thibaud, Trillat and Hirsch, *Compt. rend.* 194, p. 1223 (1932); *Jour. de Phys.* 3, p. 314 (1932).

<sup>7</sup> Myers, Byrne and Cox, *Phys. Rev.* 46, p. 777 (1934).

<sup>8</sup> Rupp, *Naturwiss.* 19, p. 109 (1931); Rupp and Szilard, *ibid.* p. 422; Rupp and Szilard, *Phys. Zeit.* 33, p. 158 (1932); Rupp, *ibid.* p. 937.

<sup>9</sup> Thomson, *Phil. Mag.* 17, p. 1058 (1934).

<sup>10</sup> Rupp, *Zeit. für Phys.* 79, p. 642 (1932), 90, p. 166 (1934).

in which he found a polarisation, in the sense demanded by Mott's theory, with two right-angled deviations from gold scatterers and energies up to 250 kv. These results are not in agreement with those found by other experimenters mentioned above, and cannot be regarded as reliable.



## NAME INDEX

### A

ADAM 197  
 Alexandrov 317  
 Alichanian 51  
 Aminoff 182, 212, 233, 235, 236  
 van Amstel 168, 181  
 Andrade 169, 281  
 Andrews 207  
 Arnot 246  
 Arsenieva 321  
 Aylmer 151

### B

BACCAREDDA 211  
 Bailey 195  
 Barengarten 278  
 Basart 225  
 Beach 259  
 Beeching 116, 160, 168, 178, 237, 241, 296, 297, 303  
 Beilby 185  
 Belwe 178  
 Berdennikov 195  
 Bethe 104, 267, 273, 282, 283 *et seq.*  
 Bewilogua 251  
 Bircumshaw 163, 178  
 Blackman 93, 104, 292  
 Blodgett 208  
 Boersch 114, 125  
 Bohr 12, 317  
 Born 17, 88  
 Bound 235  
 Bowden 191  
 Bragg, Sir William, 74  
 Bragg, W. L., 23, 25, 71, 93, 96, 97, 99, 184  
 Breit 322  
 Bresler 195, 211  
 Bridgman 238  
 Brill 130  
 Brillouin 12  
 Brinckman 87  
 Brindley 95  
 Brockway 230, 233, 248, 253, 254, 257, 259, 260  
 de Broglie 12, 14, 17, 33, 37, 47, 50, 51, 52, 58, 59, 68  
 Broomé 182, 212, 233, 236

Bruce 190  
 Brück 76, 165, 166, 167, 169, 174, 175  
 Bruni 211  
 Bühl 263, 281  
 Burgers 135, 167, 168, 169, 181, 225  
 Busch 226  
 Byrne 322

### C

CATES 178, 179  
 Chase 322  
 Cochrane 76, 85, 105, 113, 152, 171, 189, 237  
 Cooper 79, 132, 150, 178, 180, 234  
 Coper 167  
 Cosslett 249  
 Coster 125  
 Cox 321, 322  
 Curran 52

### D

DAMES 280  
 Darbyshire 79, 132, 150, 152, 153, 159, 177, 178, 180, 184, 187, 188, 191, 192, 234  
 Darwin 64, 65, 311 *et seq.*  
 Davey 136  
 David 318  
 Davisson 30, 33, 34, 37, 102, 159, 180, 263, 266 *et seq.*, 299, 321  
 Debye 27, 125, 195, 251  
 Desch 238  
 Dippel 167, 168, 169  
 Dirac 53, 311  
 Dixit 160, 161, 167, 169, 187, 188, 191, 192, 241  
 Dobinski 188  
 Dornte 234, 249  
 Drude 4  
 Dymond 318, 319

### E

ECKART 267  
 Ehrenberg 278  
 Ehrenfest 187, 251  
 Einstein 12

## 326 THEORY AND PRACTICE OF ELECTRON DIFFRACTION

Eisenhut 213  
 Elsasser 29  
 Emslie 49, 117, 120, 121  
 Ewald 70, 283

### F

FARNSWORTH 171, 273 *et seq.*  
 Fermat 14  
 Fermi 93  
 Finch 82, 83, 84, 117, 120, 123, 124,  
     127, 134, 137, 151, 153, 163, 170,  
     173, 174, 175, 176, 180, 191, 193,  
     194, 209, 210, 213, 226, 231, 239,  
     240, 241, 242  
 Fordham 123, 151, 163, 195, 214  
 Förster 317  
 Fourier 7, 8, 10, 53, 72, 73, 106, 284  
 Fraser 216  
 French 146, 186, 238  
 Frenkel 317  
 Fresnel 4, 5  
 von Friesen 50, 51, 54, 55  
 Fröhlich 272  
 Frommer 167

### G

GAERTNER 214  
 Garrido 199  
 Gen 164  
 Germer 30, 33, 34, 37, 102, 159, 180,  
     190, 194, 204, 207, 208, 215, 229,  
     233, 263, 266 *et seq.*, 299, 321  
 Gether 249  
 Glasstone 259  
 Goudsmit 311  
 Green 307  
 Gregg 243

### H

HAIDUCK 280  
 Halpern 317, 320  
 Hamilton 14  
 Hampson 243  
 Harding 99, 297, 298  
 Hardy 197  
 Harkins 280  
 Hartree 92  
 Hass 164  
 Hauer 87  
 Hautot 105, 298  
 Havigurst 296  
 Hayashi 309  
 Heisenberg 61, 66

Hellmann 318, 320  
 Hendricks 212, 213, 234, 249, 259  
 Hengstenberg 199  
 Henneberg 86  
 Hirsch 82, 163, 198, 242, 322  
 Hopkins 180, 188, 193  
 Howe 151, 234, 236  
 Hughes 52, 191, 224  
 Hull 27, 136

### I

IITAKE 179  
 Imori 179  
 Ironside 44, 46, 47

### J

JAKOWLEW 280  
 James 95  
 Jefferson 234, 239  
 Jenkins, G. I., 243  
 Jenkins, R. O., 144, 145, 160, 180,  
     183, 195, 209, 224, 236  
 Jones, E. Taylor, 150  
 Jones, P. L. F., 243, 254, 257  
 Joffe 321

### K

KAKESITA 195  
 Kallaschnikow 280  
 Kassatotschkin 280  
 Kaupp 213  
 Kaye 232  
 Kelvin 11  
 Kikuchi 49, 79, 80, 81, 111 *et seq.*,  
     122, 125, 127, 146, 149, 157, 158,  
     160, 232, 283, 297 *et seq.*, 304  
 Kirchhoff 4, 5  
 Kirchner, 76, 77, 98, 101, 103, 105,  
     130, 137, 164, 173, 189, 230, 236,  
     241, 322  
 Klinger 49  
 Knauer 185  
 Konobievski 44  
 Kosman 51  
 Kossel 306  
 Krylow 211  
 Kurrelmeyer 322  
 Kusmin 125, 278, 280

### L

LABY 232  
 Lamla 309, 310

Langmuir 197  
Langstroth 322  
Laplace 6  
Lark-Horovitz 96, 151  
Laschkarew 96, 125, 157, 159, 161,  
212, 276, 278, 279, 280, 301  
Lassen 76, 165, 166, 167  
de Laszlo 233, 235, 248  
von Laue 23, 75, 76, 77, 132, 135,  
136, 142, 143, 282, 300, 301, 307,  
308, 309  
Lebedeff 198, 226, 228  
Lees 189  
Lennard-Jones 123  
Lorentz 12  
Loria 49  
Louw 224

## M

M'CANDLESS 181  
M'Farlane 223  
M'Ilwraith 322  
Mann 213  
Mark 87, 150, 151, 246  
Martindale 169, 281  
Massey 94, 246  
Matukawa 302, 306, 308  
Maxwell 208, 213, 234, 242, 249, 259  
Mehl 181  
Meibonn 114  
Menke 195  
Menzer 77  
Merigoux 214  
Miller 21  
Miwa 188  
Miyake 158, 160, 163, 177, 179, 182,  
183, 301  
Mongan 228, 234, 241  
Moon 280  
Moore 191  
Morgan 229  
Morse 104, 251, 271, 276, 283, 299  
Mosley 234, 249, 259  
Mott 88, 91, 94, 246, 317, 318, 320  
Motz 151, 211, 214  
Müller 197, 205  
Murison 160, 163, 167, 177, 199 *et seq.*,  
213, 240  
Muto 48, 241  
Myers 321, 322

## N

NAKAGAWA 116, 146, 149, 157, 158,  
160, 298, 299

Natta 211  
Nelson 179, 181, 207  
Newton 185  
Nishikawa 49, 113

## O

OGAWA 164  
Oketani 162, 163  
Ornstein 87, 91  
Otty 177, 180

## P

PAPSDORF 189, 195  
Pauling 253, 254, 257, 259  
Planck 12  
Ponte 48  
Preston 163, 178, 180  
Prins 187

## Q

QUARRELL 117, 132, 134, 135, 165,  
169, 175, 180, 191, 226, 231, 239,  
241, 242

## R

RAETHER 137, 145, 146, 150, 187, 188,  
191, 192, 193, 195  
Rayleigh 185  
Reid 36, 37, 40, 150  
Rhines 181  
Richards 212, 235  
Richter 318, 319, 320  
Ridler 191  
Riedmiller 230  
Roebuck 191  
Rollier 213  
Rüdiger 166, 167, 174, 175, 235  
Rupp 114, 223, 263, 281, 321, 322  
Rydberg 51

## S

SAUTER 318, 319  
Schalnikoff 164  
Scherrer 27  
Schomaker 254  
Schoon 153, 160, 208, 230, 235  
Schrödinger 17, 18, 58, 59, 69, 89  
Schwinger 320  
Sherman 255  
Shinohara 115, 116, 117, 120, 155,  
160, 161, 273, 296 *et seq.*  
Shirai 95

# 328 THEORY AND PRACTICE OF ELECTRON DIFFRACTION

Shishacow 212  
 Shurman 280  
 Smith, P. T., 100  
 Smith, N., 177, 179, 229  
 Snell 107  
 Sommerfeld 12, 58, 59  
 Springall 254  
 Sproull 275 *et seq.*  
 Steinheil 135, 136, 178  
 Stern 185  
 Storks 204, 207, 208  
 Strauff 195, 211  
 Stuart 167, 213, 240  
 Sun 170, 173, 174, 176, 241  
 Sutton 243  
 Szilard 322

## T

TARTAKOWSKY 263, 281  
 Tashaban 96  
 Thibaud 322  
 Thiessen 160, 208, 230, 235  
 Thomas 93  
 Thomson, G. P., 37, 39, 42, 46, 87, 88,  
 105, 138, 141, 162, 163, 164, 165,  
 167, 171, 177, 179, 181, 199, 212,  
 213, 216, 223, 231, 236, 240, 244,  
 251, 275, 281, 299, 318, 319, 322  
 Thomson, Sir J. J., 283  
 Tillman 117, 122, 146, 156, 158, 159,  
 160, 226, 234  
 Tol 87  
 Trendelenburg 132, 234, 241, 244  
 Trillat 82, 105, 150, 151, 162, 163, 195,  
 198, 211, 214, 223, 242, 298, 322  
 Tyson 195, 214

## U

UHLÉNBECK 311  
 Usyskin 212  
 Uyeda 160

## V

VOLMER 168

## W

WEISSKOPF 318  
 White 103, 104  
 Whitmore 193  
 Wieland 132, 234, 241  
 Wierl 87, 187, 195, 234, 246, 257, 258  
 Williams 170, 176  
 Wilman 82, 83, 84, 117, 123, 124, 134,  
 137, 153, 193, 194, 209, 210, 226,  
 231, 239, 241, 242  
 Winter 318  
 Wolf 321  
 Wood 171

## Y

YAMAGUTI 48, 155, 157, 158, 159, 160,  
 181, 182, 241  
 Yearian 95, 151, 234, 236  
 Young 37

## Z

VAN ZANTEN 125  
 Zelmanoff 164, 195, 211  
 Zocher 167

## SUBJECT INDEX

### A

ABSORPTION 297, 301  
 accommodation coefficient 213  
 acetylene 258  
 adhesion 197  
 adsorbed gas 35, 269, 281  
 alcohols 206  
 alkali halides 123, 124, 259  
 aluminium 44, 82, 87, 105, 165 *et seq.*,  
     233  
     — silicate 132  
 amalgams 151  
 ammonium chloride 213  
 amplitude 1  
 amyl acetate 241  
 anodic polishing 191  
 anomalous dispersion 268  
 'anpassung' 288  
 anthracene 127, 209  
 antimony 159, 160  
 apparatus 39, 49, 216 *et seq.*, 246 *et*  
     *seq.*, 263 *et seq.*  
 applications 211 *et seq.*  
 'arcing' 128, 162  
 arcs, in reflection patterns, 140, 206  
 atomic scattering 86 *et seq.*  
 'aufhellung' 115  
 auripigmentum 242

### B

BACKGROUND 48, 103  
 bands from polycrystalline films 134  
 bands, Kikuchi, 113, 125, 302 *et seq.*  
 barium stearate 208  
 beads 137  
 beaten films 46, 162, 240  
 beats 9, 290  
 beeswax 151  
 Beilby layer 185  
 benzene 254, 258, 259  
 beta rays 52, 321, 322  
 Bethe's theory 283 *et seq.*  
 bismuth 159, 164  
 blackening produced by electrons 244  
 bond distances 258 *et seq.*  
 boundary conditions 285, 300  
 'Bragg' reflection 24, 147, 267  
 bromine 258

bromostearic acid 200  
 brucite 242  
 Brück's law 174  
 brushing 222  
 burnishing 188

### C

CADMIUM 173, 188  
     — iodide 83, 164, 173  
 calcite 49, 160, 192, 239  
 calcium fluoride 117, 160, 167, 168,  
     192  
 calomel 164  
 camera, electron diffraction, 39, 216  
     *et seq.*  
     — length 219, 243  
 cast-iron 210  
 cell, unit, 20  
 celluloid 36, 38, 123, 150, 241  
 cellulose 211  
     — acetate 136, 240, 241  
 central maximum 103, 173  
 cetyl alcohol 201  
     — palmitate 153, 208  
 charcoal 265  
 'charging-up' 239  
 chromium 166, 172, 186, 190, 238  
 circles 80, 117 *et seq.*  
 clay 212  
 cleavage slips 242  
     — surfaces 146, 155, 159, 239  
 cobalt 132, 134, 172  
     — crystal, surface of, 76  
 collimating tube 221, 247  
 collodion 241  
 colloid precipitation 241  
 comparison photograph 229, 230  
 conductivity electrons, collisions with  
     308  
 conservation of energy 63, 67  
 contamination 149 *et seq.*, 237  
 copper 46, 91, 134, 151, 171, 173, 186,  
     188, 191, 213, 238, 241, 273 *et seq.*,  
     321  
 cross-grating patterns 78 *et seq.*, 141  
     *et seq.*  
 cross-gratings 132, 135, 150  
 crystal axes 20, 136

### 330 THEORY AND PRACTICE OF ELECTRON DIFFRACTION

crystal growth 162 *et seq.*  
 — lattice 20  
 — size 78, 130, 140, 165, 240  
 — — and lattice constant, 123  
 cubic crystals 26  
 current density and crystal growth  
   171, 172  
 — — of electrons 59, 314  
 cyclohexane 258  
 cyclopentane 258

#### D

DETERMINISM 63  
 deviation of electrons 293, 298, 299  
 diamond 146, 160, 239, 297  
 diaphragms 228  
 1, 2-dibromoethane 258  
 1, 2-dichloroethane 258  
 dichloroethylene 258  
 diffraction, *see* scattering  
 diffuse rings 164, 177, 186, 190 *et seq.*,  
   200, 205, 211, 243, 252  
 diffuse streak 146, 195  
 diffusion of metals 213  
 discharge tube 221, 228, 230  
 dispersion 8  
 —, anomalous, 268  
 distortion 79, 141, 215  
 Dixit's law 167  
 Dobson tank 244  
 double-acceleration camera 231  
 double-shutter 229  
 'dust' specimens 241  
 dynamical theory 271 *et seq.*, 283 *et seq.*

#### E

$E(\theta)$ , definition of, 93, 251  
 —, graph of, for aluminium, 97  
 —, — of, for gold, 87  
 —, measurement of, 87, 244  
 $\{E(\theta)\}^2$ , Tables of, 92, 93  
 electric density 17, 59  
 electrical measurements 236  
 electrodeposition 238  
 electrolytic deposits 170 *et seq.*  
 electron beam, 'aiming' of, 224  
 — —, current in, 224  
 — gun 263  
 electrostatic lens 232  
 'elliptical rings' 46  
 elongated spots 145, 146  
 envelopes 117, 309  
 etched crystal 76, 141 *et seq.*, 156  
 etching 238, 265

ethylene 258  
 evaporated layers 164 *et seq.*  
 evaporation 238, 240  
 Ewald sphere 71, 288  
 'excitation error' 288  
 extension of reciprocal lattice points  
   75, 80, 140, 144, 300  
 extinction 291  
 'extra' rings and spots 82, 149, 171

#### F

$f$ , definition of, 86, 91  
 —, graph of, for aluminium, 97  
 F, definition of, 86  
 facets, developed by heating, 275, 278  
 Faraday cylinder 30, 237, 244, 263,  
   281, 319  
 fatty acids 197, 198, 206  
 Fermat's principle 3, 14  
 finite crystal 72  
 fluorescent screen 219, 230  
 fluorite, *see* calcium fluoride  
 focal length 226  
 focusing 223, 226, 232, 234  
 'forbidden' rings and spots 82, 150,  
   281, 296  
 Fourier analysis of crystal 72, 284  
 — — of wave 53  
 — component 74, 106  
 — integral 7  
 — series 7  
 four-vector 16  
 fractional indices 82  
 free rotation 258  
 frequency 1  
 Fresnel zones 97, 99

#### G

GALENA 49, 160, 192, 215  
 gas in metals 165  
 gas layer 35, 269, 281  
 gas molecules 246 *et seq.*  
 gaskets 225  
 gauze 239, 241  
 gelatine 214  
 gems 155, 194  
 geometrical optics 6  
 gold 43, 87, 103, 123, 134, 151, 152,  
   162 *et seq.*, 188, 190, 213, 229, 233,  
   238, 273 *et seq.*, 317 *et seq.*  
 — alloy 162  
 — amalgam 151  
 graphite 48, 82, 83, 124, 159, 160, 209,  
   242, 278, 280

grating, plane, 32, 317, *see also* cross-grating  
 grazing beams 35, 269  
 grease 127, 197 *et seq.*, 219, 220, 237  
   — pattern 204, 208  
 Green's theorem 307  
 grinding 238  
 group velocity 9, 13  
   — of waves 9, 54, 64, 316  
 growth of crystals 162 *et seq.*  
 gypsum 160

## H

HAEMATITE 160, 191  
 haloes 37, *see also* diffuse rings  
 Hamiltonian 18  
 heating, by electron bombardment, 265  
   — of thin films 162  
 heavy negative ions 228  
 hexane 258  
 high tension equipment 222, 230  
   — voltages 51  
 horns attached to reciprocal lattice points 75  
 hot cathode 230  
 Huygens' construction 3  
 hydrocarbons 197  
 hydrogen atoms, position of, 212  
 hyperbolae 137

## I

IDENTIFICATION 136  
 illumination of plates 243  
 imaginary quantities 65  
 impurities 149  
 inclined films 44, 128, 162, 164  
 induction coil 222  
 inelastic collisions 48, 99, 103, 115, 251, 301, 307  
 inhomogeneity of electrons 224  
 inner potential 106 *et seq.*, 122, 145, 155 *et seq.*, 209, 267, 275 *et seq.*, 282  
   — —, Table of, 160  
   — —, theory of, 157  
 intensities 86 *et seq.*, 105, 131  
   —, measurement of, 244  
 iron 166, 173, 174, 186, 188, 238, 321

## J

JETS for vapour stream 247 *et seq.*

## K

KIKUCHI bands 113, 125, 302 *et seq.*  
   — circles 80  
   — lines 80, 111 *et seq.*, 125, 127, 146, 301, 307  
   — — and Laue spots, interference of, 116  
   — — as test for distortion 141  
   — —, envelopes of, 117, 309  
   — —, indices of, 148  
   — —, intersections of, 115, 302  
   — —, width of, 303  
 Kirchhoff's theorem 4  
 Kossel lines 306

## L

LARD 201, 207  
 Laue beams 266  
   — case and Bragg case in Bethe's theory 292  
   — conditions 23, 71, 111  
   — numbers 25  
   — spots 146  
   — zones 81, 141, 149  
 layer lattice 132  
 leak 223  
 linear diffraction 120  
 lines, regularly arranged, 171  
 liquids, surfaces of, 236  
 long-chain compounds 38, 151, 160, 197  
 lubrication 197 *et seq.*

## M

MAGNESIUM 180  
 magnetic field 67, 312  
   — lens 226  
   — moment of electron 311  
 measuring patterns 242  
 mercury 195  
 metal films 39  
 methyl stearate 207  
 mica 49, 79, 98, 101, 103, 105, 111, 114, 117, 122, 127, 135, 136, 153, 160, 167, 242  
 microphotometer 244, 252  
 migration of atoms 168, 176  
 Miller indices 21  
 minimum layer to give pattern 152 *et seq.*  
 mischmetal 265  
 molecular rays 185  
   — structures, Table of, 260  
 molybdenite 82, 136, 160, 242

### 332 THEORY AND PRACTICE OF ELECTRON DIFFRACTION

molybdenum 166, 167  
monomolecular layer of gas 269 *et seq.*  
— — of stearate 208

#### N

NATURAL surfaces 155, 239  
net plane 20  
nickel 30, 46, 134, 152, 159, 165, 171, 188, 263 *et seq.*, 321  
nickel-iron 135  
nomographs 136  
nozzle for gases 247 *et seq.*  
nuclear scattering 317  
'Nujol' 208

#### O

OCTAHEDRAL boundaries 76  
'Oildag' 209  
oils 197 *et seq.*  
operators 18  
optical reflection 146  
order of reflection 25  
organic compounds 160, 261, 262  
orientation 46, 128, 140, 144, 162 *et seq.*, 184, 192, 194, 197 *et seq.*, 240  
— and temperature 166, 175  
— as a single crystal 165 *et seq.*  
orpiment 242  
outgassing 265, 278, 279  
oxide, *see also* oxides  
—, cadmium 48  
—, copper, 163, 177, 191  
—, lead, 144, 160, 242  
—, magnesium, 48, 96  
—, platinum, 213  
—, tin, 160  
—, zinc, 48, 95, 114, 123, 160, 175, 241  
— -coated filaments 214  
oxides 177 *et seq.*, 238  
—, growth of, 181  
—, inner potentials of, 145, 160

#### P

PALLADIUM 134, 151, 163, 166, 173  
parabolae 117 *et seq.*  
paraffin 151, 153, 160, 197 *et seq.*, 242  
— wax 204  
parallelepiped, scattering by, 77  
passivated iron 179  
patterns, types of, 126  
Pauling-Sidgwick rule 259  
penetration of electrons 99, 139, 152

pentadecane 208  
pentane 258  
phase 1  
— velocity 2, 59  
photographic action 214  
— plate 223  
phytol 208  
picein 204, 218, 221  
plane grating beams 266  
plate holder 218, 229, 234 *et seq.*  
platinised asbestos 212  
platinum 46, 82, 134, 163, 167, 173, 212, 213  
polarisation 311 *et seq.*  
polish 155, 185 *et seq.*  
polished copper as substrate 136  
polonium 213  
potassium chloride 95  
powder method 27  
precision measurements 50  
probability 17, 59, 69  
projections on surface 76, 138, 189  
protective coatings 178, 180  
pseudomorphism 176, 180  
pumping system 222  
pyrites 124, 145, 159, 160, 192

#### Q

QUARTZ 166

#### R

RADIAL distribution method 253, 257  
ray 6  
reciprocal lattice 70, 80, 84, 128, 131, 142, 145, 284  
reciprocity law 307  
reflection 49  
— patterns, interpretation of, 137  
— specimens 238  
refraction 107 *et seq.*, 145, 147, 188, 190, 195, 267  
— in transmission 108  
— of Kikuchi lines 122  
—, single, 110  
refractive index 19, 106  
reproduction of patterns 244  
'Resoglaz' 208  
resolving power 32, 53  
'resonance errors' 287  
ring patterns by reflection 138  
rings, diameters of, 45  
—, width of, 53, 78, 130  
rock-salt 145, 146, 160, 161, 165, 192, 239, 297, 302

rotation photographs, reflection, 116,  
158  
— —, transmission, 136  
rubber 211  
Rubinglimmer 178  
rust 178

## S

SATURATED diode 231  
satellites 274, 276  
scalar product 70  
scattering by atoms 86  
— by gas molecules 249  
— by lattice 22, 71  
— by nucleus 317  
—, diffuse, 111  
Schomaker's formula 254  
scums on molten metals 180  
selective reflection 291  
selenium 191  
semi-permeable membranes 214  
sharpness of patterns 53  
shutter 221, 234, 248  
silica 194  
silicon 191  
— carbide 194  
silver 87, 134, 151, 166, 172, 186, 188,  
214, 273 *et seq.*  
— bromide 214  
single crystals 238  
size of crystals 78, 123, 130, 140, 165,  
240  
slow electrons 30 *et seq.*, 124, 159, 263  
*et seq.*, 321  
Snell's law 107  
sodium nitrate 174, 193  
'soots' 241  
spacing, Bragg, 25, 38, 71, 187, 243  
spark gap 40, 222, 225  
sparking potentials and wave-lengths,  
Table of, 243  
specimen holder 219, 229, 236  
specimens, preparation of, 237 *et seq.*  
specular reflection 116  
speculum 185  
'sphere' method 238  
spherulites 170  
spider's web 48  
spin 52, 68, 311  
spluttering 46, 165 *et seq.*, 238, 240  
spreading of wave 10, 19, 63, 67  
spurious ring 224  
stearic acid 154, 197, 198, 207, 208,  
242  
steel, polished, 185

steel, stainless, 179, 241  
Stern-Gerlach experiments 311, 317  
stibnite 117, 160, 182  
straight line pattern 201, 207  
streak, diffuse, 146, 195  
structure factor 26, 77, 94  
subsidiary peaks 274, 276  
— rings 83  
substrate, effect of, on deposit 173  
successive diffractions 150  
superposition of waves 3  
surface, contour of, 76, 139, 189  
— layers, scattering by, 98  
Sutton's method 178

## T

TALC 160, 212, 242  
tallow 201  
technique 216 *et seq.*  
tellurium 159  
temperature effect 124, 280, 281  
tenorite 177  
tetrachlorides 258  
tetradecane 208  
thermal agitation 103  
thermionic emission 214  
thinning of films 239  
tilting thin film 44, 128, 162, 164  
transmission experiments 36 *et seq.*  
— patterns 126 *et seq.*  
— specimens 239  
tripalmitin 201  
tristearin 197, 207  
tungsten 277, 280  
twinning 171

## U

UNCERTAINTY principle 54, 61, 317  
'unctuous' metals 207  
unit cube, size of, 47

## V

VAPOURS, diffraction by, 246 *et seq.*  
vaseline 204  
vector product 70  
'Velox' 223  
'visual' method 252  
voltage, measurement of, 38, 40, 232  
*et seq.*

## W

WAVE, de Broglie, 13

## 334 THEORY AND PRACTICE OF ELECTRON DIFFRACTION

wave equation 3, 15, 17  
— front 2  
— length 1, 29, 41, 315  
— —, measurement of, 232 *et seq.*  
— —, Table of, 243  
— mechanics 12 *et seq.*  
—, plane, 8  
— train 53, *see also* group  
— velocity 3, 59  
—, water, 10  
waves, theory of, 1 *et seq.*  
waxes 199  
wedge-shaped specimens 242  
width of reflections 295 *et seq.*

width of rings 78, 123, 130, 140, 240,  
298  
Wierl's formula 187, 251  
willemite 40, 219  
'windows' in thin films 281

### Y

X-RAYS, scattering of, 86, 91, 96

### Z

ZINC 159, 160, 167, 173, 191, 281  
zinc blende 117, 145, 160, 182, 239

THE END

## BOOKS ON PHYSICS

AN INTRODUCTION TO LABORATORY TECHNIQUE. By A. J. ANSLEY. 12s. 6d. net.

INTRODUCTION TO CONTEMPORARY PHYSICS.  
By KARL K. DARROW, Ph.D. 25s. net.

INTRODUCTION TO THEORETICAL PHYSICS.  
By Prof. LEIGH PAGE, Ph.D. 30s. net.

ATOMIC ARTILLERY : MODERN ALCHEMY FOR EVERYMAN. By Prof. J. K. ROBERTSON. 10s. 6d. net.

X-RAYS IN THEORY AND EXPERIMENT. By Prof. ARTHUR H. COMPTON, Ph.D., Sc.D., and Prof. SAMUEL K. ALLISON, Ph.D. 31s. 6d. net.

PHYSICAL OPTICS. By ROBERT W. WOOD, LL.D. Third Edition (1934). 31s. 6d. net.

THEORETICAL HYDRODYNAMICS. By Prof. L. M. MILNE-THOMSON, M.A., F.R.S.E. 31s. 6d. net.

THE MEASUREMENT OF INDUCTANCE, CAPACITANCE, AND FREQUENCY. By A. CAMPBELL, M.A., and E. C. CHILDS, Ph.D. 30s. net.

MACMILLAN AND CO. LTD. LONDON

## BOOKS ON PHYSICS

A TEXTBOOK OF HEAT. By Prof. H. S. ALLEN and  
R. S. MAXWELL.

HEAT FOR ADVANCED STUDENTS. By E. EDSER,  
A.R.C.Sc. Revised Edition (1936) by N. M. BLIGH,  
A.R.C.Sc. 6s.

THE THEORY OF LIGHT. By THOMAS PRESTON,  
F.R.S. Fifth edition (1928), edited by Prof. A. W.  
PORTER, D.Sc. 25s. net.

A TEXT-BOOK ON SOUND. By Prof. EDWIN H.  
BARTON, D.Sc. (Lond.), F.R.S. 15s. net.

LIGHT FOR STUDENTS. By E. EDSER, A.R.C.Sc.  
New Edition (1931) with an Appendix by N. M.  
BLIGH, A.R.C.Sc. 7s.

A TEXT-BOOK OF LIGHT. By G. R. NOAKES, M.A.  
6s.

THE THEORY OF HEAT. By THOMAS PRESTON,  
F.R.S. Fourth Edition (1929), edited by J.  
ROGERSON COTTER, M.A. 25s. net.

THE SCIENCE OF SEEING. By MATTHEW LUC-  
KIESH, D.Sc., D.E., and FRANK K. MOSS, E.E.  
25s. net.

MACMILLAN AND CO. LTD. LONDON

## BOOKS ON CHEMISTRY

A SHORT HISTORY OF CHEMISTRY. By Prof. J. R. PARTINGTON, D.Sc. 7s. 6d.

HISTORICAL INTRODUCTION TO CHEMISTRY. By Prof. T. M. LOWRY, C.B.E., D.Sc., F.R.S. New Impression, with Additions (1936). 10s. 6d. net.

ELEMENTARY PHYSICAL CHEMISTRY. By Prof. HUGH S. TAYLOR, D.Sc., F.R.S., and Prof. H. AUSTIN TAYLOR, Ph.D. Second Edition (1937). 16s. net.

A TREATISE ON PHYSICAL CHEMISTRY. A Co-operative Effort by a Group of Physical Chemists. Edited by Prof. HUGH S. TAYLOR, D.Sc., F.R.S. Second Edition (1931) thoroughly revised. 2 vols. 30s. net each.

THE FUNDAMENTALS OF CHEMICAL THERMODYNAMICS. By J. A. V. BUTLER, D.Sc.

PART I. ELEMENTARY THEORY AND ELECTROCHEMISTRY. Third Edition (1939). 7s. 6d.

PART II. THERMODYNAMICAL FUNCTIONS AND THEIR APPLICATIONS. 8s. 6d.

THE PHASE RULE AND PHASE REACTIONS: THEORETICAL AND PRACTICAL. By S. T. BOWDEN, D.Sc. 10s. net.

CATALYSIS: FROM THE STANDPOINT OF CHEMICAL KINETICS. By Prof. GEORG-MARIA SCHWAB. Translated by Prof. HUGH S. TAYLOR, D.Sc., F.R.S., and R. SPENCE. 18s. net.

THEORETICAL ELECTROCHEMISTRY. By N. A. MCKENNA, B.A. 15s.

MACMILLAN AND CO. LTD. LONDON

## BOOKS ON MATHEMATICS

HIGHER MATHEMATICS FOR STUDENTS OF  
ENGINEERING AND SCIENCE. By F. G. W.  
BROWN, M.Sc. 10s.

THE ELEMENTS OF MATHEMATICAL ANALYSIS.  
By Prof. J. H. MICHELL, M.A., F.R.S., and M. H.  
BELZ, M.Sc. 2 vols. 42s. net each.

AN INTRODUCTION TO THE THEORY OF IN-  
FINITE SERIES. By T. J. I'A BROMWICH, Sc.D.,  
F.R.S. Second Edition (1926). Revised with the  
assistance of T. M. MACROBERT, D.Sc. 30s. net.

INTRODUCTION TO THE THEORY OF  
FOURIER'S SERIES AND INTEGRALS. By  
Prof. H. S. Carslaw, Sc.D. Third Edition, revised  
and enlarged (1930). 20s. net.

INTRODUCTION TO THE MATHEMATICAL  
THEORY OF THE CONDUCTION OF HEAT IN  
SOLIDS. By Prof. H. S. CARSLAW, Sc.D. 30s. net.

FUNCTIONS OF A COMPLEX VARIABLE. By  
Prof. THOMAS M. MACROBERT, M.A., D.Sc. Second  
Edition (1933). 14s. net.

THE CALCULUS OF FINITE DIFFERENCES. By  
Prof. L. M. MILNE-THOMSON, M.A., F.R.S.E.  
30s. net.

A TREATISE ON BESSEL FUNCTIONS AND  
THEIR APPLICATIONS TO PHYSICS. By  
Prof. A. GRAY, F.R.S., and G. B. MATHEWS,  
F.R.S. Revised Edition by Prof. A. GRAY and  
Prof. T. M. MACROBERT. 36s. net.

STANDARD FOUR-FIGURE MATHEMATICAL  
TABLES. By Prof. L. M. MILNE-THOMSON,  
M.A., and L. J. COMRIE, M.A., Ph.D. Edition A :  
With Positive Characteristics in the Logarithms.  
Edition B : With Negative Characteristics in the  
Logarithms. 10s. 6d. net each.

MACMILLAN AND CO. LTD. LONDON

